

Electron-Electron Interactions in Quantum Point Contacts and Finite Quantum Wires

Ph.D. Thesis in Physics

Anders Mathias Lunde

Niels Bohr Institute
University of Copenhagen
Denmark

Supervisor: Karsten Flensberg

17th of July 2007

ELECTRON-ELECTRON INTERACTIONS IN QUANTUM POINT CONTACTS AND
FINITE QUANTUM WIRES

Ph.D. thesis

© Anders Mathias Lunde 2007

E-mail: lunan@fys.ku.dk

The Niels Bohr Institute
Faculty of Science
University of Copenhagen

Universitetsparken 5
2100 Copenhagen Ø
Denmark

Abstract

This thesis is on the effect of electron-electron interactions on the transport properties in two cases: (\mathcal{A}) Finite length clean quantum wires and (\mathcal{B}) point-like constrictions. In both situations, the system is connected adiabatically to non-interacting leads. The main difference between the two cases is that the finite length quantum wire has approximately translational symmetry and the point-like constriction does not. Therefore the electron-electron interaction have to conserve momentum in the case of finite quantum wires (\mathcal{A}), but not for point-like constrictions (\mathcal{B}). In both cases, the change in conductance G and thermopower S due to interactions are considered. Common for both cases is that *without* interactions the conductance is $\frac{2e^2}{h}$ times the number of modes and the thermopower is exponentially suppressed at low temperatures T , i.e. $\propto e^{-T_F/T}$ (T_F being the Fermi temperature). This thesis present three main effects of interactions:

- (\mathcal{A}) In a single mode quantum wire two-particle interactions cannot change the distribution of electrons due to momentum and energy conservation. Therefore multi-mode wires are considered and we find that the *interaction induced resonances* in the conductance and thermopower at particular values of the Fermi level (i.e. gate voltage). The magnetic field splitting of the resonances provide a unique signature of the effect.
- (\mathcal{A}) *Three-particle collisions* in a single-mode finite wire can change the electron distribution, but the contribution to the conductance and thermopower turns out to be exponentially suppressed in temperature to lowest order in the interaction. However, several interesting properties of the tree-particle scattering rate are found.
- (\mathcal{B}) For a point-like constriction, two-particle scattering can change the current *even* for a single-mode. Therefore a weak interaction V_0 changes the current as $I(T, V)/V \simeq \frac{2e^2}{h} - \alpha|V_0|^2T^2 - \gamma|V_0|^2V^2$ and the thermopower as $S \propto |V_0|^2T^3$ for low temperature T and/or small bias V (α and γ being constants). Furthermore, the noise is reduced compared to the single-particle case. In a large magnetic field, the interaction among electrons of *equal* spin suppress the low-temperature corrections to the transport properties by two extra powers of temperature. The conductance versus temperature (for $B = 0$) beyond the perturbative regime was found in a self-consistent 2nd order approach. Based on numerical results, we conjecture that the conductance approach $\sim e^2/h$ for higher temperatures, however, still lower than T_F . These results are all in qualitative agreement with experimental studies on the 0.7 anomaly in quantum point contacts.

On the technical side, the Boltzmann equation approach is used for the finite quantum wires whereas the Green's function approach is used for the point-like constriction. In both cases, the regime of weak interactions are studied using perturbation theory to second order in the interaction.

Preface

The present Ph.D. thesis is submitted in candidacy for the Ph.D. degree in physics at the University of Copenhagen. It presents the main parts of my research activities from May 2004 to July 2007 in the area of mesoscopic electron transport theory. It was carried out under the supervision of Associate Professor Karsten Flensberg at the Niels Bohr Institute, University of Copenhagen, Denmark.

First of all, I would like to thank my supervisor **Karsten Flensberg** for his tremendous amount of ideas, patience, inspiration and work. It has truly been a great pleasure to learn from him over the last years and I have enjoyed his open-minded attitude both within and outside of physics. I am also impressed and inspired by his way of attacking an unknown problem and his ability to figure out and describe a complex problem in very simple terms (which often leads to a simple model that captures the essential physics).

During my Ph.D. studies, I spend the winter of 2005/2006 at the William I. Fine Theoretical Physics Institute (University of Minnesota, Minneapolis, USA) under the supervision of Leonid I. Glazman. I am sincerely grateful to **Leonid Glazman** for the excellent supervision, ideas and inspiration that I have received from him. He always gave me the time and patience, I needed during my stay and I have learned many interesting and useful skills from him. I admire him for his sharp mind and kind personality. During my stay in Minnesota, I also got in contact with several other interesting persons. In particular, I want to thank Markus Garst, Maxim Khodas and Roman M. Lutchyn of the condensed matter physics theory group for great discussion on physics and bison for instance during wonderful lunch breaks with asian cuisine.

An obligatory part of the Ph.D. program at the University of Copenhagen is to teach. I have enjoyed being a teaching assistant in statistical physics and in applications of quantum mechanics. Furthermore, I supervised Jesper Nissen (in collaboration with Karsten Flensberg) during his master thesis on carbon nanotubes - A fun task and I want to thank Jesper for some good and hectic months.

Another obligatory part of the Ph.D. program is to take courses. To this end, I have enjoyed the pleasure of learning the non-equilibrium Green's function technique from Antti-Pekka Jauho together with Christian Flindt. Furthermore, I have participated in a study group on theoretical condensed matter physics with Thomas Frederiksen, Dan Bohr, Christian Flindt and Mikkel Strange from the Technical University of Denmark. I want to thank them for an inspiring and fun time together trying to understand the wonders of physics.

I also want to acknowledge Reinhold Egger and Alessandro De Martino from the Heinrich-Heine University in Düsseldorf for an interesting, fun, energetic and fruitful collaboration on transport in short quantum point contacts (see chapter 6). I want to thank them for numerous interesting and very useful discussions both in person and by e-mail.

In the last years at the Niels Bohr institute, I have had numerous valuable discussions with several individuals from the the experimental and theoretical condensed matter group at the institute. For instance, I have had the pleasure of sharing an office with some of them. In particular, the experimentalists have also been very helpful in explaining me the reality in a laboratory and how experiments really work and what can actually be measured - something everyone should keep in mind. Furthermore, I have had numerous entertaining lunch breaks with them. The transport theory group is acknowledged for a lot of interesting debates, e.g. at our weekly group meeting.

At last but not least, I want to thank my girlfriend Arancha, my family and my friends for understanding, patience and support during my Ph.D. studies and especially in the last hectic months.

A. Mathias Lunde, Copenhagen, July 2007.

Contents

| | |
|---|-------------|
| Abstract | I |
| Preface | III |
| List of symbols | VIII |
| 1 Introduction | 1 |
| 1.1 Mesoscopic transport | 1 |
| 1.2 Quantum point contacts | 2 |
| 1.3 Thermopower | 4 |
| 1.4 The Landauer formula | 5 |
| 1.4.1 Dissipation for a clean 1D system perfectly connected to the leads? | 6 |
| 1.4.2 A historic note on the Landauer formula | 7 |
| 1.5 Non-interacting current through a quantum point contact | 7 |
| 1.5.1 The saddle-point model of a quantum point contact | 8 |
| 1.5.2 Analytic results for an ideal quantum point contact | 10 |
| 1.6 The secret behind the Landauer formula | 12 |
| 1.7 Thermopower and electron-hole asymmetry | 13 |
| 1.8 A first look at electronic interactions in quantum point contacts | 13 |
| 1.9 The 0.7 anomaly in quantum point contacts | 16 |
| 1.9.1 Experimental features of the 0.7 anomaly | 17 |
| 1.9.2 Available explanations of the 0.7 conductance anomaly | 21 |
| 1.10 Outline of the thesis | 23 |
| 2 The Mott formula for non-interacting electrons | 25 |
| 2.1 The Mott formula | 25 |
| 2.2 Why study the Mott formula? | 25 |
| 2.3 The lowest order approximation in $k_B T$ | 26 |
| 2.4 Validity of the Mott formula | 27 |
| 2.4.1 Numerical investigation | 27 |
| 2.4.2 A power series expansion of the transmission | 29 |
| 2.4.3 An analytically solvable case: The ideal point contact | 30 |

| | | |
|----------|---|-----------|
| 2.5 | Beyond non-interacting electrons? | 31 |
| 2.6 | Concluding remarks | 32 |
| 3 | Transport in finite quantum wires: A Boltzmann equation approach | 33 |
| 3.1 | Relaxation in a one-dimensional system with perfect leads | 33 |
| 3.2 | The Boltzmann equation approach | 35 |
| 3.2.1 | The Boltzmann equation for a wire with leads | 36 |
| 3.2.2 | Collision integrals for electronic interactions | 37 |
| 3.2.3 | The current to lowest order in the scattering rate | 39 |
| 3.3 | A requirement on the scattering to change the current | 41 |
| 3.4 | Outlook | 45 |
| 4 | Interaction-induced resonances in multi-mode wires | 47 |
| 4.1 | The physical picture of the interaction-induced resonances | 47 |
| 4.1.1 | Interaction-induced resonances at certain Fermi energies . | 47 |
| 4.1.2 | Conductance dip at the resonance | 50 |
| 4.1.3 | Sign change of the thermopower at the resonance | 52 |
| 4.1.4 | The conductance and thermopower have scaling forms . . | 53 |
| 4.2 | Is the resonance observable? An order of magnitude estimate . . | 54 |
| 4.3 | The current to lowest order in the interaction | 55 |
| 4.3.1 | The electron-electron interaction matrix element | 59 |
| 4.3.2 | The current to lowest order in the temperature | 61 |
| 4.3.3 | Higher orders in temperature | 66 |
| 4.4 | The Mott formula | 67 |
| 4.5 | Magnetic field splitting of the resonance | 68 |
| 4.5.1 | The magnetic field splits the subbands | 68 |
| 4.5.2 | The interaction-induced resonances in a magnetic field . . | 69 |
| 4.5.3 | Suppression of resonant scattering between equal spins . . | 71 |
| 4.5.4 | Resonant scattering between opposite spins | 75 |
| 4.6 | Summary | 77 |
| 5 | Three-particle scattering in finite quantum wires | 79 |
| 5.1 | The three-particle interactions within the wire | 79 |
| 5.2 | The perturbative approach | 80 |
| 5.2.1 | The dominant three-particle scattering process | 81 |
| 5.2.2 | The conductance and thermopower corrections | 81 |
| 5.2.3 | A simple picture for the sign of the thermopower | 82 |
| 5.2.4 | A simple picture of the conductance correction | 83 |
| 5.2.5 | The three-particle scattering rate | 83 |
| 5.3 | The long wire limit: An open question | 85 |

| | | |
|----------|---|------------|
| 6 | Non-momentum conserving interactions in point contacts | 87 |
| 6.1 | The physics of non-momentum conserving interactions in quantum point contacts | 88 |
| 6.1.1 | The point-like interaction model | 91 |
| 6.2 | The problem of the Boltzmann equation | 92 |
| 6.3 | The Green's function approach | 92 |
| 6.3.1 | Average values in the quantum point contact setup | 93 |
| 6.3.2 | The Green's functions and the Langreth rules | 96 |
| 6.3.3 | The Dyson equation | 100 |
| 6.4 | A non-perturbative current formula for the point-like interaction . | 102 |
| 6.4.1 | Connection to the Meir-Wingreen formula for an Anderson model | 106 |
| 6.5 | Perturbative results for the current using the point-like interaction | 107 |
| 6.5.1 | The current to first order in the interaction | 108 |
| 6.5.2 | The current to second order in the interaction | 109 |
| 6.6 | The low-temperature perturbative transport coefficients beyond the point-like interaction | 117 |
| 6.6.1 | The perturbative large magnetic field results | 120 |
| 6.7 | The conductance in the self-consistent second order approach . . . | 122 |
| 6.7.1 | The self-consistent second-order approximation | 123 |
| 6.7.2 | The idea of the 2nd order self-consistent approach | 123 |
| 6.7.3 | The non-perturbative conductance and thermopower . . . | 126 |
| 6.7.4 | Connection to the Anderson model: A new parameter regime | 133 |
| 6.8 | The noise due to non-momentum conserving interactions | 134 |
| 6.9 | Discussion and summary | 136 |
| | Appendix A: A general current formula | 139 |
| A.1 | The Hamiltonian | 139 |
| A.2 | The current | 140 |
| A.3 | A general formula for the current | 141 |
| A.4 | Electron-electron interactions for a general basis and interaction . | 142 |
| A.4.1 | The free-electron plane wave basis | 144 |
| | Paper I: Journal of Physics: Condensed Matter 17, 3879 (2005) | 145 |
| | Paper II: Physical Review Letters 97, 256802 (2006) | 153 |
| | Paper III: Physical Review B 75, 245418 (2007) | 159 |
| | Paper IV: submitted (2007) | 173 |
| | Bibliography | 179 |

List of symbols

GENERAL NOTATION

| Symbol | Description | |
|----------------------|---|------------|
| QPC | Short for quantum point contact | |
| 1D | Short for one-dimensional | |
| 2D | Short for two-dimensional | |
| $a \equiv b$ | Means that a is <i>defined</i> to be b | |
| I | The particle current | |
| I_e | The electric current (i.e. $I_e = (-e)I$) | |
| G | The linear conductance | eq.(1.2) |
| G_T | The thermoelectric coefficient | eq.(1.2) |
| S | The thermopower | eq.(1.3) |
| T | Temperature | |
| ε_F | Fermi level (Fermi energy) | |
| T_F | Fermi temperature: $T_F = \varepsilon_F/k_B$ | |
| μ | Chemical potential | |
| V_g | Gate voltage | |
| $f^0(\varepsilon)$ | The (equilibrium) Fermi distribution | |
| $f_L^0(\varepsilon)$ | The Fermi distribution of the left lead | eq.(1.5) |
| $f_R^0(\varepsilon)$ | The Fermi distribution of the right lead | eq.(1.5) |
| $e > 0$ | Elementary charge (defined as positive) | |
| $\theta(x)$ | The step function (zero for $x < 0$, one for $x > 0$) | |
| c_i^\dagger | Operator creating a particle in state i | |
| c_i | Operator annihilating a particle in state i | |
| k_i | (Quasi-)momentum <i>before</i> the scattering event | |
| $k_{i'}$ | (Quasi-)momentum <i>after</i> the scattering event | |
| $\mathcal{T}(E)$ | The transmission | eq. (1.4) |
| S^M | The result of the Mott formula | eq. (2.1) |
| $V_{1'2',12}$ | The direct interaction | eq. (4.37) |
| \mathcal{S} | The noise of the current | p. 19 |
| \mathcal{P} | The principal part of an integral | |

BOLTZMANN EQUATION NOTATION

| Symbol | Description | Reference |
|-------------------------|--|--------------|
| L | Length of the wire | fig. (3.1) |
| \mathcal{L} | Normalization length | p. 40 |
| $f_{kn}(x)$ | Distribution function | |
| $f^{(n)}$ | The n^{th} order distribution function | eq.(3.13) |
| $I_e^{(0)}$ | The non-interacting contribution to the current | eq.(3.17) |
| $I_e^{(1)}$ | The 1 st order scattering contribution to the current | eq.(3.17) |
| $I_e^{(\text{int})}$ | The full scattering contribution to the current | eq.(3.19) |
| $\mathcal{I}_{knx'}[f]$ | The collision integral | sec. 3.2.2 |
| $W_{12;1'2'}$ | Two-body transition rate | eq.(3.7,3.9) |
| $W_{123;1'2'3'}$ | Three-body transition rate | eq.(3.11) |
| T_{Fb} | Given by $T_{\text{Fb}} = (\varepsilon_{\text{F}} - \varepsilon_0)/k_{\text{B}}$ | |
| ε_0 | Subband spacing | eq.(4.2) |
| $n_B(x)$ | The Bose function for $\mu = 0$ and $x = \varepsilon/k_{\text{B}}T$ | eq.(4.68) |

THE GREEN'S FUNCTION NOTATION

| Symbol | Description | Reference |
|--------------------------|---|------------|
| $B_H(t)$ | Operator B in the Heisenberg picture | eq.(6.11) |
| $\langle B_H(t) \rangle$ | The average value of B defined in eq.(6.10) | |
| $\mathcal{G}(1, 1')$ | The contour ordered Green's function | eq.(6.21) |
| $\mathcal{G}^<(1, 1')$ | The lesser Green's function | eq.(6.22a) |
| $\mathcal{G}^>(1, 1')$ | The greater ordered Green's function | eq.(6.22b) |
| $\mathcal{G}^a(1, 1')$ | The retarded ordered Green's function | eq.(6.22c) |
| $\mathcal{G}^r(1, 1')$ | The advanced ordered Green's function | eq.(6.22d) |
| \mathcal{G}_0^i | The non-interacting Green's function ($i = r, a, \lessgtr$) | p. 99 |
| $A(1, 1')$ | The spectral function | eq.(6.23) |
| $\Sigma(1, 1')$ | The (irrecusable) contour ordered self-energy | eq.(6.45) |
| $\Sigma_{(2)}$ | The 2nd order self-energy | fig. 6.4 |
| Σ_{sc} | The self-consistent 2nd order self-energy | fig. 6.7) |
| V_0 | Interaction constant in $V(x, x') = V_0\delta(x)\delta(x')$ | eq.(6.6) |
| T^* | The non-perturbative temperature scale | eq.(6.116) |
| $d(\omega)$ | The density of states for a quadratic band | eq.(6.64) |
| $W(\Delta k, q)$ | General non-momentum conserving interaction | eq.(6.103) |

Chapter 1

Introduction

1.1 Mesoscopic transport

From our everyday life, we all know examples of conductors such as the copper wires that provide power to our lamps, computers, etc. However, many do not imagine the fascinating range of phenomenon that occurs, when a conductor becomes smaller. This is studied within the field of mesoscopic transport, where the word mesoscopic refers to the size of the active component in the circuit, which is between the dimensions of the everyday macroscopic world and the microscopic world of atoms. One of the challenges of mesoscopic systems is that they are so small that we often cannot use the thermodynamic limit¹ used for macroscopic systems, and yet, so large that it is not feasible to describe them taking every atom into account. However, to perform a transport measurement on a mesoscopic system it has to be connected to the macroscopic world by contacts having well-defined thermodynamical properties such as temperature and chemical potential.

One of the interesting phenomenon that takes place on a mesoscopic scale is for a small, mesoscopic ring. Here the wave nature of the electrons shows up by making an interference pattern in the magnetoresistance. More precisely, the conductance is periodic in the magnetic field with a period of h/e . This experiment is very similar to the famous double-slit experiment and is called the Aharonov-Bohm effect [2, 3]. Another fascinating effect also due to the interference of the electrons in a mesoscopic conductor is the universal conductance fluctuations [4, 5, 6]. Here the shape and impurities in a mesoscopic conductor creates some random scattering and interference pattern in the sample, which in terms make a random variation of the conductance (e.g. as a function of magnetic field or cool down). The characteristic size of these conductance variations are e^2/h and does *not* dependent on the specific device.

¹This limit is that the number of particles and volume go to infinity while the density is constant [1].

Yet another fundamental effect originating in the wave nature of the electrons is the conductance quantization in units of $2e^2/h$. This quantization appears in various experimental systems like a string of gold atoms [7], cleaved edge overgrowth quantum wires [8]² or in quantum point contacts in a two-dimensional (2D) electron gas [9, 10]. The general features of the conductance quantization can be understood within the framework of non-interacting electrons as we shall see below [11]. The question under investigation in this thesis is:

How does the transport properties change due to electron-electron interaction in quantum point contacts?

We view a quantum point contact in two ways: As a short quantum wire and as a point-like region. In both cases, the system is perfectly connected to non-interacting leads. The main difference between the two viewpoints is that the electron-electron scattering can occur *without* momentum conservation for point-like regions in contrast to quantum wires.

In this thesis, only open systems are considered, i.e. systems that are very well contacted to the macroscopic reservoirs and thereby neglect the regime of poor contacts, where other interesting phenomenon occur such as Coulomb blockade and Kondo physics [12, 13, 14].

It is interesting to note that in all the examples mentioned above, fundamental constants appear as an essential part of the description. Of course, the details might depend slightly on other parameters as well, but it illuminates that mesoscopic transport is a fundamental and interesting part of science and not just the next natural step in the search for better and faster electronics!

For a general introduction to mesoscopic physics, see Imry [15], for quantum transport, see Beenakker [3] or Bruus and Flensberg [14, chap. 7 and 10], or for an overview including references, see Glazman [16].

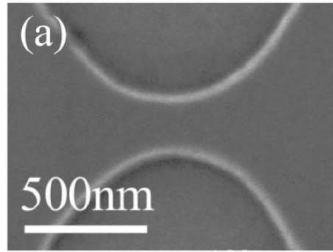
1.2 Quantum point contacts

One of the most studied and fundamental systems in mesoscopic physics is the quantum point contact (QPC). Generally, a QPC is a small connection between two reservoirs, where the width of the connection is comparable to the Fermi wavelength of the electrons (see [18] for a non-technical introduction). A QPC can, for instance, be made by an electrostatic gate on top of a 2D electron gas made in a semiconductor heterostructure, see figure 1.1(a). The gate depletes the underlying electron gas and thereby changes the width of the region, where the current has to pass through. It is the number of transverse modes (i.e. transverse quantum states³) that are energetically available for a given width of the QPC

²Note that for cleaved edge overgrowth wires the conductance is not quantized perfectly in steps of $2e^2/h$. However, it is still in steps, see ref. [8].

³Often other words like channel, level or 1D band are used instead of transverse mode.

QUANTUM POINT CONTACT



CONDUCTANCE QUANTIZATION

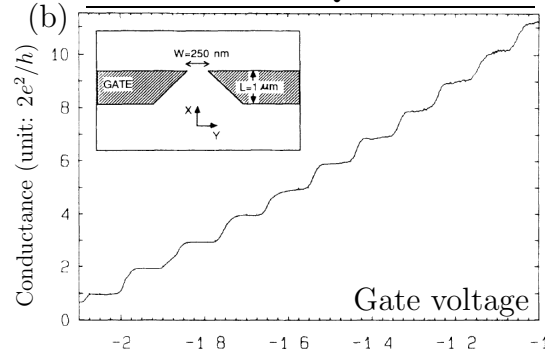


Figure 1.1: (a) A scanning electron microscope picture of a quantum point contact. The two parabola shaped objects are gates that deplete the underlying two-dimensional electron gas and thereby form the point contact. The picture is taken from A. Kristensen *et al.* [17], where further experimental details can be found. (b) One of the first experimental evidence by van Wees *et al.* [9] of the conductance quantization as a function of gate voltage. The temperature is $T = 0.6\text{K}$. The insert shows a schematic picture of their experimental setup (also taken from [9]). Despite the geometric difference between the inset and figure (a) both experiments ([9] and [17]) show the conductance steps.

that determines the conductance G , i.e.:

$$G = \frac{2e^2}{h} \times \text{Number of transverse modes.} \quad (1.1)$$

The number of transverse modes is equal to the number of half Fermi wavelengths one can fit into the width of the QPC. One of the two first experimental examples of conductance quantization in a QPC by van Wees *et al.* [9] is seen on figure 1.1(b), where steps of size $2e^2/h$ are seen as a function of the gate voltage (i.e. the width of the QPC). The factor of 2 in the conductance quantum $2e^2/h$ is a manifestation of spin degeneracy and vanish for a high magnetic field⁴ [19].

The quantized conductance value eq.(1.1) is actually the maximal conductance for any mesoscopic conductor for a given number of channels. To have an integer number of fully occupied transverse modes it is essential that the temperature is low, so there is no partly thermal occupation of higher transverse modes. Apart from the thermal smearing of the conductance quantization, it can also suffer from all sorts of other imperfections like poor contacts, scattering on the internal barrier created by the gates and so on. For a QPC to have perfectly smooth quantized conductance, the shape of the contacts to the leads need to be sufficiently smooth⁵. Sufficient smooth shape means that the curvature of the

⁴The field should be high enough to spin split the bands more than the temperature to see plateaus of size e^2/h .

⁵Otherwise reflection at the contacts and mode mixing can change conductance, e.g. an abrupt contact to the QPC will induce winks at the beginning of each conductance step [20].

boundary of the potential created by the gates should be larger than the width of the constriction [11]. If this is fulfilled, the contacts are connected to the point contact adiabatic, meaning that a propagating state from the contact can propagate through the QPC without being mix with other propagating modes.

The geometry of the QPC can differ as seen e.g. by comparing figure 1.1(a) and the inset of figure 1.1(b). However, as long as the smoothness criterion of the contacts is fulfilled the conductance quantization will appear. Despite the name, "point" contact, QPC's can have a finite length⁶ of order ~ 100 nm to $1 \mu\text{m}$ depending on the sample geometry. Therefore it could also be called a short clean quantum wire. Of course, the length should be compared to the Fermi wavelength, which in GaAs systems are roughly of order 40 nm [3]. Experimentally, there has been some reports on longer QPC's or short clean quantum wires up to $\sim 10 \mu\text{m}$ also fabricated by depleting some of a 2D electron gas by gates [21, 22, 23, 24]. They all show conductance quantization, but also some conductance decrease as a function of temperature. In this thesis, QPC's are modelled both as a finite length clean quantum wires and as point-like constrictions having in common that they are both adiabatically connected to the leads.

1.3 Thermopower

For a macroscopic conductor, a temperature gradient as well as a chemical potential gradient (i.e. a voltage drop) can drive an electric current. For a mesoscopic conductor, the situation is similar, except that often the conductor is too small to have a well-defined temperature gradient inside. This is indeed the case for a QPC. Therefore the electric current I_e is driven by a temperature difference ΔT and/or a chemical potential difference $\Delta\mu = eV$ between the contacts of the conductor. The current in the linear transport regime is

$$I_e = GV + G_T\Delta T, \quad (1.2)$$

where G is the conductance and G_T is the thermoelectric coefficient. The current is taken positive, if the electric charge is transported from left to right.

To get information about the thermoelectric coefficient G_T in an actual experiment, one considers the amount of voltage it takes to cancel a current produced by a temperature difference. This leads to the introduction of the thermopower S as

$$I_e = GV + G_T\Delta T = 0 \quad \Rightarrow \quad S \equiv - \lim_{\Delta T \rightarrow 0} \frac{V}{\Delta T} \Big|_{I_e=0} = \frac{G_T}{G}, \quad (1.3)$$

⁶However, it might look like QPC's are really point-like on the scanning electron microscopy picture, e.g. figure 1.1(a). However, one should be careful to measure the length from the SEM picture, because the electrostatic shape of the QPC in the 2D electron gas due to the gates might be different than the one seen.

which is the experimental relevant quantity to model. The thermopower is sometimes referred to as the Seebeck coefficient. Note that, as for macroscopic conductors, a related subject is to study the heat current, however, this is not the subject of the present thesis⁷.

For a QPC, the thermopower turns out to have a peak every time the conductance changes from one plateau to the next and at the conductance plateau the thermopower goes to zero, see figure 1.3. The first thermopower measurements on QPC's were made by L. W. Molenkamp *et al.* [30, 28, 26]. Experimentally, the different temperatures of each side of the QPC are obtained e.g. by a current through only one of the contacts to heat it up. An application of the thermopower of a QPC is as a thermometer for a 2D electron gas [31].

1.4 The Landauer formula

A general way to describe transport phenomenon in coherent mesoscopic conductors for non-interacting electrons is by the famous *Landauer formula*. In the case of conductance, it states that the zero-temperature conductance is simply given by the quantum mechanical transmission probability to pass through the mesoscopic conductor. For an electric current at non-zero temperature in a two lead setup the Landauer formula is ($e > 0$)

$$I_e = \frac{2(-e)}{h} \int dE \mathcal{T}(E) [f_L^0(E) - f_R^0(E)], \quad (1.4)$$

where the integral is integrated over all available energies E , $\mathcal{T}(E)$ is the transmission and $f_i^0(E)$ is the Fermi function for the right ($i = R$) or left ($i = L$) lead, i.e.

$$f_i^0(E) = \frac{1}{1 + \exp[(E - \mu_i)/k_B T_i]}. \quad (1.5)$$

Here T_i and μ_i are the temperature and chemical potential of the left/right lead, respectively. The Landauer formula is very general and is a part of a general scattering approach to quantum transport in mesoscopic systems often referred to as the *Landauer-Büttiker formalism*. It was pioneered by R. Landauer [32], M. Büttiker [33] and Y. Imry [34, 15, 35]. In the Landauer formula, the current is fully coherent and the transmission $\mathcal{T}(E)$ can be given in terms of the quantum mechanical transmission amplitude matrix $\mathbf{t}(E)$ as

$$\mathcal{T}(E) = \text{Tr}[\mathbf{t}^\dagger(E)\mathbf{t}(E)]. \quad (1.6)$$

⁷A heat current I_Q can also be driven by a voltage and/or a temperature difference, i.e. $I_Q = MV + K\Delta T$, where time-reversal symmetry leads to $M \propto G_T$. The heat current can be carried both by phonons and electrons in macroscopic solids as well as in the mesoscopic regime. For further discussion see e.g. [1, 25, 26, 27, 28, 29], where [26, 28] focuses on non-interacting electrons in QPC's including measurements on the thermal conductance K and [29] has more refined measurements of K in QPC's.

A generalization of eq.(1.4) to more than two leads is very intuitive [33]. See e.g. the book [14, chap.7] for a detailed introduction to the Landauer-Büttiker formalism.

In the linear response regime the Landauer formula eq.(1.4) gives the conductance G , thermoelectric coefficient G_T and thermopower S in terms of the transmission. Due to the linear response the Fermi functions $f_{R/L}^0(E)$ are expanded around the equilibrium chemical potential μ and temperature T as

$$f_i^0(E) \simeq f^0(E) - \partial_E f^0(E)(\mu_i - \mu) - \partial_E f^0(E)(E - \mu) \frac{T_i - T}{T} \quad (1.7)$$

valid for a small bias $V = (\mu_L - \mu_R)/(-e)$ and temperature difference⁸ $\Delta T = T_R - T_L$, i.e. $|eV| \ll \mu$ and $|\Delta T| \ll T$. Here $f^0(E)$ is the equilibrium Fermi function with chemical potential μ and temperature T . Inserting this into the Landauer formula the linear transport coefficients become [36]

$$G(\mu, T) = \frac{2e^2}{h} \int dE \mathcal{T}(E) [-\partial_E f^0(E)], \quad (1.8)$$

$$G_T(\mu, T) = \frac{2ek_B}{h} \int dE \mathcal{T}(E) \left(\frac{E - \mu}{k_B T} \right) [-\partial_E f^0(E)], \quad (1.9)$$

$$S(\mu, T) = \frac{k_B}{e} \frac{\int dE \mathcal{T}(E) \left(\frac{E - \mu}{k_B T} \right) [-\partial_E f^0(E)]}{\int dE \mathcal{T}(E) [-\partial_E f^0(E)]}. \quad (1.10)$$

Note that the natural unit becomes e^2/h for conductance and k_B/e for thermopower. It immediately follows that for zero temperature we have

$$S(\mu, T = 0) = 0 \quad \text{and} \quad G(\mu, T = 0) = \frac{2e^2}{h} \mathcal{T}(\mu), \quad (1.11)$$

i.e. conductance is the transmission, and the thermopower is zero.

1.4.1 Dissipation for a clean 1D system perfectly connected to the leads?

Historically, it was a dilemma how a 1D wire with perfect transmission (i.e. integer) and no impurities could have a finite conductance (see also subsection 1.4.2, p. 7) [34, 18].

An important point of the Landauer formula is that for a fully open QPC (integer transmission) the dissipation *does not happen in the QPC*, but in the reservoirs. The dissipation can be thought to happen in the following way: Consider an electron passing from the left to the right reservoir. It will leave the QPC

⁸Note that V and ΔT is defined such that $V > 0$ and/or $\Delta T > 0$ leads to $I_e > 0$ for non-interacting electrons.

being in thermal equilibrium with the left reservoir, however, now belonging to the right reservoir. Therefore it will now equilibrate with the right reservoir and thereby the dissipation happens here. This is how the contacts leads to a finite conductance for a perfectly open QPC with no impurities.

Physically, the equilibration in the leads is due to different relaxation processes and mainly electron-electron interactions at low temperatures, since the leads are two or three dimensional.

But what if such relaxation processes like interactions are also present in the one-dimensional constriction? This is investigated further in chapter 3.

1.4.2 A historic note on the Landauer formula

The original Landauer formula [32] for conductance is $G_b = \frac{2e^2}{h} \frac{\mathcal{T}(\mu)}{1-\mathcal{T}(\mu)}$, which *only* describes the conductance of the barrier, which the electrons are transported through (for a single channel, $0 \leq \mathcal{T}(\mu) \leq 1$). The modern version, $G = \frac{2e^2}{h} \mathcal{T}(\mu)$ cited here, is the conductance of the barrier *and* the perfect leads. This can be understood as an addition of resistors in series $G^{-1} = G_b^{-1} + G_c^{-1}$, where the resistance of the two perfect leads are $G_c^{-1} = \frac{h}{2e^2}$ [34]. This interpretation have been confirmed by measurements on cleave edge overgrowth wires, where the resistance of the inner barrier G_b^{-1} was found to be zero for unity transmission in a four terminal measurement [37, 38]. For a historical review including reference and a linear response calculation of the Landauer formula see Stone and Szafer [39] or Beenakker [3, sec. III.A.2] for a shorter version.

1.5 Non-interacting current through a quantum point contact

Next, we take a closer look at how to understand a QPC within the theory of non-interacting electrons and use this to calculate the current through the QPC using the Landauer formula. This is only meant to illuminate some of the important points in the analysis and not to be a detailed review (for details see either [11] or one of the books [14, sec. 7.3] or [40, sec. 2.4]).

The single-particle Schrödinger equation for an electron in the 2D electron gas confined by the electrostatic potential from the gate $V_{\text{gate}}(x, y)$ is

$$\left[-\frac{\hbar^2}{2m}(\partial_x^2 + \partial_y^2) + V_{\text{gate}}(x, y) \right] \psi(x, y) = E\psi(x, y), \quad (1.12)$$

where $\psi(x, y)$ is the 2D eigenstate, E is the energy and m is the effective mass. Here x is along the QPC and y is perpendicular to it, see figure 1.2. For each value of x , it is possible to expand the wave function on a complete set of eigenfunctions $\{\varphi_{nx}(y)\}$ in transverse y -direction, i.e. $\psi(x, y) = \sum_n \varphi_{nx}(y)\phi_n(x)$, where $\phi_n(x)$

are the expansion coefficients. If the curvature of the shape of the potential is small compared to the width of the constriction [11], then the two-dimensional Schrödinger equation reduces to a one-dimensional equation of the form:

$$\left[-\frac{\hbar^2}{2m} \partial_x^2 + \varepsilon_n(x) \right] \phi_n(x) \simeq E \phi_n(x), \quad (1.13)$$

where $\varepsilon_n(x)$ is the transverse quantization energy and depends on the specific model of the confining potential⁹. For any model, this is a 1D Schrödinger equation describing scattering of a potential barrier of the form $\varepsilon_n(x)$ (since it goes to zero for $x \rightarrow \pm\infty$). Therefore the transmission and reflection of the barrier can be calculated (e.g. in the WKB approximation) and then related to fully coherent current through the barrier by the Landauer formula.

In eq.(1.13) the index n can be interpreted as the mode number. The narrowest point of the QPC is $x = 0$, so $\varepsilon_n(0)$ is the maximum of $\varepsilon_n(x)$. For a given energy E (and neglecting tunnelling), we have perfect transmission through all the modes with $\varepsilon_n(0) < E$ and no transmission through the modes with $\varepsilon_n(0) > E$. Therefore at zero temperature, we have an integer number of conducting modes. By changing the gate voltage the width (and depth) of the QPC changes and thereby $\varepsilon_n(0)$ and in terms the number of fully transmitting modes. This leads to the conductance quantization as a function of gate voltage. However, it is not obvious that each mode contributes $2e^2/h$ to the conductance and this fact originates in the one dimensionality of the channel (as we shall see in section 1.6).

1.5.1 The saddle-point model of a quantum point contact

To understand the QPC better, we consider a specific model of the gate potential. It is the so-called saddle-point model [41], where $V_{\text{gate}}(x, y)$ is expanded around the middle of the constriction $x = y = 0$ assumed to be a saddle-point (see figure 1.2(b)), i.e.

$$V_{\text{gate}}(x, y) = \frac{1}{2} m \omega_y^2 y^2 - \frac{1}{2} m \omega_x^2 x^2 + V_0 \quad (1.14)$$

where V_0 is the height of the saddle-point and ω_y, ω_x parameters describing the form of the QPC. In the transverse direction y , this is a harmonic oscillator so the transverse quantization energy is $\varepsilon_n(x) = \hbar \omega_y (n + \frac{1}{2}) - \frac{1}{2} m \omega_x^2 x^2$, where the value of ω_y depends on the width of the QPC. For the saddle-point model, it is possible to show that there is no mode mixing and that the transmission through the n^{th} mode is [42, 43]:

$$\mathcal{T}_n(E) = \frac{1}{1 + \exp \left[-2\pi (E - \hbar \omega_y (n + \frac{1}{2}) - V_0) / \hbar \omega_x \right]}. \quad (1.15)$$

⁹In general, it should satisfy the equation: $\left[-\frac{\hbar^2}{2m} \partial_y^2 + V_{\text{gate}}(x, y) \right] \varphi_{nx}(y) = \varepsilon_n(x) \varphi_{nx}(y)$. If a hard wall potential is chosen, then $\varepsilon_n(x) = \pi^2 \hbar^2 / (2m d(x)^2)$, where $d(x)$ is the width of the constriction (varying slowly compared to its minimum value [11]).

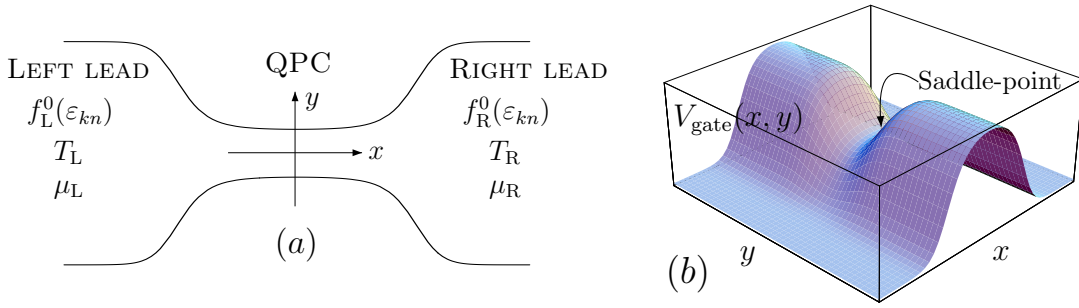


Figure 1.2: (a) A schematic top view of a QPC. The left and right reservoirs are in equilibrium with their own temperature $T_{R/L}$ and chemical potential $\mu_{R/L}$. The shape of the QPC is seen to be smooth compared to the width of the QPC. (b) An illustration of the possible form of the electrostatic potential the gate induced in the two-dimensional electron gas. The formation of a quantum point contact is clearly seen. The saddle-point in the middle of the QPC is the bottleneck of electronic transport through the QPC. The saddle-point model [41] eq.(1.14) only uses the quadratic terms of the potential in an expansion around the middle of the QPC.

To get the full transmission $\mathcal{T}(E)$ one simply has to sum over all modes, i.e.

$$\mathcal{T}(E) = \sum_n \mathcal{T}_n(E). \quad (1.16)$$

The next step is to insert this into the conductance eq.(1.8) and thermopower eq.(1.10). The integrals can easily be done numerically and the result is seen on figure 1.3(left).

The experimental results are G and S as a function of gate voltage V_g whereas the theoretical results are G and S as a function of the chemical potential μ . Varying the gate voltage the potential landscape $V_{\text{gate}}(x, y)$ varies and therefore in principle also the parameters ω_x and ω_y of the model. However, roughly speaking one can argue that the gate voltage and chemical potential are linear dependent, $\mu \propto V_g + \text{constant}$, for an open contact. However, to make qualitative statements the electrostatic problem has to be investigated in detail [44, 45].

The smearing of the conductance steps are due to temperature $k_B T$ and the curvature across the barrier $\hbar\omega_x$. Note that the smaller the curvature of the barrier in the x -direction, $\hbar\omega_x$, the longer the QPC, so in the saddle-point model longer QPC's should have sharper conductance steps. For the thermopower, the peaks are broadened by $k_B T$ and $\hbar\omega_x$, respectively. The parameter $\hbar\omega_y$ is the confinement in the transverse direction and gives the length of the conductance steps (and the thermopower valleys).

Taboryski *et al.* fit their experimental data to the saddle-point model for two different AlGaAs/GaAs samples. They find the parameters $\hbar\omega_y = 0.90\text{meV}$ and $\hbar\omega_x = 0.35\text{meV}$ (i.e. $\omega_y/\omega_x \simeq 2.6$) and $\hbar\omega_y = 0.9\text{meV}$ and $\hbar\omega_x = 0.35\text{meV}$ (i.e. $\omega_y/\omega_x \simeq 3.0$), respectively¹⁰ [47]. The ratio ω_y/ω_x of about 3 is widely

¹⁰Remembering that $1\text{K}=0.086\text{meV}$.

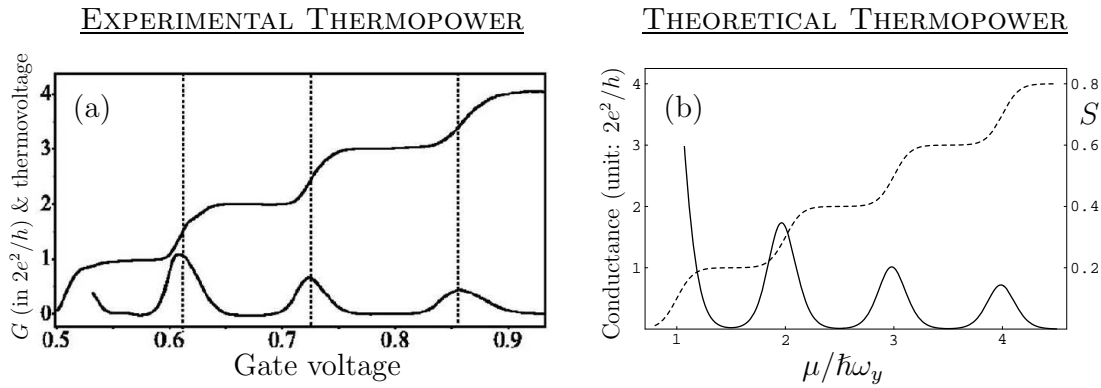


Figure 1.3: (a) Experimental measurement of the thermopower and conductance of a QPC at $T = 4.2\text{K}$ measured by Proskuryakov *et al.* [46]. The thermopower has a peaks between the conductance plateaus and is zero on the plateaus. To be precise, it is the thermovoltage which is measured and shown (in arbitrary units), since the method of heating the reservoir by a current does not allow for an easy measurement of the temperature difference. The definition of the thermovoltage V_{th} is: the voltage required to stop a current produced by an (unknown) temperature difference ΔT , i.e. $V_{\text{th}} = (G_T/G)\Delta T$ from eq.(1.3). (b) The conductance (dashed) and thermopower in the saddle point model as a function of the chemical potential μ (in units of $\hbar\omega_y$). The parameters are: $V_0 = -1/2$, $k_B T = 0.05$ and $\hbar\omega_x/(2\pi) = 0.05$ both in units of $\hbar\omega_y$. The resemblance to the experimental results is striking. In experiments, the ratio ω_y/ω_x is about 3 [47].

spread in the literature as being realistic (including the original saddle-point model article [41] by Büttiker).

1.5.2 Analytic results for an ideal quantum point contact

If the barrier of the QPC in the x -direction is absent the point contact is ideally connected to the leads. This means that $\omega_x = 0$ and (for a quadratic transverse confinement potential) the transmission eq.(1.15) becomes a step-function¹¹

$$\mathcal{T}(E) = \sum_{n=1}^{\infty} \theta(E - n\hbar\omega_y), \quad (1.17)$$

which allows us to get analytic results for the conductance and thermopower [36, 26] as we shall see now.

¹¹For simplicity we choose $V_0 = -\hbar\omega_y/2$.

The conductance becomes¹²

$$\begin{aligned} G(\mu, T) &= \frac{2e^2}{h} \int_0^\infty dE \sum_{n=1}^\infty \theta(E - n\hbar\omega_y) [-\partial_E f^0(E)] \\ &= \frac{2e^2}{h} \sum_{n=1}^\infty \int_{n\hbar\omega_y}^\infty dE [-\partial_E f^0(E)] = \frac{2e^2}{h} \sum_{n=1}^\infty \frac{1}{1 + \exp\left(\frac{n\hbar\omega_y - \mu}{k_B T}\right)}, \end{aligned} \quad (1.18)$$

where it is clear that temperature smears the conductance steps. Note that in the high temperature limit, $k_B T \rightarrow \infty$, we have $\exp[(n\hbar\omega_y - \mu)/k_B T] \rightarrow 1$, so e.g. the conductance for a single channel goes to e^2/h . However, for $k_B T \sim \hbar\omega_y$ the conductance steps are smeared to a straight line.

The thermoelectric coefficient eq.(1.9) (defined in eq.(1.2)) is

$$\begin{aligned} G_T(\mu, T) &= \frac{2e^2}{h} \frac{k_B}{e} \int_0^\infty dE \mathcal{T}(E) \left(\frac{E - \mu}{k_B T} \right) [-\partial_E f^0(E)] \\ &= \frac{2e^2}{h} \frac{k_B}{e} \sum_{n=1}^\infty \int_{n\hbar\omega_y}^\infty dE \left(\frac{E - \mu}{k_B T} \right) \frac{1/k_B T}{4 \cosh^2\left(\frac{E - \mu}{2k_B T}\right)} \\ &= \frac{2e^2}{h} \frac{k_B}{e} \sum_{n=1}^\infty \left[\ln(1 + e^{\Delta_n}) - \frac{\Delta_n}{1 + e^{-\Delta_n}} \right], \end{aligned} \quad (1.19)$$

where $\Delta_n = (n\hbar\omega_y - \mu)/k_B T$. The function in the square bracket is even in Δ_n and maximal for $\Delta_n = 0$. Therefore G_T has a peak (of width $\sim k_B T$) every time $\mu = n\hbar\omega$ as expected. Note that

$$\ln(1 + e^{\Delta_n}) - \frac{\Delta_n}{1 + e^{-\Delta_n}} = \begin{cases} \ln 2 & \text{for } \frac{|n\hbar\omega_y - \mu|}{k_B T} = 0 \\ \frac{|n\hbar\omega_y - \mu|}{k_B T} \exp\left[-\frac{|n\hbar\omega_y - \mu|}{k_B T}\right] & \text{for } \frac{|n\hbar\omega_y - \mu|}{k_B T} \gg 1 \end{cases}, \quad (1.20)$$

so away from the peak the thermopower $S = G_T/G$ is exponentially suppressed in temperature and the peak height of the thermoelectric coefficient is $G_T^{\max} = \frac{2ek_B}{h} \ln 2$. Therefore at $\mu = n\hbar\omega_y$ the thermopower is $S = \frac{k_B}{e} \frac{\ln 2}{n - \frac{1}{2}}$, where n is the number of the mode that came into the energy window¹³ ($G = \frac{2e^2}{h}(n - 1/2)$).

The exponential suppression in temperature of the thermopower at the conductance plateau is not specific for this model. If the temperature is much lower than the variation of the transmission at $\varepsilon = \mu$, then the exponential suppression¹⁴ follows from eq.(1.10).

¹²The integration over energy is from 0 to ∞ , since the model is a free-electron model in the x -direction and therefore has a quadratic dispersion.

¹³Note that the peaks of S are slightly shifted compared to those of G_T due to the $1/G$ factor. For $n = 1$ the S has no peak (since $G \rightarrow 0$), but G_T does.

¹⁴To be precise, we should also assume that the Fermi level is not symmetrically placed between the band edges, because in this special case we would get exactly zero for a symmetric transmission.

1.6 The secret behind the Landauer formula

One of the secrets behind the Landauer formula is that the density of states and the velocity cancel each other in one dimension. This is the reason why every conducting mode contributes equally to the current in the Landauer formula.

To illustrate this cancellation, we consider the case of a QPC with a single fully open channel (i.e. $\mathcal{T}(E) = 1$). The electric current I_e is determent by the distribution function $f_k^{(0)}$ by ($e > 0$)

$$I_e = \frac{(-e)}{\mathcal{L}} \sum_{k\sigma} v_k f_k^{(0)}, \quad (1.21)$$

where k is the 1D wave vector, \mathcal{L} the normalization length¹⁵ and v_k the velocity given by [1, Appendix E]

$$v_k = \frac{1}{\hbar} \frac{d\varepsilon_k}{dk}, \quad (1.22)$$

where ε_k is the 1D dispersion relation along the QPC. The distribution function in the QPC $f_k^{(0)}$ is simply given by the lead from which the electrons originate:

$$f_k^{(0)} = \begin{cases} f_L^0(\varepsilon_k) & \text{for } k > 0, \\ f_R^0(\varepsilon_k) & \text{for } k < 0, \end{cases} \quad (1.23)$$

i.e. the right movers ($k > 0$) originates from the left lead and therefore is in equilibrium with this electronic reservoir, so if the reservoir is non-interacting the distribution function is the Fermi function $f_L^0(\varepsilon_k)$, eq.(1.5). (Note that $f_k^{(0)}$ changes if interactions, phonons, etc. are present, noted with the superscript (0)). Therefore the current is¹⁶:

$$\begin{aligned} I_e &= (-e) \sum_{\sigma} \int_{-\infty}^{\infty} \frac{dk}{2\pi} v_k f_k^{(0)} = 2(-e) \int_0^{\infty} \frac{dk}{2\pi} v_k [f_L^0(\varepsilon_k) - f_R^0(\varepsilon_k)] \quad (1.24) \\ &= \frac{2(-e)}{2\pi} \int_{D_l}^{D_u} d\varepsilon \underbrace{\frac{v_k}{\frac{d\varepsilon_k}{dk}}}_{(\star)} [f_L^0(\varepsilon_k) - f_R^0(\varepsilon_k)] = \frac{2(-e)}{h} \int_{D_l}^{D_u} d\varepsilon [f_L^0(\varepsilon) - f_R^0(\varepsilon)], \end{aligned}$$

where the cancellation of the velocity and density of states (\star) happened regardless of the dispersion relation ε_k . This is unique for 1D systems and is the foundation of why the Landauer formula works.

In this thesis, we will see that this cancellation also happens in the case of the interaction correction to the current. This leads to the conclusion that the electron-electron interactions only change the particle current if they change the number of left and right movers. This unique conclusion is really mesoscopic in the sense that it is not true for infinite 1D wires or bulk systems, where a velocity change due to the interaction can be enough to change the current.

¹⁵One can imagine the QPC in a long box in the x -direction of length \mathcal{L} .

¹⁶The long wire limit ($\mathcal{L} \rightarrow \infty$) is used, so $\sum_k(\dots) = \frac{\mathcal{L}}{2\pi} \int dk(\dots)$

1.7 Thermopower and electron-hole asymmetry

Often it is claimed that the thermopower of some system is a measure of the electron-hole asymmetry. The mathematical origin can often be traced back to a thermopower of the form

$$S \propto \int dE d(E) \underbrace{(E - \mu)[- \partial_E f^0(E)]}_{\text{odd function around } \mu} \mathcal{F}(E), \quad (1.25)$$

where $d(E)$ is the density of states and $\mathcal{F}(E)$ is some function. The factor $(E - \mu)$ is the essential ingredient (normally not present for conductance), since $(E - \mu)[- \partial_E f^0(E)]$ is an odd function of E around μ . Therefore the integral is zero (or exponentially small in temperature), if the density of states $d(E)$ or the function $\mathcal{F}(E)$ do not vary around μ on the scale of the temperature $k_B T$. The density of states contains information about the electron-hole asymmetry of the dispersion relation and therefore the connection between electron-hole symmetry and thermopower. However, in general one needs to be careful before making claims from the thermopower [1, p.258].

However, in the case of a QPC the density of state leaves the problem as we saw in eq.(1.24) and so does the dependence on dispersion relation. (For non-interacting electrons only the maximum D_u and minimum energy D_l of the dispersion can affect the current via the limits of the integral in the Landauer formula eq.(1.4)). Therefore in a QPC the (non-interacting) thermopower is *not* a measure of the electron-hole asymmetry of the dispersion. Rather for non-interacting electrons, it is a measure of the asymmetry of the transmission, since the factor $(E - \mu)$ is still present as seen in eq.(1.10).

1.8 A first look at electronic interactions in quantum point contacts

There is in general no a priori reason to believe that the electron-electron interaction should be absent nor weak inside a QPC, since the constricted region of a QPC is essentially one-dimensional. Despite this fact, we saw that the main features of the experimental observations can be explained by non-interacting Landauer-Büttiker theory. An important point of the description of a QPC is that the *contacts play an essential role* in the physics. Therefore a QPC should not be thought of as an (infinitely long clean) one-dimensional electron gas. This is still true, when the interactions are considered.

Let us first consider the phase space in 1D for pair electron-electron interactions in a single mode. Assume that the interaction conserves energy ε_k and

momentum,

$$\varepsilon_{k_1} + \varepsilon_{k_2} = \varepsilon_{k_{1'}} + \varepsilon_{k_{2'}}, \quad (1.26)$$

$$k_1 + k_2 = k_{1'} + k_{2'}, \quad (1.27)$$

where k_i [$k_{i'}$] denote the (quasi-)momentum before [after] the scattering event. These constrictions only leave two possible solutions: $(k_1, k_2) = (k_{1'}, k_{2'})$ or the exchange solution $(k_1, k_2) = (k_{2'}, k_{1'})$. In either case the electron-electron interaction cannot redistribute the electrons in the system. The solution is easily found in the case of a quadratic dispersion, $\varepsilon_k \propto k^2$, but is generally true for any dispersion with positive¹⁷ curvature.

The situation changes in the case of more than a single mode, if inter-mode scattering is considered. Such inter-mode scattering processes do have sufficient phase space and some of them turn out to change the current as we will see in chapter 4.

Infinitely long 1D electron gases

For an *infinitely long* one-dimensional electron gas the Fermi liquid theory breaks down in the sense that the lifetime of the quasi-particles does not become small compared to the excitation energy itself [14, p.352]. Therefore the elementary excitations of a 1D electron gas are not quasi-particle-like excitations and therefore, strictly speaking, the concept of quasi-particles does not make sense in this situation. Instead one introduces the concept of a Luttinger liquid [48]¹⁸, where the low-energy elementary excitations are collective oscillations of the density¹⁹ called plasmons.

The Luttinger model [49, 50] is a model for the Luttinger liquid describing the low-energy physics of an infinite clean 1D fermion gas. By using a linear dispersion, $\varepsilon_{k,s=\pm 1} = s\hbar v_F k$, the Luttinger model can be manipulated to a quadratic form and thereby the eigenenergies can be found²⁰. To do this, one cannot include all the possible kinds of scattering processes, but the ones that cannot be included, can be shown to be unimportant at low energies by Renormalization-group methods [14]. The assumption of linear bands in the Luttinger model is essential to solve the model exactly and makes it particle-hole symmetric. Furthermore, without linearized bands the model can no longer be solved exactly

¹⁷Note that in the special case of a linear dispersion, $\varepsilon_{k,s=\pm 1} = s\hbar v_F k$, this is no longer true. However, the pair interaction still cannot redistribute the electron among left and right movers.

¹⁸Note that the original paper by Haldane Ref.[48] is an excellent and readable paper on the subject, even for a beginner.

¹⁹Note that one of the special features of a Luttinger Liquid is that the spin density waves and charge density waves propagate independently, a phenomenon without counterparts in higher dimensions known as spin-charge separation.

²⁰This manipulation requires a special analytical form of the interaction. Often this form is taken to be different constants for different scattering processes.

and it turns out that the physics might change substantially, see e.g. [51]. Another limitation of the Luttinger liquid is that low temperature (compared to the interaction) is needed.

A central parameter in the Luttinger model is the g parameter, which is one ($g = 1$) for non-interacting electrons, less than one ($g < 1$) for repulsive interactions and greater than one ($g > 1$) for attractive interactions. The specific form of g depends on the included interaction processes²¹. The charge density wave excitations have the velocity renormalized by g to be $\tilde{v} = v_F/g$ and their energy is $\omega_q = q\tilde{v}$. Furthermore, it is found that for an infinite Luttinger model the interactions also renormalize the conductance for a single mode to be [52]:

$$G = g \frac{2e^2}{h}, \quad (L = \infty). \quad (1.28)$$

To show this, more of the formalism for the Luttinger model is needed. For more information in this fascinating subject, see e.g. one of the books [53] or [14, chap.19] or the review on transport in (spinless) Luttinger liquids [52].

Finite Luttinger liquids

The next question that naturally arises in the context of QPC's is: What happens for a *finite* Luttinger liquid, i.e. including the effect of the leads? For the conductance, the answer is the striking reappearance of the conductance quantum [54, 55, 56, 57]:

$$G = \frac{2e^2}{h}, \quad (L < \infty). \quad (1.29)$$

To show this, Maslov and Stone used a x -dependent g , setting it equal to the non-interacting value one in the leads. Kane and Fisher noted it via the ac conductance crossover²² from $g \frac{2e^2}{h}$ to $\frac{2e^2}{h}$ at the frequencies lower than $\omega_c = v_F/L$. The result is for a Luttinger liquid without any impurities or non-momentum conserving backscattering terms in the interaction (such as e.g. Umklap terms).

Next we make a rough estimate of the length, where Luttinger liquid physics is no longer relevant for QPC's. The length of the QPC, where Luttinger liquid theory is *not* important is given by comparing the smallest possible plasmon

²¹For a spinless Luttinger model, including inter and intra band processes the g parameter is [14, p.362]: $g = [1 + (V_{q=0} - V_{q=2k_F})/\pi v_F]^{-1/2}$, where V_q is the 1D Fourier transformed Coulomb interaction cut off e.g. by the width of the wire.

²²The dc conductance is the $\omega \rightarrow 0$ part of the frequency dependent ac conductance. Therefore this statement might seem contradictory to eq.(1.28), where the limit $\omega \rightarrow 0$ was taken. However, in calculating the conductance it is important, if one takes the $q \rightarrow 0$ limit or $\omega \rightarrow 0$ limit first, since it gives different results and applies to different physical situations, see e.g. [55][14, p.286].

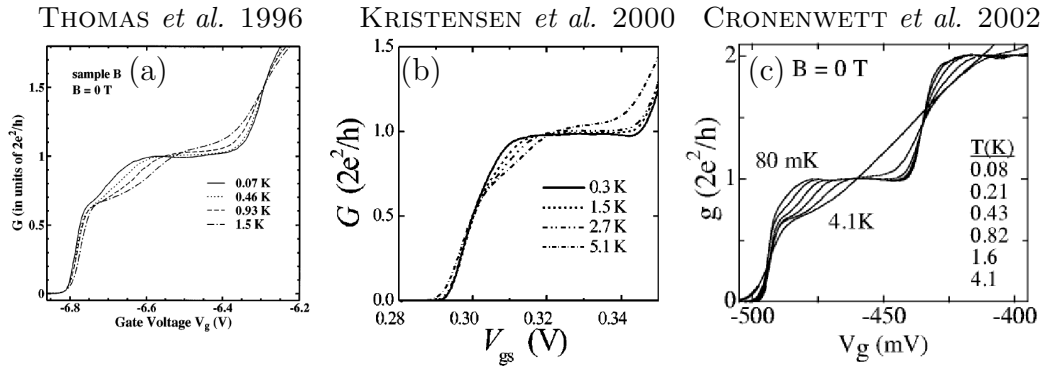


Figure 1.4: The experimental data of the linear conductance as a function of gate voltage for three different experiments (a) Thomas *et al* [58], (b) Kristensen *et al* [17] and (c) Cronenwett *et al.* [59]. All the experiments show a reduced conductance when the temperature is increased in the beginning of the first quantized conductance plateau. In the beginning of the first conductance step the electron density is low in the QPC.

energy $(\hbar v_F/g)\frac{2\pi}{L}$ to the available thermal energy $k_B T$:

$$k_B T < \frac{\hbar v_F}{g} \frac{2\pi}{L}, \quad \Rightarrow \quad L < \frac{\hbar v_F}{g k_B T}, \quad (\text{Luttinger physics not relevant}) \quad (1.30)$$

so for short QPC's or low temperatures the Luttinger liquid state is not reached. However, a better estimate of the length could consider, when the Luttinger liquid ground state of the system is really gone and it might be bigger, since the contacts destroy the Luttinger liquid state.

1.9 The 0.7 anomaly in quantum point contacts

All the main experimental features of QPC's can be explained within the non-interacting Landauer-Büttiker theory. However, in the beginning of the first conductance plateau there is a shoulder-like feature, which cannot be explained within this framework, see figure 1.4. It is often refereed to as *the 0.7 anomaly* or the 0.7 structure in lack of a better name, since it is a reduction of the conductance to something like $0.7 \times 2e^2/h$, however, the magnitude varies depending on the sample. Below we outline several important experimental features of the 0.7 anomaly and some of the available explanations. An explanation should be able to explain all the experimental features consistently. It seems like there is no generally accepted explanation of the 0.7 anomaly, even though the first experiments were done more than a decade ago [58, 60]²³. However, there is an overall consensus that it is somehow related to the spin degree of freedom.

²³Note that the first systematic study including temperature and magnetic field dependencies was properly by Thomas *et al.* [58], but the effect is also clearly seen in the data by van Wees *et al.* [60] (see figure 6 in the paper).

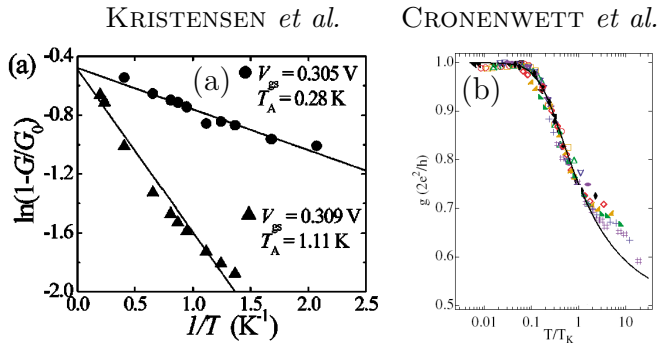


Figure 1.5: Experimental data of the conductance reduction as a function of temperature at the 0.7 anomaly. The data by (a) Kristensen *et al.* [17] and (b) Cronenwett *et al.* [59] show essentially the same feature: The conductance is reduced from $2e^2/h$ at low temperatures to $\sim e^2/h$ at higher temperatures (see the text for details).

1.9.1 Experimental features of the 0.7 anomaly

There have been numerous experimental studies of the 0.7 anomaly. Here we list some of the important features without calving to review the effect.

The conductance versus gate voltage and temperature

In figure 1.4, we see three different experimental studies [58, 17, 59] all showing the same feature: In the beginning of the first quantized plateau there is a conductance reduction at elevated temperatures. At the lowest possible temperature, there is no anomaly and the data looks like the Landauer result (see figure 1.3), but at higher temperatures the conductance reduces from $2e^2/h$ to something like $0.7 \times 2e^2/h$ depending on gate voltage. In some experiments like Cronenwett *et al.* [59] 1.4(c), the anomaly looks like a 0.7 *plateau*, but in many others it is more a shoulder-like feature e.g. Kristensen *et al.* [17] in figure 1.4(b).

The gate voltage is a measure of the density of electrons in the QPC, i.e. near pinch off the contact the density is low. Therefore the density is low near the 0.7 anomaly. If the electron density becomes smaller the anomaly have been reported to become more pronounced [61].

A detailed study of the temperature dependence of the conductance anomaly has also done by Cronenwett *et al.* [59] and Kristensen *et al.* [17] and it is seen in figure 1.5. They essentially find the same feature: The conductance in the beginning of the first plateau goes from $2e^2/h$ at low temperature to about e^2/h at higher temperatures. However, the two papers use different models to fit the data. In Kristensen *et al.* a activated temperature behavior is used of the form

$$G(T) = 1 - C \exp(-T_A/T), \quad (1.31)$$

where C and T_A are fitted to the data for different gate voltages V_g (and they find that $T_A \sim V_g^2$). The solid lines in figure 1.5(a) are the fit to this form and we note that at $1/T = 0$ the fit approach $\ln[1 - G/(2e^2/h)] \simeq 0.5$ so the conductance

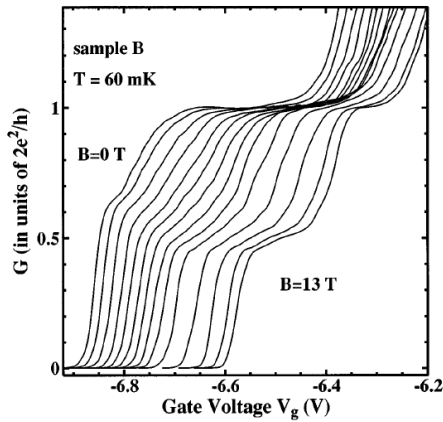


Figure 1.6: Experimental data of the 0.7 anomaly for an in-plane magnetic field increased from 0 T to 13 T. As the field is increased the 0.7 anomaly gradually becomes a plateau at e^2/h . Therefore the anomaly disappears in a high magnetic field, since the quantized plateau e^2/h is in agreement with the Landauer formula. The curves are slightly off set for clarity. The data is from Thomas *et al.* [58] and other experiments obtain similar results.

approaches $G \sim 0.4(2e^2/h)$ at high temperature²⁴. In Cronenwett *et al.* they can also fit their data to the above form (see their ref. [25]), but they chose to fit it to another form inspired by Kondo-physics (see below). Therefore they have a single fit parameter T_K (the Kondo temperature) and each gate voltage has its own T_K . In the end, they scale all their data onto a single curve by making a plot of G versus T/T_K , which is seen in figure 1.5(b). Note that their T/T_K axis is logarithmic. Further studies of the temperature dependence include [62, 63].

Note that in Kristensen *et al.* [17] the geometric and lithographic details of the QPC's in the GaAs/AlGaAs heterostructures were also investigated in detail. It is found that these details do not change the 0.7 feature substantially.

The magnetic field dependence

The magnetic field dependence of the anomaly has also been investigated [58, 59, 64, 63]. In figure 1.6, the experimental data of Thomas *et al.* [58] is seen. It shows that the 0.7 feature gradually goes to the plateau at e^2/h , when turning up the magnetic field. The effect of a magnetic field in the plane²⁵ of a 2D electron gas is to spin split the transversal modes and therefore the Landauer formula predicts conductance quantization in steps of e^2/h in a high magnetic field. Therefore the experimental data approaches the expected result from the Landauer formula, when the field is turned up, so in that sense the anomaly disappears in a high magnetic field.

The non-linear conductance

The current through a QPC have also been investigated in the non-linear regime, i.e. as a function of the source-drain bias V . When turning up the bias, the

²⁴Amazingly, we find the same value in fits to our numerical calculation, see table 6.1 (p. 132) in chapter 6.

²⁵If the field is not in the plane, quantum Hall physics would play a role.

conductance steps as a function of gate voltage split up as $\frac{2e^2}{h}(n - 1/2)$ (for $n = 1, 2, \dots$), which can be explained by the Landauer formula [65, 66].

In connection to the 0.7 anomaly, the non-linear regime has also been investigated [17, 59, 63, 67]. Roughly, the effect of increasing the bias is the same as increasing the temperature: The conductance is reduced compared to the non-interacting result from the Landauer formula. In [17] it is shown that the scale associated with nonzero bias is the same as the one associated with nonzero temperatures.

The thermopower near the anomaly

Appleyard *et al.* [68] have experimentally demonstrated that the thermopower is enhanced compared to the Landauer formula prediction at gate voltages, where the 0.7 anomaly appears. Furthermore, they report that the thermopower enhancement breaks the so-called Mott formula. The Mott formula is an approximation for the thermopower in terms of the conductance: $S \simeq S^M \propto (1/G)dG/d\varepsilon_F$ (more about the Mott formula in chapter 2). This is a good approximation for non-interacting electrons, so Appleyard *et al.* conclude that the 0.7 anomaly is related to some kind of many-body effect. However, it should be noted that in comparing the measured conductance via the Mott formula to the thermopower, the Fermi level ε_F is replaced by the gate voltage V_g , i.e. $S^M \propto (1/G)dG/d\varepsilon_F \rightarrow S^M \propto (1/G)dG/dV_g$, which is valid if $V_g \propto \varepsilon_F$. However, that is not an obvious statement, especially close to pinch off of the QPC.

Appleyard *et al.* [68] also observes that for large magnetic fields, the Mott formula again becomes a good approximation for the thermopower. This is consistent with the conductance measurements in the sense that the 0.7 anomaly disappears in a large magnetic field²⁶.

The shot noise for the 0.7 anomaly

The noise is a measure of the amount of fluctuations in the current (for a review see [69]). Formally, the (zero frequency) noise is given by $\mathcal{S} = \int dt \langle \delta I_e(t) \delta I_e(0) \rangle$, where $\delta I_e(t)$ is the current fluctuation in time, $\delta I_e(t) = I_e(t) - \langle I_e \rangle$, and $\langle I_e \rangle$ is the average current. Therefore \mathcal{S} can be understood as the average amount of current fluctuations in time, i.e. the noise. The noise is a function of temperature T and bias V and often one distinguish between the thermal noise (where $V \rightarrow 0$ and $T \neq 0$) and the shot-noise (where $V \neq 0$ and T low). The noise in the thermal-noise limit ($eV/k_B T \rightarrow 0$) is given in terms of the conductance by $\mathcal{S} = 4k_B T G$ (using the fluctuation-dissipation theorem), so to get new information about a system, the shot-noise is investigated.

²⁶The thermopower is a difficult measurement to perform and to the best of our knowledge, there has been no further published results in relation to the 0.7 anomaly.

For a QPC the Landauer-Büttiker theory gives a shot-noise of the form [70]

$$\mathcal{S}^s = 2(2e^2/h)eV\mathcal{T}(1 - \mathcal{T}) \coth(eV/2k_B T) \quad (1.32)$$

for a single mode and a energy independent transmission²⁷ \mathcal{T} , i.e. the QPC is shot-noiseless on the conductance plateau. Note that a QPC always has thermal noise and this contribution is $2(2e^2/h)2k_B T\mathcal{T}^2$, so adding the thermal and shot-noise and taking the limit $eV/2k_B T \rightarrow 0$ the result $\mathcal{S} = 4k_B T(2e^2/h)\mathcal{T} = 4k_B T\mathcal{G}$ is obtained in agreement with the dissipation-fluctuation theorem. The shot-noise relation for QPC's has been experimentally verified [72, 73].

Recently, the noise has also been measured in relation to the 0.7 anomaly [71, 74, 75, 76]. The result is that the noise is reduced compared to the value one would expect from the Büttiker formula eq.(1.32). This should be understood in the following way: The current at the anomaly is reduced corresponding to some transmission through the QPC. If this transmission is used to calculate the shot-noise from eq.(1.32), then a larger value than the measured value is obtained.

Furthermore, in Dicarolo *et al.* [76] (figure 6 in their paper) they also measure the noise at the higher conductance plateaus and find that here the non-interacting Büttiker formula works well (including the energy dependence of the transmission). This seems to indicate that the 0.7 anomaly does not have any multi-mode counterpart and only occurs in the beginning of the first plateau²⁸. However, the opposite view point has also been reported [77], in any case the anomaly seems smaller on the higher conductance plateaus.

The length dependence of the 0.7 anomaly

If the length of the QPC becomes longer [78], then the anomaly becomes more pronounced. Reilly *et al.* [78] report that the long wires $L \sim 2\mu\text{m}$ even has a dip in the conductance as a function of gate voltage in the beginning of the first plateau. Other experimental studies [22] note that longer wires have an anomalous conductance reduction to $\sim e^2/h$.

The 0.7 anomaly in other 1D systems?

All the studies of the 0.7 feature that we have described so far have been done in QPC's made in 2D electron gases in semiconductor heterostructures. Recently, the anomaly has also been found for a QPC made in a 2D *hole* gas [79].

Features similar to the 0.7 structure have been seen in similar systems to QPC's, like the so-called cleaved edge overgrowth quantum wires [80] and even

²⁷Note that for more than one channel this result is generalized to include a sum over the transmission channels $\mathcal{T}(1 - \mathcal{T}) \rightarrow \sum_n T_n(1 - T_n)$. If the transmission is not energy independent, then an integration over energy is needed including Fermi functions of the leads, see e.g. [71].

²⁸The same conclusion is also found from the thermopower data [68].

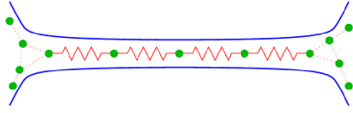


Figure 1.7: In the low density regime of a 1D wire the electrons (green dots) can form a Wigner-crystal, which is a crystalline structure similar to the lattice of a solid. The figure is taken from a poster by Matveev.

carbon nanotubes [81] (however, the nanotube data is rather weak). These observations seem to suggest that the 0.7 phenomenon has a more general nature and does not depend on the details of the QPC's. However, so far only really convincing experiments have only been conducted in semiconductor heterostructures²⁹.

1.9.2 Available explanations of the 0.7 conductance anomaly

Below we go through a few of the available explanations of the 0.7 anomaly. Again, we do not pretend to review the field, just to give a taste of the various models.

The Wigner-crystal model

A interesting proposal was given by Konstantin A. Matveev in 2004 [82, 83]. He proposed that the electrons in a low density quantum wire connected to leads can have a short-range crystalline order, i.e. form a so-called Wigner-crystal³⁰, see figure 1.7. Generally, a Wigner-crystal is formed, when the interaction energy becomes more important than the kinetic energy. In 1D this happens at low densities n , because the kinetic energy is $E_{\text{kin}} \propto k_F^2 \propto n^2$ whereas the Coulomb energy is $E_{\text{int}} \propto 1/r \propto n$. In this crystalline state, the spins of the electrons form a 1D Heisenberg chain with exchange coupling J , which is described by the Hamiltonian $H = \sum_n J \mathbf{S}_n \cdot \mathbf{S}_{n+1}$ with $J > 0$ (antiferromagnetic). The coupling J is much smaller than the Fermi energy and exponentially suppressed in density (i.e. $J \propto \varepsilon_F \exp(-\pi/\sqrt{n}a_B)$, where a_B is the Bohr radius). In this model, the conductance becomes $2e^2/h$ at low temperatures $k_B T \ll J \ll \varepsilon_F$ and e^2/h and higher temperatures $J \ll k_B T \ll \varepsilon_F$. This reduction of the conductance can be understood as a high temperature suppression of the spin excitations through the wire. Note that the spin-charge separation phenomenon does not take place in this setup, because the density is inhomogeneous.

Numerous further studies have been conducted along these lines by Matveev and co-workers [85, 86, 87]. Similar studies include a Hubbard chain connected to leads, which have been investigated using a Monte Carlo method and finds

²⁹To the best of our knowledge.

³⁰Note that Spivak and Zhou [84] also consider Wigner-crystal formation in the QPC, but claims to have a ferromagnetic order in the QPC in contrast to Matveev.

that the conductance reduces for increasing length [88]. A related subject are the so-called spin-incoherent Luttinger liquids, see e.g. [89, 90, 91]

The Kondo-like model

A heavily debated proposal is the so-called Kondo-like explanation of the 0.7 anomaly by Meir *et al.* [92]. It states that the conduction anomaly is due to the Kondo effect in the QPC close to pinch off.

The Kondo effect is known from metals with magnetic impurities and quantum dots [14, 93, 12]. A quantum dot with tunnelling contacts to the leads has Coulomb blockade peaks in the linear conductance as a function of gate voltage (or equivalently the Fermi level of the dot), because the current can only pass through the dot if an energy level of the dot is aligned with the Fermi level of the leads. The Kondo effect is a dramatic (i.e. several orders of magnitude) increase of the conduction between the peaks for an odd number of electrons on the dot, when the temperature is decreased below the so-called Kondo temperature T_K , which depends on the system. The conductance of a quantum dot in the Kondo regime is $2e^2/h$ for low temperatures $T \ll T_K$ and goes to zero at higher temperatures $T \gg T_K$. The functional form is well approximated by [94]

$$G^{\text{Kondo}}(T) = \frac{2e^2}{h} \left(\frac{1}{1 + (2^{1/s} - 1)(T/T_K)^2} \right)^s, \quad (\text{with } s = 0.22) \quad (1.33)$$

which only depends on T through T/T_K , a general feature of Kondo physics.

Therefore Meir *et al.* [92] explains the 0.7 anomaly by assuming that the electron forms a localized spin in the QPC, which can exhibit a Kondo effect in analog to a quantum dot. With this assumption they can show many of the experimental features, e.g. the shot-noise [95]. However, as seen above the Kondo effect *does not* lead to the same temperature dependence as observed for the 0.7 anomaly, since the Kondo effect goes from $2e^2/h$ to zero for increasing temperature whereas the observed dependence is from $2e^2/h$ to $\sim e^2/h$ for increased temperature. To cure this, it is simply postulated that the conductance follows

$$G^{\text{QPC}}(T) = \frac{1}{2}G^{\text{Kondo}}(T) + \frac{e^2}{h}, \quad (1.34)$$

which is the form used to fit the temperature dependence in Cronenwett *et al.* [59] shown in figure 1.5(b).

To justify the assumption of the localized electron in the QPC, Rejec and Meir [96] performed spin density functional theory calculations and indeed found bound states in the QPC geometry. According to this, electrons can localize in these bound states and perform Kondo physics leading the anomaly. However, other spin density functional theory calculations [97, 98] did not find bound states and Hartree-Fock calculations [99] could not confirm the Kondo scenario either.

The phenomenological spin-split model

Already in the early papers (e.g. [58]) the idea of a spontaneous spin polarization in zero magnetic field was discussed. Bruus *et al.* [100, 101] constructed a phenomenological model, where the spin up and spin down subbands are split by an amount that depends on the density of the electrons. A variety of this model³¹ was also considered by Reilly [102]. These models are able to explain all the experimental features, but lack a microscopic origin.

Some other explanations

There have been numerous attempts to explain the 0.7 anomaly. One of these models describe backscattering of the electrons by acoustic phonons [103, 104], which can explain the temperature and the bias dependence of the anomaly. However, the model also predicts an anomaly in the case of a large magnetic field, i.e. on the e^2/h plateau, which is not observed in the experiments.

Another model showing activated temperature dependence is that a localized plasmon exist inside the QPC, which can backscatter the electrons [105]. This model have also been investigated in relations to experiments [62].

Recently, more simple models have been investigated considering the electron-electron interaction in the QPC as the essential ingredient [106, 107, 108]. In chapter 6, we give another proposal using a model of non-momentum conserving electron-electron interaction in the QPC. Using perturbation theory, this model can explain all the observed features qualitatively and even in the non-perturbative regime we calculate the temperature dependence of the conductance showing similar features to the experiments.

1.10 Outline of the thesis

In this thesis, we consider electron-electron interaction effects in two regimes of the length of a QPC (or finite length quantum wire): (i) Long enough to have momentum conserving electron-electron interactions, i.e. $k_F L \gg 1$. (ii) So short that the translational invariance is broken leading to non-momentum conserving electron-electron interactions, i.e. $k_F L \sim 1$.

For the finite length quantum wires, we consider the multi-mode case and find interesting resonances in the conductance and thermopower at certain values of the Fermi energy (i.e. the gate voltage). Furthermore, we study the possibility of three-particle interactions in a single mode. However, this only leads to exponentially suppressed corrections of the transport properties at low temperatures

³¹On of the subtle difference between the models are that in Bruus *et al.* the Fermi level of the leads are pinned to the one of the spin bands in the beginning of the plateau, which is not the case in [102].

($\propto e^{-T_F/T}$) in the perturbative limit of weak interactions. In this regime of length, we are able to use the Boltzmann equation approach.

In the case of a short QPC, we find interaction corrections to the transport properties even in the single-mode case. Here we use a Green's function approach and develop a non-perturbative current formula, which is used to find the conductance beyond the perturbative limit in the interaction.

However, before we begin to understand the interaction effects, we consider the so-called Mott formula for thermopower of non-interacting electrons in order to better understand the experimental results of QPC's.

Chapter 2

The Mott formula for non-interacting electrons

In this chapter, the so-called *Mott formula* for thermopower is introduced and discussed in the context of non-interacting electrons. This is important to understand possible deviations from the Mott formula due to electronic interactions and other effects. The main parts of this discussion was published in *Journal of Physics: Condensed Matter*, see paper I (p. 145).

2.1 The Mott formula

The *Mott formula*¹ is an approximation relating the thermopower to the derivative of the conductance (conductivity) with respect to the chemical potential, originally developed for bulk systems [109, 110]. For a quantum point contact the Mott formula is

$$S^M(\mu, T) = \frac{\pi^2}{3} \frac{k_B}{e} T \frac{1}{G(\mu, T)} \frac{dG(\mu, T)}{d\mu}, \quad (2.1)$$

where $G(\mu, T)$ is the *temperature-dependent* conductance.

2.2 Why study the Mott formula?

Experimentally, the Mott formula is a valuable tool, because it allows for a comparison between the measured conductance and thermopower. The comparison is done using the gate voltage V_g instead of the chemical potential in the Mott

¹Sometimes also called the Cutler-Mott formula after the paper in Ref. [109].

formula², i.e.

$$S^M \propto k_B T \frac{d \ln G(V_g, T)}{dV_g}, \quad (2.2)$$

where $G(V_g, T)$ is the measured conductance. Since the Mott formula is expected to be valid for non-interacting electron, it has been argued that deviations from the Mott formula could be a sign of some extra information in the thermopower compared to the conductance. This extra information could for instance be many-body effects as reported in an experiment by Appleyard *et al.* [68]. However, it is not certain that interaction effects will break the Mott formula and we shall see an example of this in chapter 4 (paper II, p. 153).

The purpose of this chapter is to determine the validity of the Mott formula as an approximation to the thermopower for non-interacting electrons. This will help us to distinguish deviation from the Mott formula due to single-particle behavior and due to more complicated behavior in the experiments [31, 68, 111].

2.3 The lowest order approximation in $k_B T$

As found in chapter 1, eq.(1.10), the Landauer formula leads to the following formula for the non-interacting thermopower³ [36]

$$S(\mu, T) = \frac{2ek_B}{h} \frac{1}{G(\mu, T)} \int_0^\infty d\varepsilon \mathcal{T}(\varepsilon) \left(\frac{\varepsilon - \mu}{k_B T} \right) [-\partial_\varepsilon f^0(\varepsilon)], \quad (2.3)$$

where

$$G(\mu, T) = \frac{2e^2}{h} \int_0^\infty d\varepsilon \mathcal{T}(\varepsilon) [-\partial_\varepsilon f^0(\varepsilon)]. \quad (2.4)$$

An approximation to the non-interacting thermopower is now derived, valid when the temperature is the smallest energy scale in the problem. If the temperature $k_B T$ is much smaller than scale of variation of the transmission $\mathcal{T}(\varepsilon)$ around the chemical potential μ , then we can expand the transmission to lowest

²Note that since one measures the thermovoltage, $V_{th} = (G_T/G)\Delta T$, instead of the thermopower, it is not the absolute magnitude that can be compared, but rather the functional shape (see e.g. the caption of figure 1.3).

³Here we chosen the additive constant in the energy such that the lower limit of the integrals are zero. Furthermore, since we are not interested in exponentially small corrections, the upper limit is chosen to be infinity.

order (i.e. a Sommerfeld expansion) in the integrands in eq.(2.3) and (2.4), i.e.

$$\begin{aligned}
S^{(1)}(\mu, T) &= \frac{k_B}{e} \frac{\int_0^\infty d\varepsilon \left\{ \mathcal{T}(\mu) + \partial_\mu \mathcal{T}(\mu)(\varepsilon - \mu) \right\} \left(\frac{\varepsilon - \mu}{k_B T} \right) [-\partial_\varepsilon f^0(\varepsilon)]}{\int_0^\infty d\varepsilon \mathcal{T}(\varepsilon) [-\partial_\varepsilon f^0(\varepsilon)]} \\
&\simeq \frac{\pi^2}{3} \frac{k_B}{e} k_B T \frac{\partial_\mu \mathcal{T}(\mu)}{\mathcal{T}(\mu)} \\
&= \frac{\pi^2}{3} \frac{k_B}{e} k_B T \frac{1}{G(\mu, T=0)} \frac{\partial G(\mu, T=0)}{\partial \mu}, \tag{2.5}
\end{aligned}$$

where we used the integral

$$\begin{aligned}
\int_0^\infty d\varepsilon \left(\frac{\varepsilon - \mu}{k_B T} \right)^2 [-\partial_\varepsilon f^0(\varepsilon)] &= \int_{-\frac{\mu}{k_B T}}^\infty dx \frac{x^2}{4 \cosh^2(x/2)} \\
&\simeq \int_{-\infty}^\infty dx \frac{x^2}{4 \cosh^2(x/2)} = \frac{\pi^2}{3} \quad \text{for } k_B T \ll \mu. \tag{2.6}
\end{aligned}$$

Note that integrals leading to exponentially small contributions in temperature, i.e. $\propto \exp(-\mu/k_B T)$, are neglected for $k_B T \ll \mu$.

Therefore the Sommerfeld expansion lead us to a well-defined approximation for the thermopower, $S \simeq S^{(1)}$, valid for temperatures lower than μ and the scale of variation of $\mathcal{T}(\varepsilon)$ around μ . This formula is similar to the Mott formula eq.(2.1), *but* it uses the zero-temperature conductance $G(\mu, T=0)$ instead of $G(\mu, T)$. Therefore the Mott formula is good approximation, when $k_B T$ is the smallest scale in the problem. In the experiments, the temperature dependent conductance is used to analyze the results and the modern⁴ version of the Mott formula is therefore the one stated in eq.(2.1).

2.4 Validity of the Mott formula

It is harder to argue rigorously for the Mott formula eq.(2.1) including the temperature-dependent conductance than the lowest order expansion $S^{(1)}$ eq.(2.5). Here a numerical investigation is performed followed by some analytical considerations in order to identify the regime of validity of the Mott formula.

2.4.1 Numerical investigation

Here we numerically compare the thermopower S eq.(2.3), the Mott formula S^M eq.(2.1) and the lowest order approximation $S^{(1)}$ eq.(2.5) for a QPC. To make a numerical integration (of eq.(2.3), (2.1) and (2.4)) a specific form of the

⁴Originally, $S^{(1)}$ was called the Mott formula [109, 110, 1].

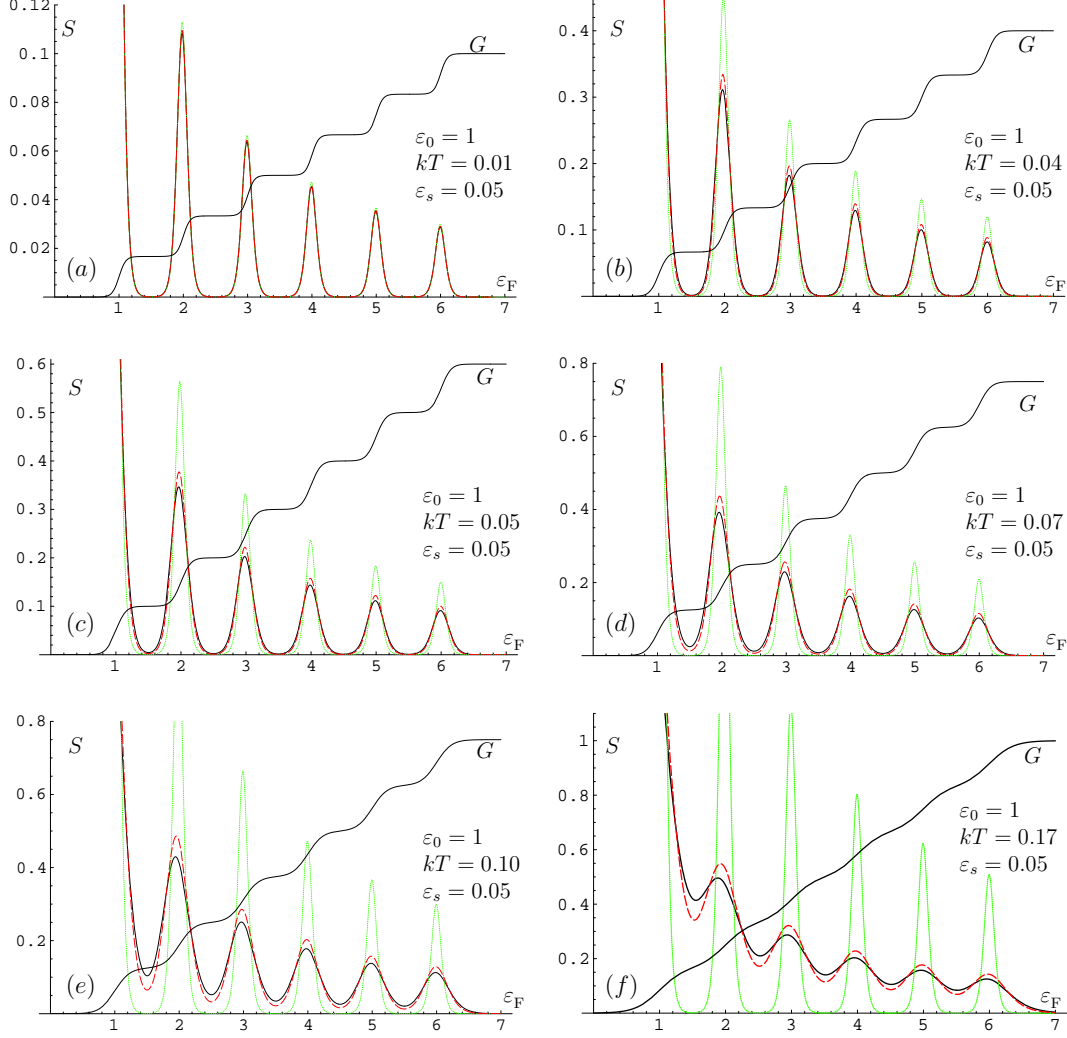


Figure 2.1: The results of a numerical evaluation of the thermopower S eq.(2.3) (black full line), the Mott formula S^S eq.(2.1) (red dashed line) and the lowest order approximation $S^{(1)}$ (green full line) as a function of the chemical potential $\mu = \varepsilon_F$ for the saddle-point transmission model eq.(2.7). The smearing of the transmission is kept constant at $\varepsilon_s = 0.05$ and from (a) to (f) the temperature $k_B T$ is varied from $k_B T = 0.01 < \varepsilon_s$ to $k_B T = 0.17 > \varepsilon_s$. All energies are in units of ε_0 and the unit of the vertical axis is k_B/e . The point is that the Mott formula is a fairly good approximation to the thermopower for non-interacting electrons even for temperatures larger than the smearing of the transmission. The conductance (in arbitrary units) is seen for a comparison.

transmission $\mathcal{T}(\varepsilon)$ is needed. The saddle-point model [41] (see section 1.5.1, p. 8) has a Fermi function like transmission,

$$\mathcal{T}(\varepsilon) = \sum_{n=1}^{n_{\max}} \frac{1}{\exp(\frac{n\varepsilon_0 - \varepsilon}{\varepsilon_s}) + 1}, \quad (2.7)$$

which is used to obtain the results of figure 2.1. The transmission has two different energy scales: (i) The smearing of the conductance steps ε_s and (ii) the length of the conductance steps ε_0 . In terms of the saddle-point potential eq.(1.14), these parameters are given by $\varepsilon_s = \hbar\omega_x/(2\pi)$ and $\varepsilon_0 = \hbar\omega_y$ (see eq.(1.15)), respectively.

The parameter regimes under investigation are:

$$k_{\text{B}}T < \varepsilon_s \text{ [fig. 2.1(a)]}, \quad k_{\text{B}}T \sim \varepsilon_s \text{ [fig. 2.1(b-d)]} \quad \text{and} \quad k_{\text{B}}T > \varepsilon_s \text{ [fig. 2.1(e-f)]}.$$

In all three regimes the temperature is still low in the sense that $k_{\text{B}}T \ll \mu$, where μ is of order the step length ε_0 . Note that all three parameter regimes are experimentally relevant, since they all have a staircase like conductance.

From the figures 2.1 we can draw the following conclusions

- For $k_{\text{B}}T < \varepsilon_s$ (figure 2.1(a)) both the Mott formula and the lowest order approximation work very well, as expected from the derivation of $S^{(1)}$ in section 2.3.
- When $k_{\text{B}}T \sim \varepsilon_s$ (figure 2.1(b-d)) the Mott formula is still a good approximation, but not the lowest order approximation $S^{(1)}$.
- Even for $k_{\text{B}}T > \varepsilon_s$ the Mott formula remains a good approximation, (figure 2.1(e-f)).

Therefore the Mott formula seem to be good approximation for non-interacting electrons in QPC's. Note that as $k_{\text{B}}T$ increases S^{M} and $S^{(1)}$ has a tendency to overestimate the thermopower at the peaks and underestimate it in the valleys.

2.4.2 A power series expansion of the transmission

To understand better why the Mott formula works for temperature comparable to and even larger than the smearing of the transmission ε_s , we insert

$$\mathcal{T}(\varepsilon) = \sum_{n=0}^{\infty} \frac{1}{n!} \frac{\partial^n \mathcal{T}(\mu)}{\partial \varepsilon^n} (\varepsilon - \mu)^n, \quad (2.8)$$

in the Mott formula eq.(2.1) and the thermopower eq.(2.3), i.e. we include all orders instead of only keeping the lowest order as in $S^{(1)}$ eq.(2.5). Inserting the

transmission eq.(2.8) in the thermopower eq.(2.3) and Mott formula eq.(2.1), we get⁵

$$S(\mu, T) \simeq \frac{k_B}{e} \frac{1}{G(\mu, T)} \frac{2e^2}{h} \sum_{n=0}^{\infty} \left[\frac{I_{2n+2}}{(2n+1)!} \frac{\partial^{2n+1} \mathcal{T}(\mu)}{\partial \varepsilon^{2n+1}} (k_B T)^{2n+1} \right], \quad (2.9)$$

$$S^M(\mu, T) \simeq \frac{k_B}{e} \frac{1}{G(\mu, T)} \frac{2e^2}{h} \sum_{n=0}^{\infty} \left[\frac{I_2 I_{2n}}{(2n)!} \frac{\partial^{2n+1} \mathcal{T}(\mu)}{\partial \varepsilon^{2n+1}} (k_B T)^{2n+1} \right], \quad (2.10)$$

assuming that $k_B T \ll \mu$ to make the even powers of temperature vanish by using

$$\int_{-\frac{\mu}{k_B T}}^{\infty} dy \frac{y^n}{4 \cosh^2(y/2)} \xrightarrow{\text{for } k_B T \ll \mu} \int_{-\infty}^{\infty} dy \frac{y^n}{4 \cosh^2(y/2)} \equiv I_n, \quad (2.11)$$

which is zero for odd integers n . The integrals I_n can be calculated and the first few values are:

$$I_0 = 1, \quad I_2 = \frac{\pi^2}{3}, \quad I_4 = \frac{7\pi^4}{15}, \quad I_6 = \frac{31\pi^6}{21}, \quad I_8 = \frac{127\pi^8}{15}, \quad I_{10} = \frac{2555\pi^{10}}{33}, \quad \dots \quad (2.12)$$

We observe that only the first order in $k_B T$ is the same in the power series of S and S^M , but they both only have odd powers of $k_B T$ at low temperature $k_B T \ll \mu$ and share the factor $\partial_{\varepsilon}^{2n+1} \mathcal{T}(\mu)$. However, the numerical prefactors behave rather differently as a function of n :

$$\frac{I_{2n+2}}{(2n+1)!} \sim 4.00 \times n + \frac{\pi^2}{3} \quad \text{and} \quad \frac{I_2 I_{2n}}{(2n)!} \rightarrow 6.58 \quad \text{for } n \gtrsim 10, \quad (2.13)$$

as seen on figure 1 in paper I (p.145). Therefore the similarity really depends on the n^{th} derivative of the transmission.

2.4.3 An analytically solvable case: The ideal point contact

In this section, the extreme limit of zero smearing of the conductance steps due to the barrier, $\varepsilon_s = 0$, is considered, i.e. the limit $k_B T \gg \varepsilon_s$. This case has a step function transmission and is analytically solvable, see section 1.5.2.

Using eq.(1.18) for the conductance the Mott formula eq.(2.1) gives

$$S^M(\mu, T) = \frac{k_B}{e} \frac{2e^2}{h} \frac{1}{G(\mu, T)} \sum_{n=1}^{\infty} \left[\frac{\pi^2}{3} \frac{1}{4 \cosh^2(\Delta_n/2)} \right], \quad (2.14)$$

which should be compared to the thermopower $S = G_T/G$ using eq.(1.19)

$$S(\mu, T) = \frac{k_B}{e} \frac{2e^2}{h} \frac{1}{G(\mu, T)} \sum_{n=1}^{\infty} \left[\ln(1 + e^{\Delta_n}) - \frac{\Delta_n}{1 + e^{-\Delta_n}} \right], \quad (2.15)$$

⁵See paper I (p. 145) section 3.2 for more details of this calculation.

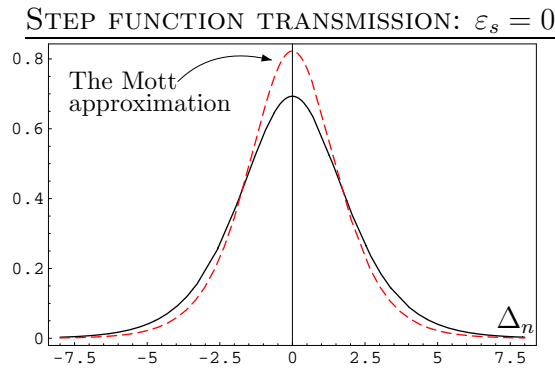


Figure 2.2: A comparison between the Mott formula and the exact thermopower for a step-function transmission (i.e. $\varepsilon_s = 0$). The solid black curve is the function in the square brackets in eq.(2.15) (i.e. the exact result) and the red dashed curve is the Mott approximation to this result (i.e. the function in the square brackets in eq.(2.14)). The Mott formula is remarkably good considering that we are in the regime $k_B T \gg \varepsilon_s$.

where $\Delta_n = (n\varepsilon_0 - \mu)/k_B T$. We see that the functions in the square brackets are not analytically alike, however, their functional form are not too different as seen on figure 2.2. The tendency that the Mott formula overestimates the thermopower at the peaks is the same as in the numerics, see figure 2.1. The Mott formula also shows exponential suppression on the plateaus,

$$\frac{\pi^2}{3} \frac{1}{4 \cosh^2(\Delta_n/2)} \simeq \frac{\pi^2}{3} \exp(-|\Delta_n|) \quad \text{for} \quad k_B T \ll |n\varepsilon_0 - \mu|, \quad (2.16)$$

but the prefactor misses a factor $\propto |\Delta_n|$ compared to the thermopower S , see eq.(1.20).

Therefore this simple step model for the transmission confirms the surprising result from the numerical investigation: The Mott formula works fairly well even for $k_B T \gg \varepsilon_s$.

2.5 Beyond non-interacting electrons?

The Mott formula has been investigated in many kinds of systems. For instance in metals it was found to be a good approximation even in the presence of a static lattice and electron-phonon scattering [112, 113]. However, one should be careful extending these results and methods to the mesoscopic regime and especially to QPC's, since they rely on thermodynamical consideration of the system⁶. None the less, the thermopower often -but not always- comes in the form seen in eq.(1.25), i.e.

$$S = \frac{k_B}{e} \frac{2e^2}{h} \frac{1}{G} \int d\varepsilon d(\varepsilon) \left(\frac{\varepsilon - \mu}{k_B T} \right) [-\partial_\varepsilon f^0(\varepsilon)] \mathcal{F}(\varepsilon), \quad (2.17)$$

⁶Especially, considering the heat current one often uses $dQ = TdS = dU - \mu dN$ in bulk systems (see e.g.[1, p.253]). For interacting systems one should also consider, which energy is being transported when constructing the heat current [114].

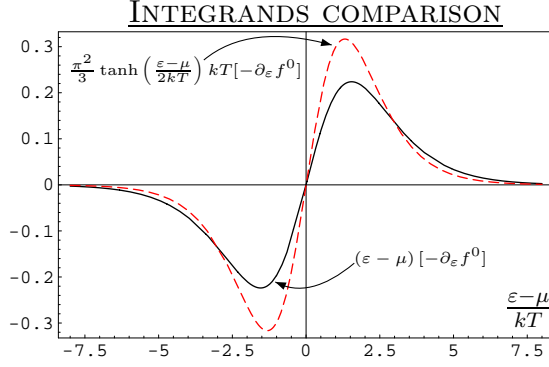


Figure 2.3: A comparison between important parts of the integrands in the thermopower eq.(2.17) and the Mott formula eq.(2.18). The integrals of S and S^M are the same except for the shown functions.

where $d(\varepsilon)$ is the density of states and $\mathcal{F}(\varepsilon)$ is some function. The conductance is given by the same integral without the factor $(\varepsilon - \mu)/k_B T$. In this case, the only dependence of μ is in the derivative of the Fermi function and therefore using the Mott formula is the same as approximating $(\varepsilon - \mu)/k_B T$ in the integral by $(\pi^2/3) \tanh[(\varepsilon - \mu)/(2k_B T)]$, i.e.

$$S^M = \frac{k_B}{e} \frac{2e^2}{h} \frac{1}{G} \int d\varepsilon d(\varepsilon) \frac{\pi^2}{3} \tanh\left(\frac{\varepsilon - \mu}{2k_B T}\right) [-\partial_\varepsilon f^0(\varepsilon)] \mathcal{F}(\varepsilon). \quad (2.18)$$

Due to the presence of $[-\partial_\varepsilon f^0(\varepsilon)]$ these two integrands are not too different as seen on figure 2.3. Of course, how well the Mott formula approximates the thermopower really depends on $d(\varepsilon)\mathcal{F}(\varepsilon)$. Furthermore, if $\mathcal{F}(\varepsilon)$ depends on μ or the thermopower does not have the specific form eq.(2.17) assumed here, then the above consideration is useless. In chapter 4, we shall see an example, where interacting electrons in QPC's follow the Mott formula fairly well.

2.6 Concluding remarks

We have considered how well the Mott formula approximates the non-interacting thermopower derived from the Landauer formula for a QPC. The result is that for low temperature $k_B T \ll \mu$, it is a reasonably good approximation and it becomes better the smaller the temperature. In particular, $k_B T$ should be compared to the scale of the smearing of the transmission steps $\varepsilon_s \ll \mu$ (due to the barrier along the QPC). If $k_B T \ll \varepsilon_s$ the Mott formula can be shown to be a very good approximation by a Sommerfeld expansion of the thermopower. Surprisingly, it is still a fairly good approximation for $k_B T \gtrsim \varepsilon_s$ as found in numerical calculations and confirmed by an analytic model of a step-function transmission in the regime $k_B T \gg \varepsilon_s = 0$.

Chapter 3

Transport in finite quantum wires: A Boltzmann equation approach

In this chapter, we introduce the Boltzmann equation and the way it can be used to model the current through finite quantum wires perfectly connected to external leads. We begin by commenting on the problem of relaxation in 1D wires connected to reservoirs. Thereafter we find the current due to the electronic scattering to first order in the scattering rate, which is an extension of the Landauer formula including e.g. interactions effects. In the end, we show that a relaxation mechanism have to change the number of left and right movers to change the current through these kinds of systems.

3.1 Relaxation in a one-dimensional system with perfect leads

Here we briefly discuss the possibility of electronic relaxation in finite clean (i.e. no impurities) 1D quantum wires perfectly connected to higher dimensional leads (QPC's).

Our starting point is a semi-classical description, where the central object is the electronic distribution function $f_{kn}(x)$ depending on space x , quasi-momentum k and subband index n of the transverse quantization. We only consider the situation, where a number of transverse modes (subbands) are fully open, so we have reflectionless contacts. Therefore the right movers ($k > 0$) on the left side of the system are distributed with the distribution function of the left lead $f_L^0(\varepsilon_k)$ and vice versa. Therefore the distribution function at the ends of the system is:

$$f_{kn}(x=0) = f_L^0(\varepsilon_{kn}) \quad \text{for } k > 0, \quad (3.1a)$$

$$f_{kn}(x=L) = f_R^0(\varepsilon_{kn}) \quad \text{for } k < 0, \quad (3.1b)$$

where L is the length of the system and $f_{L/R}^0(\varepsilon_{kn})$ are the Fermi functions of the leads eq.(1.5), see figure 3.1(b).

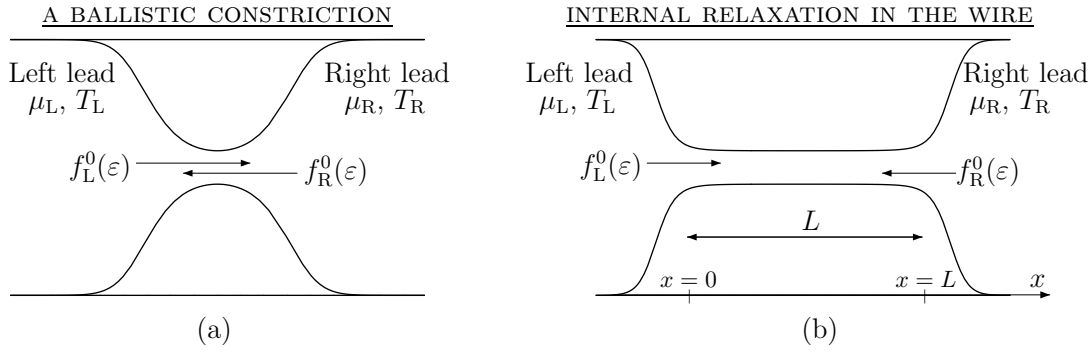


Figure 3.1: Relaxation of the electron distribution function for a ballistic point contact (a) and for a 1D wire with length L (b). In both cases, the distribution function for right moving electrons on the left side of the system is distributed with the distribution function of the left reservoir $f_L^0(\varepsilon_k)$ and vice versa. In the short system (a) without relaxation the distribution functions does not change. This is in contrast to the longer 1D wire (b) where relaxation in the wire has time to change the incoming distribution functions. The degree of relaxation in the wire of course depends on other quantities than the length and in chapter 6 we consider relaxation in an point-like constriction due to non-momentum conserving interactions.

One limit is the ballistic one, where there is no relaxation inside the wire as seen in figure 3.1(a). Therefore the distribution function is simply given by eq.(3.1) for all x and the current follows the Landauer formula with integer transmission as obtained in eq.(1.24).

On the other hand, if there is some kind of relaxation processes inside the system, then the distribution function can change. One mechanism of relaxation is electronic interactions. However, for a single mode, momentum and energy conserving two-particle interactions cannot change the distribution function as noted in section 1.8. Therefore we have to consider more than one subband (chapter 4) or higher order processes like three-particle processes (chapter 5). To obtain information about the change of the distribution function the conductance and especially the thermopower are valuable quantities.

If we consider a infinitely long clean 1D wire *without* leads, then it is translational invariant. This means that the interactions will be momentum conserving and therefore they cannot change the total momentum of the electronic system, which in terms means that the current does not change [14, exercise 8.5]. However, introducing leads changes the picture completely. In this case, one can speculate that a very long wire has two different kinds of regions. In the region near the contacts, electrons with a Fermi distributions is injected from the contact. These will try to equilibrate with the electrons coming from the inner wire and this will create a zone of equilibration near the contacts. The length of this zone will be determent by some kind of characteristic equilibration length ℓ_{eq} , so a very long wire means a wire much longer than this zone $L \gg \ell_{eq}$. In the inner wire, one might expect that the left and right movers have equilibrated completely from

the effects of the contacts. Therefore they might have reached an equilibrium in a reference frame moving with some drift velocity characterizing the current through the wire (e.g. a shifted Fermi function). The length of this inner peace should not change the current due to its translational invariance. Therefore we have argued that the contacts may change the picture of a 1D wire dramatically. To the best of our knowledge, a more precise and quantitative description of the long wire limit including the leads is currently not available and therefore remains an interesting open question.

It is interesting to note, that in the case of momentum-independent velocities of the left and right movers (i.e. linear dispersion) such as a Luttinger liquid we have the following situation: A shifted Fermi function is identical to a distribution where the left and right movers have different Fermi functions (like eq.(3.1)). Therefore the curvature of the dispersion and electron-hole asymmetry might play an essential role and hence thermopower is an interesting quantity to investigate.

In this thesis, we consider the problem perturbably to lowest order in the interaction and therefore find corrections to the ballistic result for a weak relaxation in the wire.

3.2 The Boltzmann equation approach

To calculate the particle current the Boltzmann equation is used. Generally, it is:

$$\frac{\partial f_{\mathbf{k}}(\mathbf{r}, t)}{\partial t} + \frac{d\mathbf{r}}{dt} \frac{\partial f_{\mathbf{k}}(\mathbf{r}, t)}{\partial \mathbf{r}} + \frac{d\mathbf{k}}{dt} \frac{\partial f_{\mathbf{k}}(\mathbf{r}, t)}{\partial \mathbf{k}} = \mathcal{I}_{\mathbf{k}, \mathbf{r}, t}[f], \quad (3.2)$$

where $f_{\mathbf{k}}(\mathbf{r}, t)$ is the distribution function in general depending on time t , space \mathbf{r} and (quasi-)momentum \mathbf{k} . The right hand side is the collision integral $\mathcal{I}_{\mathbf{k}, \mathbf{r}, t}[f]$, which is a functional of f describing the collisions in the system. In the case of an electronic system the collision integral can e.g. describe electron-electron interactions, interactions with static impurities or electron-phonon interactions.

The Boltzmann equation is a continuity equation in (\mathbf{r}, \mathbf{k}) -space and semi-classical in origin, since knowing the exact position and momentum of a particle is not allowed in quantum mechanics due to the Heisenberg principle. The microscopic origin of the Boltzmann equation is Fermi liquid theory, where the particles are the free-electron like excitations of the system (the so-called quasi-particles).

Generally, it is a difficult task to solve the Boltzmann equation, since the collision integral depends on f making it a partial integro-differential equation. Therefore approximation and simplification capturing the essential physics are necessary. The Boltzmann equation have been used to successfully describe a wealth of phenomena in all areas of physics. For a complete introduction to the Boltzmann equation consult the book by Smith and Jensen [115].

3.2.1 The Boltzmann equation for a wire with leads

We now describe the Boltzmann equation for a finite length quantum wire perfectly connected to the leads, which have different chemical potentials and/or temperatures, see figure 3.1. Only steady state is considered so $\frac{\partial f}{\partial t} = 0$, and the problem is one dimensional, i.e. $f = f_{kn}(x)$, where n is the band index and the spin index σ is implicit.

Steady state bulk systems like metals and semiconductors are often modelled as perfectly homogeneous, so the spatial derivative is zero. The driving fields are included in the Boltzmann equation by using the equation of motion (Newton's second law) for \mathbf{k} to write $\hbar \frac{d\mathbf{k}}{dt} = \mathbf{F}$, where \mathbf{F} is the force acting on the particles (e.g. the electric field, temperature gradient and/or Lorentz force).

In contrast, here we model the wire as being an inhomogeneous system (i.e. x dependent) and include the driving fields in the boundary condition of the distribution function. If we apply a bias across the wire, then by solving the Poisson equation one finds that in the linear response regime the potential drop happens at the contacts (i.e. at the ends of the wire) [116, and ref. therein]¹. Therefore the electrostatic potential is flat inside the wire, so we have $\frac{dk}{dt} = 0$. Therefore the Boltzmann equation for the quantum wire is

$$v_{kn} \partial_x f_{kn}(x) = \mathcal{I}_{knx}[f] \quad (3.3)$$

including the boundary conditions for reflectionless contacts eq.(3.1):

$$f_{kn}(x=0) = f_L^0(\varepsilon_{kn}) \quad \text{for } k > 0, \quad (3.4a)$$

$$f_{kn}(x=L) = f_R^0(\varepsilon_{kn}) \quad \text{for } k < 0. \quad (3.4b)$$

Here $\frac{dx}{dt} = v_{kn}$ is the velocity given in by dispersion relation ε_{kn} as

$$v_{kn} = \frac{1}{\hbar} \frac{d\varepsilon_{kn}}{dk}. \quad (3.5)$$

Note that a temperature difference between the contacts in the linear response regime can also be included and treated in the same fashion.

The Boltzmann equation eq.(3.3) including the boundary conditions eq.(3.4) is the starting point of our calculations of the conductance and thermopower and what differs is the collision integral.

The particle current I has to be conserved, which leads to a restriction of form of the collision integral. This is found by integrating over k and summing over n and σ on the right and left hand side of the Boltzmann equation (3.3):

$$\int_{-\infty}^{\infty} \frac{dk}{2\pi} \sum_{n\sigma} \mathcal{I}_{knx}[f] = \int_{-\infty}^{\infty} \frac{dk}{2\pi} \sum_{n\sigma} v_{kn} \partial_x f_{kn}(x) = \partial_x I = 0, \quad (3.6)$$

¹See also the beautiful experiment by Picciotto *et al.* [37, 38].

where the last equality ($\partial_x I = 0$) is imposed by current conservation (i.e. I is x -independent). Therefore for the current to be conserved the collision integral have to fulfill eq.(3.6).

In the present model, the collision integral is not present outside the wire ($x < 0$ and $x > L$) and it is abruptly turned on at the boundaries $x = 0$ and $x = L$. This is of course an approximation, but we expect it to capture the essential physics of a wire being connected to higher dimensional (non-interacting) reservoirs. However, it could be interesting to study a more realistic, gradual turn on of the strength of the collision integral.

The Boltzmann equation have previously been used to describe mesoscopic transport in quantum wires a number of times. Some examples include quantum hall effect in quantum wires [117], Coulomb drag between ballistic quantum wires [118], magnetoconductivity of quantum wires [119], electron-phonon interactions in finite quantum wires [120], surface roughness in QPC's [121], Phonon drag in ballistic quantum wires [122], spin transport [123] and also more numerically oriented studies [124, 125].

3.2.2 Collision integrals for electronic interactions

It is also worth to note that in the present description we have not yet constricted ourself to a specific collision integral, i.e. a specific scattering (relaxation) mechanism. Some examples of scattering events are: Scattering of static impurities, electron-electron scattering and electron-phonon scattering. Now we briefly describe the collision integrals used in this thesis.

For the two-body (multi-subband) electron-electron interaction the collision integral is:

$$\begin{aligned} \mathcal{I}_{k_1 n_1 x}[f] = & - \sum_{\substack{\sigma_2 \\ \sigma_1, \sigma_2'}} \sum_{\substack{n_2 \\ n_1, n_2'}} \sum_{\substack{k_2 \\ k_1, k_2'}} \left\{ \underbrace{W_{1'2';12} f_{k_1 n_1}(x) f_{k_2 n_2}(x) [1 - f_{k_1' n_1'}(x)] [1 - f_{k_2' n_2'}(x)]}_{\text{scattering out of the state } |k_1 n_1\rangle |k_2 n_2\rangle} \right. \\ & \left. - \underbrace{W_{12;1'2'} f_{k_1' n_1'}(x) f_{k_2' n_2'}(x) [1 - f_{k_1 n_1}(x)] [1 - f_{k_2 n_2}(x)]}_{\text{scattering into the state } |k_1 n_1\rangle |k_2 n_2\rangle} \right\}. \quad (3.7) \end{aligned}$$

This collision integral is understood in the following way: An electron in the state $|k_1 n_1\rangle$ interacts with an electron in $|k_2 n_2\rangle$ and they scatter into $|k_1' n_1'\rangle$ and $|k_2' n_2'\rangle$, see figure 3.2. This happens with a transition rate² $W_{1'2';12}$, where i is short for $k_i n_i$. The scattering rates are proportional to the occupation, i.e. the distribution function f , and to the availability of the state after the scattering event $1 - f$ (for fermions). The collision integral contains both a term for scattering into the states $|k_1 n_1\rangle$ and $|k_2 n_2\rangle$ and one for scattering out of $|k_1 n_1\rangle$ and $|k_2 n_2\rangle$. This leads to a collision integral of the form³ seen in eq.(3.7).

²Note that we use the convention from quantum mechanics for the indices: $W_{f;i}$, where i

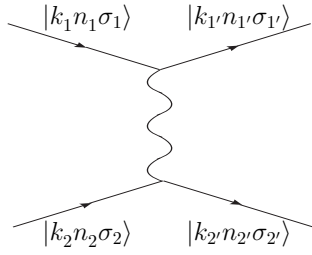


Figure 3.2: The basic two-particle scattering process, where 1 and 2 scatters into 1' and 2'. This is the basis of the collision integral eq.(3.7).

We should make sure that the restriction on the collision integral in eq.(3.6) from the current conservation is obeyed. Introducing the short hand notation $f_i = f_{k_i n_i}(x)$, we test this by inserting eq.(3.7) in eq.(3.6):

$$\begin{aligned} \sum_{k_1 n_1 \sigma_1} \mathcal{I}_{k_1 n_1 x}[f] = & \quad (3.8) \\ - \sum_{\substack{\sigma_1 \sigma_2 \\ \sigma_1' \sigma_2'}} \sum_{\substack{n_1 n_2 \\ n_1' n_2'}} \sum_{\substack{k_1 k_2 \\ k_1' k_2'}} \{ W_{1'2';12} f_1 f_2 [1 - f_{1'}][1 - f_{2'}] - \underbrace{W_{12;1'2'} f_{1'} f_{2'} [1 - f_1][1 - f_2]}_{\text{interchange } 1 \leftrightarrow 1' \text{ and } 2 \leftrightarrow 2'} \} = 0, \end{aligned}$$

i.e. the two-body collision integral conserves current as it should.

In eq.(3.7) we assume the collision integral to be local in space, so all the distribution functions are taken at x . A generalization can be done by using $f_i = f_{k_i n_i}(x_i)$ and integrating over x_2 , $x_{1'}$ and $x_{2'}$.

Furthermore, the transition rate is often⁴ symmetric $W_{12;1'2'} = W_{1'2';12}$ and can in the simplest case be found by Fermis Golden rule:

$$W_{12;1'2'} = \frac{2\pi}{\hbar} |\langle k_1' n_1' k_2' n_2' | \mathcal{V} | k_1 n_1 k_2 n_2 \rangle|^2 \delta(\varepsilon_{k_1 n_1} + \varepsilon_{k_2 n_2} - \varepsilon_{k_1' n_1'} - \varepsilon_{k_2' n_2'}), \quad (3.9)$$

where \mathcal{V} is the electron-electron interaction operator and the matrix element contains both an direct and exchange term. The transition rate given by the Fermi Golden rule is symmetric.

Note that for any symmetric and energy conserving transition rate the collision integral is zero, if Fermi functions are inserted, since

$$\begin{aligned} f^0(\varepsilon_1) f^0(\varepsilon_2) [1 - f^0(\varepsilon_{1'})][1 - f^0(\varepsilon_{2'})] = \\ f^0(\varepsilon_{1'}) f^0(\varepsilon_{2'}) [1 - f^0(\varepsilon_1)][1 - f^0(\varepsilon_2)] \end{aligned} \quad (3.10)$$

valid for $\varepsilon_1 + \varepsilon_2 = \varepsilon_{1'} + \varepsilon_{2'}$, where $\varepsilon_i = \varepsilon_{k_i n_i}$. Therefore in equilibrium ($\mu_L = \mu_R$, $T_L = T_R$) the Fermi function solves the interacting problem.

and f are the initial and final state, respectively.

³Note that the collision integral is not exact, since it could contain higher order distribution functions, for a discussion see [115, p.7].

⁴A symmetric rate means that the probability of $12 \rightarrow 1'2'$ is the same as $1'2' \rightarrow 12$ (called the detailed balance principle). If we do not have time-reversal symmetric, then this might not be true [115, 126].

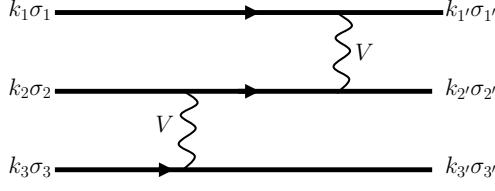


Figure 3.3: The basic three-particle scattering process, where three particles exchange momentum and energy. It consists of two 2-body scatterings, connected by a virtual-like state, so the individual 2-body scatterings do not have to conserve momentum and energy.

If we only have a single mode (subband), then two-body interactions cannot change the distribution function for a momentum and energy conserving scattering as noted in section 1.8. In this case, the three-body interactions become relevant and they have the following collision integral:

$$\mathcal{I}_{k_1 x}[f] = - \sum_{\substack{\sigma_2 \sigma_3 \\ \sigma_1' \sigma_2' \sigma_3'}} \sum_{\substack{k_2 k_3 \\ k_1' k_2' k_3'}} \left\{ W_{1'2'3';123} f_1 f_2 f_3 (1 - f_{1'}) (1 - f_{2'}) (1 - f_{3'}) \right. \\ \left. - W_{123;1'2'3'} f_{1'} f_{2'} f_{3'} (1 - f_1) (1 - f_2) (1 - f_3) \right\}, \quad (3.11)$$

where $f_i = f_{k_i}(x)$ and $W_{123;1'2'3'}$ is the three-particle transition rate (often symmetric). The form and understanding of the collision integral is the same as for the two-body case eq.(3.7), see figure 3.3. Again, we have assumed a local collision integral, but it can as before easily be expanded to a non-local one. Further, the three-body collision integral also conserves the current seen in an equivalent fashion to eq.(3.8).

Collision integrals describing scattering of electrons on static impurities or electron-phonon scattering have the same idea of scattering in and out built into them. For details consult [115] or [126].

3.2.3 The current to lowest order in the scattering rate

The Boltzmann equation (3.3) for a wire perfectly connected to leads is now solved perturbably to lowest order in the scattering rate⁵. This leads to the current through the wire to lowest order in the scattering rate. It is a general derivation, in the sense that the precise form of the collision integral is not specified.

If there is no scattering, then the collision integral is zero, $\mathcal{I}[f] = 0$, and the solution is simply given by the boundary conditions eq.(3.4) for all x , i.e.

$$f_{kn}^{(0)}(x) = \begin{cases} f_L^0(\varepsilon_{kn}), & \text{for } k > 0 \\ f_R^0(\varepsilon_{kn}), & \text{for } k < 0 \end{cases}. \quad (3.12)$$

If the wire is short or the scattering is weak, then the scattering only changes the distribution function away from the initial distribution $f^{(0)}$ by a small amount.

⁵For the collision integrals stated above, the solution is to first order in $W_{12;1'2'}$ or $W_{123;1'2'3'}$.

Therefore we expand the distribution function in orders of the scattering rate as:

$$f = f^{(0)} + f^{(1)} + \dots \quad (3.13)$$

Inserting this into the Boltzmann equation (3.3), we get:

$$v_{kn} \partial_x [f_{kn}^{(0)}(x) + f_{kn}^{(1)}(x)] + \mathcal{O}(W^2) = \mathcal{I}_{knx}[f^{(0)}] + \mathcal{O}(W^2), \quad (3.14)$$

where terms of higher order in the transition rate W have been neglected. The collision integral contains a factor of W and therefore $\mathcal{I}_{knx}[f^{(0)}]$ is to first order in W . If the scattering W does not depend on x (for $0 < x < L$), then $\mathcal{I}_{knx}[f^{(0)}]$ is x independent, since $f^{(0)}$ is x independent, i.e. $\mathcal{I}_{knx}[f^{(0)}] = \mathcal{I}_{kn}[f^{(0)}]$. This fact makes it easy to find $f^{(1)}$ from eq.(3.14) as⁶:

$$f_{kn}^{(1)}(x) = \frac{x}{v_{kn}} \mathcal{I}_{kn}[f^{(0)}] \quad \text{for } k > 0, \quad (3.15a)$$

$$f_{kn}^{(1)}(x) = \frac{x-L}{v_{kn}} \mathcal{I}_{kn}[f^{(0)}] \quad \text{for } k < 0. \quad (3.15b)$$

This gives an partial answer to how and how much the distribution function change as a function of length L for a short wire or weak scattering: For $k > 0$ the left lead injects the equilibrium distribution $f_L^0(\varepsilon_{kn})$ at $x = 0$ and then the distribution function relaxes to $f_L^0(\varepsilon_{kn}) + \frac{L}{v_{kn}} \mathcal{I}_{kn}[f^{(0)}]$ at $x = L$, which is then ejected into the right contact (see figure 3.1 and sec. 3.1). Similar for $k < 0$ the right contact injects $f_R^0(\varepsilon_{kn})$ at $x = L$, after which the wire ejects $f_R^0(\varepsilon_{kn}) - \frac{L}{v_{kn}} \mathcal{I}_{kn}[f^{(0)}]$ at $x = 0$ into the left contact.

Next the electric current I_e is found ($e > 0$):

$$I_e = \frac{(-e)}{\mathcal{L}} \sum_{\sigma nk} v_{kn} f_{kn}(x) \quad (3.16)$$

where \mathcal{L} is a normalization length. Model-wise, one can imagine the wire to be imbedded in a longer box of length \mathcal{L} , so the unperturbed eigenstates along the wire are normalized to \mathcal{L} (e.g. $\frac{1}{\sqrt{\mathcal{L}}} e^{ikx}$) and also the conversion of k -sums to integrals are with respect to this length. Of course, the final result does not depend on \mathcal{L} . However, the length of the wire and \mathcal{L} are not necessarily equal⁷.

⁶We can also find the higher order terms of the distribution function in the above described way, since we can solve the Boltzmann equation order by order. If we e.g. wanted $f^{(2)}$, we should insert $f^{(1)}$ into the collision integral and solve the equation. This iteration can -in principle- be continued to any order. However, we can see that already for $f^{(2)}$ one has to put the collision integral into the collision integral, since $f^{(1)}$ depends on $\mathcal{I}_{kn}[f^{(0)}]$. This makes the problem more and more involved to solve the higher the iteration step.

⁷Note that in paper II and III we do *not* make this distinction. However, to be precise it should be included.

The electric current to first order in the scattering is found by inserting $f = f^{(0)} + f^{(1)}$ from eq.(3.12) and (3.15) into eq.(3.16):

$$\begin{aligned}
I_e &\simeq \frac{(-e)}{\mathcal{L}} \sum_{\sigma nk} v_{kn} [f_{kn}^{(0)}(x) + f_{kn}^{(1)}(x)] \\
&= \frac{-e}{\mathcal{L}} \left[\sum_{\sigma nk > 0} v_{kn} \left(f_L^0(\varepsilon_{kn}) + \frac{x}{v_{kn}} \mathcal{I}_{kn}[f^{(0)}] \right) + \sum_{\sigma nk < 0} v_{kn} \left(f_R^0(\varepsilon_{kn}) + \frac{x-L}{v_{kn}} \mathcal{I}_{kn}[f^{(0)}] \right) \right] \\
&= \frac{(-e)}{\mathcal{L}} \sum_{\sigma nk > 0} v_{kn} [f_L^0(\varepsilon_{kn}) - f_R^0(\varepsilon_{kn})] + x \frac{(-e)}{\mathcal{L}} \overbrace{\sum_{\sigma nk} \mathcal{I}_{kn}[f^{(0)}]}^{=0} - L \frac{(-e)}{\mathcal{L}} \sum_{\sigma nk < 0} \mathcal{I}_{kn}[f^{(0)}] \\
&\equiv I_e^{(0)} + I_e^{(1)}, \tag{3.17}
\end{aligned}$$

where $I_e^{(0)}$ is the non-interacting Landauer result for integer transmission (e.g. compare to eq.(1.4) [p. 5] or eq.(1.24) [p. 12]) and $I_e^{(1)}$ is the correction to the current to first order in the scattering rate W , so $I_e^{(1)}$ is the scattering correction we set out to find. There are a few comments that should be noted about the above expression (3.17).

First of all, the term $\sum_{\sigma nk} \mathcal{I}_{kn}[f^{(0)}]$ is zero due to current conservation (to first order) eq.(3.6) and can also be seen explicitly (as in eq.(3.8)).

Secondly, the velocity in the current definition and in the first order distribution function cancel each other. This has the consequence that when inserting the collision integral in $I_e^{(1)}$, then all the wave vectors enter on equal footing, i.e. there is nothing special about the index from the Boltzmann equation $kn\sigma$. As a consequence, only scattering events that change the number of left and right moving particles can change the particle current. We take a closer look at this important statement in the next section 3.3 and show that it is true to all orders in perturbation theory.

Finally, we note that the first order current expression $I_e^{(1)}$ is proportional to the length of the wire L , i.e. $I_e^{(1)} \propto L$, regardless of the precise form of the collision integral, since it is L independent. However, the normalization length \mathcal{L} appearing in $I_e^{(1)}$ cancels out with factors from the collision integral, then taking the long wire limit and making the k -sums to integrals.

In the next chapters, we will consider the correction $I_e^{(1)}$ for two specific examples: Multi mode two-body scattering and single mode three-body scattering.

3.3 A requirement on the scattering to change the current

In this section, we show the following statement:

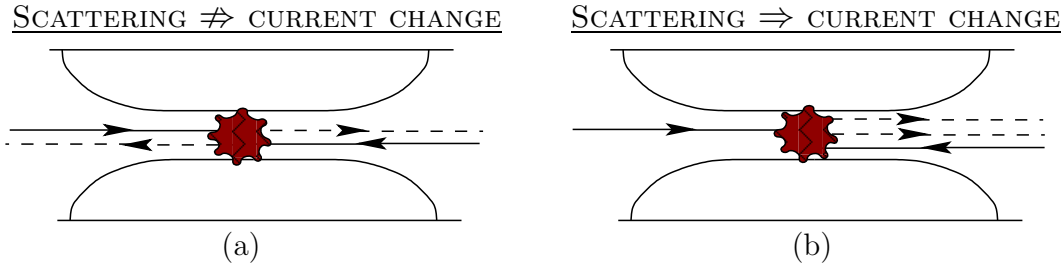


Figure 3.4: An illustration of the principle that *the current changes due to the scattering if and only if the scattering changes the number of left and right moving particles*. The full/dashed arrows represent particles before/after the scattering and the red star is (an artists impression of) the scattering event. In (a) the scattering does *not* change the number of left and right moving particles and hence not the current. The opposite situation is seen in (b). Intuitively, the statement means that it is the number of particles that pass the wire, which decides the current.

The particle current changes due to scattering if and only if the scattering changes the number of left and right moving particles.

For this statement to be true, the scattering rate needs to be symmetric under particle exchanges of (i) the incoming particles and (ii) the outgoing particles. The microscopic origin of the scattering is a priori not specified and can be two-body interactions, three-body interactions, electron-phonon interactions or any other kind that has the required symmetries of the scattering rate. An illustration for two-body scattering is given in figure 3.4.

Intuitively, the statement means that the *number* of particles passing through the wire decides the current and *not* the velocity of the particles. Therefore if the scattering in the wire does not change the number of transmitted particles, then it does not change the current. In contrast to this is e.g. an infinite 1D wire or a bulk metal⁸, where a velocity change is sufficient to change the current.

Here the above statement is shown using the Boltzmann equation (3.3) including the boundary conditions eq.(3.4)⁹. One could think that changing the velocity of a particle should change the current, since the velocity time the distribution function enters in the current definition eq.(3.16), but -surprisingly- this turns out not to be the case. Actually the origin of the statement is that *the velocity of the current definition and the distribution function cancel out* in the current due to scattering to all orders in perturbation theory (i.e. so this cancellation in eq.(3.17) was simply the first order special case). This cancellation of

⁸Of course, higher dimensional materials ($D > 1$) have more degrees of freedom than just left and right movers (with respect to some direction), so not only forward or backward scattering is possible.

⁹However, we speculate it to be independent of the Boltzmann equation approach and therefore of a more general nature.

the velocities is very similar to the cancellation leading to the Landauer formula (see eq.(1.24)) and also in this case it is a special feature of one dimension.

Next we give the explicit arguments for the above statement. We begin by formally rewriting the Boltzmann equation (3.3) including the boundary conditions as:

$$f_{kn}(x) = f_L^0(\varepsilon_{kn}) + \int_0^x dx' \frac{\mathcal{I}_{knx'}[f]}{v_{kn}} \quad \text{for } k > 0, \quad (3.18a)$$

$$f_{kn}(x) = f_R^0(\varepsilon_{kn}) + \int_L^x dx' \frac{\mathcal{I}_{knx'}[f]}{v_{kn}} \quad \text{for } k < 0. \quad (3.18b)$$

This is not a closed solution to the Boltzmann equation, since the distribution function appears in $\mathcal{I}_{knx'}[f]$ on the right hand side¹⁰. The (exact) current is found by inserting eq.(3.18) into the current definition eq.(3.16):

$$\begin{aligned} I_e &= \frac{(-e)}{\mathcal{L}} \sum_{\sigma nk > 0} v_{kn} [f_L^0(\varepsilon_{kn}) - f_R^0(\varepsilon_{kn})] \\ &\quad + \frac{(-e)}{\mathcal{L}} \sum_{\sigma nk > 0} \int_0^x dx' \mathcal{I}_{knx'}[f] + \frac{(-e)}{\mathcal{L}} \int_L^x dx' \sum_{\sigma nk < 0} \mathcal{I}_{knx'}[f] \\ &= I_e^{(0)} - \frac{(-e)}{\mathcal{L}} \int_0^L dx \sum_{\sigma nk < 0} \mathcal{I}_{knx}[f] + \frac{(-e)}{\mathcal{L}} \int_0^x dx' \overbrace{\sum_{\sigma nk} \mathcal{I}_{knx'}[f]}^{=0} \equiv I_e^{(0)} + I_e^{(\text{int})}, \end{aligned} \quad (3.19)$$

where the integrals were manipulated as $\int_L^x = \int_L^0 + \int_0^x$ and the restriction on $\mathcal{I}_{knx'}[f]$ due to current conservation eq.(3.6) make the x -depend term vanish. Here we have found the current change due to scattering $I_e^{(\text{int})}$ and seen that in this term the velocity from the current definition and distribution function cancels. Note the connection to the first order calculation eq.(3.17): $I_e^{(\text{int})} = I_e^{(1)} + \mathcal{O}(W^2)$. Note also that the above derivation does not distinguish between local and non-local collision integrals. It is important to stress that this does not solve the problem, since the unknown distribution function still enters the current, however, we can get information out from this form as we shall see now.

To show that the scattering events that conserve the number of left and right movers do not change the current $I_e^{(\text{int})}$, we focus on a specific example: Three-particle scattering in a single band. The other cases like two-body scattering or electron-phonon scattering are done easily after seeing this example. The current contribution due to three-body interactions are found by inserting

¹⁰This rewriting might enlighten the iterative scheme, which could be follow to find the distribution function numerically or otherwise.

the three-particle collision integral eq.(3.11) into $I_e^{(\text{int})}$ eq.(3.19)¹¹:

$$I_e^{(\text{int})} = \frac{(-e)}{\mathcal{L}} \int_0^L dx \sum_{\substack{\sigma_1 \sigma_2 \sigma_3 \\ \sigma_{1'} \sigma_{2'} \sigma_{3'}}} \sum_{\substack{k_1 < 0, k_2, k_3 \\ k_{1'} k_{2'} k_{3'}}} \left\{ W_{1'2'3';123} f_1 f_2 f_3 (1 - f_{1'}) (1 - f_{2'}) (1 - f_{3'}) \right. \\ \left. - W_{123;1'2'3'} f_{1'} f_{2'} f_{3'} (1 - f_1) (1 - f_2) (1 - f_3) \right\}. \quad (3.20)$$

Next we can divide the summation over the k quantum numbers into positive ($k > 0$) and negative ($k < 0$) intervals and to this end, we introduce the convenient notation:

$$\sum_{\substack{k_1 < 0, k_2 > 0, k_3 < 0 \\ k_{1'} > 0, k_{2'} > 0, k_{3'} < 0}} (\cdot) \equiv \sum_{\substack{-+- \\ ++-}} (\cdot), \quad \sum_{\substack{\sigma_1 \sigma_2 \sigma_3 \\ \sigma_{1'} \sigma_{2'} \sigma_{3'}}} (\cdot) \equiv \sum_{\text{spin}} (\cdot), \quad (3.21)$$

where the order of the k_1, k_2 etc. matters.

If the scattering conserves the number of left and right movers, then the number of positive (and negative) k quantum numbers before and after the scattering remains the same. Therefore we want to show that terms in $I_e^{(\text{int})}$ that have the same number of positive and negative k numbers before and after the scattering are zero. We take an illustrative example of this, where one can also see the importance of the symmetry of particle interchange in $W_{123;1'2'3'}$:

$$\begin{aligned} & \sum_{\text{spin}} \sum_{\substack{-+- \\ +--}} \left[W_{1'2'3';123} f_1 f_2 f_3 (1 - f_{1'}) (1 - f_{2'}) (1 - f_{3'}) \right. \\ & \quad \left. - W_{123;1'2'3'} f_{1'} f_{2'} f_{3'} (1 - f_1) (1 - f_2) (1 - f_3) \right] \\ &= \overbrace{\sum_{\text{spin}} \sum_{\substack{-+- \\ +--}}^{1' \leftrightarrow 2'}} \left[W_{2'1'3';123} f_1 f_2 f_3 (1 - f_{1'}) (1 - f_{2'}) (1 - f_{3'}) \right. \\ & \quad \left. - W_{123;2'1'3'} f_{1'} f_{2'} f_{3'} (1 - f_1) (1 - f_2) (1 - f_3) \right] \\ &= \sum_{\text{spin}} \sum_{\substack{-+- \\ +--}} W_{1'2'3';123} f_1 f_2 f_3 (1 - f_{1'}) (1 - f_{2'}) (1 - f_{3'}) \\ & \quad - \sum_{\text{spin}} \sum_{\substack{-+- \\ +--}} \underbrace{W_{123;1'2'3'} f_{1'} f_{2'} f_{3'} (1 - f_1) (1 - f_2) (1 - f_3)}_{\text{interchange } (123) \rightleftharpoons (1'2'3')} = 0, \quad (3.22) \end{aligned}$$

where $1'$ and $2'$ were interchanged at the first equality and in the second equality we used that the scattering rate is assumed to be symmetric under particle exchange among the initial and final states respectively, e.g. $W_{123;1'2'3'} = W_{123;2'1'3'}$.

¹¹Here we drop the subband index n for simplicity. However, the statement is still true including it.

All order terms having the same number of positive (negative) k quantum numbers cancel in the same way. Therefore we have now showed that the scattering have to change the number of left and right movers to change the current. Note that the statement is not limited to three-particle interactions and the same proof can be given e.g. in the case of multi-mode two-particle scattering or electron-phonon scattering (as long as the scattering rate has the required symmetries).

However, the distribution function *can* be changed by processes that conserve the number of left and right moving particles. This change of the distribution function can make processes that change the number of left and right movers more probable and -in this indirect way- change the current. This is a higher order effect in the scattering rate and could therefore become important in the non-perturbative regime. However, note that if there do not exist any processes that changes the number of left and right movers, then the current never changes - no matter the order.

3.4 Outlook

In this chapter, we have found the current due to electronic scattering in the Boltzmann equation approach for a wire perfectly connected to external leads. To first order in the scattering rate this contribution is:

$$I_e^{(1)} = -L \frac{(-e)}{\mathcal{L}} \sum_{\sigma n k < 0} \mathcal{I}_{kn}[f^{(0)}], \quad (3.23)$$

where $f^{(0)}$ is the initial distribution function of the leads. This term stems from the scattering such as electron-electron interaction or electron-phonon interaction and is an extension of the famous Landauer formula (for integer transmission). We also discussed the statement that the scattering has to change the number of left and right movers to change the current of the wire. In the next chapters, we are going to consider $I_e^{(1)}$ in the case of multi-mode two-body scattering and single-mode three-body scattering.

Chapter 4

Interaction-induced resonances in multi-mode wires

In this chapter, we consider two-body multi-mode electronic interactions perturbatively in a wire perfectly connected to external leads. The Boltzmann equation approach of chapter 3 is used. We find interaction induced resonances in the conductance and thermopower as a function of the Fermi level (i.e. gate voltage). Surprisingly, the Mott formula is found to be a good approximation. Furthermore, the splitting of the resonances in a magnetic field is studied. These results are published in paper II (p. 153).

4.1 The physical picture of the interaction-induced resonances

Before we give a detailed account of the calculations, we try to give a physical picture of the interaction induced resonances as a function of the Fermi level. We focus on how it come about and how it affects the conductance and thermopower with and without a magnetic field.

4.1.1 Interaction-induced resonances at certain Fermi energies

Here we consider wires long enough for the electron-electron interaction to be momentum and energy conserving. Furthermore, as we found in section 3.3, the particle current changes *if and only if* the number of left and right movers change in the interaction process. The interaction process also have to happen *near the Fermi level*, otherwise the processes will be exponentially suppressed in temperature by the filled Fermi sea. Here we consider perturbative effects only, so a redistribution of the Fermi sea due to higher order processes in the interaction is not taken into account. In section 1.8, we saw that in 1D the momentum and

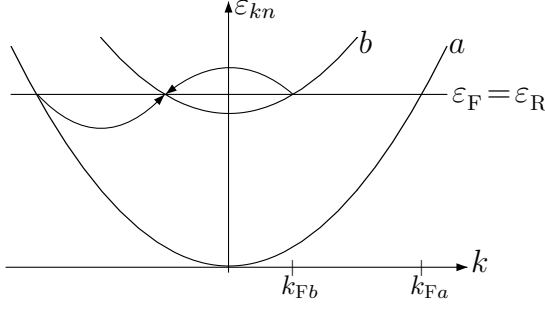


Figure 4.1: An energy and momentum conserving electron-electron interaction process that also changes the number of left and right movers. For this to happen near ε_F , we have to require that $k_{Fa} = 3k_{Fb}$. If the Fermi level is increased or decreased, then the process no longer conserves momentum at the Fermi level, i.e. we have identified a resonance $\varepsilon_F = \varepsilon_R$.

energy conservation forbids the electrons to redistribute due to two-body intra-band interaction processes. Therefore we have to consider inter-band processes. To summarize, the relevant interaction processes have to

- conserve energy,
- conserve momentum,
- change the number of left and right movers,
- have final and initial states near the Fermi level and
- be inter-band interaction processes.

This is only possible for certain values of the Fermi level¹ ε_F , or equivalently, the gate voltage. Therefore as the Fermi level is varied the special points will appear at certain values of ε_F .

In the case of two modes, labelled as $n = a$ (the lowest one) and $n = b$, the situation is seen on figure 4.1. At the special resonance point $\varepsilon_F = \varepsilon_R$ all the above requirements for the interaction process are fulfilled. At the resonance point, momentum conservation at the Fermi level leads to the following requirement for the Fermi wave vectors of the two modes:

$$k_{Fb} - k_{Fa} = -2k_{Fb} \quad \Rightarrow \quad k_{Fa} = 3k_{Fb}, \quad (4.1)$$

i.e. they need to have a ratio of 3 to 1. We use quadratic bands ε_{kn} ,

$$\varepsilon_{ka} = \frac{\hbar^2 k^2}{2m}, \quad \varepsilon_{kb} = \frac{\hbar^2 k^2}{2m} + \varepsilon_0, \quad (4.2)$$

where m is the effective mass and ε_0 the spacing between the two first subbands ($\varepsilon_0 = \varepsilon_{k=0b} - \varepsilon_{k=0a}$). For simplicity the effective mass is taken to be equal for the two bands, $m_a = m_b \equiv m$. Therefore at the resonance, $k_{Fa} = 3k_{Fb}$, the energy is:

$$\varepsilon_R = \frac{9}{8} \varepsilon_0 \quad (\text{quadratic bands}) \quad (4.3)$$

¹Note that at low temperature, the chemical potential and the Fermi level are equal; Keeping in mind that the Fermi level is defined as the zero temperature chemical potential.

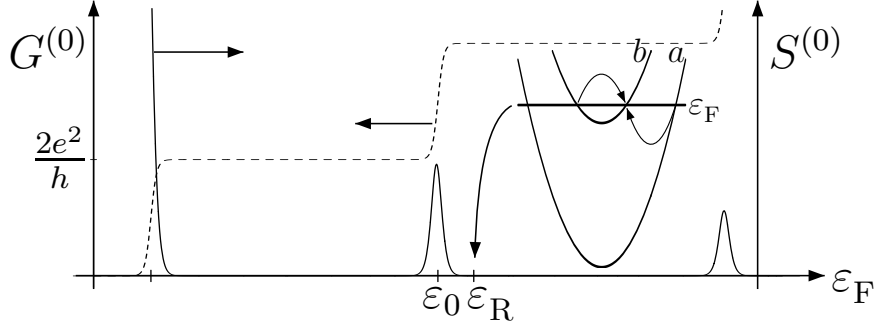


Figure 4.2: The non-interacting conductance $G^{(0)}$ (dashed line) and non-interacting thermopower $S^{(0)}$ (full line) versus the Fermi energy ε_F . We point out the special resonance point $\varepsilon_F = \varepsilon_R$, where a dip in the conductance and a wave in the thermopower is predicted to appear as will be explained in section 4.1.2 and 4.1.3.

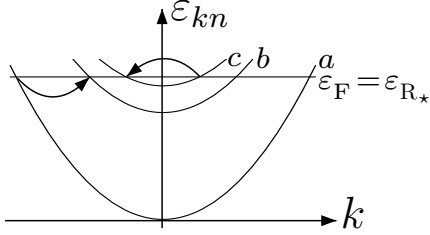


Figure 4.3: An example of a resonance in the case of three modes. Again, the scattering conserves momentum and energy and changes the number of left and right movers. The requirement here is $k_{Fa} = 2k_{Fc} + k_{Fb}$ to have a resonance. In the figure, the subband spacing is $\varepsilon_1 = \varepsilon_0/4$, see eq.(4.6)

using the definition

$$\varepsilon_F = \frac{\hbar^2 k_{Fa}^2}{2m} = \frac{\hbar^2 k_{Fb}^2}{2m} + \varepsilon_0. \quad (4.4)$$

The fraction $9/8$ changes for a non-quadratic dispersion relation or if $m_a \neq m_b$, but $k_{Fa} = 3k_{Fb}$ stemming from momentum conservation remains true. This is the only resonance for two modes. The position of the resonance is just after the second mode appears as a function of the Fermi energy as seen in figure 4.2. The effect of the resonance on the conductance and thermopower will be explained shortly.

If we have three or more modes, then more resonances will appear. An example of a resonance for three modes is seen on figure 4.3 and momentum conservation requires

$$k_{Fa} = 2k_{Fc} + k_{Fb} \quad (4.5)$$

at the resonance. For quadratic bands

$$\varepsilon_{ka} = \frac{\hbar^2 k^2}{2m}, \quad \varepsilon_{kb} = \frac{\hbar^2 k^2}{2m} + \varepsilon_0, \quad \varepsilon_{kc} = \frac{\hbar^2 k^2}{2m} + \varepsilon_0 + \varepsilon_1, \quad (4.6)$$

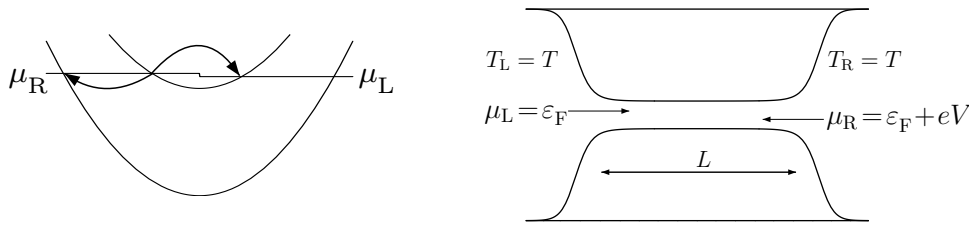


Figure 4.4: An illustration of how the scattering at the resonance $\varepsilon_F = \varepsilon_R$ leads to a conductance dip. Without the interaction (and $V > 0$), the left movers have a higher chemical potential than the right movers and the particle current is from the right to the left contact (so $I_e^{(0)} = \frac{4e^2}{h}V > 0$). At the resonance point, $\varepsilon_F = \varepsilon_R$, the interaction will effectively produce more right movers (since $\mu_R > \mu_L$), which in terms reduces the particle current. By moving away from the resonance point, $\varepsilon_F \lesseqgtr \varepsilon_R$, the scattering is suppressed by the Fermi sea. Therefore we obtain a dip in conductance at the resonance point.

this leads to a resonance energy of the form

$$\varepsilon_{R*} = \varepsilon_0 + \varepsilon_1 + \frac{\varepsilon_0^2}{8(\varepsilon_0 + 2\varepsilon_1)} \quad (\text{quadratic bands}), \quad (4.7)$$

which moves closer to the conductance step at $\varepsilon_F = \varepsilon_0 + \varepsilon_1$ for increasing $\varepsilon_1/\varepsilon_0$ (and for $\varepsilon_1 = \varepsilon_0$ the resonance is at $\varepsilon_{R*} = 49\varepsilon_0/24$). Another resonance for three modes is the one similar to the two band situation (figure 4.1) $k_{Fa} = 3k_{Fc}$ or in energy for quadratic bands $\frac{9}{8}(\varepsilon_0 + \varepsilon_1)$.

Therefore by tuning the gate voltage, i.e. the Fermi level ε_F , the resonances will appear at different special values, see figure 4.2. The next question is what kind of signal one should expect at these resonance points. In the following, we focus exclusively on the two mode case seen in figure 4.1.

4.1.2 Conductance dip at the resonance

For two fully open modes the non-interacting conductance is $G^{(0)} = 4e^2/h$. The effect of the interaction-induced resonance is a dip (i.e. a negative peak) at $\varepsilon_F = \varepsilon_R$ as will be argued in the following. Remember that a *left* mover comes from the *right* lead and vice versa.

In the scattering process seen on figure 4.1, a right mover is backscattered to a left mover. The opposite is of course also possible at $\varepsilon_F = \varepsilon_R$. Therefore if there is no difference between the left and right movers, then the scattering processes does not redistribute left and right movers.

However, if we apply a bias, then the left and right movers will have different chemical potentials as seen on figure 4.4(left). In this situation, there will be a tendency to scatter particles from the higher to the lower chemical potential at the resonance, i.e. for $\mu_R > \mu_L$ this will create more right movers. The non-interacting

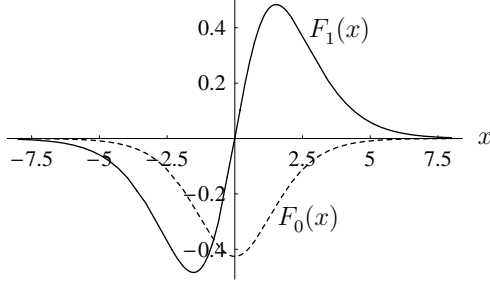


Figure 4.5: The dimensionless scaling functions $F_0(x)$ and $F_1(x)$ entering the conductance correction eq.(4.8) and the interaction-induced thermopower eq.(4.11), respectively.

particle current for $\mu_R > \mu_L$ will have an excess of left movers² (see figure 4.4), so the resonance reduces the conductance at $\varepsilon_F = \varepsilon_R$ compared to $4e^2/h$. Due to momentum conservation, the resonant scattering have to happen near $\varepsilon_F = \varepsilon_R$, so by tuning ε_F away from ε_R the scattering process will be suppressed by the Fermi sea. This leads to a dip in the conductance at the resonance.

Qualitative prediction of the conductance dip

The interaction induced correction to the conductance $G^{(0)} = 4e^2/h$ is:

$$G^{(1)} = \frac{4e^2}{h} \frac{L}{\ell_{ee}} \frac{T}{T_F} F_0 \left(\frac{\varepsilon_F - \varepsilon_R}{k_B T} \right), \quad (4.8)$$

which is to lowest order in temperature and perturbative in the interaction. Here $F_0(x)$ is a dimensionless function seen in figure 4.5 and ℓ_{ee} is the effective scattering length for the described scattering at the resonance (seen in figure 4.1) given by

$$\ell_{ee} = \frac{2}{27} \frac{2\pi}{k_{Fa}} \left(\frac{\hbar v_{Fa}}{|V_{2k_{Fb}}^{babb}|} \right)^2, \quad (4.9)$$

where $v_{Fa} = \hbar k_{Fa}/m$ and $V_{2k_{Fb}}^{babb}$ is the inter band electron-electron interaction for the process seen in figure 4.1 with a momentum change of $2k_{Fb}$. Therefore the correction is proportional to the interaction squared, the length of the wire L and temperature: $G^{(1)} \propto L |V_{2k_{Fb}}^{babb}|^2 T$. The dimensionless function $F_0(x)$ is a negative peak, so the width of the conductance dip is of order a few $k_B T$. The explicit form of $F_0(x)$ will be derived in section 4.3.

The expression for $G^{(1)}$ is valid for

$$L \ll (T_F/T) \ell_{ee}, \quad (4.10)$$

which amount to short lengths, low temperatures, weak scattering or a combination them. Note that this is the range, where the Luttinger liquid physics is not relevant for a finite 1D system connected to the leads, see eq.(1.30). For longer wires, the resonance still exists, but it is not described by the form above.

²Of course, this assumes that $V > 0$ in figure 4.4(right), so that $I_e^{(0)} = \frac{4e^2}{h} V > 0$

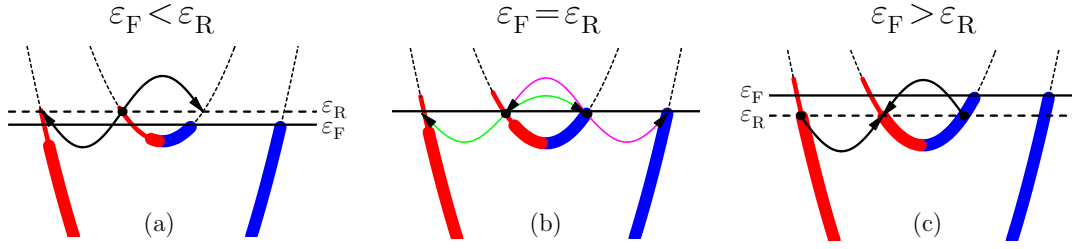


Figure 4.6: A physical picture of the how the interaction induces a sign change of the thermopower at the resonance. The right movers (blue) have a lower temperature than the left movers (red) and therefore the left movers have a larger smearing of the Fermi level illustrated by the thin red lines. (Of course, the degree of smearing is largely exaggerated for illustrative purposes.) The dashed black lines are unpopulated energy bands. Due to momentum conservation the scattering have to happen at the resonance ε_R . Therefore (and due to the temperature difference) the interaction for $\varepsilon_F < \varepsilon_R$ leads to more right movers in contrast to $\varepsilon_F > \varepsilon_R$, which leads to more left movers and hence a sign-change of the current due to a temperature difference $T_R - T_L > 0$ is found.

4.1.3 Sign change of the thermopower at the resonance

The non-interacting thermopower is exponentially suppressed in temperature on the conductance plateaus, see section 1.5.2. Here we argue that the interaction induces a sign change in the thermopower S at the resonance $\varepsilon_F = \varepsilon_R$ from $S(\varepsilon_F < \varepsilon_R) < 0$ to $S(\varepsilon_F > \varepsilon_R) > 0$. Furthermore, if $|\varepsilon_F - \varepsilon_R| \gtrsim 5k_B T$, then S is exponentially suppressed in temperature. Therefore we predict a wave-like structure centered at $\varepsilon_F = \varepsilon_R$.

To understand the thermopower $S = G_T/G$, it is enough to understand G_T . Therefore consider a wire only with a temperature difference across: $\mu_R = \mu_L$ and $T_R = T + \Delta T > T_L = T$. In this case, the non-interacting particle current is from the right to the left lead: $I_e^{(0)} \propto e^{-T_{Fb}/T} \Delta T > 0$, where $T_{Fb} \equiv (\varepsilon_F - \varepsilon_0)/k_B$. Figure 4.6 shows the three situations: $\varepsilon_F < \varepsilon_R$, $\varepsilon_F = \varepsilon_R$ and $\varepsilon_F > \varepsilon_R$, which we will now consider one by one.

Exactly at the resonance, $\varepsilon_F = \varepsilon_R$, the difference in temperature between the left and right movers does not lead to any preference for scattering, which produces an excess of left or right movers, i.e. the purple and green scattering processes on figure 4.6(b) are equally³ likely. In other words, the difference in smearing of the Fermi level of the right and left movers, does not give a different in the scattering at $\varepsilon_F = \varepsilon_R$. Therefore the interaction does not produce thermopower at $\varepsilon_F = \varepsilon_R$.

Next consider the Fermi level below the resonance, $\varepsilon_F < \varepsilon_R$, but still within a few $k_B T$ from ε_R . Due to momentum conservation, the interaction process

³As we shall see later, the curvature of the band induces a slight difference between left and right movers leading to a small thermopower. However, this effect is to higher order in temperature and only shifts the zero of the sign-change of the thermopower.

still has to happen near the resonance energy. The left movers have a higher temperature and therefore their Fermi level is more smeared out. This gives more left movers (than right movers) with an energy near ε_R , which can scatter into a right moving state⁴, see figure 4.6(a). Therefore more right movers are created and hence a negative electric current, i.e. negative G_T and thermopower.

In the opposite case, $\varepsilon_F > \varepsilon_R$, seen on figure 4.6(c), the right moving states near ε_R have a larger tendency to be filled than the left moving ones⁵ (since $T_R > T_L$). Therefore the scattering is mainly out of the right moving states and hence producing more left movers and in terms a positive electric current, i.e. a positive thermopower.

Therefore we have seen that $S(\varepsilon_F < \varepsilon_R) < 0$ and $S(\varepsilon_F > \varepsilon_R) > 0$ and hence the thermopower S must change sign. Furthermore, if the Fermi level is tuned far away from the resonance (more than a few $k_B T$), then for $\varepsilon_F \ll \varepsilon_R$ there are simply no electrons with an energy near ε_R and for $\varepsilon_F \gg \varepsilon_R$ all the states near ε_R are completely filled, i.e. we have an exponential suppression for $|\varepsilon_F - \varepsilon_R| \gg k_B T$ due to Fermi factors. In conclusion, the interaction at the resonance induces a thermopower with a wave-like structure centered at the resonance.

Qualitative prediction of the interaction-induced thermopower

Since the non-interaction thermopower $S^{(0)}$ is exponentially suppressed in temperature, the interaction-induced thermopower $S^{(1)}$ completely dominates the thermopower: $S = S^{(0)} + S^{(1)} + \dots \simeq S^{(1)}$. Therefore to lowest order in temperature and perturbative in the interaction the thermopower is

$$S = \frac{k_B}{e} \frac{L}{\ell_{ee}} \frac{T}{T_F} F_1 \left(\frac{\varepsilon_F - \varepsilon_R}{k_B T} \right), \quad (4.11)$$

where the length ℓ_{ee} is given in eq.(4.9) and $F_1(x)$ is a dimensionless function seen in figure 4.5. We see the wave-like structure of $S \propto F_1[(\varepsilon_F - \varepsilon_R)/k_B T]$, which we have argued for above. As in the case of the conductance correction, we see that $S \propto L |V_{2k_F}^{babb}|^2 T$.

4.1.4 The conductance and thermopower have scaling forms

An interesting observation is that the conductance correction $G^{(1)}$ eq.(4.8) and the interaction-induced thermopower eq.(4.11) have a *scaling form* as a function of the Fermi level at low temperatures in the sense that the dimensionless functions only depend on $(\varepsilon_F - \varepsilon_R)/k_B T$. This means that measurements performed at different (low) temperatures are predicted to collapse to a single curve, when the

⁴In the extreme case of zero temperature of the right moving electrons, there are simply no right moving electrons near ε_R and therefore no production of left moving electrons.

⁵Again in the extreme case of zero temperature right movers, it is impossible to scatter into the filled right moving Fermi sea and hence only left moving electrons are produced.

data is properly scaled. These curves are the dimensionless functions $F_0(x)$ and $F_1(x)$ seen in figure 4.5 for the conductance and thermopower, respectively.

4.2 Is the resonant scattering observable?

An order of magnitude estimate

Before we dwell into the calculation of G and S near the resonance, we discuss the possibility of actually observing it.

To the best of our knowledge, nobody has observed it yet (or tried to) in the traditional QPC's made in semiconductor heterostructures even though they have been around for a couple of decades now⁶. However, the effect might also be found in other 1D systems, such as the cleaved-edge overgrowth 1D wires by Jacobi *et al.* [80]. Furthermore, measuring thermopower in experiments is more difficult than measuring the conductance.

One of the reasons, it might be hard to find the resonance is the position at $\varepsilon_F = 9\varepsilon_0/8$. This is either in the beginning of the second conductance plateau or in the worst case on the step between the first and second plateau depending on the smearing of the steps (determent by temperature and the QPC potential). In the case that ε_R is on the step, or equivalently, in the non-interacting thermopower peak, then the resonance might be difficult to distinguish on top of the non-interacting signal. At least in principle, it is a matter of engineering and low temperature to make sure that the resonance is on the second plateau and in this case it might be possible to observe the resonance in G and S . Also as we shall see, the magnetic field dependence is a good candidate for experimental verification.

Let us now turn to the magnitude of the resonant signal in G and S . Here we simply give a very rough order of magnitude estimate. From Appleyard *et al.* [31] we extract that $\varepsilon_0 \sim 10$ meV from the subband spacing in their QPC's. Therefore near the resonance $T_{Fa} \sim 110$ K, $T_{Fb} \sim 10$ K and $k_{Fa}^{-1} \sim 7$ nm using the effective mass $m^* = 0.067m_e$ for GaAs. The interaction is difficult to estimate, because it depends on many effects like screening, but roughly it is $|V_{2k_{Fb}}^{babb}| \sim e^2/4\pi\epsilon_0^*$, where $\epsilon_0^* \simeq 13\epsilon_0$ (ϵ_0 being the vacuum permittivity). This leads to

$$\frac{\hbar v_{Fa}}{V_{2k_{Fb}}^{babb}} \sim k_{Fa} a_0^* = k_{Fa} a_0 \frac{13}{0.067} \sim 1.4, \quad (4.12)$$

⁶In an unpublished paper from 2004 by Proskuryakov, Nicholls, Hadji-Ristic, Kristensen and Sørensen, some shoulder-like feature on the second single-particle thermopower peak is observed, which *could be* the discussed effect. However, it violates the Mott formula in contrast to the interaction-induced thermopower effect. In the same paper, a negative thermopower is observed near the 0.7 structure. It would require more experimental work to make any definite conclusions, however, the present author might - of course - be easily convinced!

where $a_0 = \frac{\hbar^2}{m_e e^2 / 4\pi\epsilon_0}$ is the Bohr radius and a_0^* is the effective Bohr radius. This gives $\ell_{ee} \sim 7$ nm, which is much smaller than a typical length $L \sim 100$ nm. Therefore $T_{Fa}\ell_{ee}/L \sim 110\text{K} \frac{7\text{nm}}{100\text{nm}} \sim 8$ K and the prefactor for say $T \sim 1$ K is about 0.1, so using $F_0(0) \sim 0.4$ the conductance dip is of order a few $\sim 4\%$ percent of $4e^2/h$ and like-wise for the interaction-induced thermopower wave⁷.

However, this might be a overestimation, since the interaction is an *inter*-band interaction and therefore suppressed compared to an intra-band interaction by the orthogonality of the transverse eigenstates. This statement will be more clear later, see p. 61. Instead of estimating the interaction, it will be possible to extract it from the experiment and in this way, measuring the thermopower signal would be a direct way to measure the inter-band interaction. A quantity which is hard to get by other methods.

4.3 The current to lowest order in the interaction

In this section, we will give a detailed calculation of the conductance correction $G^{(1)}$ in eq.(4.8) and the interaction-induced thermopower in eq.(4.11). The reason for the many details is that paper II (p. 153) was only a four page paper not leaving room for details.

The calculation is an application of the Boltzmann equation approach discussed in chapter 3. Here the electric current I_e is expanded in orders of the scattering rate $W_{12;1'2'}$ (proportional to the interaction strength squared) as

$$I_e = I_e^{(0)} + I_e^{(1)} + \dots, \quad (4.13)$$

where $I_e^{(0)}$ is the non-interacting result, see section 3.2.3. Therefore the starting point is to find the electric current to first order in the scattering rate given by eq.(3.17) as

$$I_e^{(1)} = -L \frac{(-e)}{\mathcal{L}} \sum_{\sigma_1 n_1 k_1 < 0} \mathcal{I}_{k_1 n_1}[f^{(0)}], \quad (4.14)$$

where the relevant collision integral $\mathcal{I}_{k_1 n_1}[f]$ is the two-body collision integral eq.(3.7):

$$\mathcal{I}_{k_1 n_1}[f] = - \sum_{\substack{\sigma_2 \\ \sigma_1' \sigma_2' n_1' n_2' k_1' k_2'}} \sum_{n_2} \sum_{k_2} W_{12;1'2'} [f_1 f_2 (1 - f_{1'}) (1 - f_{2'}) - f_{1'} f_{2'} (1 - f_1) (1 - f_2)], \quad (4.15)$$

where we use the short hand notation $f_1 = f_{k_1 n_1}(x)$ and suppress the spin index completely in the notation. The labelling is such that the states before (after)

⁷Interestingly, this estimate shows that the non-perturbative regime $(L/\ell_{ee})(T/T_F) \gtrsim 1$ might not be out of reach experimentally.

the scattering are unprimed (primed), see figure 3.2. The scattering rate is here symmetric and found by using Fermis Golden rule:

$$W_{12;1'2'} = \frac{2\pi}{\hbar} |\langle k_1' n_1' k_2' n_2' | \mathcal{V} | k_1 n_1 k_2 n_2 \rangle|^2 \delta(\varepsilon_1 + \varepsilon_2 - \varepsilon_{1'} - \varepsilon_{2'}), \quad (4.16)$$

where $\varepsilon_i = \varepsilon_{k_i n_i}$, \mathcal{V} is the electron-electron interaction operator and the matrix element contains both an direct and exchange term. The non-interacting distribution function $f^{(0)}$ that we need to insert in eq.(4.14) is given by the reservoirs:

$$f_{kn}^{(0)} = f_L^0(\varepsilon_{kn})\theta(k) + f_R^0(\varepsilon_{kn})\theta(-k). \quad (4.17)$$

Linear response in ΔT and V and the non-interacting current

Now we calculate the current $I_e^{(0)}$ and $I_e^{(1)}$ to linear order in the apply bias V and temperature difference ΔT , i.e. in the linear response limit. The temperatures and chemical potentials of the two reservoirs are taken to be:

$$T_L = T, \quad T_R = T + \Delta T, \quad \mu_L = \varepsilon_F + eV, \quad \mu_R = \varepsilon_F. \quad (4.18)$$

With this convention for V and ΔT we have

$$I_e = -GV + G_T \Delta T. \quad (4.19)$$

Note that in linear response it does not matter that we apply ΔT and V asymmetrically, but we do it for calculational simplicity. With the above convention for V and ΔT the non-interacting current $I_e^{(0)}$ eq.(3.17) for the two bands in eq.(4.2) in linear response becomes:

$$\begin{aligned} I_e^{(0)} &= \frac{(-e)}{\mathcal{L}} \sum_{n=a,b} \sum_{\sigma k > 0} v_{kn} (f_L^0(\varepsilon_{kn}) - f_R^0(\varepsilon_{kn})) \\ &= -\frac{2e^2}{h} V \left[h \left(\frac{T_F}{T} \right) + h \left(\frac{T_{Fb}}{T} \right) \right] + \frac{2e}{h} k_B \Delta T \left[D \left(\frac{T_F}{T} \right) + D \left(\frac{T_{Fb}}{T} \right) \right], \end{aligned} \quad (4.20)$$

where

$$T_F = \varepsilon_F / k_B, \quad T_{Fb} \equiv (\varepsilon_F - \varepsilon_0) / k_B, \quad (4.21)$$

$D(x) = \frac{x}{1+e^x} + \ln(1 + e^{-x})$ and $h(x) = \frac{1}{1+e^{-x}}$. To lowest non-vanishing order in temperature $T \ll T_{Fb} \ll T_F$ this is

$$I_e^{(0)} = -\frac{4e^2}{h} V + \frac{2e}{h} \frac{T_{Fb}}{T} e^{-T_{Fb}/T} k_B \Delta T, \quad (4.22)$$

which only has exponential corrections on the conductance plateau.

As a general tool, we introduce the deviation $\psi_{kn}(x)$ from the equilibrium distribution function by the relation [115]

$$f_{kn}(x) = f^0(\varepsilon_{kn}) + f^0(\varepsilon_{kn})[1 - f^0(\varepsilon_{kn})]\psi_{kn}(x). \quad (4.23)$$

This definition is a cleaver one, if the distribution function changes mostly around the Fermi level. To first order in ψ , the term in the square bracket of the collision integral eq.(4.15) becomes:

$$\begin{aligned} f_1 f_2 (1 - f_{1'}) (1 - f_{2'}) - f_{1'} f_{2'} (1 - f_1) (1 - f_2) = \\ f_1^0 f_2^0 (1 - f_{1'}^0) (1 - f_{2'}^0) [\psi_1 + \psi_2 - \psi_{1'} - \psi_{2'}] + \mathcal{O}(\psi^2) \end{aligned} \quad (4.24)$$

using the H -theorem $f_1^0 f_2^0 (1 - f_{1'}^0) (1 - f_{2'}^0) = f_{1'}^0 f_{2'}^0 (1 - f_1^0) (1 - f_2^0)$ valid for energy conserving scattering and the short hand notation $\psi_i = \psi_{k_i n_i}(x)$ and $f_i^0 = f^0(\varepsilon_{k_i n_i})$.

In our case, we only use this general expression to get the linear response limit of $I_e^{(1)}$. To this end, we expand the Fermi functions for the left and right lead as:

$$f_L^0(\varepsilon_{kn}) = f^0(\varepsilon_{kn}) + [-\partial_\varepsilon f^0(\varepsilon_{kn})] eV + \mathcal{O}(V^2), \quad (4.25a)$$

$$f_R^0(\varepsilon_{kn}) = f^0(\varepsilon_{kn}) + [-\partial_\varepsilon f^0(\varepsilon_{kn})] (\varepsilon_{kn} - \varepsilon_F) \frac{\Delta T}{T} + \mathcal{O}(\Delta T^2), \quad (4.25b)$$

where $f^0(\varepsilon_{kn})$ is the Fermi function with the equilibrium temperature T and Fermi energy ε_F inserted. By noting the identity

$$f^0(\varepsilon)(1 - f^0(\varepsilon)) = k_B T [-\partial_\varepsilon f^0(\varepsilon)] \quad (4.26)$$

and using eq.(4.25), the zeroth order deviation $\psi_{kn}^{(0)}$ from the equilibrium distribution function is identified to be

$$\psi_i^{(0)} = \begin{cases} \frac{eV}{k_B T}, & \text{for } k_i > 0 \\ \frac{\varepsilon_{k_i n_i} - \varepsilon_F}{k_B T} \frac{\Delta T}{T}, & \text{for } k_i < 0 \end{cases}. \quad (4.27)$$

Therefore to find $I_e^{(1)}$ eq.(4.14) to linear order in V and ΔT , we insert $\psi^{(0)}$ eq.(4.27) into eq.(4.24) and then into the collision integral $\mathcal{I}_{k_1 n_1}[f^{(0)}]$ eq.(4.15), i.e.

$$I_e^{(1)} = L \frac{(-e)}{\mathcal{L}} \sum_{\substack{\sigma_1 \sigma_2 \\ \sigma_{1'} \sigma_{2'}}} \sum_{\substack{n_1 n_2 \\ n_{1'} n_{2'}}} \sum_{\substack{k_1 < 0, k_2 \\ k_{1'} k_{2'}}} \Delta_{12;1'2'} [\psi_1^{(0)} + \psi_2^{(0)} - \psi_{1'}^{(0)} - \psi_{2'}^{(0)}] + \mathcal{O}(V^2, \Delta T^2), \quad (4.28)$$

where

$$\Delta_{12;1'2'} \equiv W_{12;1'2'} f_1^0 f_2^0 (1 - f_{1'}^0) (1 - f_{2'}^0), \quad (4.29)$$

which is the linear response expression for $I_e^{(1)}$.

The interaction needs to change the number of left and right movers

To proceed, the $\psi_i^{(0)}$ is inserted into the current correction $I_e^{(1)}$ eq.(4.28). Since $\psi_i^{(0)}$ is different for positive and negative k_i , we need to separate each summation over k into two terms. This creates $2^3 = 8$ terms (since $k_1 < 0$). It is at this stage of the calculation, where all the processes that do *not* change the number of left and right movers in the interaction cancel out. This is a special case of the more general statement made in section 3.3: A scattering process changes the current, if and only if, it changes the number of left and right movers. As an example of the cancellation consider the term representing the simultaneous backscattering of a left and a right mover to a right and a left mover, i.e.

$$\sum_{\substack{\sigma_1\sigma_2 \\ \sigma_1'\sigma_2'}} \sum_{\substack{n_1n_2 \\ n_1'n_2'}} \sum_{\substack{-+ \\ ++}} \Delta_{12;1'2'} [\psi_1^{(0)-} + \psi_2^{(0)+} \underbrace{-\psi_{1'}^{(0)+} - \psi_{2'}^{(0)-}}_{1' \leftrightarrow 2 \text{ and } 2' \leftrightarrow 1}] = 0, \quad (4.30)$$

using that $\Delta_{12;1'2'} = \Delta_{2'1';21}$, the short-hand notation $\psi_i^{(0)} = \theta(k_i)\psi_i^{(0)+} + \theta(-k_i)\psi_i^{(0)-}$ and the convention

$$\sum_{\substack{k_1 < 0, k_2 > 0 \\ k_{1'} > 0, k_{2'} < 0}} (\dots) \equiv \sum_{\substack{-+ \\ +-}} (\dots). \quad (4.31)$$

The invariance of $\Delta_{12;1'2'}$ under exchange of the indices follows from eq.(4.29) and eq.(4.16)⁸. Furthermore, one term is backscattering of two left movers to two right movers ($-- \rightarrow ++$), which is not allowed due to momentum conservation present in $W_{12;1'2'}$. Doing variable changes in the last four terms and using the symmetry under variable change in $\Delta_{12;1'2'}$ (e.g. $\Delta_{12;1'2'} = \Delta_{21;1'2'}$ and $\Delta_{12;1'2'} = \Delta_{1'2';12}$) and energy conservation, we get:

$$\begin{aligned} I_e^{(1)} = & L \frac{(-e)}{\mathcal{L}} \sum_{\substack{\sigma_1\sigma_2 \\ \sigma_1'\sigma_2'}} \sum_{\substack{n_1n_2 \\ n_1'n_2'}} \sum_{\substack{-+ \\ ++}} \Delta_{12;1'2'} \left[\frac{\Delta T}{k_B T^2} (\varepsilon_1 - \varepsilon_F) - \frac{eV}{k_B T} \right] \\ & + L \frac{(-e)}{\mathcal{L}} \sum_{\substack{\sigma_1\sigma_2 \\ \sigma_1'\sigma_2'}} \sum_{\substack{n_1n_2 \\ n_1'n_2'}} \sum_{\substack{+- \\ --}} \Delta_{12;1'2'} \left[\frac{\Delta T}{k_B T^2} (\varepsilon_1 - \varepsilon_F) - \frac{eV}{k_B T} \right]. \end{aligned} \quad (4.32)$$

If we also use that $\Delta_{12;1'2'}$ is invariant under all $k_i \rightarrow -k_i$ ($i = 1, 2, 1', 2'$) simultaneously due to time invariance symmetry, then $I_e^{(1)}$ becomes

$$I_e^{(1)} = 2L \frac{(-e)}{\mathcal{L}} \sum_{\substack{\sigma_1\sigma_2 \\ \sigma_1'\sigma_2'}} \sum_{\substack{n_1n_2 \\ n_1'n_2'}} \sum_{\substack{-+ \\ ++}} \Delta_{12;1'2'} \left[\frac{\Delta T}{k_B T^2} (\varepsilon_1 - \varepsilon_F) - \frac{eV}{k_B T} \right]. \quad (4.33)$$

⁸As an example consider: $\Delta_{12;1'2'} = \Delta_{1'2';21}$, which can be argued in the following way: The final and initial states can be interchange due to the H -theorem for the Fermi functions eq.(3.10) and in $W_{12;1'2'}$, since this is a matrix element times an even function of $\varepsilon_1 + \varepsilon_2 - \varepsilon_{1'} - \varepsilon_{2'}$. Within the final/initial states the indices can also be exchanges since $|12\rangle = -|21\rangle$ and the sign vanish, when taking the square to get $W_{12;1'2'}$.

Next we constrict ourself to the situation of two bands and do the summation over the band indices consisting of 16 terms. In the k -summation, we have one left mover ($k_1 < 0$) and three right movers. By using this fact combined with momentum and energy conservation, there is only one possible combination of band indices: $n_1 = b$, $n_2 = a$ and $n_{1'} = n_{2'} = b$. This correspond exactly to the resonant scattering process described in section 4.1.1 (p. 47) and seen on figure⁹ 4.1. Therefore we have now seen how this resonant scattering process appears formally. Momentum conservation restricts the scattering process, so it is only possible near $k_{Fa} = 3k_{Fb}$, (see section 4.1.1). Therefore $I_e^{(1)}$ only has non-exponential terms, if the Fermi level is close to the resonance energy, i.e.

$$I_e^{(1)} = 2L \frac{(-e)}{\mathcal{L}} \sum_{\substack{\sigma_1 \sigma_2 \\ \sigma_{1'} \sigma_{2'}}} \sum_{\substack{-- \\ ++}} \Delta_{12;1'2'} \left[\frac{\Delta T}{k_B T^2} (\varepsilon_1 - \varepsilon_F) - \frac{eV}{k_B T} \right] \Big|_{\substack{n_2=a, n_1=b \\ n_{1'}=n_{2'}=b}} + \mathcal{O}\left(e^{-\frac{T_{Fb}}{T}}\right). \quad (4.34)$$

The task is now to evaluate this to lowest order in the temperature.

4.3.1 The electron-electron interaction matrix element

To calculate $I_e^{(1)}$ eq.(4.34), the matrix element of the electron-electron interaction entering the scattering rate $W_{12;1'2'}$ eq.(4.16) is now considered¹⁰.

First of all, in the perturbative approach it is the non-perturbed states, which are used to calculate the matrix element. Here this is the single-particle (non-interacting) states

$$\psi_{kn\sigma}(x, y) = \frac{1}{\sqrt{\mathcal{L}}} e^{ikx} \varphi_n(y) \chi_\sigma, \quad (4.35)$$

where $\varphi_n(y)$ is the eigenstate of the transverse mode¹¹ ($n = a, b$) and χ_σ is the spin eigenstate. In general, any two-body interaction operator in second quantization is [14, chap. 1]

$$\mathcal{V} = \frac{1}{2} \sum_{121'2'} V_{1'2';12} c_{1'}^\dagger c_{2'}^\dagger c_2 c_1, \quad (4.36)$$

where c_i^\dagger (c_i) is the creation (annihilation) operator and

$$V_{1'2';12} = \int d\mathbf{r}_1 \int d\mathbf{r}_2 \psi_{1'}^*(\mathbf{r}_1) \psi_{2'}^*(\mathbf{r}_2) V(\mathbf{r}_1, \mathbf{r}_2) \psi_1(\mathbf{r}_1) \psi_2(\mathbf{r}_2) \quad (4.37)$$

⁹Note that on figure 4.1, we have actually shown the process where a left mover is produced instead of a right mover as in the present calculation. Note that we could just as well have manipulated the result eq.(4.33) into the \sum_{+-} form, which would match the process on figure 4.1.

¹⁰Note that this calculation of course can be done without using second quantization.

¹¹For simplicity, we take the transverse mode to be one dimensional. We could, however, equally well have described it as being two dimensional.

in terms of the first quantization operator $V(\mathbf{r}_1, \mathbf{r}_2)$. In the case of electron-electron interactions in a 1D wire inserting the single-particle states of eq.(4.35) gives

$$\mathcal{V} = \frac{1}{2\mathcal{L}} \sum_{\sigma_1 \sigma_2} \sum_{\substack{n_1 n_2 \\ n_1' n_2'}} \sum_{k_1 k_2 q} V_q^{n_1 n_2 n_1' n_2'} c_{k_1 + q n_1' \sigma_1}^\dagger c_{k_2 - q n_2' \sigma_2}^\dagger c_{k_2 n_2 \sigma_2} c_{k_1 n_1 \sigma_1}, \quad (4.38)$$

where the electron-electron interaction is only Fourier transformed along the wire keeping the transverse modes in real space i.e.

$$V_q^{n_1 n_2 n_1' n_2'} = \int_{-\frac{\mathcal{L}}{2}}^{\frac{\mathcal{L}}{2}} dx e^{-iqx} \int_{-\frac{d}{2}}^{\frac{d}{2}} dy_1 \int_{-\frac{d}{2}}^{\frac{d}{2}} dy_2 \varphi_{n_1'}^*(y_1) \varphi_{n_2'}^*(y_2) V(x, y_1 - y_2) \varphi_{n_1}(y_1) \varphi_{n_2}(y_2), \quad (4.39)$$

where d is the width of the channel and $V(x, y)$ is the interaction, e.g. a screened Coulomb interaction. Here we have incorporated the momentum conservation¹² $k_1 + k_2 = k_1' + k_2'$ and spin conservation $\sigma_i = \sigma_{i'}$ into the operator in eq.(4.38). To calculate the matrix element $\langle 1'2' | \mathcal{V} | 12 \rangle$ the symmetrized two-particle states,

$$|12\rangle = |k_1 n_1 \sigma_1 k_2 n_2 \sigma_2\rangle = c_{k_1 n_1 \sigma_1}^\dagger c_{k_2 n_2 \sigma_2}^\dagger |0\rangle, \quad (4.40)$$

$$|1'2'\rangle = |k_1' n_1' \sigma_1' k_2' n_2' \sigma_2'\rangle = c_{k_1' n_1' \sigma_1'}^\dagger c_{k_2' n_2' \sigma_2'}^\dagger |0\rangle, \quad (4.41)$$

and the electron-electron operator eq.(4.38) is used to obtain:

$$\begin{aligned} \langle 1'2' | \mathcal{V} | 12 \rangle = \frac{1}{2\mathcal{L}} \delta_{k_1 + k_2, k_1' + k_2'} & \left[(V_{k_1' - k_1}^{n_1 n_2 n_1' n_2'} + V_{k_1 - k_1'}^{n_2 n_1 n_2' n_1'}) \delta_{\sigma_1, \sigma_1'} \delta_{\sigma_2, \sigma_2'} \right. \\ & \left. - (V_{k_2' - k_1}^{n_1 n_2 n_2' n_1'} + V_{k_1 - k_2'}^{n_2 n_1 n_1' n_2'}) \delta_{\sigma_1, \sigma_2'} \delta_{\sigma_2, \sigma_1'} \right]. \quad (4.42) \end{aligned}$$

If we use that the interaction is only a function of the distance between the electrons, then it is even in both coordinates, e.g. $V(x, -y) = V(\sqrt{x^2 + y^2}) = V(x, y)$. This leads to the relations

$$V_q^{n_1 n_2 n_1' n_2'} = V_q^{n_2 n_1 n_2' n_1'} \quad \text{and} \quad V_{-q}^{n_1 n_2 n_1' n_2'} = V_q^{n_1 n_2 n_1' n_2'} \quad (4.43)$$

using eq.(4.39). Therefore the matrix element simplifies to

$$\langle 1'2' | \mathcal{V} | 12 \rangle = \frac{1}{\mathcal{L}} \delta_{k_1 + k_2, k_1' + k_2'} \left[\underbrace{V_{k_1' - k_1}^{n_1 n_2 n_1' n_2'} \delta_{\sigma_1, \sigma_1'} \delta_{\sigma_2, \sigma_2'}}_{\text{The direct term}} - \underbrace{V_{k_2' - k_1}^{n_1 n_2 n_2' n_1'} \delta_{\sigma_1, \sigma_2'} \delta_{\sigma_2, \sigma_1'}}_{\text{The exchange term}} \right], \quad (4.44)$$

¹²Note that in order to have exact momentum conservation coming out of the $V_{1'2',12}$, we need $L = \mathcal{L}$. Therefore the momentum conservation is here an ansatz working well for $L \gg k_F^{-1}$.

which is the matrix element needed for $I_e^{(1)}$. The first term is often called the direct interaction and the second term is called the exchange interaction, since the last term can be obtained from the first term by exchanging the final states $(k_{1'}, n_{1'}, \sigma_{1'}) \leftrightarrow (k_{2'}, n_{2'}, \sigma_{2'})$. The exchange term is a manifestation of the fact that quantum particles are indistinguishable.

Inserting $n_2 = a$ and $n_1 = n_{1'} = n_{2'} = b$ for the particular process in mind and doing the summation over spin as it is required in the current eq.(4.34), we obtain

$$\sum_{\substack{\sigma_1 \sigma_2 \\ \sigma_{1'} \sigma_{2'}}} |\langle k_{1'} b \sigma_{1'} k_{2'} b \sigma_{2'} | \mathcal{V} | k_1 b \sigma_1 k_2 a \sigma_2 \rangle|^2 = \frac{4}{\mathcal{L}^2} \delta_{k_1+k_2, k_{1'}+k_{2'}} \left\{ |V_{k_{1'}-k_1}^{babb}|^2 + |V_{k_{2'}-k_1}^{babb}|^2 - \text{Re} \left[V_{k_{1'}-k_1}^{babb} (V_{k_{2'}-k_1}^{babb})^* \right] \right\}. \quad (4.45)$$

This is the result for zero magnetic field. Later we shall see that it is at this point of the calculation that a finite magnetic field changes the situation, since the 1D subbands spin split and so does the resonance.

Magnitude of the *inter-subband* interaction

The magnitude of the inter-band interaction $|V^{babb}|^2$ decides the magnitude of the interaction-induced resonances in G and S and is therefore an important quantity.

In eq.(4.39) for $V_q^{n_1 n_2 n_{1'} n_{2'}}$ the transverse eigenstates $\varphi_n(y)$ appears. Since the transverse modes of the subbands are orthogonal, $\int dy \varphi_n^*(y) \varphi_{n'}(y) = \delta_{n,n'}$, the *inter*-subband interactions such as V^{babb} are suppressed compared to the *intra*-subband interactions such as V^{bbbb} . If we were to use a model of the interaction where $V(x, y) \propto \delta(y)$, then the inter-subband interaction would be exactly zero. However, for a general dependence of y in $V(x, y)$, the inter-subband interaction is nonzero. How much the inter-subband interaction is suppressed compared to the intra-subband interaction depends heavily on the model for the transverse states and the interaction. However, note that no intra-subband processes can induce a resonance due to the criteria presented in section 4.1.1.

4.3.2 The current to lowest order in the temperature

Next we calculated the current correction $I_e^{(1)}$ in eq.(4.34) in the low temperature limit:

$$T \ll T_{Fb} = (\varepsilon_F - \varepsilon_0)/k_B \ll T_F. \quad (4.46)$$

The strategy of finding the low temperature limit is to introduce new dimensionless integration variables in the k -integrals and then expand the integrand

in orders of $T/T_{\text{F}b}$. This is a rigorous procedure and can be used in various situations apart from the present one.

We begin by inserting the matrix element including the spin sums from eq.(4.45) into eq.(4.34) and transforming the sums over the wave vectors into integrals, $\sum_k \rightarrow \frac{\mathcal{L}}{2\pi} \int dk$, i.e.:

$$I_e^{(1)} = \frac{2(-e)L}{\pi^2 \hbar} \int_{-\infty}^0 dk_1 \int_0^\infty dk_2 \int_0^\infty dk_{1'} \int_0^\infty dk_{2'} f_1^0 f_2^0 (1 - f_{1'}^0)(1 - f_{2'}^0) \quad (4.47)$$

$$\times \left\{ |V_{k_{1'}-k_1}^{babb}|^2 + |V_{k_{2'}-k_1}^{babb}|^2 - \text{Re} \left[V_{k_{1'}-k_1}^{babb} (V_{k_{2'}-k_1}^{babb})^* \right] \right\}$$

$$\times \delta(k_1 + k_2 - k_{1'} - k_{2'}) \delta(\varepsilon_1 + \varepsilon_2 - \varepsilon_{1'} - \varepsilon_{2'}) \left[\frac{\Delta T}{k_{\text{B}} T^2} (\varepsilon_1 - \varepsilon_{\text{F}}) - \frac{eV}{k_{\text{B}} T} \right]$$

where the normalization length \mathcal{L} cancels out¹³ and the band indices from now on are $n_2 = a$ and $n_1 = n_{1'} = n_{2'} = b$. In order to expand in temperature new dimensionless integration variables are introduced as

$$z_j = \frac{\varepsilon_j - \varepsilon_{\text{F}}}{k_{\text{B}} T} \quad \text{for } j = 1, 2, 1', 2'. \quad (4.48)$$

Next we express all quantities in eq.(4.47) in the new variables and expand them to lowest order non-vanishing order in temperature. First of all the integral change as (remembering that $k_1 < 0$)

$$\int_{-\infty}^0 dk_1 (\dots) = \int_{-\infty}^{\varepsilon_0} d\varepsilon_1 \left(-\sqrt{\frac{m}{2\hbar^2(\varepsilon_1 - \varepsilon_0)}} (\dots) \right) \Big|_{k_1 = -\sqrt{\frac{2m(\varepsilon_1 - \varepsilon_0)}{\hbar^2}}} \quad (4.49)$$

$$= \frac{k_{\text{F}b}}{2} \frac{T}{T_{\text{F}b}} \int_{-T_{\text{F}b}/T}^{\infty} dz_1 \frac{(\dots)}{\sqrt{1 + z_1 \frac{T}{T_{\text{F}b}}}} \Big|_{k_1 = -k_{\text{F}b} \sqrt{1 + z_1 \frac{T}{T_{\text{F}b}}}},$$

$$\int_0^\infty dk_2 (\dots) = \int_0^\infty d\varepsilon_2 \sqrt{\frac{m}{2\hbar^2 \varepsilon_2}} (\dots) \Big|_{k_2 = \sqrt{\frac{2m\varepsilon_2}{\hbar^2}}} \quad (4.50)$$

$$= \frac{k_{\text{F}a}}{2} \frac{T}{T_{\text{F}a}} \int_{-T_{\text{F}a}/T}^{\infty} dz_2 \frac{(\dots)}{\sqrt{1 + z_2 \frac{T}{T_{\text{F}a}}}} \Big|_{k_2 = k_{\text{F}a} \sqrt{1 + z_2 \frac{T}{T_{\text{F}a}}}},$$

$$\int_0^\infty dk_{1'} (\dots) = \int_{\varepsilon_0}^\infty d\varepsilon_{1'} \sqrt{\frac{m}{2\hbar^2(\varepsilon_{1'} - \varepsilon_0)}} (\dots) \Big|_{k_{1'} = \sqrt{\frac{2m(\varepsilon_{1'} - \varepsilon_0)}{\hbar^2}}} \quad (4.51)$$

$$= \frac{k_{\text{F}b}}{2} \frac{T}{T_{\text{F}b}} \int_{-T_{\text{F}b}/T}^{\infty} dz_{1'} \frac{(\dots)}{\sqrt{1 + z_{1'} \frac{T}{T_{\text{F}b}}}} \Big|_{k_{1'} = k_{\text{F}b} \sqrt{1 + z_{1'} \frac{T}{T_{\text{F}b}}}},$$

¹³The Kronecker-delta function for momentum conservation are made into a Dirac delta function as $\sum_k \delta_{k,q}(\dots) = \int dk \delta(k - q)(\dots)$, i.e. without the factor of $\frac{\mathcal{L}}{2\pi}$, so the normalization length \mathcal{L} does indeed cancel out in $I_e^{(1)}$ as it should.

where $k_{2'}$ is as $k_{1'}$ and $T_{Fa} \equiv T_F$ was introduced for notational consistency¹⁴. The wave vectors k as a function of z was indicated. To lowest order in temperature the above density of states are simply constant, i.e.

$$\frac{1}{\sqrt{1 + z_i \frac{T}{T_{Fb}}}} = 1 + \mathcal{O}\left(\frac{T}{T_{Fb}}\right). \quad (4.52)$$

This approximation is equivalent to using linear bands and including higher order terms in T is the same as including curvature effects of the dispersion. The wave vectors k as a function of z to lowest order in T is also the same as using a linear dispersion:

$$k_1 = -k_{Fb} \sqrt{\left(1 + z_1 \frac{T}{T_{Fb}}\right)} \simeq -k_{Fb} \left(1 + \frac{1}{2} z_1 \frac{T}{T_{Fb}}\right), \quad (4.53)$$

and

$$k_2 \simeq k_{Fa} \left(1 + \frac{1}{2} z_2 \frac{T}{T_{Fa}}\right), \quad k_{i'} \simeq k_{Fb} \left(1 + \frac{1}{2} z_{i'} \frac{T}{T_{Fb}}\right), \quad (i = 1, 2). \quad (4.54)$$

Therefore the momentum conservation term in eq.(4.47) becomes

$$\delta(k_1 + k_2 - k_{1'} - k_{2'}) \simeq \frac{2}{k_{Fb}} \frac{T_{Fb}}{T} \delta\left(-z_1 + \frac{k_{Fb}}{k_{Fa}} z_2 - z_{1'} - z_{2'} - \frac{8}{3} \frac{\Delta\varepsilon_F}{k_B T}\right), \quad (4.55)$$

where we have introduced the parameter

$$\frac{\Delta\varepsilon_F}{k_B T} \equiv \frac{3 \hbar v_{Fb} (3k_{Fb} - k_{Fa})}{8 k_B T} \quad (4.56)$$

measuring the detuning away from the resonance at $k_{Fa} = 3k_{Fb}$. At the resonance we have $\Delta\varepsilon_F = 0$ and $\Delta\varepsilon_F$ is positive (negative) for $\varepsilon_F > \varepsilon_R$ ($\varepsilon_F < \varepsilon_R$). An expansion of $\Delta\varepsilon_F$ in ε_F around $\varepsilon_R = 9\varepsilon_0/8$ gives:

$$\frac{\Delta\varepsilon_F}{k_B T} \simeq \frac{(\varepsilon_F - \varepsilon_R)}{k_B T}, \quad (4.57)$$

which is seen on figure 4.7 to be a rather good approximation in the low temperature regime of interest (i.e. for ε_F within a few $k_B T$ of ε_R). Here we take $\Delta\varepsilon_F/k_B T$ as a parameter of order ~ 1 and in the end of the calculation it turns out to be the argument of the functions F_0 and F_1 in $G^{(1)}$ eq.(4.8) and S eq.(4.11), respectively. Returning to the momentum conservation eq.(4.55), we note that

¹⁴Each band has its own temperature scale: $T_{Fa} = \varepsilon_F/k_B$ for band a and $T_{Fb} = \hbar^2 k_{Fb}^2 / (2m) = (\varepsilon_F - \varepsilon_0)/k_B$ for band b .

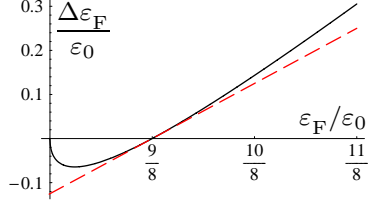


Figure 4.7: The parameter $\Delta\varepsilon_F$ as a function of ε_F (full line) from eq.(4.56) and the approximation $\Delta\varepsilon_F \simeq (\varepsilon_F - \varepsilon_R)$ (red dashed line) in units of ε_0 . For low temperatures $T \ll (\varepsilon_F - \varepsilon_0)/k_B$ the approximation is good in the regime of interest, where ε_F is up to a few $k_B T$ from $\varepsilon_R = 9\varepsilon_0/8$. Note that the band edge $\varepsilon_F = \varepsilon_0$ is not of interest in the present calculation.

$$\frac{k_{Fa}}{k_{Fb}} = 3 - \frac{8}{6} \frac{T}{T_{Fb}} \frac{\Delta\varepsilon_F}{k_B T} \simeq 3 \quad (4.58)$$

to lowest order in temperature, which is inserted into the momentum conservation eq.(4.55), i.e.

$$\delta(k_1 + k_2 - k_{1'} - k_{2'}) \simeq \frac{2}{k_{Fb}} \frac{T_{Fb}}{T} \delta\left(-z_1 + \frac{1}{3}z_2 - z_{1'} - z_{2'} - \frac{8}{3} \frac{\Delta\varepsilon_F}{k_B T}\right). \quad (4.59)$$

The energy conservation is easily rewritten as

$$\delta(\varepsilon_1 + \varepsilon_2 - \varepsilon_{1'} - \varepsilon_{2'}) = \frac{1}{k_B T} \delta(z_1 + z_2 - z_{1'} - z_{2'}) \quad (4.60)$$

and so are the Fermi function

$$f_1^0 f_2^0 (1 - f_{1'}^0) (1 - f_{2'}^0) = g(z_1) g(z_2) g(-z_{1'}) g(-z_{2'}) \quad (4.61)$$

defining

$$g(z) \equiv \frac{1}{1 + e^z}. \quad (4.62)$$

Now we only need the interaction factor to lowest order in T to have all the ingredients for $I_1^{(1)}$ in eq.(4.47). The direct interaction $V_{k_{1'}-k_1}^{babb}$ and the exchange interaction $V_{k_{2'}-k_1}^{babb}$ are functions of the differences $k_{1'} - k_1$ and $k_{2'} - k_1$, respectively. To lowest order in temperature both these differences are equal to $2k_{Fb}$, so

$$\left\{ |V_{k_{1'}-k_1}^{babb}|^2 + |V_{k_{2'}-k_1}^{babb}|^2 - \text{Re} \left[V_{k_{1'}-k_1}^{babb} (V_{k_{2'}-k_1}^{babb})^* \right] \right\} = |V_{2k_{Fb}}^{babb}|^2 + \mathcal{O}\left(\frac{T}{T_{Fb}}\right), \quad (4.63)$$

and the higher orders in temperature will include derivatives of the interaction $\partial_q V_{2k_{Fb}}^{babb}$ with respect to the momentum transfer $q = k_{i'} - k_1$. Therefore $I_e^{(1)}$ eq.(4.47) to lowest order in temperature is:

$$\begin{aligned} I_e^{(1)} = & \frac{2(-e)L}{\pi^2 \hbar} \frac{(k_{Fb})^2 k_{Fa}}{8(\varepsilon_F - \varepsilon_0)} |V_{2k_{Fb}}^{babb}|^2 \frac{T}{T_{Fb}} \\ & \times \int_{-\infty}^{\infty} dz_1 \int_{-\infty}^{\infty} dz_2 \int_{-\infty}^{\infty} dz_{1'} \int_{-\infty}^{\infty} dz_{2'} g(z_1) g(z_2) g(-z_{1'}) g(-z_{2'}) \\ & \times \delta(z_1 + z_2 - z_{1'} - z_{2'}) \delta\left(-z_1 + \frac{1}{3}z_2 - z_{1'} - z_{2'} - \frac{8}{3} \frac{\Delta\varepsilon_F}{k_B T}\right) \left[\frac{\Delta T}{T_{Fa}} z_1 - \frac{eV}{\varepsilon_F} \right], \end{aligned} \quad (4.64)$$

where all the lower limits of the integrals are extended to infinity, $-T/T_{Fb/a} \rightarrow -\infty$, since this only amount to include the extra exponentially small tales of the integrand and therefore only includes an exponentially small (i.e. $\propto e^{-T_{Fb/a}/T}$) number. Furthermore, the prefactor can be rewritten using $k_{Fa} \simeq 3k_{Fb}$ eq.(4.58) as

$$\frac{2(-e)L}{\pi^2\hbar} \frac{(k_{Fb})^2 k_{Fa}}{8(\varepsilon_F - \varepsilon_0)} |V_{2k_{Fb}}^{babb}|^2 \frac{T}{T_{Fb}} = \overbrace{\frac{9(-e)\varepsilon_F}{\pi^2\hbar}}^{\text{Unit of current}} Lk_{Fa} \left(\frac{|V_{2k_{Fb}}^{babb}|}{\hbar v_{Fa}} \right)^2 \frac{T}{T_F} + \mathcal{O}\left[\left(\frac{T}{T_F}\right)^2\right].$$

The lowest order expansion in temperature in eq.(4.64) is equivalent to using the (momentum independent) value of the interaction at the Fermi level and linear bands from the beginning from the calculation, however, here we have presented the rigorous justification of this (often used approximation).

Next we show how to manipulate $I_e^{(1)}$ in eq.(4.64) into the form of the functions F_1 and F_0 in $G^{(1)}$ eq.(4.8) and S eq.(4.11), respectively.

First of all, we note that for $\Delta\varepsilon_F = 0$ the term proportional to ΔT is zero, since the z_1 integrand is odd. This can be seen explicitly by making a variable transformation $(z_2, z_{1'}, z_{2'}) \rightarrow (-z_2, -z_{1'}, -z_{2'})$ and using

$$g(-z_1)g(-z_2)g(z_{1'})g(z_{2'})\delta(-z_1 - z_2 + z_{1'} + z_{2'}) = g(z_1)g(z_2)g(-z_{1'})g(-z_{2'})\delta(z_1 + z_2 - z_{1'} - z_{2'}). \quad (4.65)$$

However for $\Delta\varepsilon_F \neq 0$ this is not true and for the eV term the z_1 integrand is even. Therefore it is now evaluated.

To do some of the integrals in eq.(4.64) analytically, new variables are introduced as

$$z_s = z_{1'} + z_{2'} \quad \text{and} \quad z_d = z_{1'} - z_{2'}, \quad (4.66)$$

and the determinant for the variable change is 1/2. The integral over z_d can be done separately, since z_d does not enter in the delta functions. It is

$$\begin{aligned} \int_{-\infty}^{\infty} dz_d g(-z_{1'})g(-z_{2'}) &= \\ \int_{-\infty}^{\infty} dz_d g\left[-\frac{1}{2}(z_s + z_d)\right]g\left[-\frac{1}{2}(z_s - z_d)\right] &= -2z_s n_B(-z_s) \end{aligned} \quad (4.67)$$

where

$$n_B(x) = \frac{1}{e^x - 1}. \quad (4.68)$$

Using the energy conservation to do the z_s -integral (i.e. $z_s = z_1 + z_2$) and afterwards using the momentum conservation delta function to do the z_2 -integral

(i.e. $z_2 = -3z_1 - 4\Delta\varepsilon_F/k_B T$), we arrive at

$$I_e^{(1)} = -\frac{3}{2} \frac{9(-e)\varepsilon_F}{\pi^2 \hbar} L k_{Fa} \left(\frac{|V_{2k_{Fb}}^{babb}|}{\hbar v_{Fa}} \right)^2 \frac{T}{T_F} \int_{-\infty}^{\infty} dz_1 g(z_1) g\left(-3z_1 - 4\frac{\Delta\varepsilon_F}{k_B T}\right) \\ \times \left\{ -2z_1 - 4\frac{\Delta\varepsilon_F}{k_B T} \right\} n_B\left(2z_1 + 4\frac{\Delta\varepsilon_F}{k_B T}\right) \left[\frac{\Delta T}{T_F} z_1 - \frac{eV}{\varepsilon_F} \right]. \quad (4.69)$$

This is rewritten into a more appealing form by introducing

$$h(z, x) \equiv g(z)g(-3z - 4x)(-2z - 4x)n_B(2z + 4x) \\ = \frac{-(z + 2x)}{4 \sinh(2x + z) \cosh(z/2) \cosh(2x + 3z/2)} \quad (4.70)$$

and the length scale ℓ_{ee} in eq.(4.9) and we get

$$I_e^{(1)} = \frac{4e}{h} \frac{L}{\ell_{ee}} \frac{T}{T_F} \int_{-\infty}^{\infty} dz h\left(z, \frac{\Delta\varepsilon_F}{k_B T}\right) [k_B \Delta T z - eV] = G_T^{(1)} \Delta T - G^{(1)} V, \quad (4.71)$$

using eq.(4.19). The thermopower $S = G_T/G$ to lowest order in temperature is $S \simeq G_T^{(1)}/G^{(0)}$ (since $G_T^{(0)} \propto e^{-T_{Fb}/T}$), so we can read off the conductance and thermopower to lowest order in the interaction and lowest order in temperature to be:

$$G = \frac{4e^2}{h} + \frac{4e^2}{h} \frac{L}{\ell_{ee}} \frac{T}{T_F} F_0\left(\frac{\varepsilon_F - \varepsilon_R}{k_B T}\right), \quad (4.72a)$$

$$S = \frac{k_B}{e} \frac{L}{\ell_{ee}} \frac{T}{T_F} F_1\left(\frac{\varepsilon_F - \varepsilon_R}{k_B T}\right), \quad (4.72b)$$

using that $\Delta\varepsilon_F/k_B T \sim (\varepsilon_F - \varepsilon_R)/k_B T$ eq.(4.57), where $F_n(x)$ is

$$F_n(x) = \int_{-\infty}^{\infty} dz z^n h(z, x), \quad (4.73)$$

seen in figure 4.5 for $n = 0, 1$. This is the result we set out to find.

4.3.3 Higher orders in temperature

We have also calculated the next order in temperature of the current of first order in the interaction $I_e^{(1)}$ in eq.(4.47). This is done by extending the calculation presented above. This amounts to going beyond linear bands and thereby including curvature effects of the dispersion. Furthermore, the derivative of the interaction $\partial_q V_{2k_{Fb}}^{babb}$ begins to play a role.

One of the results of the higher order calculation is that the thermopower at the resonance $k_{Fa} = 3k_{Fb}$ is nonzero, i.e.

$$G_T^{(2)}(\Delta\varepsilon_F = 0) = -\frac{4ek_B}{\hbar} 0.86 \frac{3}{\pi} \frac{L}{\ell_{ee}} \left(\frac{T}{T_F} \right)^2, \quad (4.74)$$

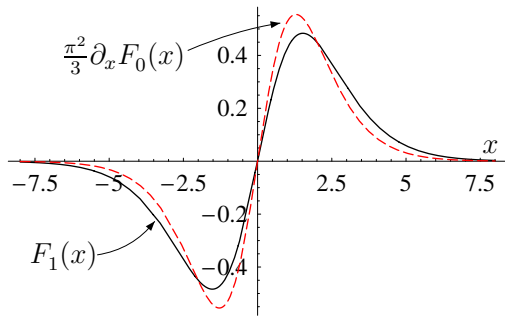


Figure 4.8: A comparison of $F_1(x)$ (full line) and $\frac{\pi^2}{3} \frac{dF_0(x)}{dx}$ (dashed line) appearing in the interaction-induced thermopower eq.(4.72b) and the Mott formula result eq.(4.76), respectively. It is observed that the Mott formula is a good approximation here, even though the thermopower is only due to interactions.

where the prefactor 0.86 is the result of a numerical evaluation of an integral. This result is purely due to the curvature of the dispersion, since the second order term in T proportional to $\partial_q V_{2k_{Fb}}^{babb}$ is zero at the resonance. This result shows that the curvature of the dispersion shifts the resonance point slightly to a higher value of the Fermi level. However, the sign change of the thermopower as a function of ε_F still appears.

To lowest order in temperature S and G eq.(4.72) are symmetric in ε_F around ε_R (apart from the prefactor), see figure 4.5. Another result of the next order in temperature calculation is that the form becomes asymmetric. This asymmetry is only due to the derivative of the dispersion $\partial_q V_{2k_{Fb}}^{babb}$ and the term from the curvature of the dispersion still gives a symmetric contribution. However, to say more about these issues, one could e.g. make a numerical evaluation of $I_e^{(1)}$ in eq.(4.47).

4.4 The Mott formula

The Mott formula gives the thermopower in terms of the conductance as

$$S^M = \frac{\pi^2}{3} \frac{k_B}{e} k_B T \frac{1}{G} \frac{dG}{d\varepsilon_F}, \quad (4.75)$$

and it is often argued to be a low temperature approximation valid for *non-interacting* electrons (e.g. in Ref. [68]). Here we simply try to use the Mott formula and find that it is a surprisingly good approximation, even though we are dealing with a thermopower solely due to interaction effects.

Inserting the conductance $G \simeq G^{(0)} + G^{(1)}$ eq.(4.72a) into the Mott formula gives

$$S^M \simeq \frac{k_B}{e} \frac{L}{\ell_{ee}} \frac{T}{T_F} \frac{\pi^2}{3} \frac{dF_0(x)}{dx} \bigg|_{x=\left(\frac{\varepsilon_F - \varepsilon_R}{k_B T}\right)} \quad (4.76)$$

to lowest order in temperature for ε_F within a few $k_B T$ of ε_R . In figure 4.8, we observe that $F_1(x)$ is well approximated by $\frac{\pi^2}{3} \frac{dF_0(x)}{dx}$ and hence the Mott formula

result eq.(4.76) is a good approximation to the interaction-induced low temperature thermopower S in eq.(4.72b). Therefore the resonance due to interactions cannot be detected by a violation of the Mott formula.

4.5 Magnetic field splitting of the resonance

In this section, the effect of a magnetic field on the interaction-induced resonance is discussed. First we describe how a magnetic field spin split the 1D modes in the quantum wire and in terms splits the resonance at $\varepsilon_F = \varepsilon_R$ into four resonances $\varepsilon_F = \varepsilon_R^{\sigma\sigma'}$. Next we argue that two of the resonances describing scattering between equal spins are significantly suppressed compared to the scattering between opposite spins due to the Pauli principle. In the end, we make an explicit calculation of the effect.

4.5.1 The magnetic field splits the subbands

The finite quantum wire connected to leads is imbedded into a 2D electron gas. Here we imagine a uniform and constant magnetic field \mathbf{B} being applied in the plane of the 2D electron gas and thereby we are not in the quantum hall regime¹⁵. (Note that for a small magnetic field component perpendicular to the plane the following is still qualitatively true.) Therefore it is only the electrons magnetic moment $\bar{\mu}$ due to its spin σ that couples to the magnetic field as $H_B = -\bar{\mu} \cdot \mathbf{B}$. This leads to a spin-splitting of the energy bands as:

$$\varepsilon_{ka\downarrow} = \frac{\hbar^2 k^2}{2m} - \frac{1}{2}g\mu_B B, \quad \varepsilon_{ka\uparrow} = \frac{\hbar^2 k^2}{2m} + \frac{1}{2}g\mu_B B, \quad (4.77a)$$

$$\varepsilon_{kb\downarrow} = \frac{\hbar^2 k^2}{2m} + \varepsilon_0 - \frac{1}{2}g\mu_B B \quad \text{and} \quad \varepsilon_{kb\uparrow} = \frac{\hbar^2 k^2}{2m} + \varepsilon_0 + \frac{1}{2}g\mu_B B, \quad (4.77b)$$

where $\mu_B = \frac{e\hbar}{2m}$ is the Bohr magneton, g is the so-called g -factor¹⁶ and $B = |\mathbf{B}|$ is the magnitude of the magnetic field. A natural definition of the Fermi wave vectors $k_{Fa\sigma}$ and $k_{Fb\sigma}$ for the spin-split bands is

$$\varepsilon_F = \frac{\hbar^2 k_{Fa\sigma}^2}{2m} + \sigma \frac{1}{2}g\mu_B B, \quad \varepsilon_F = \frac{\hbar^2 k_{Fb\sigma}^2}{2m} + \varepsilon_0 + \sigma \frac{1}{2}g\mu_B B \quad (4.78)$$

where $\sigma = \uparrow = +1$ and $\sigma = \downarrow = -1$. This also defines the spin-split Fermi temperatures as $k_B T_{Fn\sigma} = \hbar^2 k_{Fn\sigma}^2 / (2m)$.

¹⁵In general, the effect of a magnetic field on the motion of a spinless particle with charge q is to change the Hamiltonian to $H = \frac{1}{2m}(\mathbf{p} - q\mathbf{A})^2$, where $\mathbf{B} = \nabla \times \mathbf{A}$ and $\mathbf{p} = -i\hbar\nabla$. This gives rise to Landau levels and if we apply the field along the wire, then the wave function in the plane of the 2D gas presented in eq.(4.35.) is not changed, see e.g. [127].

¹⁶In vacuum it is about two, but in solids the effective g -factor can vary in size and sign due to a number of effects, e.g. spin-orbit coupling.

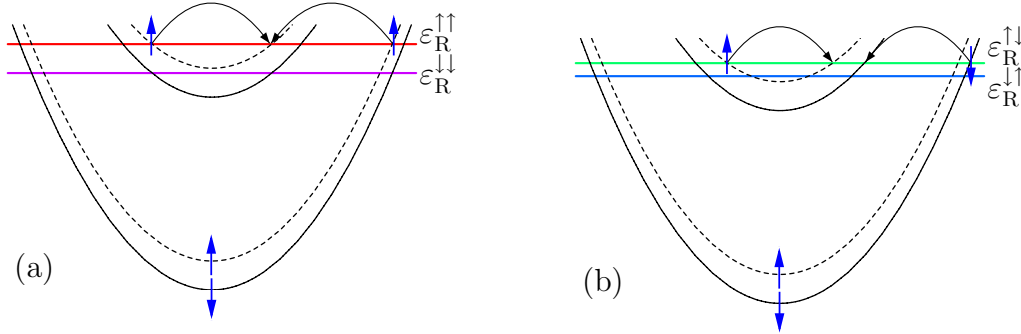


Figure 4.9: For a nonzero magnetic field the resonance at $\varepsilon_F = \varepsilon_R$ for $B = 0$ splits up into four resonances: (a) Two for scattering between electrons with the same spin and (b) two for scattering between electrons with opposite spin. The four resonance energies $\varepsilon_R^{\uparrow\uparrow}$ (red), $\varepsilon_R^{\downarrow\downarrow}$ (purple), $\varepsilon_R^{\uparrow\downarrow}$ (green) and $\varepsilon_R^{\downarrow\uparrow}$ (blue) are seen for $g\mu_B B = 0.15\varepsilon_0$, but we have only show the scattering process for $\varepsilon_R^{\uparrow\uparrow}$ and $\varepsilon_R^{\downarrow\downarrow}$ to keep the illustration simple. In the case of scattering between equal spins in (a), the final states are the same, which is forbidden by the Pauli principle and hence the scattering is heavily suppressed compare to the scattering between different spins (see the text for further explanation).

If the spin-splitting $g\mu_B B$ is larger than $k_B T$ and the smearing of the transmission due to geometry¹⁷, then additional conductance steps of size e^2/h appears and also the thermopower peaks splits up as seen on figure 4.10. Experimentally this is also a well-known fact, see e.g. [19].

4.5.2 The interaction-induced resonances in a magnetic field

The principle leading to a interaction-induced resonance is the same with and without a magnetic field. Therefore a resonant scattering process still has to obey the requirements stated in section 4.1.1, i.e. change the number of left and right movers, conserve momentum and energy, and happen near the Fermi energy. Furthermore, the scattering conserves the spin in the sense that the final and initial state of an electron has the same spin, since the interaction cannot produce spin-flipping. Therefore there is *no* resonances at e.g. $k_{Fa\downarrow} = 3k_{Fa\uparrow}$.

However, the resonance for $k_{Fa} = 3k_{Fb}$ with $B = 0$ is split into four resonances: Two resonant scattering processes between electrons with equal spins seen in figure 4.9(a) and two scattering processes between electrons with opposite spins, see figure 4.9(b). Momentum conservation $k_1 + k_2 = k_{1'} + k_{2'}$ gives the resonant conditions and using the quadratic dispersion eq.(4.77) the resonant energies $\varepsilon_R^{\sigma\sigma'}$

¹⁷In the saddle-point model, this is $\hbar\omega_x$ (see section 1.5.1).

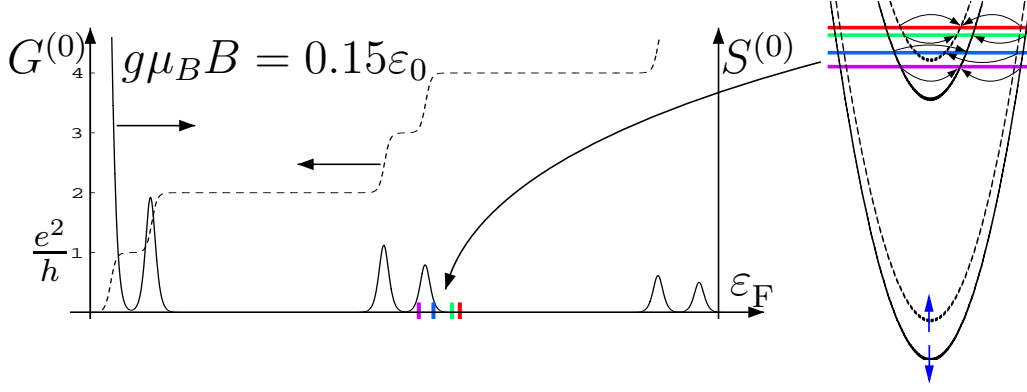


Figure 4.10: The non-interaction conductance steps and thermopower peaks spin split due to the magnetic field. So does the interaction-induced resonance and here we illustrate the position of the resonances for $g\mu_B B = 0.15\varepsilon_0$. Each color indicates a specific resonance, see eq.(4.79). The resonances in G and S might be masked by the non-interaction signal depending on the value of $g\mu_B B$. In this case, $\varepsilon_R^{\downarrow\downarrow}$ and $\varepsilon_R^{\uparrow\uparrow}$ might be hidden in the non-interacting signal.

are also found, i.e.:

$$\uparrow\uparrow: k_{Fa\uparrow} = 3k_{Fb\uparrow}, \quad \varepsilon_R^{\uparrow\uparrow} = \frac{9}{8}\varepsilon_0 + \frac{1}{2}g\mu_B B, \quad (\text{Red}) \quad (4.79a)$$

$$\downarrow\downarrow: k_{Fa\downarrow} = 3k_{Fb\downarrow}, \quad \varepsilon_R^{\downarrow\downarrow} = \frac{9}{8}\varepsilon_0 - \frac{1}{2}g\mu_B B, \quad (\text{Purple}) \quad (4.79b)$$

$$\uparrow\downarrow: k_{Fa\downarrow} = 2k_{Fb\uparrow} + k_{Fb\downarrow}, \quad \varepsilon_R^{\uparrow\downarrow} = \varepsilon_0 \frac{9 + 20\frac{g\mu_B B}{\varepsilon_0} + 8\left(\frac{g\mu_B B}{\varepsilon_0}\right)^2}{8\left(1 + 2\frac{g\mu_B B}{\varepsilon_0}\right)}, \quad (\text{Green}) \quad (4.79c)$$

$$\downarrow\uparrow: k_{Fa\uparrow} = 2k_{Fa\downarrow} + k_{Fb\uparrow}, \quad \varepsilon_R^{\downarrow\uparrow} = \varepsilon_0 \frac{9 - 20\frac{g\mu_B B}{\varepsilon_0} + 8\left(\frac{g\mu_B B}{\varepsilon_0}\right)^2}{8\left(1 - 2\frac{g\mu_B B}{\varepsilon_0}\right)}, \quad (\text{Blue}) \quad (4.79d)$$

where the color indicates the color used for that resonance in figures 4.9, 4.10 and 4.11. Note that the scattering at $\varepsilon_R^{\uparrow\uparrow}$ can only conserve momentum and energy for $g\mu_B B < \varepsilon_0/4$ and for a larger splitting it no longer exist. Likewise $\varepsilon_R^{\uparrow\downarrow}$ is only present for $g\mu_B B > -\varepsilon_0/4$. Furthermore, for small subband splitting $g\mu_B B \ll \varepsilon_0$ the resonances energies are $\varepsilon_R^{\sigma\bar{\sigma}} \simeq \frac{9}{8}\varepsilon_0 + \sigma\frac{1}{4}g\mu_B B$ for $\sigma = +1(-1) = \uparrow(\downarrow)$ and $\bar{\sigma} = -\sigma$. On figure 4.10 the resonances are seen together with the non-interaction conductance and thermopower for $g\mu_B B = 0.15\varepsilon_0$. A word of warning is that the resonances might be hard to observe, if they fall on top of the non-interaction thermopower peaks (i.e. on the conductance steps). The resonant energies as a function of the magnetic field splitting is seen on figure 4.11.

The conductance and thermopower response at the resonances have the same physics as in the $B = 0$ case and in the following we shall focus on what effects the spins have on the scattering.

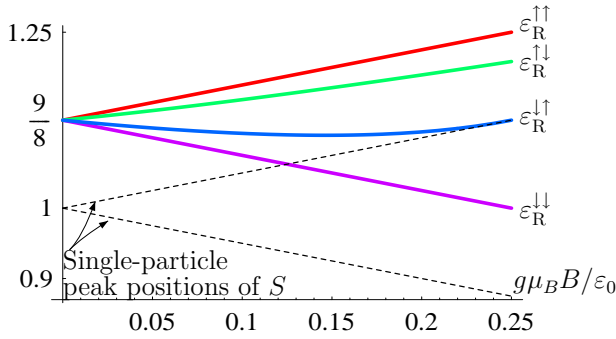


Figure 4.11: The resonance energies in eq.(4.79) as a function of the magnetic field splitting $g\mu_B B$ in units of the subband splitting ε_0 . The dashed lines illustrate the bottoms of the spin-split $n = b$ band, or equivalently, the single particle peaks of the thermopower. Note that $\varepsilon_R^{\downarrow\uparrow}$ does not exist for $g\mu_B B > \varepsilon_0/4$.

4.5.3 Suppression of resonant scattering between equal spins

Violation of the Pauli principle leads to suppression of the scattering

In figure 4.9(a) the scattering at $\varepsilon_R^{\uparrow\uparrow}$ between two spin up electrons is seen. *Exactly* at the Fermi level $\varepsilon_F = \varepsilon_R^{\uparrow\uparrow}$ the scattering is

$$(k_1, k_2) = (-k_{Fb\uparrow}, k_{Fa\uparrow}) \rightarrow (k_{1'}, k_{2'}) = (k_{Fb\uparrow}, k_{Fb\uparrow}), \quad (4.80)$$

so since the electrons have the same spin, the final states $|k_i n_i \sigma_i\rangle$ ($i = 1, 2$) are the same. This is forbidden by the Pauli principle and therefore *exactly* at the Fermi level this scattering process cannot happen! Therefore the electrons have to scattering into states slightly different from the Fermi level, but still within $k_B T$ of $\varepsilon_R^{\uparrow\uparrow}$. Analyzing any other scattering at $\varepsilon_R^{\uparrow\uparrow}$ than the one shown in figure 4.9(a) would lead to the same result, e.g. $(k_1, k_2) = (k_{Fb\uparrow}, k_{Fb\uparrow}) \rightarrow (k_{1'}, k_{2'}) = (k_{Fa\uparrow}, -k_{Fb\uparrow})$ has two electrons in the same initial state. The same arguments hold for $\varepsilon_R^{\downarrow\downarrow}$. This effect will suppress the resonant scattering between equal spins at $\varepsilon_R^{\uparrow\uparrow}$ and $\varepsilon_R^{\downarrow\downarrow}$.

Tendency of the direct and exchange terms of the interaction to cancel

Next we argue for the suppression of the resonant scattering between equal spins in a slightly more formal way by considering the electron-electron interaction matrix element. This has the advantage of leading to a quantitatively way of calculating the suppression.

The matrix element eq.(4.44) for the electron-electron interaction has a direct and exchange term. For the scattering *exactly at the Fermi level* the direct and exchange terms cancel each other, since $k_{1'} - k_1 = k_{2'} - k_1 = 2k_{Fb\uparrow}$ (inserting eq.(4.80)), i.e.

$$\langle 1'2' | \mathcal{V} | 12 \rangle = \frac{1}{\mathcal{L}} \left[V_{k_{1'} - k_1 = 2k_{Fb\uparrow}}^{babb} - V_{k_{2'} - k_1 = 2k_{Fb\uparrow}}^{babb} \right] = 0 \quad \text{exactly at } \varepsilon_F = \varepsilon_R^{\uparrow\uparrow}. \quad (4.81)$$

Again, the same result is obtained in the case of scattering with two spin \downarrow electrons.

Furthermore, it is clear from eq.(4.44) that for any momentum independent interaction in Fourier space (i.e. local interaction in real space¹⁸) equal spins cannot interact, since the direct and exchange terms cancel. This rather general statement can be understood physical as the facts that the Pauli principle forbids electrons in the same spin state to touch. However, if the interaction is *non-local* in space, i.e. the interaction has a momentum dependence in Fourier space, then electrons with equal spins can interaction, *but* there is still a tendency for the interaction to be weaker due to the Pauli principle, or equivalently, due to an almost¹⁹ cancellation of the direct and exchange terms.

Therefore to calculate the effect of the scattering between equal spins, we need to include the momentum dependence q in the interaction V_q^{babb} . To do this to lowest order in temperature²⁰, V_q^{babb} is expanded in q around $2k_{Fb\sigma}$, which is the momentum transfer at the Fermi level $\varepsilon_F = \varepsilon_R^{\sigma\sigma}$ for both the direct and exchange term, i.e.

$$V_q^{babb} \simeq V_{2k_{Fb\sigma}}^{babb} + \partial_q V_{2k_{Fb\sigma}}^{babb} (q - 2k_{Fb\sigma}) + \dots \quad (4.82)$$

Inserting this expansion in the matrix element eq.(4.44) for the scattering between equal spins seen in figure 4.9(a), we have

$$\langle k_1' b \sigma k_2' b \sigma | \mathcal{V} | k_1 a \sigma k_2 b \sigma \rangle = \frac{1}{\mathcal{L}} \delta_{k_1+k_2, k_1'+k_2'} \partial_q V_{2k_{Fb\sigma}}^{babb} (k_1' - k_2') + \dots \quad (4.83)$$

We will now use this to calculate the interaction-induced conductance and thermopower response near the resonant scattering of equal spins.

The current to lowest order in the interaction and temperature

For a small magnetic field splitting $g\mu_B B \lesssim k_B T$, it is possible to have several of the different scattering processes seen in figure 4.9 active for the same value of ε_F . To be able to separate the signal of one resonance from the other, we investigate the regime of large splitting compared to temperature:

$$k_B T \ll g\mu_B B. \quad (4.84)$$

In this regime, we can calculate the current to lowest order in the interaction and temperature close to $\varepsilon_R^{\uparrow\uparrow}$ or $\varepsilon_R^{\downarrow\downarrow}$ separately using the same approach as in section 4.3, but now having two spin-polarized subbands (e.g. $\varepsilon_{ka\uparrow}$ and $\varepsilon_{kb\uparrow}$) instead of two spin-degenerate subbands (ε_{ka} and ε_{kb}). The only difference from the calculation in section 4.3 is the matrix element and the spin summation.

¹⁸In a local interaction the particle have to touch to interact, which is modelled by a delta function interaction, $V(\mathbf{r}, \mathbf{r}') \propto \delta(\mathbf{r} - \mathbf{r}')$.

¹⁹By almost we mean that the cancellation is not exact, but only suppresses the interaction.

²⁰That this is to lowest order in temperature can be seen by using the same rational as in section 4.3 and will be clear shortly.

Following section 4.3, the current contribution $I_e^{(1)}$ for ε_F near $\varepsilon_R^{\sigma\sigma}$ is (see e.g. eq.(4.34) and eq.(4.47))

$$I_e^{(1)} = 2L \frac{(-e)}{\mathcal{L}} \sum_{\substack{++ \\ --}} f_1^0 f_2^0 (1 - f_{1'}^0) (1 - f_{2'}^0) \delta(\varepsilon_1 + \varepsilon_2 - \varepsilon_{1'} - \varepsilon_{2'}) \quad (4.85)$$

$$\times \frac{2\pi}{\hbar} \left\{ \sum_{\substack{\sigma_1 \sigma_2 \\ \sigma_{1'} \sigma_{2'}}} |\langle k_{1'} n_{1'} k_{2'} n_{2'} | \mathcal{V} | k_1 n_1 k_2 n_2 \rangle|^2 \right\} \left[\frac{\Delta T}{k_B T^2} (\varepsilon_1 - \varepsilon_F) - \frac{eV}{k_B T} \right] \Bigg|_{\substack{n_2=a, n_1=b \\ n_{1'}=n_{2'}=b}}.$$

Introducing the new variables $z_i = \frac{\varepsilon_i - \varepsilon_F}{k_B T}$ and expanding in temperature the calculation follows the one in section 4.3.2, replacing $k_{Fn} \rightarrow k_{Fn\sigma}$ and $T_{Fn} \rightarrow T_{Fn\sigma}$, except for the spin summation and the matrix element. Using eq.(4.83) this is:

$$\sum_{\substack{\sigma_1 \sigma_2 \\ \sigma_{1'} \sigma_{2'}}} |\langle k_{1'} b k_{2'} b | \mathcal{V} | k_1 b k_2 a \rangle|^2 = \frac{1}{\mathcal{L}^2} \delta_{k_1+k_2, k_{1'}+k_{2'}} |\partial_q V_{2k_{Fb\sigma}}^{babb}|^2 (k_{1'} - k_{2'})^2$$

$$= \frac{1}{\mathcal{L}^2} \delta_{k_1+k_2, k_{1'}+k_{2'}} |\partial_q V_{2k_{Fb\sigma}}^{babb}|^2 \frac{k_{Fb\sigma}^2}{4} \left(\frac{T}{T_{Fb\sigma}} \right)^2 (z_{1'} - z_{2'})^2, \quad (4.86)$$

where all the spin are the same: $\sigma_1 = \sigma_2 = \sigma_{1'} = \sigma_{2'} = \sigma$. This equation replaces eq.(4.45) in the calculation in subsection 4.3.2. Here $k_{1'}$ and $k_{2'}$ are inserted in terms of $z_{1'}$ and $z_{2'}$, respectively, to lowest order in $T/T_{Fb\sigma}$. We see that the matrix element eq.(4.86) is to lowest order in $T/T_{Fb\sigma}$, since including higher orders in the expansion of V_q^{baab} in eq.(4.83) would only lead to higher order terms in $T/T_{Fb\sigma}$. Inserting eq.(4.86) and using z variables to lowest order the current is

$$I_e^{(1)} = \frac{2(-e)L}{\pi^2 \hbar} \frac{(k_{Fb\sigma})^4 k_{Fa\sigma}}{128 k_B T_{Fb\sigma}} |\partial_q V_{2k_{Fb\sigma}}^{babb}|^2 \left(\frac{T}{T_{Fb\sigma}} \right)^3 \quad (4.87)$$

$$\times \int_{-\infty}^{\infty} dz_1 \int_{-\infty}^{\infty} dz_2 \int_{-\infty}^{\infty} dz_{1'} \int_{-\infty}^{\infty} dz_{2'} (z_{1'} - z_{2'})^2 g(z_1) g(z_2) g(-z_{1'}) g(-z_{2'})$$

$$\times \delta(z_1 + z_2 - z_{1'} - z_{2'}) \delta\left(-z_1 + \frac{1}{3} z_2 - z_{1'} - z_{2'} - \frac{8}{3} \frac{\Delta \varepsilon_F^{\sigma\sigma}}{k_B T}\right) \left[\frac{\Delta T}{T_{Fa\sigma}} z_1 - \frac{eV}{k_B T_{Fa\sigma}} \right],$$

where the important difference compared to eq.(4.64) is the extra T^2 factor and the factor $(z_{1'} - z_{2'})^2$ in the integrand. Here we have introduced

$$\frac{\Delta \varepsilon_F^{\sigma\sigma}}{k_B T} \equiv \frac{3 \hbar v_{Fb\sigma} (3k_{Fb\sigma} - k_{Fa\sigma})}{8 k_B T} \simeq \frac{(\varepsilon_F - \varepsilon_R^{\sigma\sigma})}{k_B T}, \quad (4.88)$$

so $k_{Fa\sigma}/k_{Fb\sigma} \simeq 3$ to lowest order in temperature and the prefactor becomes

$$\begin{aligned} & \frac{2(-e)L}{\pi^2\hbar} \frac{(k_{Fb\sigma})^4 k_{Fa\sigma}}{128k_B T_{Fb\sigma}} |\partial_q V_{2k_{Fb\sigma}}^{babb}|^2 \left(\frac{T}{T_{Fb\sigma}} \right)^3 \\ &= \frac{81(-e)k_B T_{Fa\sigma}}{16\pi^2\hbar} L k_{Fa} \left(\frac{k_{Fa\sigma} |\partial_q V_{2k_{Fb\sigma}}^{babb}|}{\hbar v_{Fa\sigma}} \right)^2 \left(\frac{T}{T_{Fa\sigma}} \right)^3 + \mathcal{O}\left[\left(\frac{T}{T_{Fa\sigma}}\right)^4\right]. \end{aligned}$$

Again we introduce the new variables z_d and z_s eq.(4.66) and calculate the z_d integral by using that

$$\begin{aligned} & \int_{-\infty}^{\infty} dz_d (z_{1'} - z_{2'})^2 g(-z_{1'}) g(-z_{2'}) = \\ & \int_{-\infty}^{\infty} dz_d z_d^2 g\left[-\frac{1}{2}(z_s + z_d)\right] g\left[-\frac{1}{2}(z_s - z_d)\right] = -2z_s n_B(-z_s) \left(\frac{4\pi^2}{3} + \frac{1}{3} z_s^2 \right). \end{aligned} \quad (4.89)$$

and remember the factor of 1/2 from the determinant of the variable change. Doing the z_s and z_2 integrals using the delta functions, we find

$$\begin{aligned} I_e^{(1)} &= \frac{4e}{h} \frac{9L}{\ell_{ee}^{\sigma\sigma}} \left(\frac{T}{T_{Fa\sigma}} \right)^3 \frac{1}{16} \int_{-\infty}^{\infty} dz h\left(z, \frac{\Delta\varepsilon_F^{\sigma\sigma}}{k_B T}\right) \left[\frac{4\pi^2}{3} + \frac{1}{3} \left(2z + 4 \frac{\Delta\varepsilon_F^{\sigma\sigma}}{k_B T} \right)^2 \right] \\ &\quad \times (k_B \Delta T z - eV) = G_T^{(1)\sigma\sigma} \Delta T - G^{(1)\sigma\sigma} V, \end{aligned} \quad (4.90)$$

in terms of the $h(z, x)$ function defined in eq.(4.70) and introducing the length

$$\ell_{ee}^{\sigma\sigma} = \frac{2}{27} \frac{2\pi}{k_{Fa\sigma}} \left(\frac{\hbar v_{Fa\sigma}}{k_{Fa\sigma} |\partial_q V_{2k_{Fb\sigma}}^{babb}|} \right)^2. \quad (4.91)$$

Therefore the conductance and thermopower response at the resonances for scattering between equal spins near $\varepsilon_R^{\sigma\sigma}$ ($\sigma = \uparrow, \downarrow$) are:

$$G^{(1)\sigma\sigma} = \frac{4e^2}{h} \frac{9L}{\ell_{ee}^{\sigma\sigma}} \left(\frac{T}{T_{Fa\sigma}} \right)^3 \tilde{F}_0 \left(\frac{\varepsilon_F - \varepsilon_R^{\sigma\sigma}}{k_B T} \right), \quad (4.92a)$$

$$S^{\sigma\sigma} = \frac{k_B}{e} \frac{9L}{\ell_{ee}^{\sigma\sigma}} \left(\frac{T}{T_{Fa\sigma}} \right)^3 \tilde{F}_1 \left(\frac{\varepsilon_F - \varepsilon_R^{\sigma\sigma}}{k_B T} \right), \quad (4.92b)$$

where $\tilde{F}_n(x)$ is defined by

$$\tilde{F}_n(x) = \frac{1}{16} \int_{-\infty}^{\infty} dz z^n h(z, x) \left[\frac{4\pi^2}{3} + \frac{1}{3} (2z + 4x)^2 \right], \quad (4.93)$$

and for $n = 0, 1$ seen on figure 4.12 to be of order $F_n(x)$ eq.(4.73) by comparing figure 4.5 and 4.12. It is evident from eq.(4.92) that $G^{(1)\sigma\sigma}$ and $S^{\sigma\sigma}$ are suppressed

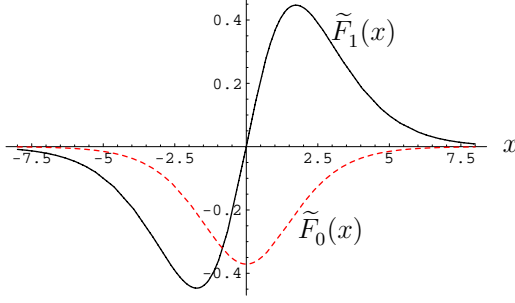


Figure 4.12: The dimensionless scaling functions $\tilde{F}_0(x)$ and $\tilde{F}_1(x)$ entering the conductance correction $G^{(1)\sigma\sigma}$ and the interaction-induced thermopower $S^{\sigma\sigma}$ eq.(4.92) due to the scattering between equal spins. Note the similarity to the functions $F_0(x)$ and $F_1(x)$ seen in figure 4.5 entering the $B = 0$ result.

compared to the $B = 0$ result in eq.(4.72) by two powers of temperature and by the fact that $k_{Fa\sigma}|\partial_q V_{2k_{Fb\sigma}}^{babb}|$ enters $\ell_{ee}^{\sigma\sigma}$ whereas $|V_{2k_{Fb}}^{babb}|$ enters ℓ_{ee} . We have hidden some of the magnetic field splitting in the parameters²¹, e.g. $T_{Fa\sigma} = (\varepsilon_F - \sigma g\mu_B B/2)/k_B$. In the thermopower $S^{\sigma\sigma}$ given above, we have assumed that $G^{(0)} = 4e^2/h$, which is always true for $\varepsilon_R^{\uparrow\uparrow}$, but for $\varepsilon_R^{\downarrow\downarrow}$ it is only true for $g\mu_B B \lesssim 0.11\varepsilon_0$ (see figure 4.11) and for $g\mu_B B \gtrsim 0.13\varepsilon_0$ one should use $G^{(0)} = 3e^2/h$ to get $S^{\downarrow\downarrow}$. As in the $B = 0$ case, the Mott formula is found to be a good approximation to lowest order in temperature, i.e. $\tilde{F}_1(x) \simeq \frac{\pi^2}{3} \frac{d\tilde{F}_0(x)}{dx}$.

4.5.4 Resonant scattering between opposite spins

Next the resonant scattering for electrons of opposite spin seen in figure 4.9(b) is discussed in the regime $k_B T \ll g\mu_B B$, so it is possible to consider the scattering at $\varepsilon_R^{\downarrow\downarrow}$ and $\varepsilon_R^{\uparrow\uparrow}$ separately. In this case, there is no suppression of the effect due to the Pauli principle. On the contrary, due to the opposite spins the exchange term will be zero in the matrix element eq.(4.44), because for the scattering near $\varepsilon_F = \varepsilon_R^{\uparrow\downarrow}$ or $\varepsilon_F = \varepsilon_R^{\downarrow\uparrow}$ the spins are $\sigma_1 = \sigma_{1'} \equiv \sigma$ and $\sigma_2 = \sigma_{2'} = \bar{\sigma} = -\sigma$, so

$$\begin{aligned} \langle k_1' b \sigma k_2' b \bar{\sigma} | \mathcal{V} | k_1 b \sigma k_2 a \bar{\sigma} \rangle &= \frac{1}{\mathcal{L}} \delta_{k_1+k_2, k_{1'}+k_{2'}} \left[V_{k_{1'}-k_1}^{babb} \delta_{\sigma, \sigma} \delta_{\bar{\sigma}, \bar{\sigma}} - V_{k_{2'}-k_1}^{babb} \delta_{\sigma, \bar{\sigma}} \delta_{\bar{\sigma}, \sigma} \right], \\ &= \frac{1}{\mathcal{L}} \delta_{k_1+k_2, k_{1'}+k_{2'}} V_{k_{1'}-k_1}^{babb}. \end{aligned} \quad (4.94)$$

To lowest order in the temperature, we can use $V_{k_{1'}-k_1}^{babb} = V_{2k_{Fb\sigma}}^{babb}$ (for $\varepsilon_R^{\sigma\bar{\sigma}}$), so including the spin summation for one of the resonances $\varepsilon_R^{\sigma\bar{\sigma}}$ we get

$$\sum_{\substack{\sigma_1 \sigma_2 \\ \sigma_{1'} \sigma_{2'}}} |\langle k_1' b \sigma k_2' b \bar{\sigma} | \mathcal{V} | k_1 b \sigma k_2 a \bar{\sigma} \rangle|^2 = \frac{1}{\mathcal{L}^2} \delta_{k_1+k_2, k_{1'}+k_{2'}} |V_{2k_{Fb\sigma}}^{babb}|^2. \quad (4.95)$$

At this point, it is instructive to compare to the case without a magnetic field given in eq.(4.45). For $B = 0$, the lowest order result comes from scattering

²¹If we expand in the magnetic field splitting $g\mu_B B/(\varepsilon_F - \varepsilon_0)$, then the lowest order term is to replace $(T_{Fa\sigma}, v_{Fa\sigma}, k_{Fb\sigma}, k_{Fa\sigma}) \rightarrow (T_{Fa}, v_{Fa}, k_{Fb}, k_{Fa})$ everywhere except in $\varepsilon_R^{\sigma\sigma}$. This is the result stated in paper II.

between opposite spins (see e.g. the above discussion in section 4.5.3). However, for $B = 0$ the summation over spin gives $4 \frac{1}{\mathcal{L}^2} \delta_{k_1+k_2, k_{1'}+k_{2'}} |V_{2k_{Fb}}^{babb}|^2$, whereas scattering at each of the two resonances $\varepsilon_R^{\sigma\bar{\sigma}}$ only contributes $\frac{1}{\mathcal{L}^2} \delta_{k_1+k_2, k_{1'}+k_{2'}} |V_{2k_{Fb\sigma}}^{babb}|^2$ in the separable regime $k_B T \ll g\mu_B B$. Therefore the $B = 0$ resonance in the conductance or thermopower is 2 times larger than just adding the two separate resonances at $\varepsilon_R^{\uparrow\downarrow}$ and $\varepsilon_R^{\downarrow\uparrow}$, respectively. This is because the exchange term in the interaction gives a contribution in the $B = 0$ case and no contribution in the spin-split case, where exchange of the final states $1' \rightleftharpoons 2'$ is not possible. To make this statement clearer, the summation over spin in the $B = 0$ case eq.(4.45) is performed again (in the low temperature limit: $V_{k_{1'}-k_1}^{babb} \rightarrow V_{2k_{Fb}}^{babb}$):

$$\begin{aligned}
& \sum_{\substack{\sigma_1 \sigma_2 \\ \sigma_{1'} \sigma_{2'}}} |\langle k_{1'} b \sigma_{1'} k_2 b \sigma_{2'} | \mathcal{V} | k_1 b \sigma_1 k_2 a \sigma_2 \rangle|^2 \\
&= \frac{1}{\mathcal{L}^2} \delta_{k_1+k_2, k_{1'}+k_{2'}} |V_{2k_{Fb}}^{babb}|^2 \sum_{\substack{\sigma_1 \sigma_2 \\ \sigma_{1'} \sigma_{2'}}} (\delta_{\sigma_1, \sigma_{1'}} \delta_{\sigma_2, \sigma_{2'}} - \delta_{\sigma_1, \sigma_{2'}} \delta_{\sigma_2, \sigma_{1'}})^2 \\
&= \frac{1}{\mathcal{L}^2} \delta_{k_1+k_2, k_{1'}+k_{2'}} |V_{2k_{Fb}}^{babb}|^2 \left\{ \underbrace{(\delta_{\uparrow, \uparrow} \delta_{\downarrow, \downarrow} - \delta_{\uparrow, \downarrow} \delta_{\downarrow, \uparrow})^2}_{\text{direct like } \varepsilon_R^{\uparrow\downarrow}} + \underbrace{(\delta_{\uparrow, \downarrow} \delta_{\downarrow, \uparrow} - \delta_{\uparrow, \uparrow} \delta_{\downarrow, \downarrow})^2}_{\text{exchange of } \varepsilon_R^{\uparrow\downarrow}: \sigma_{1'} \rightleftharpoons \sigma_{2'}} \right. \\
&\quad \left. + \underbrace{(\delta_{\downarrow, \downarrow} \delta_{\uparrow, \uparrow} - \delta_{\downarrow, \uparrow} \delta_{\uparrow, \downarrow})^2}_{\text{direct like } \varepsilon_R^{\downarrow\uparrow}} + \underbrace{(\delta_{\downarrow, \uparrow} \delta_{\uparrow, \downarrow} - \delta_{\downarrow, \downarrow} \delta_{\uparrow, \uparrow})^2}_{\text{exchange of } \varepsilon_R^{\downarrow\uparrow}: \sigma_{1'} \rightleftharpoons \sigma_{2'}} \right\} = \frac{4}{\mathcal{L}^2} \delta_{k_1+k_2, k_{1'}+k_{2'}} |V_{2k_{Fb}}^{babb}|^2.
\end{aligned} \tag{4.96}$$

Here we observe that the exchange terms gives a contribution at $B = 0$, which is not present in the spin-split case, where the exchange processes are simply not possible. Therefore the mentioned factor of two is a consequence of the exchange terms.

The calculation of the conductance and thermopower response at the resonances $\varepsilon_R^{\sigma\bar{\sigma}}$ is a bit different than the previous calculations since $k_{Fa\bar{\sigma}} = 2k_{Fb\sigma} + k_{Fb\bar{\sigma}}$ at the resonance. This will e.g. enter in the momentum conservation, when using the new variables z_i . However, here we restrict ourself to the limit

$$k_B T \ll g\mu_B B \ll \varepsilon_F - \varepsilon_0, \tag{4.97}$$

so we can both separate the resonances and expand in the magnetic field splitting $g\mu_B B/(\varepsilon_F - \varepsilon_0)$. To lowest order in $g\mu_B B/(\varepsilon_F - \varepsilon_0)$ we get:

$$G^{(1)\sigma\bar{\sigma}} = \frac{4e^2}{h} \frac{1}{4} \frac{L}{\ell_{ee}} \frac{T}{T_F} F_0 \left(\frac{\varepsilon_F - \varepsilon_R^{\sigma\bar{\sigma}}}{k_B T} \right), \tag{4.98a}$$

$$S^{\sigma\bar{\sigma}} = \frac{k_B}{e} \frac{1}{4} \frac{L}{\ell_{ee}} \frac{T}{T_F} F_1 \left(\frac{\varepsilon_F - \varepsilon_R^{\sigma\bar{\sigma}}}{k_B T} \right), \tag{4.98b}$$

where the factor of 1/4 comes from the above discussion regarding the exchange term in the interaction.

4.6 Summary

In this chapter, we have described how the electron-electron interaction can induce resonances at particular Fermi energies in the conductance and thermopower of a multi-mode 1D wire well connected to external reservoirs. At these resonant points, the conductance gets a small dip (negative peak) on top of the non-interacting conductance steps. For the thermopower the non-interacting signal is exponentially suppressed in temperature and therefore the interaction-induced thermopower is the leading order in temperature around the resonance points. At these points the thermopower has a wave-like structure as a function of the Fermi level ε_F : Negative below the resonance point ε_R , positive above ε_R and exponentially suppressed far away from ε_R . For an interaction-induced resonance to occur the interaction has to conserve momentum and energy, change the number of left and right moving electrons and happen at the Fermi level. This restricts the possible resonant points substantially, nevertheless, they do exist.

In particular, the case of two transverse modes were discussed here with and without a magnetic field. Without magnetic field there is only one resonance point at $\varepsilon_F = 9\varepsilon_0/8$, where ε_0 is the subband spacing. We found that a magnetic field in the plane of the wire, spin-splits the resonances into four resonances: Two for scattering between electrons with equal spin and two for scattering between opposite spin electrons. Due to the Pauli principle, the scattering between equal spins are suppressed compared to scattering between opposite spins.

The thermopower and conductance correction calculation was an application of the Boltzmann equation approach discussed in chapter 3. It is perturbative²² in the interaction and to lowest order in the temperature.

An experimental verification of the effect is yet to come and here we have presented a number of features to look for, e.g. the magnetic field dependence and the fact that the thermopower (conductance correction) for different low temperatures can be scaled onto a single function.

²²Note that the same perturbative result can be obtained by a Green's functions approach.

Chapter 5

Three-particle scattering in finite quantum wires

In this chapter, the effect of three-body interaction on the conductance and thermopower of a single-mode finite quantum wire is explained. The chapter only contains a brief description of the subject, because paper III (p.159) is rather long and hence contain most details needed to understand the subject.

5.1 The three-particle interactions within the wire

A finite length single-mode quantum wire with reflectionless contacts is considered using the Boltzmann equation approach of chapter 3, see figure 5.1. The leads are non-interacting and their distribution functions are given by the Fermi functions $f_{L/R}^0(\varepsilon_k)$ each with their own chemical potential $\mu_{L/R}$ and temperature $T_{L/R}$. The wire is considered to be clean, i.e. no impurity or roughness scattering, so only the electron-electron interaction can redistribute the electrons in the wire and hence change the conductance and thermopower.

Why three-particle interactions?

The electron-electron interaction processes in the wire conserve the momentum and energy. As a consequence, two-particle interactions cannot redistribute the electrons in the single-mode wire, i.e. for an interaction between two electrons in

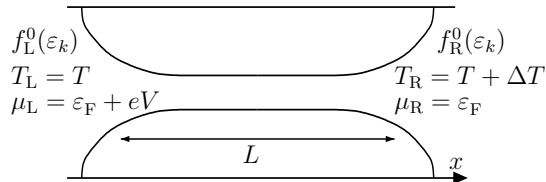


Figure 5.1: A schematic picture of a clean 1D wire of length L perfectly connected to non-interacting leads having different chemical potentials $\mu_{L/R}$ and temperatures $T_{R/L}$.

k_1 and k_2 the only possible outcome is $(k_{1'}, k_{2'}) = (k_1, k_2)$ or $(k_{1'}, k_{2'}) = (k_2, k_1)$ and in neither case, have the electrons been redistributed. This is easily seen explicitly for a quadratic dispersion $\varepsilon_k \propto k^2$, see p.14. However, it is generally true *for any dispersion with positive curvature*. To show this, one can assume that other solutions than the trivial ones are possible and then show that this leads to a contradiction. Let us consider an example: $0 < k_1, k_{1'} < k_2, k_{2'}$ (e.g. two small q processes on the positive branch of the dispersion). Since the distance $k_{1'} - k_1$ is the same as $-(k_{2'} - k_2)$, then using the positive curvature we must have $|\varepsilon_{1'} - \varepsilon_1| < |\varepsilon_{2'} - \varepsilon_2|$, however, this is in contradiction to energy conservation $\varepsilon_{1'} - \varepsilon_1 = -(\varepsilon_{2'} - \varepsilon_2)$, so the scattering is simply one of the trivial ones and a situation with $k_1, k_{1'} < k_2, k_{2'}$ is not possible. The others cases are similar.

Therefore we consider three-particle scattering, where the momentum and energy is conserved among three particles in the interaction process, see figure 3.3, so the conservation laws are

$$\varepsilon_{k_1} + \varepsilon_{k_2} + \varepsilon_{k_3} = \varepsilon_{k_{1'}} + \varepsilon_{k_{2'}} + \varepsilon_{k_{3'}}, \quad (5.1a)$$

$$k_1 + k_2 + k_3 = k_{1'} + k_{2'} + k_{3'}, \quad (5.1b)$$

which leave more phase space for the scattering. Here we consider, what kind of effects this type of interaction can have on the conductance and thermopower.

5.2 The perturbative approach

To calculate the conductance and thermopower change due to the three-particle interactions, the Boltzmann approach is used in the limit of weak interactions and/or short lengths L , so the (linear response) current is expanded in the scattering rate as $I_e = I_e^{(0)} + I_e^{(1)} + \dots$. Here $I_e^{(0)}$ is the non-interacting current for a perfectly conducting wire

$$I_e^{(0)} \simeq -\frac{2e^2}{h}V (1 - e^{-T_F/T}) + \frac{2e}{h}k_B\Delta T \frac{T_F}{T} e^{-T_F/T} \quad (5.2)$$

for low temperatures (i.e. to first order in $e^{-T_F/T}$) and $I_e^{(1)}$ is the result due to weak three-particle scatterings (see section (3.2.3))

$$I_e^{(1)} = -L \frac{(-e)}{\mathcal{L}} \sum_{\sigma k < 0} \mathcal{I}_k[f^{(0)}], \quad (5.3)$$

where $\mathcal{I}_k[f^{(0)}]$ is the three-particle collision integral eq.(3.11). Note that we have applied the bias V and temperature difference ΔT as in figure 5.1, so $I_e = -GV + G_T\Delta T$. The task is now to find $I_e^{(1)}$ to lowest order in temperature $T/T_F \ll 1$, and we refer to the paper III for details.

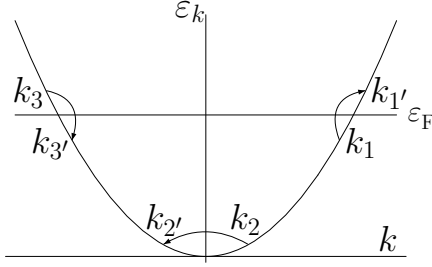


Figure 5.2: The dominant current changing three-particle scattering process at low temperatures. The process requires the state $k_{2'}$ at the bottom of the Fermi sea to be unoccupied, and therefore it only leads to an exponentially suppressed correction $\propto e^{-T_F/T}$ to the thermopower and conductance. (The opposite process creating right movers of course also exists.)

5.2.1 The dominant three-particle scattering process

From section 3.3, we know that the scattering needs to change the number of left and right movers to change the current. However, even though the three-particle interactions have more phase space than the two-particle interactions, they still *cannot* conserve momentum and energy at the Fermi level, *if* the interaction process also should change the number of left and right movers. Therefore the current changing three-particle interactions require empty states deep in the Fermi sea (or occupation of states far above from ε_F). Therefore the correction to the current at low temperatures is exponentially suppressed, $\propto e^{-T_F/T}$. As a consequence, it is unlikely, to detect the correction from three-particle interactions at low-temperatures for short clean wires, where the interaction is weak.

We have identified the most important low-temperature scattering process to be the one seen on figure 5.2. Here all the exchanged momentum differences $(k_{i'} - k_i)$ are small and in the bottom of the band, a right mover is changed to a left mover. Therefore the process is changing two right movers and one left mover into two left movers and a right mover. The exponential suppression $e^{-T_F/T}$ comes from the requirement that the state $k_{2'}$ deep in the Fermi sea needs to be empty.

5.2.2 The conductance and thermopower corrections

The result of the low-temperature $T/T_F \ll 1$ calculation of the current correction $I_e^{(1)}$ to first order in the three-particle scattering rate leads to the following conductance and thermopower:

$$S = \frac{k_B}{e} \frac{T_F}{T} e^{-T_F/T} \left[1 + \frac{L}{\ell_{eee}} \right], \quad (5.4)$$

$$G = \frac{2e^2}{h} - \frac{2e^2}{h} e^{-T_F/T} \left[1 + \frac{L}{\ell_{eee}} \right], \quad (5.5)$$

where the effective length ℓ_{eee} is introduced as

$$\ell_{eee}^{-1} = \frac{8505}{2048\pi^3} \frac{(V_0 k_F)^4}{\varepsilon_F^4} \left(\frac{k_F}{q_0} \right)^4 \left(\frac{T}{T_F} \right)^7 k_F. \quad (5.6)$$

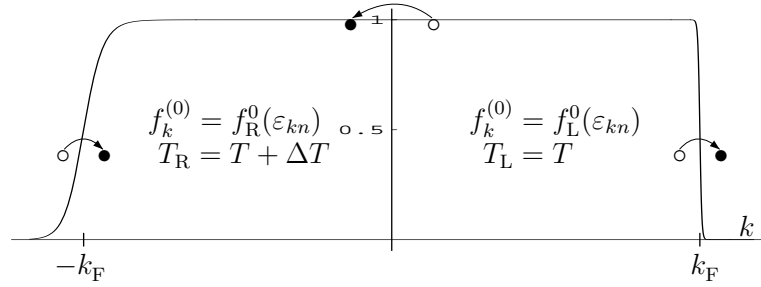


Figure 5.3: The non-interacting initial distribution function, which is changed slightly by the three-particle scattering process seen in figure 5.2. In the initial distribution function the left movers ($k < 0$) are warmer than the right movers ($k > 0$) (see figure 5.1). Since the left movers have a higher temperature than the right movers, it is easier to scattering into states with $k < 0$ at the bottom of the Fermi sea. Therefore this process dominates over the opposite process and more left movers than right movers are created and in terms a positive thermopower contribution is produced.

The symmetrized interaction in k -space $\tilde{V}_q \equiv V_q + V_{-q}$ enters the calculation, where V_q is the Fourier transform of the interaction. It is expanded in q as

$$\tilde{V}_q \equiv V_q + V_{-q} = V_0 \left[1 - \left(\frac{q}{q_0} \right)^2 + \mathcal{O}(q^4) \right], \quad (5.7)$$

since only small q are relevant for the scattering process seen in figure 5.2. Here $q_0 \ll k_F$ describes the screening of the interaction due to the nearby metallic gates and V_0 is (twice) the $q = 0$ Fourier component of the interaction (cut off by screening). Furthermore, we have used a quadratic dispersion and only used the direct three-particle interaction term in the matrix element, since this is the most important one for small $q_i = k_{i'} - k_i$ for $i = 1, 2, 3$. This approximation will be clear in eq.(5.13). Note that for a contact interaction $V_q = \text{constant}$ (i.e. $q_0 \rightarrow \infty$), we do not have any effect of the three-particle interactions.

The important point of the interaction correction (apart from being exponentially suppressed) is that it is proportional to the length L , the interaction cubed V_0^4 and some power of temperature $(T/T_F)^n$ ($n = 7$ for conductance and $n = 6$ for thermopower).

5.2.3 A simple picture for the sign of the thermopower

The sign of the thermopower contribution due to the interactions is positive, which means that the interactions *increase* the particle current due to a temperature difference. This is in contrast to the current due to a bias voltage V , which is decreased by the interactions.

Here the positive sign of S is explained by considering the dominant scattering process in figure 5.2. For $\Delta T > 0$ the non-interacting *particle* current is going

from right to left (opposite to the electric current) leading to $S^{(0)} > 0$. Figure 5.3 shows the initial distribution function with warmer left movers ($k < 0$) than right movers ($k > 0$). (Here $\mu_R = \mu_L$, since it is enough to consider G_T .) The dominant scattering process can a priori create both left and right movers (i.e. the opposite process of the one shown in figure 5.2 is of course also allowed). However, if the left movers have a higher temperature, then it is easier to scatter into states with $k < 0$ than $k > 0$. (E.g. for zero temperature right movers, it is impossible to insert an extra electron in the bottom of the Fermi sea of the right movers.) Therefore the scattering process will create more left movers, which in terms produce more particle current to the left and a higher thermopower. This explains the sign of the thermopower correction.

5.2.4 A simple picture of the conductance correction

The conductance correction can be explained in a similar manner as the thermopower one above. In this case, the non-interacting particle current is from left to right (opposite to the electric current), i.e. $I_e^{(0)} = -G^{(0)}V$, see figure 5.1. The initial distribution function have different chemical potential (and the same temperature) for the right and left movers. Since the chemical potential of the right movers is higher than for the left movers, scattering at the bottom of the band (figure 5.2) favors scattering into the left movers and hence reduce the particle current, and in terms gives a negative conductance correction.

5.2.5 The three-particle scattering rate

One of the most interesting issues in connection with the three-particle scattering is the three-particle scattering rate found as

$$W_{123;1'2'3'} = \frac{2\pi}{\hbar} |\langle 1'2'3' | V G_0 V | 123 \rangle_c|^2 \delta(\varepsilon_1 + \varepsilon_2 + \varepsilon_3 - \varepsilon_{1'} - \varepsilon_{2'} - \varepsilon_{3'}). \quad (5.8)$$

This is a generalization of Fermis Golden rule using the T -matrix, $T = V + V G_0 T$, iterated to second order to obtain the three-particle scatterings, see e.g. [14, p. 87-88]. It turns out that the three-particle interaction matrix element $\langle 1'2'3' | V G_0 V | 123 \rangle_c$ have interesting properties. Here the index c means that it should be a real 3-body interaction and not just an effective two-body scattering, where one of the incoming particles does not participate in the scattering. Furthermore,

$$G_0 = \frac{1}{\varepsilon_1 + \varepsilon_2 + \varepsilon_3 - H_0 + i\eta}, \quad (\eta \rightarrow 0^+) \quad (5.9a)$$

$$V = \frac{1}{2L} \sum_{k_1 k_2 q} \sum_{\sigma_1 \sigma_2} V_q c_{k_1+q\sigma_1}^\dagger c_{k_2-q\sigma_2}^\dagger c_{k_2\sigma_2} c_{k_1\sigma_1}, \quad (5.9b)$$

where H_0 is the unperturbed Hamiltonian (i.e. kinetic energy with some dispersion). After some operator algebra (using $|123\rangle = c_{k_1\sigma_1}^\dagger c_{k_2\sigma_2}^\dagger c_{k_3\sigma_3}^\dagger |0\rangle$) the matrix element becomes

$$\langle 1'2'3'|VG_0V|123\rangle_c = \frac{1}{(2L)^2} \sum_{(abc) \in P(123)} \sum_{(a'b'c') \in P(1'2'3')} \text{sgn}(abc) \text{sgn}(a'b'c') \quad (5.10)$$

$$\times \frac{\tilde{V}_{a'-a} \tilde{V}_{c'-c} \delta_{a+b+c, a'+b'+c'}}{\varepsilon_b + \varepsilon_c - \varepsilon_{c'} - \varepsilon_{b+c-c'} + i\eta} \delta_{\sigma_{a'}, \sigma_a} \delta_{\sigma_{b'}, \sigma_b} \delta_{\sigma_{c'}, \sigma_c},$$

where $\tilde{V}_q = V_q + V_{-q}$ is the symmetrized interaction and the set of all permutations is

$$P(123) = \{(123)^+, (231)^+, (312)^+, (132)^-, (321)^-, (213)^-\}, \quad (5.11)$$

where the sign of the permutation $\text{sgn}(abc)$ was given as a superscript. The matrix element contains 36 terms and therefore the scattering rate contains $36^2 = 1296$ terms¹. This expression does not rely on a quadratic band or on the assumption of energy conservation. A visualization of the matrix element is seen on figure 3 in paper III.

Next the matrix element is rewritten in a more appealing manner. This is inspired by the two-particle matrix element, which contains a direct and an exchange term, i.e.

$$\langle 1'2'|V|12\rangle = \frac{\delta_{k_1+k_2, k_{1'}+k_{2'}}}{\mathcal{L}} \left[\overbrace{\tilde{V}_{k_{1'}-k_1} \delta_{\sigma_1, \sigma_{1'}} \delta_{\sigma_2, \sigma_{2'}}}^{\text{direct term}} - \overbrace{\tilde{V}_{k_{2'}-k_1} \delta_{\sigma_1, \sigma_{2'}} \delta_{\sigma_2, \sigma_{1'}}}^{\text{exchange term } 1' \leftrightarrow 2'} \right]. \quad (5.12)$$

The concept of direct and exchange terms originate in the quantum mechanical principle of indistinguishable particles. Therefore it can be used for the three-particle the matrix element as well. By rewriting eq.(5.10), we obtain

$$\langle 1'2'3'|VG_0V|123\rangle_c = \delta_{k_1+k_2+k_3, k_{1'}+k_{2'}+k_{3'}} \left[\mathbb{V}(11', 22', 33') + \mathbb{V}(12', 23', 31') \right. \quad (5.13)$$

$$\left. + \mathbb{V}(13', 21', 32') - \mathbb{V}(11', 23', 32') - \mathbb{V}(13', 22', 31') - \mathbb{V}(12', 21', 33') \right],$$

where

$$\mathbb{V}(11', 22', 33') = \frac{\delta_{\sigma_{1'}, \sigma_1} \delta_{\sigma_{2'}, \sigma_2} \delta_{\sigma_{3'}, \sigma_3}}{4L^2} \quad (5.14)$$

$$\times \left[\frac{\tilde{V}_{1'-1} \tilde{V}_{3'-3}}{\varepsilon_3 + \varepsilon_2 - \varepsilon_{3'} - \varepsilon_{2+3-3'}} + \frac{\tilde{V}_{2'-2} \tilde{V}_{1'-1}}{\varepsilon_1 + \varepsilon_3 - \varepsilon_{1'} - \varepsilon_{3+1-1'}} + \frac{\tilde{V}_{3'-3} \tilde{V}_{2'-2}}{\varepsilon_2 + \varepsilon_1 - \varepsilon_{2'} - \varepsilon_{1+2-2'}} \right.$$

$$\left. + \frac{\tilde{V}_{1'-1} \tilde{V}_{2'-2}}{\varepsilon_2 + \varepsilon_3 - \varepsilon_{2'} - \varepsilon_{3+2-2'}} + \frac{\tilde{V}_{3'-3} \tilde{V}_{1'-1}}{\varepsilon_1 + \varepsilon_2 - \varepsilon_{1'} - \varepsilon_{2+1-1'}} + \frac{\tilde{V}_{2'-2} \tilde{V}_{3'-3}}{\varepsilon_3 + \varepsilon_1 - \varepsilon_{3'} - \varepsilon_{1+3-3'}} \right].$$

¹By neglecting (the important) Fermi statistics of electrons the same scattering rate was found in [128] (i.e. setting all $\text{sgn}(\dots) = +1$).

In eq.(5.13) $\mathbb{V}(11', 22', 33')$ play the role of the direct term. The final states $1'$, $2'$ and $3'$ can be exchanged (i.e. permuted) in five other ways that $(1'2'3')$ leading to five exchange terms also seen in eq.(5.13). The signs in front of each term is determined by the sign of the permutation. The arguments in the function $\mathbb{V}(11', 22', 33')$ are ordered in three pairs such that the differences between the elements in each pair are the only arguments of the interaction potential \tilde{V}_q , e.g. only $\tilde{V}_{2'-1}$, $\tilde{V}_{1'-2}$ and $\tilde{V}_{3'-3}$ enter the expression for $\mathbb{V}(12', 21', 33')$.

The expression of the three-particle matrix element in terms of direct and exchange terms is very useful, when constructing approximations having a specific scattering process in mind. This is valuable beyond our use here. To perform the correction calculation for the scattering process on figure 5.2 only $\mathbb{V}(11', 22', 33')$ is included in the matrix element, because only small q processes are important (see paper III for details).

Finally, we mention a few observations of the three-particle interaction, which are surprising compared to the case of two-particle interactions.

- If we use a constant interaction, $V_q = \text{constant}$, and a quadratic dispersion, then $\mathbb{V}(1a', 2b', 3c')\delta(\varepsilon_1 + \varepsilon_2 + \varepsilon_3 - \varepsilon_{a'} - \varepsilon_{b'} - \varepsilon_{c'}) = 0$, and hence the matrix element and the current correction. Here spinless electrons are not assumed.
- If we use an interaction like $\tilde{V}_q = V_0(1 - q^2/q_0^2)$, then $\langle 1'2'3' | VG_0V | 123 \rangle_\epsilon = 0$ for spinless electrons. However, each $\mathbb{V}(1a', 2b', 3c')$ is non-zero. This is expected by a mapping to a bosonic model with a contact interaction.

See paper III for further explanations and the connection of these result to exactly solvable models.

5.3 The long wire limit: An open question

The perturbative approach in the three-particle interaction gave a thermopower and conductance correction proportional to the length of the wire, i.e. $S \propto L$. This approach is valid for short wires or weak interactions. However, what happens for longer wires? A possible guess is that the thermopower and conductance correction saturates, when L exceeds some relaxation length (and thereby becomes length independent in the long wire limit). If we think in terms of distribution functions, then this is the case, where the relaxation in the middle of the wire is complete. It is interesting to note that there exist three-particle interactions at the Fermi level, which change the distribution function, but not the number of left and right movers. In perturbation theory these processes simply cancel out, but in the non-perturbative long wire limit they could play a role. The long wire limit is an interesting theoretical question for further studies, because it would give some information about how the distribution functions injected at the left and right contacts relax towards a common distribution function due interactions, see also section 3.1 (p. 33).

Chapter 6

Non-momentum conserving interactions in point contacts

In this chapter, we investigate quantum point contacts, which are so short that translational symmetry is broken and hence the electron-electron interaction processes can break momentum conservation, see figure 6.1. This effect can change the current even in the single mode case. Using perturbation theory in the electron-electron interaction within a Green's function approach, we find a low-temperature $T \ll T_F$ and/or low bias voltage $eV \ll \varepsilon_F$ conductance $G \equiv I/V$ reduction for increasing T and/or V as $G = 2e^2/h - \alpha T^2 - \gamma V^2$, where α and γ are constants (proportional to the interaction). The thermopower is enhanced as $S \propto T^3$. In a large magnetic field, the subbands are spin-split and the interaction between electrons with equal spin become important. Due to the Pauli principle, the conductance and thermopower corrections due to interactions are suppressed by two extra powers of temperature in this case.

NON-MOMENTUM CONSERVING INTERACTIONS IN QUANTUM POINT CONTACTS

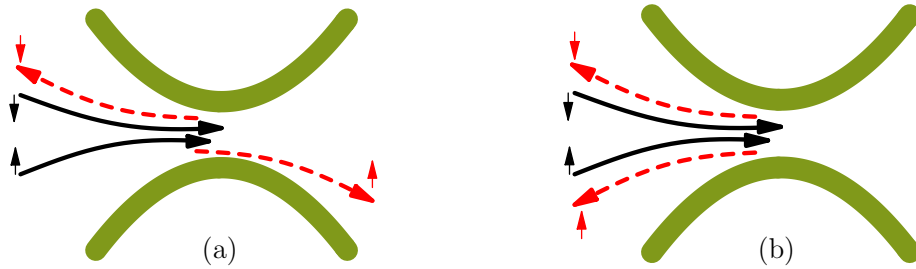


Figure 6.1: An illustration of the non-momentum conserving interaction processes in short quantum point contacts. The thick green lines are the edges of the QPC and the black full (red dashed) arrows are the incoming (outgoing) electrons before (after) the interaction. In the scattering process, the number of left and right movers can either be changed by one (a) or two (b), respectively, and they have different interaction amplitudes. We have indicated that interactions between electrons with opposite spin are most important.

Furthermore, we develop a current formula for a local interaction model $V(x, x') = V_0 \delta(x' - x) \delta(x)$ and use it to study the conductance in the non-perturbative regime making the second-order perturbative approach self-consistent. This gives a (linear) conductance numerically approaching $\sim e^2/h$ for higher temperatures T than are available by perturbative theory, but still smaller T than the Fermi temperature T_F . In the end, we discuss the noise in this model, which is suppressed compared to the non-interacting value¹. These results agrees qualitatively with the experimental data on the 0.7 anomaly in QPC's. The main results of this chapter are submitted in the form of paper IV.

6.1 The physics of non-momentum conserving interactions in quantum point contacts

In the following, we try to justify how electron-electron interaction processes can happen *without* conserving the momentum in quantum point contacts and motivate the simplistic interaction model used to mimic this behavior.

Breaking of momentum conservation in short wires

In general, the translational invariance of a system leads to momentum conservation, so for an infinitely long 1D wire the electron-electron interactions will conserve momentum. However, for a 1D wire connected to leads the translational invariance is broken in the contact region, but if the middle segment of the wire is still long compared to the Fermi wave length, then the momentum is still (approximately) conserved in the wire. This was the situation investigated in the previous chapters. In the present chapter, we consider a wire so short that the momentum does not have to be conserved in the scattering processes. Physically, the momentum of the complete system including boundaries etc. is conserved and the missing momentum in the non-momentum conserving interactions is given to other degrees of freedom of the system e.g. in the form of phonons or otherwise.

Let us consider the situation in more detail. Formally, the momentum conservation stems from the electron-electron interaction matrix element (see section 4.3.1, p. 59). For illustrative purposes, consider a very crude model of the interaction in a quantum wire connected to leads: Two electrons at x_1 and x_2 interact if they are at the same point $x_1 = x_2$ and both of them are in the wire $-L/2 < x_i < L/2$ ($i = 1, 2$ and L is the length of the wire), i.e. $V(x_1, x_2) = V_0 \delta(x_1 - x_2) \theta(L/2 - |x_1|) \theta(L/2 - |x_2|)$. For plane waves as the single particle states, $\psi_k(x) = \frac{1}{\sqrt{L}} e^{ikx}$, the interaction $V_{1'2';12}$ becomes (see

¹It should be emphasized that the noise calculation is the work of Alessandro De Martino and the numerics for the high temperature limit was done by Reinhold Egger. Both are collaborators and co-authors on paper IV.

e.g. eq.(4.36) and eq.(4.37), p. 59)

$$\begin{aligned}
 V_{1'2';12} &= \int_{-\frac{\mathcal{L}}{2}}^{\frac{\mathcal{L}}{2}} dx_1 \int_{-\frac{\mathcal{L}}{2}}^{\frac{\mathcal{L}}{2}} dx_2 \frac{1}{\mathcal{L}^2} e^{-ik_{1'}x_1} e^{-ik_{2'}x_2} V(x_1, x_2) e^{+ik_1x_1} e^{+ik_2x_2} \\
 &= \frac{V_0}{\mathcal{L}^2} \int_{-\frac{L}{2}}^{\frac{L}{2}} dx e^{i\Delta k x} = \frac{V_0}{\mathcal{L}^2} L \frac{2 \sin(L\Delta k/2)}{L\Delta k},
 \end{aligned} \tag{6.1}$$

where $\Delta k = k_1 + k_2 - k_{1'} - k_{2'}$ is the amount of broken momentum conservation and \mathcal{L} is the normalization length. If $L \rightarrow \infty$, then this is a Dirac-delta function (and if $L = \mathcal{L}$ then it is a Kronecker-delta function), so for long wires the momentum is conserved. The *essential point* is that for a short finite length L , it is possible to break the momentum conservation, $\Delta k \neq 0$, and the interaction decreases, the more the momentum conservation is broken². But how short does the wire have to be, before this is feasible? For a scattering process to change the current, the scattering have to change the number of left and right movers. For such a process to happen at the Fermi level, we have either $\Delta k = \pm 2k_F$ or $\Delta k = \pm 4k_F$ corresponding to changing the direction of one or two electrons, respectively. Therefore a crude estimate of the length L at which the non-momentum conserving processes become very important is,

$$L \sim k_F^{-1} \tag{6.2}$$

or smaller.

To obtain a better estimate of the interaction strength and it's precise dependence of $\Delta k L$ one could calculate the interaction $V_{1'2';12}$ using the wave function from the WKB approximation [127, p.253].

Estimation of $k_F L$ for a saddle-point quantum point contact

Next let us consider, if it is possible to have a fully open QPC and at the same time have a length short enough to have non-momentum conserving processes, i.e. $k_F L$ of order one.

Above L was the length at which the interactions were present. Therefore L can roughly be seen as the length, where there is only a single transverse mode energetically available, because as soon as there is more than one mode the screening begins to be more efficient, i.e. the leads begin. We now estimate this length using the saddle-point model (see section 1.5.1, p. 8). In figure 6.2,

²Note that the function in eq.(6.1) is an oscillation with decreasing amplitude as a function of Δk . This behavior is due to the sharp cut-off of the interaction at $x = \mp L/2$ and if a more smooth cut-off is used, then the oscillating behavior is absent,

e.g. $V(x_1, x_2) \propto \delta(x_1 - x_2) \exp[-(x_1 + x_2)^2/4L^2]$ leads to $V_{1'2';12} \propto \exp[-(L\Delta k)^2/4]$.

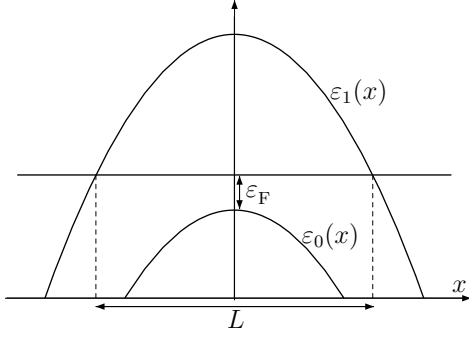


Figure 6.2: The energy barriers along a QPC in the saddle-point model. The transverse quantization energy $\varepsilon_n(x) = \hbar\omega_y(n + \frac{1}{2}) - \frac{1}{2}m\omega_x^2 x^2$ and the length, where there is only a single subband, are indicated. Note that ε_F denote the local Fermi energy, i.e. measured from the top of the barrier $\frac{1}{2}\hbar\omega_y$.

the energy landscape along a QPC is seen in the saddle-point model. The Fermi energy ε_F is the *local* Fermi energy in the QPC and therefore measured from the top of the first barrier at $\hbar\omega_y/2$. Therefore the length L is given by (two times) the point, where the second subband becomes occupied, i.e.

$$\varepsilon_F = \hbar\omega_y - \frac{1}{2}m\omega_x^2 \left(\frac{L}{2}\right)^2, \quad (6.3)$$

so using $\varepsilon_F = \hbar^2 k_F^2 / 2m$, the length compared to k_F becomes

$$k_F L = 4 \frac{\omega_y}{\omega_x} \sqrt{\frac{\varepsilon_F}{\hbar\omega_y} \left(1 - \frac{\varepsilon_F}{\hbar\omega_y}\right)}, \quad (6.4)$$

remembering that $\hbar\omega_y$ is a measure of the length of the plateau. In most experiments the ratio ω_y/ω_x is about 3 (e.g. [47], see also p. 10), so the maximum value is $k_F L \sim 6$ in the middle of the first plateau ($\varepsilon_F = \hbar\omega_y/2$), which is of order one. The sum of the single-particle transmissions for the two first subbands (at the Fermi level) in the saddle-point model eq.(1.15) is

$$\sum_{n=1,2} \mathcal{T}_n(\varepsilon_F) = \frac{1}{1 + \exp[-2\pi\varepsilon_F/\hbar\omega_x]} + \frac{1}{1 + \exp[-2\pi(\varepsilon_F - \hbar\omega_y)/\hbar\omega_x]}, \quad (6.5)$$

so it is indeed possible to have a fully open QPC and non-momentum processes present ($k_F L$ of order one) at the same time.

The above estimate for $k_F L$ eq.(6.4) becomes smaller in the beginning and in the end of the conductance plateau. As seen on figure 6.2, this is because as ε_F is moved up, k_F becomes larger and L smaller. However, it should be noted that the effective interaction strength is larger for low electron density (see e.g. [82]), i.e. in the beginning of the plateau. Therefore the combined effect of low density and small $k_F L$ gives the largest effect of non-momentum interactions in the beginning of the plateau.

6.1.1 The point-like interaction model

To treat the non-momentum conserving interaction processes in the simplest possible way, we use the interaction

$$V(x, x') = V_0 \delta(x - x') \delta(x), \quad (6.6)$$

i.e. a contact interaction in the single point $x = 0$ only. This leads to

$$V_{1'2';12} = \frac{V_0}{\mathcal{L}^2}, \quad (6.7)$$

where the momentum conservation is completely absent. In a sense this interaction model describes the limit $L \rightarrow 0$ of the problem of a wire connected to leads.

As we will see, this model is extremely useful for making a general non-perturbative current formula (section 6.4). Furthermore, in the perturbative low-temperature case, only the value of the interaction at the Fermi level is necessary as we saw in e.g. the multi-mode case studied in chapter 4. Therefore the present model will capture the relevant low-temperature perturbative physics, however, it cannot capture that different scattering processes might have different scattering amplitudes. This is studied closer in section 6.6 (using a perturbative current formula for a general interaction derived in Appendix A).

A rough estimate for the interaction strength

Next we give a very rough order of magnitude estimate for the interaction parameter V_0 in the interaction model eq.(6.6).

For low electron density the screening (e.g. due to the nearby gates) is less effective, so we use the bare Coulomb interaction $V(x, x') = \frac{e^2}{4\pi\epsilon_0|x-x'|}$ and replace $|x-x'|$ by the average length $\langle x-x' \rangle$ between electrons given in terms of the density $n = k_F/\pi$, i.e. $V(x, x') \sim \frac{e^2}{4\pi\epsilon_0} \frac{k_F}{\pi}$. To relate this to the point-like interaction, we write it without units in the delta functions as $V(x, x') = V_0 k_F^2 \delta(k_F x) \delta(k_F x')$. Therefore the rough estimate is

$$V_0 k_F^2 \sim \frac{e^2}{4\pi\epsilon_0} \frac{k_F}{\pi}. \quad (6.8)$$

The typical length of a conductance plateau $\hbar\omega_y$ of order 1-10 meV (see e.g. [47, 31, 17]) and the effective mass of GaAs is $m = 0.07m_e$ (m_e being the bare electron mass). We are interested in the beginning of the plateau, $\varepsilon_F \sim 0.2\hbar\omega_y$, so using $\hbar\omega_y \sim 5$ meV leads to $V_0 k_F^2 \sim 20$ meV ~ 230 K and $T_F \sim 12$ K.

However, it should be emphasized that this is *only* a very rough estimate. To get a realistic value one should make a realistic model of the interaction including the geometry and screening from the gates etc. This is one of the most important tasks for future theoretical work on this issue.

6.2 The problem of the Boltzmann equation

The Boltzmann equation approach to find the current cannot be used for the point-like interaction model eq.(6.6) and here we briefly discuss this issue.

If we naively try to apply the Boltzmann equation (3.3), $v_k \partial_x f_k(x) = \mathcal{I}_{kx}[f]$, by inserting the point-like interaction eq.(6.7) into the two-body collision integral eq.(3.7), we see that

$$\begin{aligned} \mathcal{I}_{kx}[f] = & - \sum_{\substack{\sigma_2 \\ \sigma_1, \sigma_2'}} \left(\frac{\mathcal{L}}{2\pi} \right)^3 \int_{-\infty}^{\infty} dk_2 \int_{-\infty}^{\infty} dk_{1'} \int_{-\infty}^{\infty} dk_{2'} \frac{2\pi}{\hbar} \frac{|V_0|^2}{\mathcal{L}^4} \delta(\varepsilon_1 + \varepsilon_2 - \varepsilon_{1'} - \varepsilon_{2'}) \\ & \times [f_1 f_2 (1 - f_{1'}) (1 - f_{2'}) - f_{1'} f_{2'} (1 - f_1) (1 - f_2)] \propto \frac{1}{\mathcal{L}}, \end{aligned} \quad (6.9)$$

whereas the right-hand side of the Boltzmann equation, $v_k \partial_x f_k(x)$, does not have an explicit dependence of the normalization length \mathcal{L} , so the normalization length \mathcal{L} does not disappear as it should in the Boltzmann equation³. This leads to nonphysical dependencies of the normalization length. For example the current becomes proportional to L/\mathcal{L} .

Conceptually, the Boltzmann equation fails because the distribution function cannot be defined properly on the length scale of the point-like interaction.

6.3 The Green's function approach

Due to the failure of the Boltzmann equation approach, we adopt a Green's function approach to calculate the current through a QPC having a point-like interaction eq.(6.6) in the middle of the contact and different chemical potentials and/or temperatures in the two leads.

Below several formal tools are presented in order to apply the Green's function technique using the famous Keldysh time contour [129]. This is not intended to be a review of the technique, but merely a minimum of basic definitions and useful relations to be used later on.

Thermopower and the Kubo formulas

By using the applied bias as a perturbation to the Hamiltonian, the linear conductance can be found as a current-current correlation function calculated e.g. by the help of equilibrium Green's functions. This approach is referred to as the Kubo

³Note that for a momentum conserving interaction, the scattering rate is $W_{12;1'2'} \propto \frac{1}{\mathcal{L}^2} \delta_{k_1+k_2, k_{1'}+k_{2'}}$, so the Kronecker delta function removes a summation over k and making the two last k sums into integrals, we observe that the normalization length \mathcal{L} cancels out from the Boltzmann equation and the current.

formula for conductance, see [14, chap.6]. If the current is driven by a temperature difference, then the situation is conceptually different, because the temperature does not enter in the Hamiltonian and therefore the driving field (i.e. the temperature difference) cannot be treated as a perturbation to the Hamiltonian. There is a way to circumvent this in bulk systems, by using the thermodynamical equality $dQ = TdS = dU - \mu dN$ leading to $J_Q = J_U - \mu J$, where J_Q , J_U and J are the heat, energy and particle currents, respectively. This can now be used in a Kubo like formula, where both the heat current and particle current enter in the correlation functions for the thermopower [112, 113, 130]. However, for QPC's it is not obvious if one is allowed to straightforwardly use the thermodynamical equality and furthermore, for interacting systems one should consider carefully which energy is being transported by the energy current [114]. Due to these considerations, we do not use this approach to the problem of a point-like interaction in a QPC.

6.3.1 Average values in the quantum point contact setup

The approach used here, is to calculate the average value of the current through the QPC (using contour ordered Green's functions). The way the average is performed is inspired by our physical situation, where the left/right reservoir inject electrons distributed by a Fermi function $f_{L/R}^0(\varepsilon_k)$ with the temperature $T_{L/R}$ and chemical potential $\mu_{L/R}$ into the QPC. Therefore we have a model, where right-movers and left movers are in different thermal equilibria and the interaction tries to equilibrate them in the QPC only. This inspires the following way to average an operator A :

$$\langle A_H(t) \rangle = \text{Tr}[\rho(H_0)A_H(t)], \quad (6.10)$$

where $A_H(t)$ is in the Heisenberg picture involving the non-interaction Hamiltonian H_0 and the interaction H_{int} , so $H = H_0 + H_{\text{int}}$ and⁴

$$A_H(t) \equiv e^{iH(t-t_0)} A e^{-iH(t-t_0)}, \quad (6.11)$$

where A is in the Schrödinger picture and t_0 is the reference (or initial) time⁵ (see e.g. [14, chapt.5]). Note that the chemical potentials are not included in H in $A_H(t)$. The density matrix $\rho(H_0)$ used in the average is

$$\rho(H_0) = \frac{e^{-\beta_L(H_{0,L} - \mu_L N_L) - \beta_R(H_{0,R} - \mu_R N_R)}}{\text{Tr} [e^{-\beta_L(H_{0,L} - \mu_L N_L) - \beta_R(H_{0,R} - \mu_R N_R)}]}, \quad (6.12)$$

⁴Here we use the traditional convention in Green's function theory and set $\hbar = 1$.

⁵Note that when using the Heisenberg picture the states do not evolve in time and it is the Schrödinger states at $t = t_0$, which should be used in the trace.

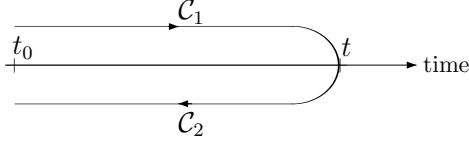


Figure 6.3: The Keldysh contour $\mathcal{C} = \mathcal{C}_1 \cup \mathcal{C}_2$ used in time ordering. This contour is a convenient mathematical tool proposed by Keldysh [129].

where $\beta_{L/R} = 1/k_B T_{L/R}$ and the number operators and the non-interacting Hamiltonians are:

$$H_0 = H_{0,L} + H_{0,R}, \quad H_{0,L} = \sum_{\sigma,k>0} \varepsilon_k c_{k\sigma}^\dagger c_{k\sigma}, \quad H_{0,R} = \sum_{\sigma,k<0} \varepsilon_k c_{k\sigma}^\dagger c_{k\sigma}, \quad (6.13)$$

$$N_0 = N_L + N_R, \quad N_L = \sum_{\sigma,k>0} c_{k\sigma}^\dagger c_{k\sigma}, \quad N_R = \sum_{\sigma,k<0} c_{k\sigma}^\dagger c_{k\sigma}. \quad (6.14)$$

The point of this way of averaging is that the bias voltage $\mu_R - \mu_L$ and temperature difference $T_R - T_L$ are in the density matrix $\rho(H_0)$ and *not* turned on as a perturbation to the Hamiltonian as it is often done, see e.g. [131, 132, 133, 134]. Furthermore, the interaction is not included in the density matrix, but in the Heisenberg picture of the operator, which is reasonable for the QPC setup with non-interacting leads.

In other works [131, 132, 133, 134]⁶, the average is done with respect to a density matrix including $H_0 + H_{\text{int}}$ (without the chemical potentials) and then the operator A is taken in a picture for the full Hamiltonian, $H = H_0 + H_{\text{int}} + H'(t)$, where $H'(t)$ is a time dependent part of H describing e.g. the applied bias voltage. Therefore here one has the bias (or another $H'(t)$) in the time evolution of A instead of in the density matrix. In this case, both the interaction H_{int} and bias $H'(t)$ are rewritten in perturbation theory (to infinite order) and one obtains two time-evolution operators ordered on the Keldysh contour, one for each perturbation. This leads to the perturbative, diagrammatic expansion of the average value using the Wicks theory as in equilibrium Green's function theory [14, 130].

The advantage of the present approach in eq.(6.10) is that we are able to treat two reservoirs having *different* temperatures. Therefore the average of the current operator can be calculated for a temperature difference, which in terms leads to the thermopower without using any thermodynamical equalities (like in the Kubo formula approach⁷).

Next we outline how the operator average $\langle A_H(t) \rangle$ can be written on the convenient Keldysh contour. See e.g. [132, chap.2] or [134] for a more detailed and complete explanation. First of all, the operator $A_H(t)$ can be written by using the interaction picture $\hat{A}(t) \equiv e^{iH_0(t-t_0)} A e^{-iH_0(t-t_0)}$ as

$$A_H(t) = v^\dagger(t, t_0) \hat{A}(t) v(t, t_0) \quad \text{with} \quad v(t, t_0) \equiv e^{+iH_0(t-t_0)} e^{-iH(t-t_0)}. \quad (6.15)$$

⁶See also [135] for an introduction using functional integrals.

⁷Calculation-wise, this route also seems to be less cumbersome.

Since the operator $v(t, t_0)$ follows the time-dependent Schrödinger-like equation $i\partial_t v(t, t_0) = \hat{H}_{\text{int}}(t)v(t, t_0)$ (with $v(t_0, t_0) = 1$), we can write it as

$$\begin{aligned} v(t, t_0) &= \sum_{n=0}^{\infty} \frac{(-i)^n}{n!} \int_{\mathcal{C}_1} dt_1 \cdots \int_{\mathcal{C}_1} dt_n T_{\mathcal{C}_1} [\hat{H}_{\text{int}}(t_1) \cdots \hat{H}_{\text{int}}(t_n)] \\ &\equiv T_{\mathcal{C}_1} \left[e^{-i \int_{\mathcal{C}_1} dt' \hat{H}_{\text{int}}(t')} \right], \end{aligned} \quad (6.16)$$

where \mathcal{C}_1 is the upper part of the Keldysh contour seen on figure 6.3, i.e. $T_{\mathcal{C}_1}$ is the normal time-ordering operator (placing operators with later times to the left) and $\int_{\mathcal{C}_1} = \int_{t_0}^t$. The hermitian conjugate $v^\dagger(t, t_0)$ is obtained by changing $\mathcal{C}_1 \rightarrow \mathcal{C}_2$, so the integrals run from t to t_0 and the time operator $T_{\mathcal{C}_2}$ orders backward in time (see figure 6.3). Inserting $v(t, t_0)$ and $v^\dagger(t, t_0)$ in eq.(6.15) one can show that (see e.g. [134, 131]):

$$\begin{aligned} A_H(t) &= T_{\mathcal{C}} \left[e^{-i \int_{\mathcal{C}} dt' \hat{H}_{\text{int}}(t')} \hat{A}(t) \right] \\ &= \sum_{n=0}^{\infty} \frac{(-i)^n}{n!} \int_{\mathcal{C}} dt_1 \cdots \int_{\mathcal{C}} dt_n T_{\mathcal{C}} [\hat{H}_{\text{int}}(t_1) \cdots \hat{H}_{\text{int}}(t_n) \hat{A}(t)], \end{aligned} \quad (6.17)$$

where $\mathcal{C} = \mathcal{C}_1 \cup \mathcal{C}_2$ is the Keldysh contour seen in figure 6.3. The time-ordering $T_{\mathcal{C}}$ orders a product of operators along the contour \mathcal{C} as:

$$T_{\mathcal{C}}[B(t_1)C(t_2)] = \begin{cases} +B(t_1)C(t_2), & \text{for } t_1 >_{\mathcal{C}} t_2 \\ -C(t_2)B(t_1), & \text{for } t_2 >_{\mathcal{C}} t_1 \end{cases}, \quad (6.18)$$

where the minus should only be included, if it involves a odd number of permutations of fermion operators to permute B and C . Here $t >_{\mathcal{C}} t'$ means that t' is before t on the contour following the arrows in figure 6.3. The integrals are also on the contour \mathcal{C} . By taking the average value of this operator using eq.(6.10), we can use Wicks theorem as in e.g. zero temperature or the equilibrium Matsubara formalism [14, 130] and formally we have the same kind of diagrammatic expansion. Note that when using Wicks theorem, one should include a slightly larger time on the creation operators in the interaction, i.e.

$$\hat{H}_{\text{int}}(t) = \frac{1}{2} \sum_{\sigma_1 \sigma_2} \sum_{\substack{k_1 k_2 \\ k_1' k_2'}} V_{1'2',12} \hat{c}_{k_1' \sigma_1}^\dagger(t^+) \hat{c}_{k_2' \sigma_2}^\dagger(t^+) \hat{c}_{k_2 \sigma_2}(t) \hat{c}_{k_1 \sigma_1}(t), \quad (6.19)$$

where t^+ is infinitesimally larger than t in the contour sense (i.e. $t^+ >_{\mathcal{C}} t$). We can use the cancellation of the disconnected diagrams in the numerator and denominator⁸ (proved in [14, p.239-241]) and obtain

$$\langle A_H(t) \rangle = \sum_{n=0}^{\infty} (-2i)^n \int_{\mathcal{C}} dt_1 \cdots \int_{\mathcal{C}} dt_n \left\langle T_{\mathcal{C}} [\hat{H}_{\text{int}}(t_1) \cdots \hat{H}_{\text{int}}(t_n) \hat{A}(t)] \right\rangle^{\text{CT}}, \quad (6.20)$$

⁸In the case of a Keldysh contour this cancellation is particularly simple, because the sum of the disconnected diagrams is one.

where CT indicates that we should only include the connected and topologically different diagrams⁹. It is at this point that the concept of the Green's functions ordered on the Keldysh contour becomes an important ingredient.

To perform actual calculations, the integrals \int_C have to be analytically continued. This can be done in basically two ways. One way is to use 2×2 matrices in Keldysh space, i.e. one entry for each possibility of having the two times in the Green's function on the upper and lower part of the Keldysh contour, see e.g. [134, 133]. Another way, which we use here, is to analytically continue the integrals using the Langreth rules [136], see e.g. [131, 132]. Below we will list some of these rules.

6.3.2 The Green's functions and the Langreth rules

In this section, we briefly go through some of the definition of the various Green's functions and state a minimum number of facts, in particular the Langreth rules and the non-interacting Green's functions, see e.g. [131, 132, 133, 134] for more details.

Definition of the various Green's functions and a few facts

The contour ordered Green's function for fermions is:

$$\mathcal{G}(1, 1') \equiv -i \langle T_C [\Psi_H(1) \Psi_H^\dagger(1')] \rangle, \quad (6.21)$$

where $\Psi_H(1)$ [$\Psi_H^\dagger(1')$] is the annihilation [creation] operator for some state and time 1 [$1'$], e.g. in real space $1 = (x_1, \sigma_1, t_1)$, but of course other quantum numbers are equally good (like $1 = (k_1, \sigma_1, t_1)$). Furthermore, it is convenient to introduce

$$\mathcal{G}^<(1, 1') \equiv +i \langle \Psi_H^\dagger(1') \Psi_H(1) \rangle, \quad (t_1 <_C t_{1'}) \quad (6.22a)$$

$$\mathcal{G}^>(1, 1') \equiv -i \langle \Psi_H(1) \Psi_H^\dagger(1') \rangle, \quad (t_1 >_C t_{1'}) \quad (6.22b)$$

$$\mathcal{G}^a(1, 1') \equiv +i \theta(t_{1'} - t_1) \langle \{ \Psi_H(1), \Psi_H^\dagger(1') \} \rangle \quad (6.22c)$$

$$\mathcal{G}^r(1, 1') \equiv -i \theta(t_1 - t_{1'}) \langle \{ \Psi_H(1), \Psi_H^\dagger(1') \} \rangle \quad (6.22d)$$

which are called the lesser $\mathcal{G}^<$, greater $\mathcal{G}^>$, advanced \mathcal{G}^a and retarded \mathcal{G}^r Green's function, respectively. Here $\{a, b\} \equiv ab + ba$ is the anti-commutator. Note that the name lesser [greater] $\mathcal{G}^<(1, 1')$ [$\mathcal{G}^>(1, 1')$] is because that t_1 is before [after] $t_{1'}$ on the contour. Furthermore, it is helpful to have the spectral function:

$$A(1, 1') \equiv i[\mathcal{G}^r(1, 1') - \mathcal{G}^a(1, 1')]. \quad (6.23)$$

⁹It is worth to notice that here we do not have to deal with a part of the contour from t_0 to $t_0 - i\beta$ due to the way the average is performed. Normally [131, 132, 134, 133], this part of the contour is excluded when taking the $t_0 \rightarrow -\infty$ limit.

From the definitions above, we observe the relations

$$\mathcal{G}^a(1, 1') = \theta(t_{1'} - t_1)[\mathcal{G}^<(1, 1') - \mathcal{G}^>(1, 1')], \quad (6.24a)$$

$$\mathcal{G}^r(1, 1') = \theta(t_1 - t_{1'})[\mathcal{G}^>(1, 1') - \mathcal{G}^<(1, 1')], \quad (6.24b)$$

which leads to

$$\mathcal{G}^r(1, 1') - \mathcal{G}^a(1, 1') = \mathcal{G}^>(1, 1') - \mathcal{G}^<(1, 1'). \quad (6.25)$$

so the four Green's functions are not independent, but there are three independent functions. This is in contrast to equilibrium theory (e.g. the Matsubara formalism), where the fluctuation-dissipation theorem connects the spectral function to all the other Green's functions, see e.g. [14, p.129].

Transforming the Green's functions between k -space and real space the Fourier transformed operators are useful,

$$\Psi^\dagger(x) = \frac{1}{\sqrt{\mathcal{L}}} \sum_k e^{-ikx} c_k^\dagger, \quad \Psi(x) = \frac{1}{\sqrt{\mathcal{L}}} \sum_k e^{+ikx} c_k, \quad (6.26)$$

$$c_k^\dagger = \frac{1}{\sqrt{\mathcal{L}}} \int_{-\frac{\mathcal{L}}{2}}^{\frac{\mathcal{L}}{2}} dx e^{+ikx} \Psi^\dagger(x), \quad c_k = \frac{1}{\sqrt{\mathcal{L}}} \int_{-\frac{\mathcal{L}}{2}}^{\frac{\mathcal{L}}{2}} dx e^{-ikx} \Psi(x), \quad (6.27)$$

since they lead to (inserting in the definition eq.(6.21))

$$\mathcal{G}(xt, x't') = \frac{1}{\mathcal{L}} \sum_{kk'} \mathcal{G}(kt, k't') e^{-ik'x' + ikx}, \quad (6.28)$$

$$\mathcal{G}(kt, k't') = \frac{1}{\mathcal{L}} \int_{-\frac{\mathcal{L}}{2}}^{\frac{\mathcal{L}}{2}} dx \int_{-\frac{\mathcal{L}}{2}}^{\frac{\mathcal{L}}{2}} dx' \mathcal{G}(xt, x't') e^{+ik'x' - ikx} \quad (6.29)$$

suppressing the spin indices. These relations do not assume translational invariance.

Furthermore, here we will only deal with steady state situations, so having performed the analytical continuation the Green's functions only depend on the time difference $t = t_1 - t_{1'}$. Therefore it is convenient to Fourier transform to frequency space as:

$$\mathcal{G}^i(11', \omega) = \int_{-\infty}^{\infty} dt e^{i\omega t} \mathcal{G}^i(11', t \equiv t_1 - t_{1'}), \quad (6.30)$$

where $i = \leq, a, r$ and we have used the same symbols 1 and 1' in $\mathcal{G}^i(11', \omega)$ as in $\mathcal{G}^i(1, 1')$, but in $\mathcal{G}^i(11', \omega)$ they do not contain any time variables, of course.

Later the following relations will turn out to be useful:

$$[\mathcal{G}^<(1, 1')]^* = -\mathcal{G}^<(1', 1) \Rightarrow [\mathcal{G}^<(11', \omega)]^* = -\mathcal{G}^<(1'1, \omega), \quad (6.31)$$

and similar for $\mathcal{G}^>$ and the retarded and advanced functions obey

$$[\mathcal{G}^r(1, 1')]^* = \mathcal{G}^a(1', 1) \Rightarrow [\mathcal{G}^r(11', \omega)]^* = \mathcal{G}^a(1'1, \omega). \quad (6.32)$$

The Langreth rules

To write the average of a physical observable in terms of integrals on the Keldysh contour \mathcal{C} eq.(6.20) and then expressing it in terms of contour ordered Green's functions is a useful theoretical tool. However, to take the last step and actually get a number in the end, we need to evaluate the integrals on the contour over the contour ordered Green's functions. To this end, the Langreth rules [136] are considered here, see also [131, 132].

Consider the following contour integral over two contour ordered functions A and B :

$$C(t, t') = \int_{\mathcal{C}} dt_1 A(t, t_1) B(t_1, t'), \quad (6.33)$$

where we have omitted all other indices that time¹⁰. Now we outline how to find, say, the lesser component of $C(t, t')$ (see [131, p.65-68]). In this case $t <_{\mathcal{C}} t'$, so the contour \mathcal{C} can be deformed into two contours leading to two integrals, one over each new contour. (The new contours are similar to \mathcal{C} , but with t and t' in the crossing point in the place of t in figure 6.3). Each of these new contours are constructed such that either $A(t, t_1)$ or $B(t_1, t')$ can be replaced by its lesser component. Along these lines the lesser component finally becomes

$$C^<(t, t') = \int_{-\infty}^{\infty} dt_1 [A^r(t, t_1) B^<(t_1, t') + A^<(t, t_1) B^a(t_1, t')], \quad (6.34)$$

and $C^>(t, t')$ by replacing all $<$ with $>$. The retarded and advanced component is found using eq.(6.24) to be

$$C^{r/a}(t, t') = \int_{-\infty}^{\infty} dt_1 A^{r/a}(t, t_1) B^{r/a}(t_1, t'). \quad (6.35)$$

These relations are easily generalized to more than two functions in the integrand, however, the time arguments have to be in a special orderly fashion, i.e.

$$D(t, t') = \int_{\mathcal{C}} dt_1 \int_{\mathcal{C}} dt_2 A(t, t_1) B(t_1, t_2) C(t_2, t'), \quad (6.36)$$

which becomes

$$\begin{aligned} D^{\geq}(t, t') = & \int_{-\infty}^{\infty} dt_1 \int_{-\infty}^{\infty} dt_2 [A^r(t, t_1) B^r(t_1, t_2) C^{\geq}(t_2, t') \\ & + A^r(t, t_1) B^{\geq}(t_1, t_2) C^a(t_2, t') + A^{\geq}(t, t_1) B^a(t_1, t_2) C^a(t_2, t')], \end{aligned} \quad (6.37)$$

$$D^{r/a}(t, t') = \int_{-\infty}^{\infty} dt_1 \int_{-\infty}^{\infty} dt_2 A^{r/a}(t, t_1) B^{r/a}(t_1, t_2) C^{r/a}(t_2, t') \quad (6.38)$$

¹⁰Note that some authors use Greek letters τ on the contour and roman t on the real axes. We do not use this convention. Instead functions without a superscript (like $>$) are on the contour and functions with a superscript are on the real time axis.

using eq.(6.34) and (6.35). The structure is now clear for this particular order of the time arguments, i.e. if we had four functions in the integrand $E = \int \int \int ABCD$ then one would get

$$E^< = \int \int \int A^r B^r C^r D^< + A^r B^r C^< D^a + A^r B^< C^a D^a + A^< B^a C^a D^a \quad (6.39)$$

and $E^r = \int \int \int A^r B^r C^r D^r$ (suppressing the time arguments).

However, sometimes the evaluation of a product of time-ordered functions without an integral is needed, i.e.

$$C_{\Leftarrow}(t, t') = A(t, t')B(t, t'), \quad (6.40a)$$

$$C_{\Rightarrow}(t, t') = A(t, t')B(t', t). \quad (6.40b)$$

The lesser components are easily seen to be

$$C_{\Leftarrow}^<(t, t') = A^<(t, t')B^<(t, t'), \quad (6.41a)$$

$$C_{\Leftarrow}^<(t, t') = A^<(t, t')B^>(t', t), \quad (6.41b)$$

and the greater components follow by $>\leftrightarrow<$. Using the definitions of the advanced and retarded Green's functions and the relations eq.(6.24), it can be seen that

$$C_{\Leftarrow}^r(t, t') = A^r(t, t')B^<(t, t') + A^<(t, t')B^r(t, t') + A^r(t, t')B^r(t, t'), \quad (6.42a)$$

$$C_{\Leftarrow}^a(t, t') = A^a(t, t')B^<(t, t') + A^<(t, t')B^a(t, t') - A^a(t, t')B^a(t, t'), \quad (6.42b)$$

$$C_{\Leftarrow}^{r/a}(t, t') = A^{r/a}(t, t')B^<(t', t) + A^<(t, t')B^{a/r}(t', t). \quad (6.42c)$$

Note the sign difference between $C_{\Leftarrow}^r(t, t')$ and $C_{\Leftarrow}^a(t, t')$ in the last term. These relations are constructed such that the greater component does not enter by the help of eq.(6.25), since we have three independent Green's functions. See e.g. Jauho and Haug [131] for further details and derivations (or [132]).

The non-interacting Green's functions

The non-interacting Green's functions $\mathcal{G}_0^i(1, 1')$ ($i = a, r, \gtrless$) of the problem are needed below and therefore given here. Due to the particular way the average is performed in eq.(6.10), we get a different result than normally (see e.g. [132, Appendix A]), since \mathcal{G}_0^{\gtrless} depend on the direction of k .

Using the definitions of the various Green's functions eq.(6.22) with $1 = (k_1 \sigma_1 t_1)$ and the average eq.(6.10), the non-interacting Green's functions become:

$$\mathcal{G}_0^r(1, 1') = -i\theta(t_1 - t_{1'})e^{-i\varepsilon_{k_1}(t_1 - t_{1'})}e^{-\eta(t_1 - t_{1'})}\delta_{k_1, k_{1'}}\delta_{\sigma_1, \sigma_{1'}}, \quad (6.43a)$$

$$\mathcal{G}_0^a(1, 1') = +i\theta(t_{1'} - t_1)e^{-i\varepsilon_{k_1}(t_1 - t_{1'})}e^{+\eta(t_1 - t_{1'})}\delta_{k_1, k_{1'}}\delta_{\sigma_1, \sigma_{1'}}, \quad (6.43b)$$

$$\mathcal{G}_0^<(1, 1') = +ie^{-i\varepsilon_{k_1}(t_1 - t_{1'})}f_{R/L}^0(\varepsilon_{k_1})\delta_{k_1, k_{1'}}\delta_{\sigma_1, \sigma_{1'}}, \quad (6.43c)$$

$$\mathcal{G}_0^>(1, 1') = -ie^{-i\varepsilon_{k_1}(t_1 - t_{1'})}[1 - f_{R/L}^0(\varepsilon_{k_1})]\delta_{k_1, k_{1'}}\delta_{\sigma_1, \sigma_{1'}}, \quad (6.43d)$$

where $f_{R/L}^0(\varepsilon_k)$ are the Fermi functions for the right(R)/left(L) reservoirs, i.e. if $k_1 > 0$ then $f_L^0(\varepsilon_{k_1})$ is used and vice versa. The non-interacting Green's functions are diagonal in k and σ and a positive infinitesimal $\eta = 0^+$ is introduced (see e.g. [14]). Note that the chemical potentials do not appear in the exponents with the energy ε_k , but in the Fermi functions. By Fourier transforming to frequency space using the convention in eq.(6.30), the non-interacting Green's functions become

$$\mathcal{G}_0^r(k, \omega) = \frac{1}{\omega - \varepsilon_k + i\eta}, \quad (6.44a)$$

$$\mathcal{G}_0^a(k, \omega) = \frac{1}{\omega - \varepsilon_k - i\eta}, \quad (6.44b)$$

$$\mathcal{G}_0^<(k, \omega) = +2\pi i \delta(\omega - \varepsilon_k) f_{R/L}^0(\varepsilon_k), \quad (6.44c)$$

$$\mathcal{G}_0^>(k, \omega) = -2\pi i \delta(\omega - \varepsilon_k) [1 - f_{R/L}^0(\varepsilon_k)], \quad (6.44d)$$

where it was used in the notation that \mathcal{G}_0^i is diagonal in k and σ , and σ was suppressed in the notation.

6.3.3 The Dyson equation

The Dyson equation known from equilibrium Green's function theory [14, 130] is still valid (due to the formal similarity) for the present approach by using the contour \mathcal{C} in the time integrals. The Dyson equation for the contour order Green's function in real space is

$$\begin{aligned} \mathcal{G}(xx', tt') = & \mathcal{G}_0(xx', tt') \\ & + \int_{-\mathcal{L}/2}^{\mathcal{L}/2} \int_{-\mathcal{L}/2}^{\mathcal{L}/2} dx_1 dx_2 \int_{\mathcal{C}} \int_{\mathcal{C}} dt_1 dt_2 \mathcal{G}_0(xx_1, tt_1) \Sigma(x_1 x_2, t_1 t_2) \mathcal{G}(x_2 x', t_2 t'), \end{aligned} \quad (6.45)$$

where we write the space and time arguments explicitly¹¹ and suppress the spin index. The Dyson equation is simply a rewriting of the Green's function \mathcal{G} using the diagrammatic expansion of the average value eq.(6.10). To this end, the irreducible self-energy $\Sigma(x_1 x_2, t_1 t_2)$ is introduced, which contains all diagrams that cannot be cut into two pieces by cutting a single Green's function line. It is important to note that Σ depends on the Green's function \mathcal{G} , which make it a difficult task to solve the Dyson equation (see e.g. [14]). Note that an external single-particle potential can easily be included in the Dyson equation, see e.g. [131, 132]. To find the lesser, greater, retarded and advanced Green's functions in terms of the self-energy components the Langreth rules eq.(6.37) and eq.(6.38) can be applied leading to three coupled (difficult) integral equations.

¹¹The order of the arguments have also been changed as $(1, 1') = (x_1 t_1, x_1 t_1') \rightarrow (x_1 x_1', t_1 t_1')$, but hopefully this does not cause any confusion.

The Dyson equation for the point-like interaction

To make a general current formula for the point-like interaction eq.(6.6), the Dyson equation is studied in this case here.

Due to the particular form of the point-like interaction, $V_0\delta(x)\delta(x')$, the self-energy can only be non-zero at $x_1 = x_2 = 0$, i.e.

$$\Sigma(x_1x_2, t_1t_2) = \delta(x_1)\delta(x_2)\Sigma(00, t_1t_2), \quad (6.46)$$

so the Dyson equation reduces to:

$$\mathcal{G}(xx', tt') = \mathcal{G}_0(xx', tt') + \int_C \int_C dt_1 dt_2 \mathcal{G}_0(x0, tt_1) \Sigma(00, t_1t_2) \mathcal{G}(0x', t_2t'). \quad (6.47)$$

Using the Langreth rule eq.(6.38) the retarded Green's functions becomes:

$$\mathcal{G}^r(xx', tt') = \mathcal{G}_0^r(xx', tt') + \int_{-\infty}^{\infty} \int_{-\infty}^{\infty} dt_1 dt_2 \mathcal{G}_0^r(x0, tt_1) \Sigma^r(00, t_1t_2) \mathcal{G}^r(0x', t_2t'), \quad (6.48)$$

and the same for \mathcal{G}^a by replacing $r \rightarrow a$. Using the Langreth rule eq.(6.37) the lesser Green's function is

$$\begin{aligned} \mathcal{G}^<(xx', tt') = & \mathcal{G}_0^<(xx', tt') + \int_{-\infty}^{\infty} \int_{-\infty}^{\infty} dt_1 dt_2 \left[\mathcal{G}_0^r(x0, tt_1) \Sigma^r(00, t_1t_2) \mathcal{G}^<(0x', t_2t') \right. \\ & \left. + \mathcal{G}_0^r(x0, tt_1) \Sigma^<(00, t_1t_2) \mathcal{G}^a(0x', t_2t') + \mathcal{G}_0^<(x0, tt_1) \Sigma^a(00, t_1t_2) \mathcal{G}^a(0x', t_2t') \right], \end{aligned}$$

and $\mathcal{G}^>$ is obtained by replacing $<$ by $>$ in all Green's functions. These equations involve a convolution in time, so Fourier transforming to frequency space using the definition (6.30) leads to a product of functions in frequency space, i.e.

$$\mathcal{G}^{r(a)}(xx', \omega) = \mathcal{G}_0^{r(a)}(xx', \omega) + \mathcal{G}_0^{r(a)}(x0, \omega) \Sigma^{r(a)}(00, \omega) \mathcal{G}^{r(a)}(0x', \omega), \quad (6.49)$$

$$\begin{aligned} \mathcal{G}^<(xx', \omega) = & \mathcal{G}_0^<(xx', \omega) + \mathcal{G}_0^r(x0, \omega) \Sigma^r(00, \omega) \mathcal{G}^<(0x', \omega) \\ & + \mathcal{G}_0^r(x0, \omega) \Sigma^<(00, \omega) \mathcal{G}^a(0x', \omega) + \mathcal{G}_0^<(x0, \omega) \Sigma^a(00, \omega) \mathcal{G}^a(0x', \omega). \end{aligned} \quad (6.50)$$

Note that there is no hidden integrals (as it is often the case in the Green's function literature). To evaluate the current average, the following rewriting of the Dyson equation becomes handy:

$$\begin{aligned} \mathcal{G}^<(xx', \omega) = & \mathcal{G}_0^<(xx', \omega) + \mathcal{G}^r(x0, \omega) \Sigma^r(00, \omega) \mathcal{G}_0^<(0x', \omega) \\ & + \mathcal{G}^r(x0, \omega) \Sigma^<(00, \omega) \mathcal{G}_0^a(0x', \omega) + \mathcal{G}^<(x0, \omega) \Sigma^a(00, \omega) \mathcal{G}_0^a(0x', \omega), \end{aligned} \quad (6.51)$$

where the order of the \mathcal{G} and \mathcal{G}_0 are opposite than in eq.(6.50). This rewriting is easily proven e.g. by iteration of eq.(6.50).

6.4 A non-perturbative current formula for the point-like interaction

In this section, a general current formula for the point-like interaction eq.(6.6) is derived, which *only* depends on the spectral function $A(00, \omega)$ in $x = x' = 0$. Of course, to find $A(00, \omega) = -2\text{Im}\mathcal{G}^r(00, \omega)$ a self-energy $\Sigma(00, \omega)$ is needed to solve the (in general) three coupled Dyson equations (6.49) and (6.50). The fact that $x = x' = 0$ in all the Green's functions in these coupled Dyson equations makes the involved functions depend on only one variable ω instead of three (x, x', ω) ; A notable simplification.

Before the derivation is given, let us recapitulate the model: A clean 1D single mode electron gas with electron-electron interactions only present in a single point $x = 0$ (corresponding to the midpoint of a QPC). The right and left movers coming into $x = 0$ have different temperatures and/or chemical potentials (i.e. distributed by the Fermi functions of the leads). Furthermore, for simplicity a quadratic band

$$\varepsilon_k = \frac{\hbar^2 k^2}{2m} \quad (6.52)$$

is used, where m is the effective mass.

Now the derivation of the current formula is given. The particle¹² current operator in the Heisenberg picture for a quadratic band is [14]

$$I_H(t) = \frac{\hbar}{2mi} \sum_{\sigma} \left[\Psi_H^{\dagger}(xt) (\partial_x \Psi_H(xt)) - (\partial_x \Psi_H^{\dagger}(xt)) \Psi_H(xt) \right]. \quad (6.53)$$

Note that if we do not have a quadratic band, then the current operator can be different¹³. This is why, we restrict ourself to a quadratic band. The average of the current operator is:

$$\begin{aligned} \langle I_H(t) \rangle &= \frac{\hbar}{2mi} \sum_{\sigma} \left[\langle \Psi_H^{\dagger}(xt) (\partial_x \Psi_H(xt)) \rangle - \langle (\partial_x \Psi_H^{\dagger}(xt)) \Psi_H(xt) \rangle \right] \\ &= \frac{\hbar}{2mi} \sum_{\sigma} \lim_{x' \rightarrow x} \partial_x \langle \Psi_H^{\dagger}(x't) \Psi_H(xt) \rangle - \lim_{x' \rightarrow x} \partial_{x'} \langle \Psi_H^{\dagger}(x't) \Psi_H(xt) \rangle \\ &= \frac{\hbar}{2mi} \sum_{\sigma} (-i) \lim_{x' \rightarrow x} [\partial_x \mathcal{G}^<(xx', tt) - \partial_{x'} \mathcal{G}^<(xx', tt)] \\ &= \frac{\hbar}{2m} \sum_{\sigma} \int_{-\infty}^{\infty} \frac{d\omega}{2\pi} \lim_{x' \rightarrow x} [\partial_{x'} - \partial_x] \mathcal{G}^<(xx', \omega) \end{aligned} \quad (6.54)$$

¹²The electric current operator is found by multiplying with $(-e) < 0$.

¹³In the derivation of the current operator in [14, p.21-23] only the kinetic part in the Hamiltonian $H_0 = \sum_{k\sigma} \varepsilon_k c_{k\sigma}^{\dagger} c_{k\sigma}$ enters. However, including a lattice potential in H of course does not change the kinetic term H_0 , *but* absorbing the (non-quadratic) band structure into the kinetic term H_0 does change it and in terms possibly the current operator.

using the definition $\mathcal{G}^<(xx', tt') = +i\langle \Psi_H^\dagger(x't')\Psi_H(xt) \rangle$. In this current formula, we can choose any point $x = x'$ to evaluate the current due to current conservation¹⁴. However, if we chose $x = x' = 0$ to evaluate the current the formula becomes particularly simple. To find $\partial_x \mathcal{G}^<(xx', \omega)$ and $\partial_{x'} \mathcal{G}^<(xx', \omega)$, we use the Dyson equations (6.50) and (6.51), respectively, so we only have to differentiate non-interaction Green's functions, i.e.

$$\begin{aligned} \partial_x \mathcal{G}^<(xx', \omega) &= \partial_x \mathcal{G}_0^<(xx', \omega) + [\partial_x \mathcal{G}_0^r(x0, \omega)] \Sigma^r(00, \omega) \mathcal{G}^<(0x', \omega) \\ &+ [\partial_x \mathcal{G}_0^r(x0, \omega)] \Sigma^<(00, \omega) \mathcal{G}^a(0x', \omega) + [\partial_x \mathcal{G}_0^<(x0, \omega)] \Sigma^a(00, \omega) \mathcal{G}^a(0x', \omega), \end{aligned} \quad (6.55a)$$

and

$$\begin{aligned} \partial_{x'} \mathcal{G}^<(xx', \omega) &= \partial_{x'} \mathcal{G}_0^<(xx', \omega) + \mathcal{G}^r(x0, \omega) \Sigma^r(00, \omega) [\partial_{x'} \mathcal{G}_0^<(0x', \omega)] \\ &+ \mathcal{G}^r(x0, \omega) \Sigma^<(00, \omega) [\partial_{x'} \mathcal{G}_0^a(0x', \omega)] + \mathcal{G}^<(x0, \omega) \Sigma^a(00, \omega) [\partial_{x'} \mathcal{G}_0^a(0x', \omega)]. \end{aligned} \quad (6.55b)$$

A major simplification occurs by using eq.(6.28) and that $\mathcal{G}_0^i(kt, k't') \propto \delta_{k,k'}$, i.e.¹⁵

$$\begin{aligned} \lim_{x \rightarrow x'} \partial_x \mathcal{G}_0^r(xx', \omega) &= \lim_{x \rightarrow x'} \partial_x \int_{-\infty}^{\infty} \frac{dk}{2\pi} \mathcal{G}_0^r(k, \omega) e^{ik(x-x')} \\ &= \int_{-\infty}^{\infty} \frac{dk}{2\pi} \mathcal{G}_0^r(k, \omega) ik = \int_{-\infty}^{\infty} \frac{dk}{2\pi} \frac{1}{\omega - \varepsilon_k + i\eta} ik \\ &= \int_{-\infty}^{\infty} \frac{dk}{2\pi} \left[\mathcal{P} \frac{1}{\omega - \varepsilon_k} - i\pi \delta(\omega - \varepsilon_k) \right] ik = 0, \end{aligned} \quad (6.56)$$

where both the principle value $\mathcal{P}(\cdot)$ term and the delta function term are odd in k (ε_k is even) and therefore zero. The same is true for the advanced non-interacting Green's function, $\lim_{x \rightarrow x'} \partial_x \mathcal{G}_0^a(xx', \omega) = 0$, and for the differentiate with respect to x' , since

$$\partial_x \mathcal{G}_0^i(xx', \omega) = \int_{-\infty}^{\infty} \frac{dk}{2\pi} \mathcal{G}_0^i(k, \omega) \partial_x e^{ik(x-x')} = -\partial_{x'} \mathcal{G}_0^i(xx', \omega) \quad (6.57)$$

for $i = <, >, r, a$. Therefore in $x = x' = 0$ we have:

$$\partial_x \mathcal{G}^<(00, \omega) = \partial_x \mathcal{G}_0^<(00, \omega) + [\partial_x \mathcal{G}_0^<(00, \omega)] \Sigma^a(00, \omega) \mathcal{G}^a(00, \omega), \quad (6.58)$$

$$\partial_{x'} \mathcal{G}^<(00, \omega) = \partial_{x'} \mathcal{G}_0^<(00, \omega) + \mathcal{G}^r(00, \omega) \Sigma^r(00, \omega) [\partial_{x'} \mathcal{G}_0^<(00, \omega)]. \quad (6.59)$$

Note that by e.g. $\partial_x \mathcal{G}_0^<(00, \omega)$ is meant that first the differentiation is done and afterwards $x = 0$. Inserting this into eq.(6.54) and using eq.(6.57) the particle

¹⁴We have checked this explicitly in the perturbative case, but we do not give the derivation here.

¹⁵Here the long wire limit $\mathcal{L} \rightarrow \infty$ is used, so $\frac{1}{\mathcal{L}} \sum_k (\dots) \rightarrow \int \frac{dk}{2\pi} (\dots)$.

current becomes:

$$\begin{aligned}
\langle I_H \rangle &= \frac{\hbar}{2m} \sum_{\sigma} \int_{-\infty}^{\infty} \frac{d\omega}{2\pi} \lim_{x' \rightarrow x} [\partial_{x'} \mathcal{G}^<(xx', \omega) - \partial_x \mathcal{G}^<(xx', \omega)] \\
&= \frac{\hbar}{2m} \sum_{\sigma} \int_{-\infty}^{\infty} \frac{d\omega}{2\pi} \left\{ -2\partial_x \mathcal{G}_0^<(00, \omega) \right. \\
&\quad \left. - \partial_x \mathcal{G}_0^<(00, \omega) \left[\mathcal{G}^r(00, \omega) \Sigma^r(00, \omega) + \Sigma^a(00, \omega) \mathcal{G}^a(00, \omega) \right] \right\} \\
&= \frac{\hbar}{2m} \sum_{\sigma} \int_{-\infty}^{\infty} \frac{d\omega}{2\pi} \left\{ \underbrace{-2\partial_x \mathcal{G}_0^<(00, \omega)}_{\text{non-interacting term}} - \underbrace{\partial_x \mathcal{G}_0^<(00, \omega) 2\text{Re} \left[\mathcal{G}^r(00, \omega) \Sigma^r(00, \omega) \right]}_{\text{current due to interaction}} \right\} \\
&\equiv I^{(0)} + I^{\text{int}}, \tag{6.60}
\end{aligned}$$

where we used $\mathcal{G}^r(xx', \omega) = [\mathcal{G}^a(x'x, \omega)]^*$ and $\Sigma^r(xx', \omega) = [\Sigma^a(x'x, \omega)]^*$ eq.(6.32). At this point, we can observe that to calculate the current it is enough to know the *local* Green's functions at $x = x' = 0$. Furthermore, from this expression it is clear that the current has two terms: A non-interacting contribution $I^{(0)}$ (still present for $\Sigma^r(00, \omega) = 0$) and a term due to the interaction I^{int} . The same is true in the Boltzmann approach, see e.g. eq.(3.19). To proceed, we need

$$\begin{aligned}
\partial_x \mathcal{G}_0^<(00, \omega) &= \int_{-\infty}^{\infty} \frac{dk}{2\pi} \mathcal{G}_0^<(k, \omega) ik = \int_{-\infty}^{\infty} \frac{dk}{2\pi} 2\pi i \delta(\omega - \varepsilon_k) f_{\text{R/L}}^0(\varepsilon_k) ik \\
&= \theta(\omega) \frac{m}{\hbar^2} [f_{\text{R}}^0(\omega) - f_{\text{L}}^0(\omega)], \tag{6.61}
\end{aligned}$$

so the current becomes

$$\langle I_H \rangle = -\frac{1}{\hbar} \sum_{\sigma} \int_0^{\infty} \frac{d\omega}{2\pi} [f_{\text{R}}^0(\omega) - f_{\text{L}}^0(\omega)] \left\{ 1 + \underbrace{\text{Re} \left[\mathcal{G}^r(00, \omega) \Sigma^r(00, \omega) \right]}_{\text{term due to interactions}} \right\}. \tag{6.62}$$

The local retarded non-interacting Green's function is

$$\mathcal{G}_0^r(00, \omega) = \int_{-\infty}^{\infty} \frac{dk}{2\pi} \frac{1}{\omega - \varepsilon_k + i\eta} = -i\pi \int_{-\infty}^{\infty} \frac{dk}{2\pi} \delta(\omega - \varepsilon_k) \equiv -i\pi d(\omega), \tag{6.63}$$

where the principal value part is zero, $\mathcal{P} \int_{-\infty}^{\infty} \frac{dk}{2\pi} \frac{1}{\omega - \varepsilon_k} = 0$, for a quadratic dispersion (and $\omega \neq 0$). In eq.(6.63) the density of states $d(\omega)$ (not including the spin) is introduced. The non-interacting local spectral function for a quadratic band is therefore

$$A_0(00, \omega) = 2\pi d(\omega) = \sqrt{\frac{2m}{\omega \hbar^2}} \theta(\omega). \tag{6.64}$$

Note that $\mathcal{G}_0^r(00, \omega) = 0$ for $\omega < 0$, so the Dyson equation (6.49) gives that $\mathcal{G}^r(00, \omega) = 0$ for $\omega < 0$ and the same for $\mathcal{G}^{a,\lessgtr}(00, \omega)$ using the local version of

eq.(6.50). Next we manipulate the term in the curly brackets in eq.(6.62) using the Dyson equation (6.49):

$$\begin{aligned} \operatorname{Re} \left[1 + \mathcal{G}^r(00, \omega) \Sigma^r(00, \omega) \right] &= \operatorname{Re} \left[\frac{\mathcal{G}^r(00, \omega)}{\mathcal{G}_0^r(00, \omega)} \right] = \operatorname{Re} \left[\frac{\mathcal{G}^r(00, \omega)}{-i\pi d(\omega)} \right] \\ &= \frac{A(00, \omega)}{2\pi d(\omega)} = \frac{A(00, \omega)}{A_0(00, \omega)}, \end{aligned} \quad (6.65)$$

so the electric current $I_e = (-e)I \equiv (-e)\langle I_H \rangle$ becomes

$$I_e = \frac{e}{h} \sum_{\sigma} \int_0^{\infty} d\omega [f_R^0(\omega) - f_L^0(\omega)] \frac{A(00, \omega)}{A_0(00, \omega)}. \quad (6.66)$$

This is the result for the general current formula and in the next sections it is applied. In the non-interacting case, $A(00, \omega) = A_0(00, \omega)$, it reduces to the Landauer formula eq.(1.4) for a single fully open channel (unity transmission). The above current formula assumes: (i) the point-like interaction model eq.(6.6), (ii) a quadratic dispersion and (iii) that we used the operator average presented in section 6.3.1. However, it is general in the sense that the self-energy $\Sigma(00, \omega)$ can be used in any sort of approximation desired. Furthermore, it can handle non-equilibrium situations as well as equilibrium ones and including a temperature difference does not propose a conceptual problem (at most a calculational one). As already mentioned, it only requires knowledge of the local Green's function (at $x = x' = 0$) to know the current, which simplifies the problem. A particularly convenient feature is that in linear response to the temperature difference ΔT or the bias voltage V these quantities are included in $[f_R^0(\omega) - f_L^0(\omega)]$, so the local spectral function $A(00, \omega)$ can be calculated in equilibrium. This makes the problem easier, since using the fluctuation-dissipation theorem there is only one independent Green's function. In section 6.7, this is used and the fluctuation-dissipation theorem will be given explicitly.

The conductance and thermopower for a point-like interaction

Next we find the conductance and thermopower for the point-like interaction using the current formula eq.(6.66).

In linear response to the bias $eV = \mu_R - \mu_L$ and temperature difference $\Delta T = T_R - T_L$ the difference between the Fermi functions of the leads is (using eq.(1.7)):

$$f_R^0(\omega) - f_L^0(\omega) = [-\partial_{\omega} f^0(\omega)] \left\{ eV + (\omega - \varepsilon_F) \frac{\Delta T}{T} \right\}, \quad (6.67)$$

so inserting this into the current formula eq.(6.66), we get the conductance G

and the thermoelectric coefficient G_T as

$$G = \frac{2e^2}{h} \int_0^\infty d\omega [-\partial_\omega f^0(\omega)] \frac{A_{\text{eq}}(00, \omega)}{A_0(00, \omega)}, \quad (6.68)$$

$$G_T = \frac{2ek_B}{h} \int_0^\infty d\omega [-\partial_\omega f^0(\omega)] \left(\frac{\omega - \varepsilon_F}{k_B T} \right) \frac{A_{\text{eq}}(00, \omega)}{A_0(00, \omega)}, \quad (6.69)$$

and the thermopower is simply $S = G_T/G$. Here $A_{\text{eq}}(00, \omega)$ is the equilibrium spectral function, because $f_R^0(\omega) - f_L^0(\omega)$ is already proportional to V and ΔT , so $V = 0$ and $\Delta T = 0$ should be used in $A(00, \omega)$ in linear response.

Including a local potential scattering term

A local potential scattering term of the form $U(x) = U_0\delta(x)$ can easily be included by adding a term to the Dyson equation. Afterwards, the same derivation as above can be done and the resulting current formula eq.(6.66) does not change, but here the $A(00, \omega)$ includes V_0 and the potential U_0 , however, $A_0(00, \omega)$ is the result for $V_0 = 0$ and $U_0 = 0$. It is not obvious how to relate the U_0 to gate voltage V_g , so we have left the detailed description of the interplay of potential scattering and interaction effects for future studies. (Furthermore, the local potential might not mimic the rather large metallic gates inducing a smooth potential particularly well.)

6.4.1 Connection to the Meir-Wingreen formula for an Anderson model

The current formula eq.(6.66) derived above is a continuum version of the famous Meir-Wingreen formula [137] for a single level Anderson model connected to two leads. Here we try to explain the connection.

The Meir-Wingreen formula is rather general and here we only need it in a special situation. Consider a tight-binding chain with spin degenerate sites i and a constant nearest neighbor hopping amplitude t . The electron-electron interaction of strength U is only included on the single site $i = 0$. This case is described by the Anderson model Hamiltonian embedded into the tight-binding chain, i.e.

$$H = \tilde{\varepsilon} \sum_{i,\sigma} c_{i\sigma}^\dagger c_{i\sigma} - t \sum_{i,\sigma} (c_{i\sigma}^\dagger c_{i+1\sigma} + c_{i+1\sigma}^\dagger c_{i\sigma}) + \sum_{\sigma} \varepsilon_0 n_{i=0\sigma} + U n_{i=0\uparrow} n_{i=0\downarrow}, \quad (6.70)$$

where $n_{i=0\sigma} = c_{i=0\sigma}^\dagger c_{i=0\sigma}$ and $\tilde{\varepsilon}$ and ε_0 are the on-site energies for $i \neq 0$ and $i = 0$, respectively. Note that the hopping onto the site $i = 0$ is the same as in the rest of the chain (which is not the usual situation in e.g. describing quantum dots).

The on-site energy $\tilde{\varepsilon}$ is often chosen as the zero of the energy for convenience. In this situation, the Meir-Wingreen formula is (see e.g. [131, 14, 137]):

$$I_e = \frac{2e}{h} \int_{-\infty}^{\infty} d\omega \pi |t|^2 d_t(\omega) A(i = i' = 0, \omega) [f_R^0(\omega) - f_L^0(\omega)], \quad (6.71)$$

where $d_t(\omega)$ is the density of states of the semi-infinite tight-binding chain (i.e. for either $i > 0$ or $i < 0$) and $A(i = i' = 0, \omega)$ is the local spectral function on the single site $i = 0$.

Physically, the tight-binding model with an interaction on a single site $i = 0$ is clearly a discrete version of the model used here, which is a 1D electron gas (without a lattice) including interactions at a single point $x = 0$. The discretization should only be visible probing short wavelength properties (or large k) compared to the distance a between the sites.

The connection between the Meir-Wingreen formula for a tight-binding chain eq.(6.71) and the current formula eq.(6.66) is evident: Both contain the local spectral function at the point, where interactions are possible, and the difference between the Fermi functions. However, the density of states are in different positions in the two formulas, but they are also different formulas. The dispersion relations are different and for a tight-binding chain it is $\varepsilon_k = -2t \cos(ka)$, where a is the distance between the sites. Therefore to obtain a formal connection¹⁶ the Fermi level of the tight-binding chain needs to be below half filling, so a quadratic dispersion is a good approximation to the dispersion.

6.5 Perturbative results for the current using the point-like interaction

As a first approach to the problem of interactions in a short point-like QPC, we perform perturbative calculations in the electron-electron interaction. We have calculated this by direct use of a perturbative (diagrammatic) expansion of the average value of the current operator eq.(6.20). This direct calculation shows that the current in the point-like model eq.(6.6) is indeed independent of the position x . However, the direct perturbative calculation in the interaction for a general x is somewhat tedious and therefore it is not shown here. Instead we simply used the current formula eq.(6.66) including the n^{th} order diagrams in the self-energy to get the interaction contribution to the current to n^{th} order.

¹⁶Note that $d(\omega) \propto 1/\sqrt{\omega}$ and using the density of states for a semi-infinite tight-binding chain it goes as $d_t(\omega) \propto \sqrt{\omega}$ for low frequencies, so the formulas correspond (see e.g. [132, Appendix C] for $d_t(\omega)$).

6.5.1 The current to first order in the interaction

The first order interaction correction is often referred to as the Hartree-Fock contribution. In the case of the point-like interaction model eq.(6.6), it is possible to show by direct calculation that the first order interaction contribution to the current is actually zero. However, in general this is not the case.

In general, the Hartree-Fock contribution correspond to that each electron interacts with the mean field of all the other electrons, so the Hartree-Fock term contributes to the single-particle (mean) field, see e.g. [14, chap.4]. Therefore it is possible to include the Hartree-Fock contribution to the interactions in the single-particle potential. In doing so, the single-particle potential becomes dependent on the electronic density. The first order contribution can also be make self-consistent, which means that the non-interacting Green's functions are replaced by the full Green's functions in the Hartree and Fock diagrams, see e.g. [138]. This self-consistent Hartree-Fock contribution still acts like a single-particle potential depending on the density, however, in this case the potential has to be treated self-consistently.

Therefore to describe the interaction corrections in a QPC, the self-consistent Hartree-Fock contribution to the current can be included into the single-particle electrostatic potential of the gates and their sum formes the single-particle potential of the QPC. The self-consistent Hartree-Fock potential can give rise to backscattering of electrons *even* at zero temperature and hence a current reduction. However, experimentally, it is possible to adjust the gates to have integer transmission (i.e. no backscattering) at the lowest possible temperatures ($T \rightarrow 0$), so this effect is compensated by tuning the electrostatic potential of the gates and this is the case of interest here. The electrostatic potential from the gates does not dependent on temperature, but the self-consistent Hartree-Fock potential could have some non-trivial temperature dependence. Lassl *et al.* [138] have considered this problem for a QPC in a realistic geometry for a contact interaction, $V(\mathbf{r} - \mathbf{r}') = \text{constant} \times \delta(\mathbf{r} - \mathbf{r}')$. In this approach the self-consistent Hartree-Fock contribution is strongest for zero temperature and decreases rapidly for higher temperatures, in complete contrast to the experimental evidence of the 0.7 anomaly. Furthermore, to see any effect of the self-consistent Hartree-Fock calculation an asymmetry between up and down spins have to be assumed corresponding to including a small magnetic field in the calculation. Note that other spin symmetry-broken mean field approaches cannot reproduce the right temperature dependence either [139].

In the present work, we do not assume any spin asymmetry and we neglect any temperature dependence of the self-consistent Hartree-Fock single-particle potential.

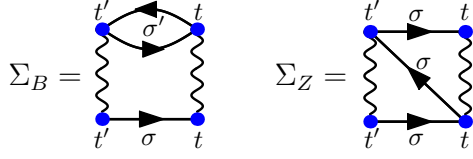


Figure 6.4: The Feynman diagrams of the self-energy to second order in the electron-electron interaction eq.(6.73) and eq.(6.74). These lead to the second order interaction term in the current $I^{(2)}$. Lines with arrows are \mathcal{G}_0 connecting the interactions (wiggled lines) at space time points $(x = 0, t^{(i)})$ (blue dots).

6.5.2 The current to second order in the interaction

Next we calculate the current to second order in the interaction for the point-like interaction eq.(6.6) using the general current formulation from section 6.4.

The particle current to second order consist of a non-interacting part $I^{(0)}$ and a second order interaction term $I^{(2)}$, i.e. $I = I^{(0)} + I^{(2)} + \dots$. Using eq.(6.60) the latter is¹⁷

$$I^{(2)} = \frac{\hbar}{2m} \sum_{\sigma} \int_{-\infty}^{\infty} \frac{d\omega}{2\pi} \left\{ -\partial_x \mathcal{G}_0^<(00, \omega) 2\text{Re} \left[\mathcal{G}_0^r(00, \omega) \Sigma_{(2)}^r(00, \omega) \right] \right\} \quad (6.72)$$

where $\Sigma_{(2)}^r(00, \omega)$ is the second order self-energy. Here the full Green's function $\mathcal{G}^r(00, \omega)$ in eq.(6.60) is replaced by \mathcal{G}_0^r to second order, because having a first order contribution in \mathcal{G}^r and a first order in Σ^r is part of the self-consistent Hartree-Fock potential included in the single-particle potential.

To find $I^{(2)}$, the topologically different second order diagrams in the self-energy are identified and shown in figure 6.4. Here the lines with arrows represent $\mathcal{G}_0(00, tt')$ going from t' to t and the wiggled lines represent the interactions connecting only $x = x' = 0$ (blue dots). There are two different contributions to the self-energy $\Sigma_{(2)}$: The bubble diagram Σ_B and the zigzag diagram Σ_Z . The contour ordered self-energies can explicitly be identified using the expansion of the average value eq.(6.20) of the Green's function to second order (see e.g. [14]). They are given in terms of the non-interacting contour ordered Green's functions by

$$\Sigma_Z(00, tt') = i^2 |V_0|^2 \mathcal{G}_0(00, tt', \sigma) \mathcal{G}_0(00, t't, \sigma) \mathcal{G}_0(00, tt', \sigma) \quad (6.73)$$

and

$$\Sigma_B(00, tt') = (-1) i^2 |V_0|^2 \mathcal{G}_0(00, tt', \sigma) \sum_{\sigma'} \mathcal{G}_0(00, t't, \sigma') \mathcal{G}_0(00, tt', \sigma') \quad (6.74)$$

where it was used that the interaction only acts at $x = 0$, so all the Green's function have to be at $x = x' = 0$. The (-1) in Σ_B is due to the Fermion-loop

¹⁷For convenience, we use eq.(6.60) instead of finding $A(00, \omega)$ to second order in the interaction and then use eq.(6.66). The two ways are of course equivalent.

(the bobble) and the i^2 is due to the second order. The Green's functions are independent of the spin, however, the spin index is temporarily included explicitly in \mathcal{G}_0 to emphasize that the spin in the loop in Σ_B can be different from the spin of the baseline in contrast to the zigzag diagram. The second order self-energy $\Sigma_{(2)} = \Sigma_B + \Sigma_Z$ becomes

$$\Sigma_{(2)}(00, tt') = |V_0|^2 \mathcal{G}_0(00, t't) \mathcal{G}_0(00, tt') \mathcal{G}_0(00, tt'). \quad (6.75)$$

Note that if the electrons are spinless (e.g. in a large magnetic field), then the two self-energy contributions cancel each other. This is similar to the cancellation of direct and exchange terms in a electron-electron interaction matrix element for spinless electrons and a momentum independent interaction, see section 4.5.3.

To find the second order current $I^{(2)}$ eq.(6.72) the retarded self-energy is needed. Using eq.(6.24) and the Langreth rule for a product eq.(6.41) it is

$$\begin{aligned} \Sigma_{(2)}^r(00, tt') &= \theta(t - t') [\Sigma_{(2)}^>(00, tt') - \Sigma_{(2)}^<(00, tt')] \\ &= \theta(t - t') |V_0|^2 [\mathcal{G}_0^<(00, t't) \mathcal{G}_0^>(00, tt') \mathcal{G}_0^>(00, tt') - \mathcal{G}_0^>(00, t't) \mathcal{G}_0^<(00, tt') \mathcal{G}_0^<(00, tt')], \end{aligned} \quad (6.76)$$

and Fourier transforming to frequency gives (making the convenient variable change $t - t' \rightarrow t$):

$$\begin{aligned} \Sigma_{(2)}^r(00, \omega) &= \\ &= |V_0|^2 \int_{-\infty}^{\infty} dt e^{i\omega t} \theta(t) [\mathcal{G}_0^<(00, -t) \mathcal{G}_0^>(00, t) \mathcal{G}_0^>(00, t) - \mathcal{G}_0^>(00, -t) \mathcal{G}_0^<(00, t) \mathcal{G}_0^<(00, t)] \\ &= |V_0|^2 \int_{-\infty}^{\infty} \frac{d\omega_1 d\omega_2 d\omega_3}{(2\pi)^3} \int_{-\infty}^{\infty} dt \theta(t) e^{i(\omega + \omega_1 - \omega_2 - \omega_3)t} e^{-\eta t} \\ &\quad \times [\mathcal{G}_0^<(00, \omega_1) \mathcal{G}_0^>(00, \omega_2) \mathcal{G}_0^>(00, \omega_3) - \mathcal{G}_0^>(00, \omega_1) \mathcal{G}_0^<(00, \omega_2) \mathcal{G}_0^<(00, \omega_3)] \\ &= |V_0|^2 \int_{-\infty}^{\infty} \frac{d\omega_1 d\omega_2 d\omega_3}{(2\pi)^3} \frac{i}{(\omega + \omega_1 - \omega_2 - \omega_3) + i\eta} \\ &\quad \times [\mathcal{G}_0^<(00, \omega_1) \mathcal{G}_0^>(00, \omega_2) \mathcal{G}_0^>(00, \omega_3) - \mathcal{G}_0^>(00, \omega_1) \mathcal{G}_0^<(00, \omega_2) \mathcal{G}_0^<(00, \omega_3)], \end{aligned} \quad (6.77)$$

where $e^{-\eta t}$ was introduced to insure convergence ($\eta = 0^+$). This has a form similar to a collision integral (see e.g. eq.(3.7)), i.e. scattering in and out of states, because $\mathcal{G}^< \sim \langle \Psi^\dagger \Psi \rangle$ is like a distribution function and $\mathcal{G}^> \sim \langle 1 - \Psi^\dagger \Psi \rangle$ is like one minus the distribution function. However, a factor is missing in each product of Green's functions. This connection will be more clear later on, see section 6.7.2.

To find Σ^r and in terms $I^{(2)}$ the non-interacting Green's functions $\mathcal{G}_0^i(k, \omega)$ (diagonal in k) eq.(6.44) are rewritten using the transformation to real space

eq.(6.28) as

$$\mathcal{G}_0^r(00, \omega) = \int_{-\infty}^{\infty} \frac{dk}{2\pi} \frac{1}{\omega - \varepsilon_k + i\eta} = -i\pi \int_{-\infty}^{\infty} \frac{dk}{2\pi} \delta(\omega - \varepsilon_k), \quad (6.78)$$

$$\mathcal{G}_0^<(00, \omega) = +2\pi i \int_{-\infty}^{\infty} \frac{dk}{2\pi} \delta(\omega - \varepsilon_k) f_{\text{R/L}}^0(\varepsilon_k), \quad (6.79)$$

$$\mathcal{G}_0^>(00, \omega) = -2\pi i \int_{-\infty}^{\infty} \frac{dk}{2\pi} \delta(\omega - \varepsilon_k) [1 - f_{\text{R/L}}^0(\varepsilon_k)], \quad (6.80)$$

where the principal part of the retarded Green's function $\mathcal{G}_0^r(00, \omega)$ is zero for $\varepsilon_k \propto k^2$ and here it turns out to be convenient to keep the delta functions for the time being. Note that the limit $\mathcal{L} \rightarrow \infty$ has already been taken at this point, making the sums over k into integrals. Inserting these into the factor $\text{Re}[\mathcal{G}_0^r(00, \omega) \Sigma_{(2)}^r(00, \omega)]$ in $I^{(2)}$ eq.(6.72), we have

$$\begin{aligned} \text{Re}[\mathcal{G}_0^r(00, \omega) \Sigma_{(2)}^r(00, \omega)] &= -\text{Im}\mathcal{G}_0^r(00, \omega) \text{Im}\Sigma_{(2)}^r(00, \omega) \\ &= -\pi^2 \left\{ \int_{-\infty}^{\infty} \frac{d\tilde{k}}{2\pi} \delta(\omega - \varepsilon_{\tilde{k}}) \right\} |V_0|^2 \int_{-\infty}^{\infty} \frac{d\omega_1 d\omega_2 d\omega_3}{(2\pi)^3} i^4 (2\pi)^3 \delta(\omega + \omega_1 - \omega_2 - \omega_3) \\ &\quad \times \int_{-\infty}^{\infty} \frac{dk_1 dk_2 dk_3}{(2\pi)^3} \delta(\omega_1 - \varepsilon_{k_1}) \delta(\omega_2 - \varepsilon_{k_2}) \delta(\omega_3 - \varepsilon_{k_3}) \\ &\quad \times [f_1^{(0)}(1 - f_2^{(0)})(1 - f_3^{(0)}) + (1 - f_1^{(0)})f_2^{(0)}f_3^{(0)}], \end{aligned} \quad (6.81)$$

where the short-hand notation $f_i^{(0)} = f_{\text{R/L}}^0(\varepsilon_{k_i})$ was used. To get $I^{(2)}$, we rewrite $\partial_x \mathcal{G}_0^<(00, \omega)$ as (see also eq.(6.61))

$$\partial_x \mathcal{G}_0^<(00, \omega) = -2\pi \int_{-\infty}^{\infty} \frac{dk}{2\pi} k \delta(\omega - \varepsilon_k) f_{\text{R/L}}^0(\varepsilon_k), \quad (6.82)$$

and insert it together with eq.(6.81) into $I^{(2)}$ eq.(6.72), i.e.

$$\begin{aligned} I^{(2)} &= \frac{\hbar}{2m} \sum_{\sigma} \int_{-\infty}^{\infty} \frac{d\omega}{2\pi} \left[2\pi \int_{-\infty}^{\infty} \frac{dk}{2\pi} k \delta(\omega - \varepsilon_k) f_{\text{R/L}}^0(\varepsilon_k) \right] 2\text{Re}[\mathcal{G}_0^r(00, \omega) \Sigma_0^r(00, \omega)] \\ &= |V_0|^2 \frac{\hbar}{2m} \sum_{\sigma} \int_{-\infty}^{\infty} \frac{dk}{2\pi} k n_k^0 2(-\pi^2) \left\{ \int_{-\infty}^{\infty} \frac{d\tilde{k}}{2\pi} \delta(\varepsilon_k - \varepsilon_{\tilde{k}}) \right\} \\ &\quad \times \int_{-\infty}^{\infty} \frac{dk_1 dk_2 dk_3}{(2\pi)^3} \delta(\varepsilon_k + \varepsilon_{k_1} - \varepsilon_{k_2} - \varepsilon_{k_3}) [f_1^{(0)}(1 - f_2^{(0)})(1 - f_3^{(0)}) + (1 - f_1^{(0)})f_2^{(0)}f_3^{(0)}], \end{aligned} \quad (6.83)$$

where delta function $\delta(\omega_i - \varepsilon_{k_i})$ in eq.(6.81) were performed. The factor in the curly brackets give $\frac{2m}{2\pi\hbar|k|}$ for a quadratic dispersion and therefore $I^{(2)}$ simplifies

to

$$\begin{aligned}
I^{(2)} &= -\frac{\pi|V_0|^2}{\hbar} \sum_{\sigma} \int_{-\infty}^{\infty} \frac{dk dk_1 dk_2 dk_3}{(2\pi)^4} \frac{k}{|k|} \delta(\varepsilon_k + \varepsilon_{k_1} - \varepsilon_{k_2} - \varepsilon_{k_3}) \\
&\quad \times f_k^{(0)} \left[f_1^{(0)} (1 - f_2^{(0)}) (1 - f_3^{(0)}) + (1 - f_1^{(0)}) f_2^{(0)} f_3^{(0)} \right] \\
&= -\frac{\pi|V_0|^2}{\hbar} \sum_{\sigma} \int_{-\infty}^{\infty} \frac{dk dk_1 dk_2 dk_3}{(2\pi)^4} \frac{k}{|k|} \delta(\varepsilon_k + \varepsilon_{k_1} - \varepsilon_{k_2} - \varepsilon_{k_3}) \\
&\quad \times \left[f_k^{(0)} f_1^{(0)} (1 - f_2^{(0)}) (1 - f_3^{(0)}) - \underbrace{(1 - f_k^{(0)})}_{(\star)} (1 - f_1^{(0)}) f_2^{(0)} f_3^{(0)} \right],
\end{aligned}$$

where the term (\star) is zero, since the integral over k is odd. Renaming the variables as $(k, k_1, k_2, k_3) \rightarrow (k_1, k_2, k_{1'}, k_{2'})$ the result of the electric current to second order in the interaction $I_e^{(2)} = (-e)I^{(2)}$ becomes

$$\begin{aligned}
I_e^{(2)} &= \frac{2\pi e|V_0|^2}{\hbar} \int_{-\infty}^{\infty} \frac{dk_1 dk_2 dk_{1'} dk_{2'}}{(2\pi)^4} \frac{k_1}{|k_1|} \delta(\varepsilon_1 + \varepsilon_2 - \varepsilon_{1'} - \varepsilon_{2'}) \\
&\quad \times \left[f_1^{(0)} f_2^{(0)} (1 - f_{1'}^{(0)}) (1 - f_{2'}^{(0)}) - (1 - f_1^{(0)}) (1 - f_2^{(0)}) f_{1'}^{(0)} f_{2'}^{(0)} \right],
\end{aligned} \tag{6.84}$$

where $f_i^{(0)} \equiv f_{\text{R/L}}^0(\varepsilon_{k_i})$ is the Fermi function of the left contact $f_{\text{L}}^0(\varepsilon_{k_i})$ for $k_i > 0$ and vice versa. This expression has the familiar structure known from the Boltzmann equation doing an expansion in the interaction (see e.g. eq.(3.17) or eq.'s(4.14) and (4.15)). However, it is free of the non-sense prefactors appearing in the Boltzmann equation approach like L/\mathcal{L} , see section 6.2. Therefore this expression means that the physics of the interaction processes can still be understood in terms of scattering in and out of the states (k_1, k_2) and $(k_{1'}, k_{2'})$. Furthermore, we observe that the derived electric current $I_e = I_e^{(0)} + I_e^{(2)} + \dots$ to second order in the interaction is *not* restricted to the linear response regime.

In the following, the second order interaction contribution to the current $I_e^{(2)}$ eq.(6.84) is used to find: (i) The analytic expressions for the conductance $G^{(2)}$ and thermopower $S^{(2)}$ to lowest order in the temperature $T/T_{\text{F}} \ll 1$, (ii) the non-linear conductance $G = I/V$ at zero temperature to lowest order in the bias, and (iii) the full temperature behavior of the second order interaction contribution of the conductance $G^{(2)}$ and thermopower $S^{(2)}$ by numerical integration.

The low-temperature conductance and thermopower to 2nd order in the interaction

The (linear) conductance G and thermopower S to second order in the interaction is now found analytically from eq.(6.84) to lowest order in the temperature, i.e. in the regime $T/T_{\text{F}} \ll 1$. The procedure is completely analogous to the one used in section 4.3.2 (p. 61) for the multi-mode wire and therefore only briefly outlined here.

First of all, the linear response limit is taken by including the temperature difference $\Delta T = T_R - T_L$ and the bias $eV = \mu_R - \mu_L$ difference in the left/right Fermi functions of the leads as $\mu_L = \varepsilon_F$, $\mu_R = \varepsilon_F + eV$, $T_L = T$ and $T_R = T + \Delta T$. In this case, the linear electric current is $I_e = GV + G_T \Delta T$. Expanding the Fermi functions gives

$$f_R^0(\varepsilon) \simeq f^0(\varepsilon) - \partial_\varepsilon f^0(\varepsilon) eV - \partial_\varepsilon f^0(\varepsilon) (\varepsilon - \varepsilon_F) \frac{\Delta T}{T} \quad \text{and} \quad f_L^0(\varepsilon) = f^0(\varepsilon), \quad (6.85)$$

and after some simplifications the linear response electric current to second order in the interaction becomes

$$I_e^{(2)} = -8 \frac{2\pi e |V_0|^2}{\hbar} \int_0^\infty \frac{dk_1 dk_2 dk_{1'} dk_{2'}}{(2\pi)^4} \delta(\varepsilon_1 + \varepsilon_2 - \varepsilon_{1'} - \varepsilon_{2'}) \times f_1^0 f_2^0 (1 - f_{1'}^0) (1 - f_{2'}^0) \left[\frac{eV}{k_B T} + \frac{\Delta T}{k_B T^2} (\varepsilon_1 - \varepsilon_F) \right], \quad (6.86)$$

where $f_i^0 \equiv f^0(\varepsilon_i) = \{1 + \exp[(\varepsilon_i - \varepsilon_F)/k_B T]\}^{-1}$. In the simplifications leading to the above result, we observe that only scattering processes changing the number of left and right movers in the scattering contribute to the current. This is completely analogous to the Boltzmann approach, see section 3.3. To expand $I_e^{(2)}$ in the temperature T/T_F , new dimensionless integration variables $z_j = (\varepsilon_j - \varepsilon_F)/k_B T$ are introduced and the linear response expression for $I_e^{(2)}$ is exactly rewritten to

$$I_e^{(2)} = -8 \frac{2\pi e |V_0|^2}{\hbar} \frac{1}{(2\pi)^4} \left(\frac{k_F}{2} \right)^4 \left(\frac{T}{T_F} \right)^2 \frac{1}{\varepsilon_F} \int_{-\frac{T_F}{T}}^\infty dz_1 \frac{1}{\sqrt{1 + z_1 \frac{T}{T_F}}} \times \int_{-\frac{T_F}{T}}^\infty dz_2 \frac{1}{\sqrt{1 + z_2 \frac{T}{T_F}}} \int_{-\frac{T_F}{T}}^\infty dz_{1'} \frac{1}{\sqrt{1 + z_{1'} \frac{T}{T_F}}} \int_{-\frac{T_F}{T}}^\infty dz_{2'} \frac{1}{\sqrt{1 + z_{2'} \frac{T}{T_F}}} \times \delta(z_1 + z_2 - z_{1'} - z_{2'}) g(z_1) g(z_2) g(-z_{1'}) g(-z_{2'}) \left[\frac{eV}{\varepsilon_F} + z_1 \frac{\Delta T}{T_F} \right], \quad (6.87)$$

where $g(z) = (1 + e^z)^{-1}$. Note that $k_F^2 |V_0|$ has units of energy, so the expression has units of current $e\varepsilon_F/\hbar$. As in section 4.3.2, the density of states are expanded in T/T_F and the integral can be calculated analytically order by order in temperature by using the variables $z_\pm = z_{1'} \pm z_{2'}$ and the useful integrals in eq.(4.67) and eq.(4.89). The result for the conductance G , thermoelectric coefficient G_T and

thermopower S is

$$G = \frac{2e^2}{h} \left[1 - \frac{1}{24} \left(\frac{|V_0|k_F^2}{\varepsilon_F} \right)^2 \left(\frac{T}{T_F} \right)^2 - \frac{\pi^2}{24} \left(\frac{|V_0|k_F^2}{\varepsilon_F} \right)^2 \left(\frac{T}{T_F} \right)^4 - \dots \right], \quad (6.88)$$

$$G_T = \frac{2e}{h} k_B \frac{\pi^2}{60} \left(\frac{|V_0|k_F^2}{\varepsilon_F} \right)^2 \left(\frac{T}{T_F} \right)^3 + \mathcal{O} \left[\left(\frac{T}{T_F} \right)^5 \right], \quad (6.89)$$

$$S = \frac{k_B}{e} \frac{\pi^2}{60} \left(\frac{|V_0|k_F^2}{\varepsilon_F} \right)^2 \left(\frac{T}{T_F} \right)^3 + \mathcal{O} \left[\left(\frac{T}{T_F} \right)^5 \right]. \quad (6.90)$$

It is interesting to observe that at least qualitatively, there is an agreement with experiments on the 0.7 anomaly: The conductance decreases for increasing temperature (e.g. [17]) and the thermopower increases at the anomaly [68] (for a description of the experiments see section 1.9).

The thermopower has one power of temperature more than the conductance correction. This is because the thermopower requires some curvature of the dispersion to avoid perfect particle-hole symmetry. This comes out naturally, when doing the expansion in temperatures of eq.(6.87).

As in the case of the multi-mode wire, the interaction contribution to the thermopower eq.(6.90) is the leading order at low temperatures compared to the exponentially suppressed non-interacting contribution, $S^{(0)} \propto \exp(-T_F/T)$. Furthermore, the thermopower S is positive, so a current due to a temperature difference is *increased* by the interactions, in contrast to the current due to a bias, which is decreased. In other words, at low temperature a positive current due to a temperature difference (for a fully open contact) is created by the electron-electron interactions.

In contrast to the multi-mode case, there is no interesting explicit dependence on ε_F in the above conductance and thermopower, i.e. no resonances. This is because that the corrections are simply caused by backscattering of one or two electrons, which can happen at any Fermi level, if the non-momentum conserving interactions are allowed ($k_F L \sim 1$). A dependence on the Fermi level is implicitly embedded in V_0 , since the non-momentum conserving processes are strongest for low $k_F L$ and interactions in general are stronger for low electron density (due to lack of screening).

We can still test the Mott formula for the thermopower eq.(2.1) and it gives the right temperature dependence, but it is off by a factor of $S^M/S = 5/3$ to lowest order in temperature. However, this factor is without taking the implicit (unknown) dependence of V_0 on ε_F into account, so we cannot make a direct comparison to the experimental data.

The full temperature dependence the conductance to 2nd order in the interaction

Above we founded that in the low temperature regime $T \ll T_F$ the conductance and thermopower to second order in the point-like interaction are proportional to T^2 and T^3 , respectively. However, what happens to the second order interaction term in G and S for higher temperatures? This question is answered below numerically and as expected the power laws are good for the lowest temperatures.

The conductance G is considered using the linear response current to second order in the interaction $I_e^{(2)}$ eq.(6.86). This is exactly rewritten to a form more accessible by numerical integration know e.g. from the Coulomb drag literature [140, 141]. The Fermi functions are rewritten using

$$f^0(\varepsilon_1)[1 - f^0(\varepsilon_{1'})] = [f^0(\varepsilon_{1'}) - f^0(\varepsilon_1)] n_B(\varepsilon_1 - \varepsilon_{1'}) \quad (6.91)$$

where $n_B(\varepsilon) \equiv [e^{\varepsilon/k_B T} - 1]^{-1}$ is the zero chemical potential Bose function and the energy conserving delta function is rewritten as

$$\delta(\varepsilon_1 + \varepsilon_2 - \varepsilon_{1'} - \varepsilon_{2'}) = \int_{-\infty}^{\infty} d\omega \delta(\varepsilon_1 - \varepsilon_{1'} - \omega) \delta(\varepsilon_2 - \varepsilon_{2'} + \omega). \quad (6.92)$$

Inserting these relations into the eV term of eq.(6.86) and using that $n_B(\omega)n_B(-\omega) = -[2 \sinh(\omega/2k_B T)]^{-2}$ one obtains after a few manipulations

$$G^{(2)} = -8 \frac{2\pi e^2 |V_0|^2}{\hbar} \frac{1}{k_B T} 2 \int_0^{\infty} d\omega \frac{[F(\omega, T/T_F)]^2}{4 \sinh^2(\omega/2k_B T)}, \quad (6.93)$$

where $G^{(2)} = I_e^{(2)}/V$ and

$$\begin{aligned} F(\omega, T/T_F) &\equiv \int_0^{\infty} \frac{dk_1}{2\pi} \int_0^{\infty} \frac{dk_{1'}}{2\pi} \delta(\varepsilon_1 - \varepsilon_{1'} - \omega) [f^0(\varepsilon_{1'}) - f^0(\varepsilon_1)] \\ &= \frac{1}{4\pi^2} \frac{m}{2\hbar^2} \int_0^{\infty} d\varepsilon \frac{f^0(\varepsilon) - f^0(\varepsilon + \omega)}{\sqrt{\varepsilon(\varepsilon + \omega)}}, \end{aligned} \quad (6.94)$$

where the quadratic dispersion was used in the last equality and above it was used that F is odd, i.e. $F(-\omega) = -F(\omega)$. To perform the numerical integration new dimensionless variables are introduced as $\Omega = \omega/k_B T$ and $E = \varepsilon/k_B T$, so

$$G^{(2)} = -\frac{2e^2}{h} \frac{1}{32\pi^2} \left(\frac{|V_0|k_F^2}{\varepsilon_F} \right)^2 \int_0^{\infty} d\Omega \frac{[\tilde{F}(\Omega, T/T_F)]^2}{\sinh^2(\Omega/2)}, \quad (6.95)$$

where

$$\tilde{F}(\Omega, T/T_F) = \int_0^{\infty} dE \frac{g(E - T_F/T) - g(E + \Omega - T_F/T)}{\sqrt{E(E + \Omega)}}, \quad (6.96)$$

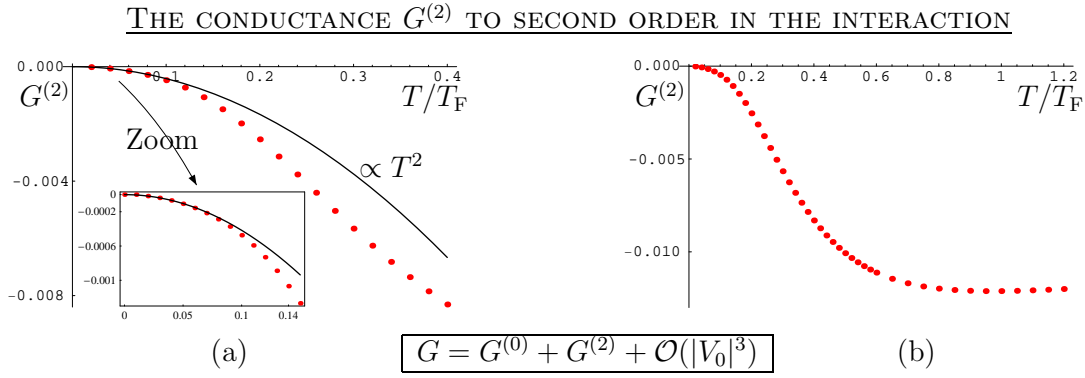


Figure 6.5: The second order interaction correction $G^{(2)}$ to the conductance $G = G^{(0)} + G^{(2)} + \dots$ in units of $\frac{2e^2}{h}(|V_0|k_F^2/\varepsilon_F)^2$ versus temperature T/T_F . The interaction correction $G^{(2)}$ (red dots) is found by numerical integration of eq.(6.95) and compared to the low temperature result $G^{(2)} \propto T^2$ (full black line) eq.(6.88) in (a). The insert in (a) shows that the power law T^2 is excellent below $T/T_F \sim 0.1$. In (b) $G^{(2)}$ is given for (unrealistically and uninterestingly) large temperatures, however, it shows that $G^{(2)}$ saturates at high enough temperatures.

and $g(x) = [1 + \exp(x)]^{-1}$. This form of $G^{(2)}$ is numerically useful, because the F functions can be done separately and then used in the ω -integral.

The result of the numerical evaluation of $G^{(2)}$ eq.(6.95) is seen in figure 6.5. We observe that the low-temperature power law, $G^{(2)} \propto T^2$ eq.(6.89), is found as expected in figure 6.5(a). In figure 6.5(b), $G^{(2)}$ is seen to saturate to a constant high temperature value $G_{\text{T-high}}^{(2)} \approx -0.012 \frac{2e^2}{h}(|V_0|k_F^2/\varepsilon_F)^2$ depending on the interaction, so the conductance G saturates to a constant value $G_{\text{T-high}} = G_{\text{T-high}}^{(0)} + G_{\text{T-high}}^{(2)}$ at high temperatures¹⁸. *However, this cannot explain the high temperature saturation for the experimental data on the 0.7 anomaly (see e.g. figure 1.5, section 1.9.1), because the saturation temperature is too high, i.e. of order T_F .* This is why, we try to go beyond perturbation theory in section 6.7 to explain this¹⁹. Note that the non-interacting conductance also has a weak temperature dependence

$$G^{(0)} = \frac{2e^2}{h} \int_0^\infty d\varepsilon [-\partial_\varepsilon f^0(\varepsilon)] = \frac{2e^2}{h} \frac{1}{1 + e^{-T_F/T}}, \quad (6.97)$$

so it saturates to e^2/h for high temperature (e.g. $G^{(0)} \approx 1.05e^2/h$ for $T/T_F = 10$ and $G^{(0)} \approx 1.76e^2/h$ for $T/T_F = 0.5$), but at low temperatures it is only an

¹⁸To do the high temperature limit analytically, we insert $f^0(\varepsilon) \simeq \exp[-(\varepsilon - \varepsilon_F)/k_B T]$ in $F(\omega, T/T_F)$ and obtain: $G^{(2, T \gg T_F)} = -\frac{2e^2}{h} \frac{1}{16} (V_0 k_F^2/\varepsilon_F)^2 e^{2T_F/T}$, where $e^{2T_F/T} \simeq 1$. However, it turns out that this approximation overestimates the numerical result by about a factor of ~ 8 . This is due to the fact that even for high temperatures the states below the Fermi level are not well approximated by only including the exponential tail.

¹⁹It is interesting to note that normally it is not the high temperature limit, which is the usual problem in mesoscopic physics.

exponential correction, $G^{(0)} \simeq \frac{2e^2}{h}(1 - e^{-T_F/T})$.

A similar analysis can be done for the thermoelectric coefficient and in terms the thermopower. However, no new interesting features appear on a scale smaller than the Fermi temperature²⁰.

The non-linear current to 2nd order in the interaction for $eV \ll \varepsilon_F$

Next the non-linear current due to an applied bias V is investigated in the regime $k_B T \ll eV \ll \varepsilon_F$ (for $T_R = T_L$). Again, the current to second order in the interaction eq.(6.84) is used, since it is also valid beyond the linear response regime. To this end, we linearize the bands, $\varepsilon_k \simeq \varepsilon_F \mp \hbar v_F(k \pm k_F)$, and use zero temperature $T = 0$, so the Fermi functions become step functions. To do the calculation the k_i -integrals of eq.(6.84) are split into positive and negative intervals (as in the low T/T_F calculation) and after some tedious calculations one obtains:

$$\frac{I_e^{(2)}(V, T = 0)}{V} = -\frac{2e^2}{h} \frac{5}{192\pi^2} \left(\frac{|V_0|k_F^2}{\varepsilon_F} \right)^2 \left(\frac{eV}{\varepsilon_F} \right)^2 \quad \text{for} \quad eV \ll \varepsilon_F. \quad (6.98)$$

The non-interacting contribution to the non-linear current for a fully open QPC at zero temperature is still linear in V ,

$$I_e^{(0)}(V, T = 0) = \frac{2e^2}{h} V, \quad (6.99)$$

as long as V is small enough not to involve other conducting subbands, see e.g. [65, 66].

Again, we observe that the non-linear current eq.(6.98) is in (at least) qualitative agreement with the experiments on the 0.7 structure: Increasing the bias will decrease the non-linear conductance (see e.g. [17] or section 1.9).

6.6 The low-temperature perturbative transport coefficients beyond the point-like interaction

In this section, we show that the low-temperature power-laws in the transport coefficients,

$$G - \frac{2e^2}{h} \propto T^2, \quad S \propto T^3 \quad \text{and} \quad \frac{I_e(V, T = 0)}{V} - \frac{2e^2}{h} \propto V^2 \quad (6.100)$$

²⁰However, at $T/T_F \simeq 0.8$ the second order interaction contribution $G_T^{(2)}$ changes sign, which can also be found by using Boltzmann factors for the Fermi functions. However, since $T/T_F \simeq 0.8$ is not small compared to one, the non-interacting contribution $G_T^{(0)}$ (see eq.(4.20)) can dominate G_T depending on the size of the interaction V_0 .

are *not* specific for the point-like interaction, but general for any interaction in the low-temperature (or voltage) regime $T \ll T_F$ (or $eV \ll \varepsilon_F$).

The current to second order in the interaction for a *general* interaction is derived in Appendix A (p. 139) and given in eq.(A.29) as:

$$I_e^{(2)} = -e\pi \sum_{k_1 k_2 k_{1'} k_{2'}} \frac{k_1}{|k_1|} \left[(1 - f_1^{(0)})(1 - f_2^{(0)})f_{1'}^{(0)}f_{2'}^{(0)} - (1 - f_{1'}^{(0)})(1 - f_{2'}^{(0)})f_1^{(0)}f_2^{(0)} \right] \\ \times \delta(\varepsilon_1 + \varepsilon_2 - \varepsilon_{1'} - \varepsilon_{2'}) \operatorname{Re} \sum_{\sigma_1 \sigma_2 \sigma_{1'} \sigma_{2'}} V_{1'2',12} \{V_{12,1'2'} - V_{21,1'2'}\}, \quad (6.101)$$

where $V_{1'2',12}$ is the direct part of the electron-electron interaction matrix element using the single-particle (non-interacting) wave function $\psi_{k\sigma}(\mathbf{r}) = \frac{1}{\sqrt{\mathcal{L}}} e^{ikx} \varphi(\mathbf{r}_\perp) \chi_\sigma$, where $\varphi(\mathbf{r}_\perp)$ is a single transverse mode ($\mathbf{r}_\perp = (y, z)$) and χ_σ is the spin part, see e.g. eq.(A.3). Therefore the interaction $V_{1'2',12}$ can be expressed as

$$V_{1'2',12} = \delta_{\sigma_1, \sigma_{1'}} \delta_{\sigma_2, \sigma_{2'}} \frac{1}{\mathcal{L}^2} \int_{-\frac{\mathcal{L}}{2}}^{\frac{\mathcal{L}}{2}} dx_a dx_b \iint d\mathbf{r}_{\perp a} d\mathbf{r}_{\perp b} |\varphi(\mathbf{r}_{\perp a})|^2 |\varphi(\mathbf{r}_{\perp b})|^2 \\ \times V(\mathbf{r}_a, \mathbf{r}_b) e^{i(k_1 - k_{1'})x_a + i(k_2 - k_{2'})x_b}, \quad (6.102)$$

and if the center of mass coordinate $X \equiv (x_a + x_b)/2$ and the distance between the electrons $\Delta x \equiv (x_a - x_b)$ are introduced then the interaction becomes

$$V_{1'2',12} = \frac{\delta_{\sigma_1, \sigma_{1'}} \delta_{\sigma_2, \sigma_{2'}}}{\mathcal{L}^2} \iint d\Delta x dX \iint d\mathbf{r}_{\perp a} d\mathbf{r}_{\perp b} |\varphi(\mathbf{r}_{\perp a})|^2 |\varphi(\mathbf{r}_{\perp b})|^2 V(\mathbf{r}_a, \mathbf{r}_b) e^{i\Delta k X + iq\Delta x}, \\ \equiv \frac{1}{\mathcal{L}^2} W(\Delta k, q) \delta_{\sigma_1, \sigma_{1'}} \delta_{\sigma_2, \sigma_{2'}}, \quad (6.103)$$

where $V(\mathbf{r}_a, \mathbf{r}_b) = V(\mathbf{r}_{\perp b}, \mathbf{r}_{\perp a}, X, \Delta x)$,

$$\Delta k \equiv k_1 + k_2 - k_{1'} - k_{2'}, \quad \text{and} \quad q \equiv \frac{(k_1 - k_{1'}) + (k_{2'} - k_2)}{2}. \quad (6.104)$$

Here Δk is the total momentum change, i.e. the amount of momentum breaking, and q can be understood as the momentum exchange in the interaction, i.e. it is the average of the momentum exchange of each electron (since for a momentum conserving interaction, $\Delta k = 0$, it is $q = k_1 - k_{1'} = k_{2'} - k_2$.) It is important to note that W is a function of both Δk and q and not only q as in the momentum conserving case, since we do not have translational invariance $V(\mathbf{r}_a, \mathbf{r}_b) \neq V(\mathbf{r}_a - \mathbf{r}_b)$. However, since $V(\mathbf{r}_a, \mathbf{r}_b) = V(\mathbf{r}_b, \mathbf{r}_a)$ leads to $V(\mathbf{r}_{\perp b}, \mathbf{r}_{\perp a}, X, \Delta x) = V(\mathbf{r}_{\perp a}, \mathbf{r}_{\perp b}, X, -\Delta x)$, we have that²¹

$$W(\Delta k, -q) = W(\Delta k, q). \quad (6.105)$$

²¹Furthermore, if the QPC is symmetric around the mid-point $x = 0$, then $V(X, \Delta x) = V(-X, \Delta x)$ so $W(\Delta k, q) = W(-\Delta k, q)$, however, here we consider a general non-symmetric QPC.

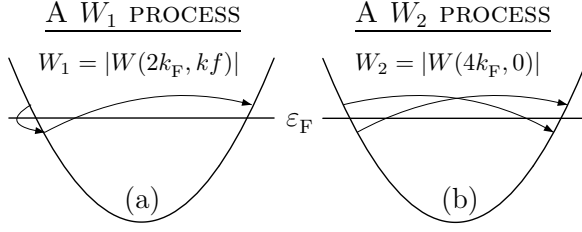


Figure 6.6: Examples of scattering processes changing the number of left and right movers by one (a) or two (b) with amplitudes W_1 and W_2 , respectively. Compare to figure 6.1.

Next we consider the linear response current to second order in a general interaction eq.(6.101) to lowest order in the temperature $T/T_F \ll 1$. The only difference to the low-temperature calculation for the point-like interaction above is that the interaction is no longer constant, so when dividing the k -integrals into positive and negative intervals, the interaction has to be taken into account. However, to lowest order in temperature, the interaction is expanded and its (momentum independent) value at the Fermi level can be used. A careful analysis of the 16 terms from dividing the four k -integrals in eq.(6.101) shows that only two kinds of the interaction processes contribute: The processes changing the number of left (right) movers by one or two shown in figure 6.6. We name these amplitudes W_1 and W_2 , respectively, and they are:

$$W_2 \equiv |W(4k_F, 0)|, \quad \text{and} \quad W_1 \equiv |W(2k_F, k_F)|, \quad (6.106)$$

using that $W(\Delta k, q)$ is even in q eq.(6.105) and that $[W(-\Delta k, -q)]^* = W(\Delta k, q)$ for a real interaction $V(\mathbf{r}_a, \mathbf{r}_b)$. The details of the low-temperature calculation are like for the multi-mode wire, see e.g. section 4.3.2 (p. 61). The low-temperature linear transport coefficients are:

$$G = \frac{2e^2}{h} \left\{ 1 - \frac{1}{48} \left[\left(\frac{W_1 k_F^2}{\varepsilon_F} \right)^2 + \left(\frac{W_2 k_F^2}{\varepsilon_F} \right)^2 \right] \left(\frac{T}{T_F} \right)^2 - \dots \right\}, \quad (6.107)$$

$$S = \frac{k_B}{e} \frac{\pi^2}{120} \left[\left(\frac{W_1 k_F^2}{\varepsilon_F} \right)^2 + \left(\frac{W_2 k_F^2}{\varepsilon_F} \right)^2 \right] \left(\frac{T}{T_F} \right)^3 + \dots, \quad (6.108)$$

Furthermore, the non-linear current due to a bias V in the regime $T = 0$ and $eV \ll \varepsilon_F$ is also found as above to be

$$\frac{I_e(V, T=0)}{V} = \frac{2e^2}{h} - \frac{2e^2}{h} \frac{1}{48\pi^2} \left[\frac{1}{4} \left(\frac{W_1 k_F^2}{\varepsilon_F} \right)^2 + \left(\frac{W_2 k_F^2}{\varepsilon_F} \right)^2 \right] \left(\frac{eV}{\varepsilon_F} \right)^2 \quad (6.109)$$

to lowest order in eV/ε_F . Note the difference in prefactors between the corrections due to W_1 and W_2 in the non-linear conductance and the linear transport coefficients. Furthermore, W_2 will be smaller than W_1 , since it involves a larger degree of momentum breaking.

These relations simplify to the point-like model results eq.(6.88), eq.(6.90) and eq.(6.98) taking $W_1 = W_2 = V_0$. Therefore we see that the amplitude V_0 of the point-like interaction $V(x, x') = V_0\delta(x)\delta(x')$ does not distinguish between different scattering processes at the Fermi level, however, it leads to the correct low-temperature (or voltage) power-laws for the interaction-induced terms in the transport coefficients.

6.6.1 The perturbative large magnetic field results

Next we study the situation of a large applied magnetic field $g\mu_B B \gg k_B T$, such that the conductance quantization is in well defined steps of e^2/h . Therefore the subbands are spin split and the interaction effects between electrons of the same spin (say $\sigma = \downarrow$) within a single subband become important. We find the conductance change perturbatively to lowest order in the (non-momentum conserving) interaction on the e^2/h plateau.

First of all, for a contact interaction in real space $V(x, x') \propto \delta(x - x')$ the Pauli principle does not allow the electrons of equal spin to interact and therefore the corrections to the current are zero (see e.g. section 4.5.3). In particular, there is no effect of the point-like interaction in eq.(6.6).

Therefore the perturbative current correction formula eq.(6.101) for a general interaction is extremely useful in the case interactions among equal spin electrons. Here we use this current formula eq.(6.101) in linear response to calculate the conductance correction to lowest order in temperature T/T_F . The calculation is very similar to the one in section 4.5.3, so only a few calculational details are discussed below. The linear response current for a single spin mode ($\sigma_1 = \sigma_2 = \sigma_{1'} = \sigma_{2'}$) and for a general interaction $W(\Delta k, q)$ is found using eq.(6.101) to be²²

$$I_e^{(2)} = -e\pi \text{Re} \int_{-\infty}^{\infty} \frac{dk_1 dk_2 dk_{1'} dk_{2'}}{(2\pi)^4} \frac{k_{1'}}{|k_{1'}|} f_1^0 f_2^0 (1 - f_{1'}^0)(1 - f_{2'}^0) [\psi_1 + \psi_2 - \psi_{1'} - \psi_{2'}] \\ \times \delta(\varepsilon_1 + \varepsilon_2 - \varepsilon_{1'} - \varepsilon_{2'}) W^*(\Delta k, q) [W(\Delta k, q) - W(\Delta k, q + k_{1'} - k_{2'})], \quad (6.110)$$

where $\psi_i = (eV/k_B T)\theta(-k_i)$ using²³ $\mu_R = \varepsilon_F + eV$, $\mu_L = \varepsilon_F$ and $T_R = T_L$. It is seen from eq.(6.110) that a q dependence of $W(\Delta k, q)$ is needed to have an effect, or equivalently, the interaction should not be a contact interaction. Otherwise, the direct term $W(\Delta k, q)$ and exchange term $W(\Delta k, q + k_{1'} - k_{2'})$ cancel out. The calculational strategy is the same as previous low-temperature calculations: Introduce new dimensionless variables $z_i = (\varepsilon_i - \varepsilon_F)/k_B T$ and expand in T/T_F . To this end, we separate all the k -integrals in positive and negative parts and in

²²Here the primed and unprimed indices were interchanged compared to eq.(6.101) for convenience.

²³To find the thermopower also, we simply have to include $\frac{\varepsilon_i - \varepsilon_F}{k_B T} \frac{\Delta T}{T} \theta(-k_i)$ in ψ_i for $T_R = T + \Delta T$ and $T_L = T$.

each term the interaction is expanded as

$$W(\Delta k, q) \simeq W(\Delta k_{\varepsilon_F}, q_{\varepsilon_F}) + \partial_q W(\Delta k_{\varepsilon_F}, q_{\varepsilon_F})[q - q_{\varepsilon_F}] + \partial_{\Delta k} W(\Delta k_{\varepsilon_F}, q_{\varepsilon_F})[\Delta k - \Delta k_{\varepsilon_F}], \quad (6.111)$$

where Δk_{ε_F} , q_{ε_F} are the values of Δk and q at the Fermi level for the particular interaction process. For example, if $k_1, k_2 > 0$ and $k_{1'}, k_{2'} < 0$, then $\Delta k_{\varepsilon_F} = 4k_{F\sigma}$ and $q_{\varepsilon_F} = 0$, where $k_{F\sigma}$ is the Fermi wave vector of the spin split band, $\varepsilon_F = \hbar^2 k_{F\sigma}^2 / 2m$. Note that expanding the interaction to higher order simply produces higher order terms in temperature and these terms are not relevant here. We use that $W(\Delta k, q)$ is even in q such that $\partial_q W(\Delta k_{\varepsilon_F}, q_{\varepsilon_F}) = -\partial_q W(\Delta k_{\varepsilon_F}, -q_{\varepsilon_F})$ and also that $W^*(\Delta k, q) = W(-\Delta k, -q)$. As in the $B = 0$ case, we find that there are two scattering processes at play: Interactions changing the number of left and right movers by one or two, respectively. These are illustrated in the figures 6.1 and 6.6 in real and momentum space, respectively. After some manipulations, we arrive at (reintroducing \hbar)

$$I_e^{(2)} \simeq (-e) \frac{2\pi}{\hbar} \left[|\partial_q W(4k_{F\sigma}, 0)|^2 + |\partial_q W(2k_{F\sigma}, k_{F\sigma})|^2 \right] \frac{eV}{\varepsilon_F} \times \int_0^\infty \frac{dk_1 dk_2 dk_{1'} dk_{2'}}{(2\pi)^4} f_1^0 f_2^0 (1 - f_{1'}^0)(1 - f_{2'}^0) \delta(\varepsilon_1 + \varepsilon_2 - \varepsilon_{1'} - \varepsilon_{2'}) (k_{1'} - k_{2'})^2, \quad (6.112)$$

where all the different terms were collected. The factor $(k_{1'} - k_{2'})^2$ stems from the expansion of the interaction. Using the dimensionless variables the lowest order expansion in T/T_F gives

$$G \simeq \frac{e^2}{h} - \frac{e^2}{h} \frac{\pi^2}{240} \left(\frac{k_{F\sigma}^6 (W_1')^2 + k_{F\sigma}^6 (W_2')^2}{\varepsilon_F^2} \right) \left(\frac{T}{T_F} \right)^4 \quad (6.113)$$

where the integrals in eq.(4.67) and eq.(4.89) were used²⁴ and we introduced the derivatives of the scattering amplitudes for the two processes in figure 6.6

$$W_1' \equiv |\partial_q W(2k_{F\sigma}, k_{F\sigma})|, \quad \text{and} \quad W_2' \equiv |\partial_q W(4k_{F\sigma}, 0)|. \quad (6.114)$$

This result shows that the interaction effect due to non-momentum conserving scattering is heavily suppressed on the e^2/h plateau (i.e. large $g\mu_B B$) by two powers of temperature compared to the $2e^2/h$ plateau ($B = 0$). It also involves the derivative of the interaction amplitude at the Fermi level instead of the interaction amplitude itself. This suppression is in (qualitative) agreement with the experiments, where no anomaly is seen on the e^2/h plateau.

The thermopower for a single spin subband can be found in the same way and goes as

$$S \propto [(W_1')^2 + (W_2')^2] \left(\frac{T}{T_F} \right)^5, \quad (6.115)$$

²⁴We also used that $\int_{-\infty}^{\infty} dx \frac{x^2}{4 \sinh^2(x/2)} = 2\pi^2/3$ and $\int_{-\infty}^{\infty} dx \frac{x^4}{4 \sinh^2(x/2)} = 8\pi^4/15$.

which again is suppressed by two powers of temperature compared to the $B = 0$ case.

6.7 The conductance in the self-consistent second order approach

In this section, we try to do better than perturbation theory. The motivation is to describe the temperature dependence of the conductance beyond the low-temperature perturbative regime, where $G - \frac{2e^2}{h} \propto -|V_0|^2 T^2$ was found. The perturbative result is correct for $T/T_F \rightarrow 0$, and fails miserably when the perturbative correction is of order the non-interacting result, i.e. $G^{(2)} \sim 2e^2/h$. This gives rise to a new temperature scale T^* of the problem²⁵ (see e.g. eq.(6.88)):

$$G^{(2)}(T^*) \sim \frac{2e^2}{h} \quad \Rightarrow \quad T^* \sim \sqrt{24} \frac{\varepsilon_F}{|V_0|k_F^2} T_F, \quad (6.116)$$

i.e. perturbation theory is valid for $T \ll T^*$. This is - of course - a rough estimate for the failure of perturbation theory. Therefore the non-perturbative regime of interest here is

$$T^* \lesssim T \ll T_F, \quad (6.117)$$

i.e. for temperature around T^* . We also require that $T \ll T_F$, because we are not interested in effects due to a large thermal smearing. Note that *if* the interaction is small enough ($|V_0|k_F^2 \ll \varepsilon_F$), then the situation $T^* \gtrsim T_F$ can appear, in which case the non-perturbative regime is not reached for $T < T_F$. The parameters used in the very rough estimate on page 91 gives T^* of order 3 K or so (for $T_F \sim 12$ K).

To approach the non-perturbative regime, we return to the point-like interaction, $V(x, x') = V_0 \delta(x) \delta(x')$, where the convenient current formula eq.(6.66) was derived, relating I_e to the local spectral function $A(00, \omega)$. To get $A(00, \omega)$, we approximate the self-energy by the self-consistent version of the second-order diagrams, see figure 6.7. This makes a numerical solution of the Dyson equation possible and we find the conductance and thermopower in the non-perturbative regime. Below we give the details of this calculation and try to motivate the approximation of the self-energy in terms of a quantum Boltzmann equation, since it is not merely a simple expansion in a small parameter or the like. It is noteworthy that the fluctuation-dissipation theorem for equilibrium Green's function comes in handy, since only the linear response regime is considered. The found temperature dependence of the conductance²⁶ seems to agree (at least) qualitatively with the experimental data on the 0.7 anomaly.

²⁵This definition is the same in spirit as in paper IV, but differs by a numerical prefactor.

²⁶To the best of our knowledge, no detailed experimental temperature study have been made for the thermopower near the anomaly.

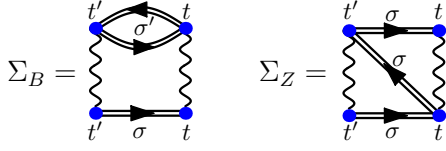


Figure 6.7: The self-consistent second-order Feynman diagrams of the self-energy eq.(6.118), which is the essential approximation make to approach the non-perturbative regime. Double lines with arrows are the full Green's functions \mathcal{G} connecting the interactions (wiggled lines) at space time points $(x = 0, t^{(i)})$ (blue dots).

6.7.1 The self-consistent second-order approximation

The self-consistent second-order approximation for the self-energy is simply to take the two second-order diagrams (seen on figure 6.4) and make the non-interacting Green's functions \mathcal{G}_0 into the full Green's functions \mathcal{G} , see figure 6.7. This will include a subclass of all possible higher order diagrams, but far from all. Therefore the approximation for the self-energy is the sum of the self-consistent bobble and zigzag diagrams (in figure 6.7), i.e.

$$\Sigma_{\text{sc}}(00, tt') = |V_0|^2 \mathcal{G}(00, t't) \mathcal{G}(00, tt') \mathcal{G}(00, tt'). \quad (6.118)$$

This is the essential approximation make to approach the non-perturbative regime. This approximation is current conserving, since the self-energy is a functional involving only full Green's functions, see e.g. [142, 143].

Below we describe how to use this approximation to solve the local Dyson equation (at $x = x' = 0$) for the local spectral function $A(00, \omega)$ by a numerical iterative scheme, which in terms leads to the conductance and thermopower.

The *GW*-approximation

Another (somewhat similar) approximation is the so-called *GW*-approximation often considered in the literature, see e.g. [144]. Here the self-energy is given by $\Sigma(1, 1') = \mathcal{G}(1, 1')W(1, 1')$, where $W(1, 1')$ is the RPA series for the interaction (see e.g. [14, chap.14]). The *GW*-approximation and the self-consistent second order approach have diagrams in common, however, they are different approximations. E.g. the *GW*-approximation includes the Fock diagram, which the self-consistent 2nd order does not.

6.7.2 The idea of the 2nd order self-consistent approach

There is no easy way to justify the self-consistent 2nd order approximation for the self-energy used here. It is not merely an expansion in a small parameter and it only includes a subset of all possible higher order diagrams in the self-energy. However, here we try to motivate the idea of the approximation by making a connection to the quantum Boltzmann equation (derivation).

First we take the usual route of deriving a quantum Boltzmann equation from the Dyson equation, see e.g. [142] or [131, 133, 143, 134]. However, the point-like interaction gives a sharp variation in space and therefore the derivation cannot be completed, so we actually cannot use a Boltzmann equation here (as noted in section 6.2). However, we will see how the self-consistent second-order approximation is like using a full collision integral instead of using $f_{\text{R/L}}^0(\varepsilon_k)$ for the distribution functions in the collision integral as in the perturbative limit.

The derivation goes as follows: We begin by writing the contour ordered (1D) Dyson equation eq.(6.45) in differential form for any self-energy $\Sigma(xx', tt')$ (see [142])²⁷:

$$\left(i\partial_t + \frac{\hbar^2}{2m} \frac{d^2}{dx^2}\right) \mathcal{G}(xx', tt') = \delta(x - x')\delta(t - t') + \int_{\mathcal{C}} dt'' \int dx'' \Sigma(xx'', tt'') \mathcal{G}(x''x', t''t') \quad (6.119a)$$

and for $\mathcal{G} = \mathcal{G}_0 + \mathcal{G}\Sigma\mathcal{G}_0$ (neglecting indices and integrals) it is

$$\left(-i\partial_{t'} + \frac{\hbar^2}{2m} \frac{d^2}{dx'^2}\right) \mathcal{G}(xx', tt') = \delta(x - x')\delta(t - t') + \int_{\mathcal{C}} dt'' \int dx'' \mathcal{G}(xx'', tt'') \Sigma(x''x', t''t'). \quad (6.119b)$$

By subtracting eq.(6.119b) from eq.(6.119a) and taking the lesser component using the Langreth rules eq.(6.34), we get

$$\begin{aligned} \left(i\partial_t + i\partial_{t'} + \frac{\hbar^2}{2m} \frac{d^2}{dx^2} - \frac{\hbar^2}{2m} \frac{d^2}{dx'^2}\right) \mathcal{G}^<(xx', tt') = \\ \int_{-\infty}^{\infty} dt'' \int dx'' \left[\Sigma^r(xx'', tt'') \mathcal{G}^<(x''x', t''t') + \Sigma^<(xx'', tt'') \mathcal{G}^a(x''x', t''t') \right. \\ \left. - \mathcal{G}^r(xx'', tt'') \Sigma^<(x''x', t''t') - \mathcal{G}^<(xx'', tt'') \Sigma^a(x''x', t''t') \right]. \end{aligned} \quad (6.120)$$

Next we Fourier transform into frequency space using the translational invariance in time, so all functions only depend on the time differences, i.e.

$$\begin{aligned} \left(\frac{\hbar^2}{2m} \frac{d^2}{dx^2} - \frac{\hbar^2}{2m} \frac{d^2}{dx'^2}\right) \mathcal{G}^<(xx', \omega) = \int dx'' \left[\Sigma^r(xx'', \omega) \mathcal{G}^<(x''x', \omega) \right. \\ \left. + \Sigma^<(xx'', \omega) \mathcal{G}^a(x''x', \omega) - \mathcal{G}^r(xx'', \omega) \Sigma^<(x''x', \omega) - \mathcal{G}^<(xx'', \omega) \Sigma^a(x''x', \omega) \right]. \end{aligned} \quad (6.121)$$

Note that the term $i\partial_t + i\partial_{t'}$ cancels out due to the time translational invariance. So far the manipulations have been completely general, but now we use

²⁷Again we neglect a possible single-particle potential, which would just give an extra term to the kinetic energy on the left hand side of the equations.

that the self-energy is local due to the point-like interaction, i.e. $\Sigma(xx', \omega) = \Sigma(00, \omega)\delta(x)\delta(x')$, so eq.(6.121) becomes

$$\left(\frac{\hbar^2}{2m} \frac{d^2}{dx^2} - \frac{\hbar^2}{2m} \frac{d^2}{dx'^2}\right) \mathcal{G}^<(xx', \omega) = \left[\delta(x) \Sigma^r(00, \omega) \mathcal{G}^<(0x', \omega) + \delta(x) \Sigma^<(00, \omega) \mathcal{G}^a(0x', \omega) - \delta(x') \mathcal{G}^r(x0, \omega) \Sigma^<(00, \omega) - \delta(x') \mathcal{G}^<(x0, \omega) \Sigma^a(00, \omega) \right]. \quad (6.122)$$

The connection to the Boltzmann equation appears, because $\mathcal{G}^<$ is like a distribution function²⁸, since it is $\sim \langle \Psi^\dagger \Psi \rangle$. We take the limit $x = x'$, so

$$\left(\frac{\hbar^2}{2m} \frac{d^2}{dx^2} - \frac{\hbar^2}{2m} \frac{d^2}{dx'^2}\right) \mathcal{G}^<(xx', \omega) \Big|_{x=x'} = \delta(x) \times [\Sigma^r(00, \omega) \mathcal{G}^<(00, \omega) + \Sigma^<(00, \omega) \mathcal{G}^a(00, \omega) - \mathcal{G}^r(00, \omega) \Sigma^<(00, \omega) - \mathcal{G}^<(00, \omega) \Sigma^a(00, \omega)] \\ = \delta(x) \left[\{ \Sigma^r(00, \omega) - \Sigma^a(00, \omega) \} \mathcal{G}^<(00, \omega) + \Sigma^<(00, \omega) \{ \mathcal{G}^a(00, \omega) - \mathcal{G}^r(00, \omega) \} \right], \quad (6.123)$$

using the relation eq.(6.25) $\mathcal{G}^r - \mathcal{G}^a = \mathcal{G}^> - \mathcal{G}^<$ (and similar for Σ) we finally arrive at

$$\frac{\hbar^2}{2m} \left(\frac{d^2}{dx^2} - \frac{d^2}{dx'^2} \right) \mathcal{G}^<(xx', \omega) \Big|_{x=x'} = \delta(x) [\Sigma^>(00, \omega) \mathcal{G}^<(00, \omega) - \Sigma^<(00, \omega) \mathcal{G}^>(00, \omega)], \quad (6.124)$$

which only involves the local lesser Green's function and its derivatives.

Normally, to derive a (quantum) Boltzmann equation one would introduce sum and difference variables²⁹ $x_\pm = x \pm x'$ and then Fourier transform in $x - x'$ to obtain a momentum dependence. In this case, the right-hand side of eq.(6.124) would be the collision integral. The next step would be to assume slow variation of $x + x'$ to make the so-called gradient-approximation, after which the left-hand of eq.(6.122) would be the driving terms in the Boltzmann equation (i.e. the left-hand side of it, see e.g. chapter 3). See e.g. [142, 131, 133, 134] for details. However, due to the point-like interaction in the short point-like QPC, slow variation cannot be assumed and the derivation of the Boltzmann equation cannot go any further.

Even though eq.(6.124) cannot be made into a Boltzmann equation, we want to use it to motivate the self-consistent second order approximation using the right-hand side as a collision integral, i.e.

$$\mathcal{I}[\mathcal{G}] \equiv \delta(x) [\Sigma^>(00, \omega) \mathcal{G}^<(00, \omega) - \Sigma^<(00, \omega) \mathcal{G}^>(00, \omega)]. \quad (6.125)$$

²⁸Formally, one can for example introduce $F(xx', \omega)$ inspired by the fluctuation-dissipation theorem as $\mathcal{G}^<(xx', \omega) = iA(xx', \omega)F(xx', \omega)$ and $\mathcal{G}^<(xx', \omega) = -iA(xx', \omega)[1 - F(xx', \omega)]$, which is nothing but expressing one unknown function by another using $\mathcal{G}^< - \mathcal{G}^> = iA$. However, in equilibrium and $x = x' = 0$ this is the Fermi function and a generalization of the concept of a distribution function is present [131, chap.6]. Furthermore, the distribution function depends on both space and momentum, so a Fourier transform from $x - x'$ to k is needed, see e.g. [142, 131].

²⁹Also in time, if time invariance was not assumed.

The lesser components of the self-consistent 2nd order self-energy eq.(6.118) are found using the Langreth rule eq.(6.41) to be

$$\begin{aligned}\Sigma_{\text{sc}}^<(00, \omega) &= |V_0|^2 \int_{-\infty}^{\infty} d(t-t') e^{i\omega(t-t')} \mathcal{G}^>(00, t'-t) \mathcal{G}^<(00, t-t') \mathcal{G}^<(00, t-t') \\ &= |V_0|^2 \int_{-\infty}^{\infty} \frac{d\omega_1 d\omega_2 d\omega_3}{(2\pi)^2} \delta(\omega + \omega_1 - \omega_2 - \omega_3) \mathcal{G}^>(00, \omega_1) \mathcal{G}^<(00, \omega_2) \mathcal{G}^<(00, \omega_3),\end{aligned}$$

and similar for $\Sigma_{\text{sc}}^>(00, \omega)$ by interchanging $>$ and $<$. Inserting these into the collision integral $\mathcal{I}[\mathcal{G}]$ (and making the variable change $(\omega, \omega_1, \omega_2, \omega_3) \rightarrow (\omega_1, \omega_2, \omega_{1'}, \omega_{2'})$), we get

$$\begin{aligned}\mathcal{I}_{\text{sc}}[\mathcal{G}] &= \delta(x) |V_0|^2 \int_{-\infty}^{\infty} \frac{d\omega_2 d\omega_{1'} d\omega_{2'}}{(2\pi)^2} \left[\mathcal{G}^<(00, \omega_1) \mathcal{G}^<(00, \omega_2) \mathcal{G}^>(00, \omega_{1'}) \mathcal{G}^>(00, \omega_{2'}) \right. \\ &\quad \left. - \mathcal{G}^>(00, \omega_1) \mathcal{G}^>(00, \omega_2) \mathcal{G}^<(00, \omega_{1'}) \mathcal{G}^<(00, \omega_{2'}) \right] \delta(\omega_1 + \omega_2 - \omega_{1'} - \omega_{2'}). \quad (6.126)\end{aligned}$$

This is like a two-body collision integral in the Boltzmann approach with a Fermi Golden rule scattering rate (compare to eq.(3.7) with eq.(3.9) inserted), since the $\mathcal{G}^<$ is like the distribution function $\sim \langle \Psi^\dagger \Psi \rangle$ and $\mathcal{G}^>$ is like one minus the distribution function, $\sim \langle 1 - \Psi^\dagger \Psi \rangle$. The second order perturbative approach (of section 6.5.2) amounts to inserting the non-interacting Green's functions above and therefore $f_{\text{L/R}}^0$ as the distribution function (leading to a current correction in the form of a Boltzmann current correction to lowest order in the interaction, compare e.g. eq.(3.17) to eq.(6.84)). The self-consistent 2nd order approximation, on the other hand, uses full Green's functions, which in the Boltzmann picture is like using the full distribution function. Using this analogue, the following qualitative statement can be made: The self-consistent 2nd order approximation amounts to a simple (i.e. Boltzmann-like) way of letting the Fermi functions of the right and left leads equilibrate towards a common distribution in the QPC. This is the basic idea of the self-consistent 2nd order approximation used here.

6.7.3 The non-perturbative conductance and thermopower

Above we argued why the self-consistent second order approximation to the self-energy *in a sense* is like using the full Boltzmann equation. Next we show how to use it to find the conductance and thermopower by an iterative procedure.

The self-consistent equation for the local equilibrium spectral function

To find the current eq.(6.66) in the point-like interaction model with a single quadratic band, only the *local* spectral function $A(00, \omega)$ (i.e. $x = x' = 0$) is needed and hence it is the central object to find. The local retarded Green's function is

$$\mathcal{G}^r(00, \omega) \equiv \frac{1}{2} [B(00, \omega) - iA(00, \omega)] \quad (6.127)$$

written in terms of its real and imaginary part (A, B are both real functions). The real part of the non-interacting local retarded Green's function is zero for a quadratic band, i.e. $B_0(00, \omega) = 0$, see eq.(6.63). Therefore the real and imaginary part of the local Dyson equation (6.49) for the retarded Green's function is

$$A(00, \omega) = A_0(00, \omega) + \frac{A_0(00, \omega)}{2} \left[\text{Re}\Sigma^r(00, \omega)B(00, \omega) + \text{Im}\Sigma^r(00, \omega)A(00, \omega) \right], \quad (6.128a)$$

$$B(00, \omega) = \frac{A_0(00, \omega)}{2} \left[\text{Im}\Sigma^r(00, \omega)B(00, \omega) - \text{Re}\Sigma^r(00, \omega)A(00, \omega) \right]. \quad (6.128b)$$

Since we are only interested in $A(00, \omega)$, the second equation is used to eliminate $B(00, \omega)$ in the first one. From eq.(6.128b) $B(00, \omega)$ is

$$B(00, \omega) = -\frac{A_0(00, \omega)\text{Re}\Sigma^r(00, \omega)}{2 - A_0(00, \omega)\text{Im}\Sigma^r(00, \omega)}A(00, \omega), \quad (6.129)$$

and inserting this into eq.(6.128a), we find the following self-consistent equation for the local spectral function

$$A(00, \omega) = \frac{1 - \pi d(\omega)\text{Im}\Sigma^r(00, \omega)}{1 - 2\pi d(\omega)\text{Im}\Sigma^r(00, \omega) + [\pi d(\omega)\text{Re}\Sigma^r(00, \omega)]^2 + [\pi d(\omega)\text{Im}\Sigma^r(00, \omega)]^2}, \quad (6.130)$$

using that $A_0(00, \omega)$ is related to the density of states $d(\omega)$ as $A_0(00, \omega) = 2\pi d(\omega)$, see eq.(6.64).

In the general non-equilibrium case, the self-energy $\Sigma^r(00, \omega)$ will depend on the spectral function $A(00, \omega)$ as well as the other Green's functions and one needs the Dyson equation for the lesser and greater component as well, to find $A(00, \omega)$ from the coupled set of Dyson equations. However, to calculate the conductance and thermopower only the equilibrium spectral function $A_{\text{eq}}(00, \omega)$ is needed, as noted in eq.(6.68) and eq.(6.69). In equilibrium all the four components of the Green's function are dependent and related to the spectral function via the fluctuation-dissipation theorem as

$$\mathcal{G}_{\text{eq}}^<(00, \omega) = iA_{\text{eq}}(00, \omega)f^0(\omega), \quad (6.131a)$$

$$\mathcal{G}_{\text{eq}}^>(00, \omega) = -iA_{\text{eq}}(00, \omega)[1 - f^0(\omega)], \quad (6.131b)$$

$$\mathcal{G}_{\text{eq}}^r(00, \omega) = \int_{-\infty}^{\infty} \frac{d\omega'}{2\pi} \frac{A_{\text{eq}}(00, \omega')}{\omega - \omega' + i\eta}, \quad (6.131c)$$

$$\mathcal{G}_{\text{eq}}^a(00, \omega) = \int_{-\infty}^{\infty} \frac{d\omega'}{2\pi} \frac{A_{\text{eq}}(00, \omega')}{\omega - \omega' - i\eta}, \quad (6.131d)$$

where $\eta = 0^+$ and $f^0(\omega) = [1 + e^{(\omega - \varepsilon_F)/k_B T}]^{-1}$ is the Fermi function. These very useful relations are only valid in equilibrium and can be shown e.g. by using

the Lehmann representation [14, p.128-130]. Therefore to find the equilibrium spectral function only a single self-consistent equation is needed:

$$A_{\text{eq}}(00, \omega) = \frac{1 - \pi d(\omega) \text{Im} \Sigma_{\text{eq}}^r(00, \omega)}{1 - 2\pi d(\omega) \text{Im} \Sigma_{\text{eq}}^r(00, \omega) + [\pi d(\omega) \text{Re} \Sigma_{\text{eq}}^r(00, \omega)]^2 + [\pi d(\omega) \text{Im} \Sigma_{\text{eq}}^r(00, \omega)]^2}, \quad (6.132)$$

where the self-energy $\Sigma_{\text{eq}}^r(00, \omega)$ is a functional of $A_{\text{eq}}(00, \omega)$ only using eq.(6.131). For the self-consistent 2nd order approximation the self-energy in eq.(6.118) is used, i.e.

$$\begin{aligned} \Sigma_{\text{sc,eq}}^r(00, \omega) = & |V_0|^2 \int_{-\infty}^{\infty} \frac{d\omega_1 d\omega_2 d\omega_3}{(2\pi)^3} \frac{A_{\text{eq}}(00, \omega_1) A_{\text{eq}}(00, \omega_2) A_{\text{eq}}(00, \omega_3)}{(\omega + \omega_1 - \omega_2 - \omega_3) + i\eta} \\ & \times [f^0(\omega_1)(1 - f^0(\omega_2))(1 - f^0(\omega_3)) + (1 - f^0(\omega_1))f^0(\omega_2)f^0(\omega_3)], \end{aligned} \quad (6.133)$$

where eq.(6.77) was used replacing \mathcal{G}_0 by \mathcal{G} and then the fluctuation dissipation theorem eq.(6.131) is used. Now it is seen explicitly that eq.(6.132) involves only one unknown function $A_{\text{eq}}(00, \omega)$, which we use a numerical iteration scheme to get out.

The numerical iteration procedure

The iterative procedure is as follows: Make an initial guess for the spectral function $A_{\text{eq}}(00, \omega)$ and calculate $\Sigma_{\text{sc,eq}}^r(00, \omega)$ and in terms the left-hand side of eq.(6.132). This gives a new guess for the spectral function (the right-hand side of eq.(6.132)), which is then used to calculate $\Sigma_{\text{sc,eq}}^r(00, \omega)$ and the left-hand side of eq.(6.132), leading to yet another guess of the spectral function. This procedure is then iterated until the same spectral function is being put in as the one coming out, since this means that it solves eq.(6.132) and hence it is the correct spectral function.

There is no guarantee that this procedure converges, but using the non-interacting spectral function $A_0(00, \omega) = 2\pi d(\omega)$ as the initial guess, we found that it does converge for the parameters used. Furthermore, in practices, one needs a way to decide, when the iteration procedure has converged. To this end, the conductance eq.(6.68) or thermopower eq.(6.69) is calculated in each iteration step and compared to the previous one, and if the difference is small enough (e.g. $0.01 \times 2e^2/h$ for G), then the iteration has converged.

Another practical information is that the full Green's functions $\mathcal{G}^i(00, \omega)$ for $i = r, a, \geq$ are zero for $\omega < 0$, since $\mathcal{G}_0^r(00, \omega) \propto A(00, \omega) = 2\pi d(\omega) \propto \theta(\omega)$.

Furthermore, numerically it is rather heavy to calculate a three dimensional integral as in eq.(6.133). Therefore $\Sigma_{\text{sc,eq}}^r(00, \omega)$ is not calculated numerically directly by using eq.(6.133), but instead by using $\mathcal{G}_{\text{eq}}^<(00, \omega) = iA_{\text{eq}}(00, \omega)f^0(\omega)$ and $\mathcal{G}_{\text{eq}}^>(00, \omega) = -iA_{\text{eq}}(00, \omega)[1 - f^0(\omega)]$ and then by Fourier transforming $\mathcal{G}_{\text{eq}}^{\geq}(00, \omega)$

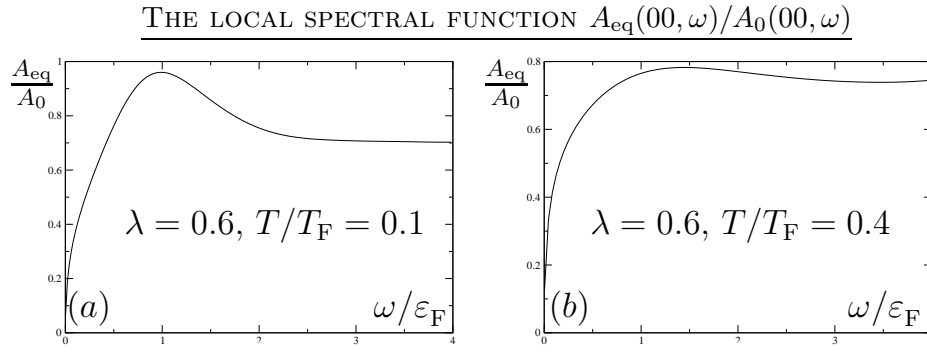


Figure 6.8: The ratio of the spectral function $A_{\text{eq}}(00, \omega)$ over the non-interacting one $A_0(00, \omega)$ for the self-consistent 2nd order approach for two values of the interaction strength λ and temperature T/T_F .

to the time domain one has

$$\Sigma_{\text{sc,eq}}^r(00, \omega) = \quad (6.134)$$

$$|V_0|^2 \int_0^\infty dt e^{i\omega t} [\mathcal{G}_{\text{eq}}^<(00, -t) \mathcal{G}_{\text{eq}}^>(00, t) \mathcal{G}_{\text{eq}}^>(00, t) - \mathcal{G}_{\text{eq}}^>(00, -t) \mathcal{G}_{\text{eq}}^<(00, t) \mathcal{G}_{\text{eq}}^<(00, t)],$$

which all are operations only involving a single integration - numerically a much simpler task.

It should be emphasized that our collaborator on paper IV Reinhold Egger did the actually implementation of the iterative scheme.

Analysis of the conductance and thermopower results

The iterative scheme was used numerically to find $A_{\text{eq}}(00, \omega)$ and from this the conductance and thermopower by using eq.(6.68) and (6.69), respectively as described above.

In the calculation, there are two parameters present: The temperature T and the interaction V_0 , which are both measured in units of the Fermi energy ε_F . We introduce the dimensionless interaction strength λ as

$$\lambda \equiv \frac{m|V_0|}{2\pi^{3/2}\hbar^2} = \frac{1}{4\pi^{3/2}} \frac{|V_0|k_F^2}{\varepsilon_F}. \quad (6.135)$$

For the parameters used in the rough estimate on page 91 the interaction strength λ is ~ 0.9 , i.e. λ is of order 1 or so. In the numerical calculation, we use $\lambda = 0.3$ (orange), 0.6 (olive), 0.8 (green), 1.0 (blue) and 2.0 (red). The numerical results for the conductance using the self-consistent 2nd order approximation for the self-energy are seen on figure 6.9, where each dot requires a self-consistent calculation. Each self-consistent calculation gives a local spectral function and

THE CONDUCTANCE IN THE 2ND ORDER SELF-CONSISTENT APPROXIMATION

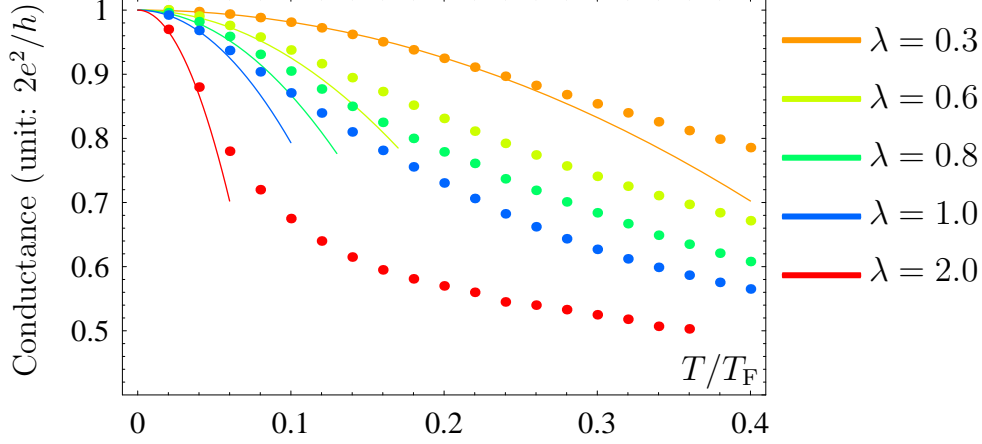


Figure 6.9: The conductance G (in units of $2e^2/h$) versus temperature T/T_F using the self-consistent 2nd order approximation for the self-energy eq.(6.118). The dots are the results of the numerical calculation for various values of the dimensionless interaction strength $\lambda = \frac{mV_0}{2\pi^{3/2}\hbar^2}$. The full lines are the low-temperature perturbative conductance to second order in the interaction, i.e. $G = \frac{2e^2}{h} \left(1 - \frac{2\pi^3}{3} \lambda^2 (T/T_F)^2\right)$.

two examples are seen in figure 6.8. In figure 6.9, the low-temperature perturbative result $G = \frac{2e^2}{h} \left[1 - \frac{2\pi^3}{3} \lambda^2 (T/T_F)^2\right]$ is also shown as full lines for comparison. The agreement between the two is good for low temperatures as expected. Note that for $\lambda = 0.3$ almost all the low temperature regime is well described by the perturbative approach, whereas for $\lambda = 2.0$ this is certainly not the case. The general trend in figure 6.9 (for various values of λ) is that *the perturbative result overestimates the interaction conductance correction for temperatures outside the perturbative regime, i.e. the corrections tends to flatten out*. Moreover, the conductance curves suggest that G saturates at temperatures beyond the perturbative regime to something like $\sim e^2/h$, however, it is hard to tell *if* the conductance really saturates or not³⁰.

The numerical iteration procedure is harder to make converge for higher values of λ and therefore calculation for $\lambda > 2$ has not been performed. The iterative calculation for $\lambda = 2$ is also very difficult to make converge and that is why not more values between $\lambda = 1$ and $\lambda = 2$ have been calculated.

In order to connect with experiments, the numerical calculations are fitted to

³⁰Note that the calculation is made in the regime $0 \leq T/T_F < 0.4$, and the non-interacting conductance is $G^{(0)}(T) = \frac{2e^2}{h} [1 + e^{-T_F/T}]^{-1}$, so a small non-interacting smearing of the conductance is present in this regime, e.g. $G^{(0)}(T/T_F = 0.3) = 0.97 \times \frac{2e^2}{h}$ and $G^{(0)}(T/T_F = 0.4) = 0.92 \times \frac{2e^2}{h}$. The non-interacting conductance saturates at e^2/h , but at a scale of order (a few) T_F .

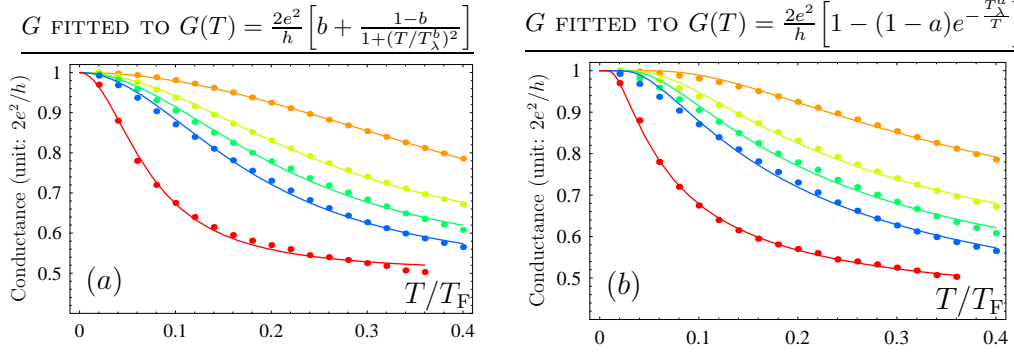


Figure 6.10: The conductance G (in units of $2e^2/h$) versus temperature T/T_F for the self-consistent 2nd order approximation (dots) and fitted (full lines) to an activation law eq.(6.136a) in (b) and to eq.(6.136b) in (a). The colors correspond to different values of the interaction strength $\lambda = 0.3$ (orange), 0.6 (olive), 0.8 (green), 1.0 (blue) and 2.0 (red). The fit parameters in eq.(6.136) are found in table 6.1. (Note that using two fit-parameters it is an easy task to fit these soft curves.)

the following three different forms:

$$G_a(T) = \frac{2e^2}{h} [1 - (1-a)e^{-T_\lambda^a/T}], \quad (\text{see fig.6.10(b)}) \quad (6.136a)$$

$$G_b(T) = \frac{2e^2}{h} \left[b + \frac{1-b}{1 + (T/T_\lambda^b)^2} \right], \quad (\text{see fig.6.10(a)}) \quad (6.136b)$$

$$G_c(T) = \frac{2e^2}{h} [c + (1-c)G^{\text{Kondo}}(T)], \quad (\text{see fig.6.11}), \quad (6.136c)$$

where the $G^{\text{Kondo}}(T)$ is the phenomenologically Kondo conductance formula (for e.g. quantum dots) given by (see e.g. p. 22 for a description)

$$G^{\text{Kondo}}(T) = \left(\frac{1}{1 + (2^{1/s} - 1)(T/T_K^c)^2} \right)^s, \quad (\text{with } s = 0.22). \quad (6.137)$$

All the fit forms are $2e^2/h$ for $T = 0$ and goes to a , b and c , respectively, for $T \rightarrow \infty$. Furthermore each fit form contains a temperature scale T_λ^a , T_λ^b and T_K^c , respectively. The fits are seen in figure 6.10 and 6.11 and the parameters are found in table 6.1. The three fitting forms all contain two fit-parameters and therefore not surprisingly, they all fit very well to the numerical calculations. However, the saturation values are somewhat different: $a \sim 0.4$, $b \sim 0.5$ and $c \sim 0.0$, and the largest fluctuations are seen in c . The temperature scales T_λ^a and T_λ^b are similar, whereas T_K^c differs and fluctuates more rapidly.

For comparison, we have also shown the temperature scale

$$T^* = \frac{1}{\lambda} \sqrt{\frac{3}{2\pi^3}} T_F \quad (6.138)$$

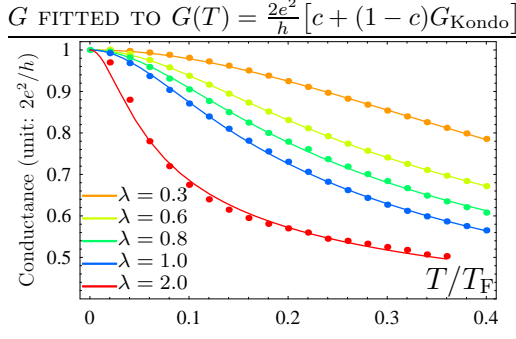


Figure 6.11: The conductance G (in units of $2e^2/h$) versus temperature T/T_F for the self-consistent 2nd order approximation (dots) and the fit to the Kondo-like form $G_c(T) = \frac{2e^2}{h} [c + (1 - c)G^{\text{Kondo}}(T)]$ (full line) for various values of the interaction λ .

| λ | T^*/T_F | T_λ^b/T_F | b | T_λ^a/T_F | a | T_K^c/T_F | c |
|-----------|-----------|-------------------|------|-------------------|------|-------------|-------|
| 0.3 | 0.7 | 0.51 | 0.43 | 0.40 | 0.43 | 1.77 | -0.40 |
| 0.6 | 0.4 | 0.26 | 0.54 | 0.24 | 0.41 | 0.80 | 0.034 |
| 0.8 | 0.3 | 0.22 | 0.51 | 0.20 | 0.38 | 0.62 | 0.027 |
| 1.0 | 0.2 | 0.19 | 0.48 | 0.17 | 0.35 | 0.50 | 0.030 |
| 2.0 | 0.1 | 0.07 | 0.50 | 0.06 | 0.42 | 0.15 | 0.23 |

Table 6.1: Temperature scales T_λ^a , T_λ^b , T_K^c and corresponding saturation values a , b and c , respectively, entering the best fits of the forms in eq.(6.136) to the numerical calculation. The temperature scale at which the problem becomes (very) non-perturbative T^* eq.(6.138) is also given for each λ .

at which the problem really becomes non-perturbative, i.e. defined as the temperature at which the perturbative low-temperature conductance becomes zero, see eq.(6.116). The temperature scales of the fit-functions eq.(6.136) are of the same order as T^* , but does not seem to be $\propto 1/\lambda$.

Next we try to motivate, why we used these fitting functions. The fit form $G_a(T)$ eq.(6.136a) is used, because it is use to fit the experimental data in Kristensen *et al.* [17]. This form is often called the activated temperature law due to the exponential dependence on temperature. Amazingly (or luckily?), we also find $a \sim 0.4$ as in the experiments [17, fig.8].

The form $G_b(T)$ eq.(6.136b) is used for the following reason: It can be found (with $b = 1/2$) by using an ansatz solution to the Boltzmann equation, where the distribution function at $x = 0$ is also a Fermi function. However, this ansatz solution to the Boltzmann equation also has the normalization factor problem (see section 6.2), since it gives $(T_\lambda^b)^2 \propto L/\mathcal{L}$, which does not make sense. However, it did inspire eq.(6.136b) and in the fits we found $b \sim 0.5$ as in the (wrong) ansatz solution.

The Kondo-like form $G_c(T)$ eq.(6.136c) has also been fitted in experiments [59], but there c is always set to $1/2$, because a conductance saturation for high temperature at e^2/h is preferred. If the parameter c is set to $1/2$, then it is still possible to fit the numerical calculation fairly well using the single parameter T_K^c . If we also use a logarithmic scale as in [59], then the fit looks as good as the one

SELF-CONSISTENT 2ND ORDER THERMOPOWER

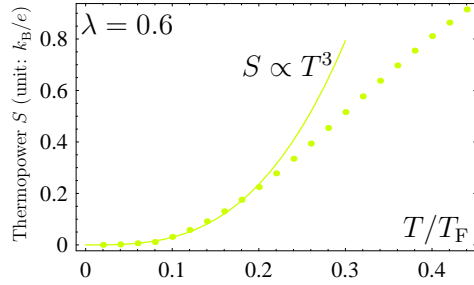


Figure 6.12: The thermopower S (in units of k_B/e) versus temperature T/T_F for the self-consistent 2nd order approximation (dots) and the low-temperature perturbative result $S = \frac{4\pi^5}{15}\lambda^2(T/T_F)^3$ (full line) for $\lambda = 0.6$.

show in Cronenwett *et al.*, see e.g. figure 1.5 p. 17.

To calculate the thermopower is a much harder numerical task than the conductance, because it requires numerically more precise knowledge of the spectral function. This can be understood by comparing eq.(6.68) for G and eq.(6.69) for S : The thermopower integral has an odd function around the Fermi energy $(\omega - \varepsilon_F)[-\partial_\omega f^0(\omega)]$, whereas the integrand in G only has a peak $[-\partial_\omega f^0(\omega)]$. However, this also makes the thermopower contain interesting information about the asymmetry of $A_{\text{eq}}(0, \omega)$ around ε_F , i.e. the electron-hole asymmetry. In figure 6.12, the thermopower is found numerically in the self-consistent 2nd order approximation. The low-temperature perturbative result $S \propto T^3$ is seen to fit well at low temperature, whereas the thermopower becomes more linear at higher temperature. The thermopower has not been fitted to any fit-functions, because so far, there are no experimental temperature dependence available.

Therefore in the non-perturbative regime $T \sim T^*$, we have found the conductance in the point-like interaction model to level off compared to the perturbative solution (using the self-consistent 2nd order approximation for the self-energy). Furthermore, the numerical calculation of the conductance shows a tendency to saturate at $\sim e^2/h$. However, more work on e.g. an analytical solution is needed to be certain of the high temperature saturation value.

6.7.4 Connection to the Anderson model: A new parameter regime

Next we turn back to the mapping between the model of a continuous 1D electron gas with interactions present in a single point $x = 0$, on one hand, and the Anderson model connected to semi-infinite tight-binding chains, on the other hand, see section 6.4.1. Here we are interested in establishing the non-perturbative regime discussed in section 6.7 in terms of the Anderson model parameters as often used to describe e.g. quantum dots [14, chap.10].

First of all, in terms of the Anderson model the coupling to the site $i = 0$ is not different from the inter-site hopping in the rest of the tight-binding chain, where it is given by t , see eq.(6.70). The so-called hybridization of the $i = 0$ site to the

leads, $\Gamma = 2\pi|t|d_t(\omega)$, is of order U , ($U \sim \Gamma$), because there is no localization at $i = 0$ in the model (i.e. no formation of a local moment). Furthermore, in order to have perfect conductance $2e^2/h$ at $T = 0$ the single-particle on-site ($i = 0$) energy ε_0 must be cancelled out such that³¹ $\varepsilon_0 = \varepsilon_F - \text{Re}[\Sigma^r(00, \omega)]$ at $T = 0$. This corresponds to having the (self-consistent) Hartree-Fock interactions included in the single-particle potential forming the QPC. Another energy scale in an Anderson model is the bandwidth D (which is $2|t|$ for a tight-binding chain). To translate between the two models, ε_F correspond to D and U to $V_0 k_F^2$. Therefore the temperature scale $k_B T^*$ correspond to D^2/U , so the non-perturbative regime of interest is (compare to eq.(6.117))

$$\frac{D^2}{U} \lesssim k_B T \ll D. \quad (6.139)$$

For this to be possible we need $U \gg D$, which is an interesting new parameter regime of the well-known Anderson model, which (to our knowledge) have not been studied before. It is our claim from the previous section, that the conductance is $\sim e^2/h$ in this regime.

Therefore, in the end, the described model of a QPC can also be understood as an Anderson model as in the papers on the Kondo effect in QPC's [92, 95] (see also p. 22). However, the model presented here is in a very different parameter regime, than the Kondo model, where $U \gg \Gamma$, $U, \Gamma \ll D$ and an on-site energy ε_0 near $-U/2$.

6.8 The noise due to non-momentum conserving interactions

The noise in the current also gives a valuable piece of information about the QPC. See p. 19 for a brief description of noise in QPC's. In this section, we briefly outline the perturbative results of the noise due to the non-momentum conserving interactions. *It is emphasized that our collaborator on paper IV Alessandro De Martino performed the actual noise calculation using a bosonization approach.*

To calculate the noise \mathcal{S} one needs to consider the zero-frequency component of the current-current correlation function, i.e. $\mathcal{S} = \int dt \langle \delta I_e(t) \delta I_e(0) \rangle$, where $\delta I_e(t)$ is the current fluctuation in time, $\delta I_e(t) = I_e(t) - \langle I_e \rangle$, and $\langle I_e \rangle$ is the average current. The following results are obtained using perturbation theory in the general interaction and linearized bands, so the different processes at the Fermi level has different amplitudes W_1 and W_2 as seen on figure 6.6. All calculations are to lowest order in the temperature and bias voltage, however, including the V^3 term in the current, since the shot-noise is a non-equilibrium phenomenon.

³¹This can be seen from the low-temperature limit of the Meir-Wingreen formula using that $\mathcal{G}^r(00, \omega) = [\omega - \varepsilon_0 - \Sigma^r(00, \omega) + i\eta]^{-1}$ and using that $\text{Im}\Sigma^r(00, \omega) = 0$ for $T = 0$ [145].

The non-equilibrium noise power of the transmitted current through the QPC is found to be

$$\mathcal{S}_T = \mathcal{S}_B + 4G_0 k_B T - 8k_B T \partial_V I_{bs}, \quad (6.140)$$

where \mathcal{S}_B is the noise in the backscattered current I_{bs} . The backscattering current I_{bs} is the lowest order interaction correction to the current through the QPC given in eq.(6.107) and (6.109) as

$$I = \frac{2e^2}{h} V - I_{bs} \quad (6.141)$$

with $I_{bs} = I_{bs1} + I_{bs2}$ and

$$I_{bs1} = \frac{1}{48} \frac{2e^2}{h} V \left(\frac{W_1 k_F^2}{\varepsilon_F} \right)^2 \left[\left(\frac{T}{T_F} \right)^2 + \frac{1}{4\pi^2} \left(\frac{eV}{\varepsilon_F} \right)^2 \right], \quad (6.142a)$$

$$I_{bs2} = \frac{1}{48} \frac{2e^2}{h} V \left(\frac{W_2 k_F^2}{\varepsilon_F} \right)^2 \left[\left(\frac{T}{T_F} \right)^2 + \frac{1}{\pi^2} \left(\frac{eV}{\varepsilon_F} \right)^2 \right], \quad (6.142b)$$

where I_{bs1} (I_{bs2}) is the current reduction due to interaction processes, where one (two) electrons change direction in the scattering process. Note that I_{bs} is defined positive for positive V . The noise in the backscattered current is found to be

$$\mathcal{S}_B(V, T) = 2e \left[2I_{bs2}(V, T) \coth \left(\frac{eV}{k_B T} \right) + I_{bs1}(V, T) \coth \left(\frac{eV}{2k_B T} \right) \right]. \quad (6.143)$$

This expression is the Schottky shot noise relation, if one takes into account that the charge of the backscattered current I_{bs2} is the double, see e.g. [106]³².

The experimental data for the noise near the 0.7 anomaly e.g. [74] shows a noise *reduction compared to the single-particle value* $\sim \mathcal{T}(1-\mathcal{T})$ (for transmission \mathcal{T} see eq.(1.32)). Here we want to know, if this is also the case in the present model for the perturbative noise calculated here. To perform this comparison in the experiment the thermal noise is subtracted from the noise leading to the so-called excess noise [74], i.e.

$$\mathcal{S}_I = \mathcal{S}_T - 4G(V, T) k_B T, \quad (6.144)$$

where $G(V, T) \equiv I(V, T)/V$ is the non-linear conductance. This part of the non-interacting single-particle noise is (see eq.(1.32) and [74, 76])

$$\mathcal{S}_I^{SP} = 2 \frac{2e^2}{h} \mathcal{R} \left[eV \coth \left(\frac{eV}{2k_B T} \right) - 2k_B T \right] + \mathcal{O}[\mathcal{R}^2], \quad (6.145)$$

³²For a model with an impurity and only the W_2 interaction process Median and Oreg [106] found the same relation, but in this case, the impurity made the noise, which is due to I_{bs1} here.

where \mathcal{R} is the reflection coefficient and we used that $\mathcal{R}(1 - \mathcal{R}) = (1 - \mathcal{T})\mathcal{T}$ and expanded to first order in \mathcal{R} , since it is small near the conductance anomaly. Now, the reflection \mathcal{R} used in the comparison between the single-particle noise and the noise due to interaction eq.(6.140) and (6.143) should be $\mathcal{R} = I_{bs}/(\frac{2e^2}{h}V)$, because it is the reflected current no matter if it is due to single-particle effects or not. Subtracting the excess noise due to interactions and the single-particle excess noise, we obtain by straightforward calculations

$$\frac{\mathcal{S}_I - \mathcal{S}_I^{SP}}{2(2e^2/h)eV(T/T_F)^2} = -2 \left[\frac{W_1^2 k_F^4}{48\pi^2 \varepsilon_F^2} \right] \frac{eV}{k_B T} + \left[\frac{W_2^2 k_F^4}{48\pi^2 \varepsilon_F^2} \right] h \left(\frac{eV}{k_B T} \right), \quad (6.146)$$

where

$$h(x) = -8x + (\pi^2 + x^2) \tanh(x/2). \quad (6.147)$$

The left-hand side of this expression is negative for $eV < 6.507 \times k_B T$ regardless of the values of W_1 and W_2 and hence we find a noise reduction compared to the non-interacting value as in the experiment. Note that in the experiment by Dicarolo *et al.* [74] $eV \lesssim 5k_B T$ is used.

Therefore (at least) qualitatively the perturbative noise calculation for non-momentum conserving interaction processes can explain the experimental noise reduction near the conductance anomaly.

6.9 Discussion and summary

In this chapter, we have studied the effect of electron-electron interactions on the transport properties of very short quantum wires (i.e. quantum point contacts) perfectly connected to the leads. The wires are so short, $L \sim k_F^{-1}$, that the translational symmetry is broken and hence the electron-electron interaction can happen *without* momentum conservation. Therefore two-particle interactions within a *single* mode can affect the current. Here we have restricted ourself to the situation of perfect transmission at zero temperature and magnetic field. Furthermore, the leads are considered to be non-interaction with each their own temperature and chemical potential.

By using perturbation theory to second order in the interaction in the Green's function approach, we found that the current is reduced compared to the non-interacting value by increasing the temperature T and/or voltage V , i.e.

$$\begin{aligned} \frac{I_e(V, T)}{V} \simeq \frac{2e^2}{h} \left\{ 1 - \frac{1}{48} \left[\left(\frac{W_1 k_F^2}{\varepsilon_F} \right)^2 + \left(\frac{W_2 k_F^2}{\varepsilon_F} \right)^2 \right] \left(\frac{T}{T_F} \right)^2 \right. \\ \left. - \frac{1}{48\pi^2} \left[\frac{1}{4} \left(\frac{W_1 k_F^2}{\varepsilon_F} \right)^2 + \left(\frac{W_2 k_F^2}{\varepsilon_F} \right)^2 \right] \left(\frac{eV}{\varepsilon_F} \right)^2 - \dots \right\} \quad (6.148) \end{aligned}$$

in the low temperature and/or voltage regime, i.e. $T/T_F \ll 1$ and $eV/\varepsilon_F \ll 1$. Here W_1 and W_2 are the scattering amplitudes to change the number of left and right movers by one or two, respectively. The thermopower to second order in the interaction and to lowest order in the temperature is found to be

$$S = \frac{k_B}{e} \frac{\pi^2}{120} \left[\left(\frac{W_1 k_F^2}{\varepsilon_F} \right)^2 + \left(\frac{W_2 k_F^2}{\varepsilon_F} \right)^2 \right] \left(\frac{T}{T_F} \right)^3, \quad \text{for } T/T_F \ll 1. \quad (6.149)$$

At low temperatures the interaction induced thermopower dominates the non-interacting value, since this is exponentially suppressed, $S^{(0)} \propto e^{-T_F/T}$. We also found the noise including the non-momentum conserving interactions and it is reduced compared to the non-interacting value.

In the case of a large applied magnetic field, $g\mu_B B \gg k_B T$, the interactions between electrons of equal spin become important. Here we found that the interaction contribution to the conductance and thermopower is suppressed by two extra powers of temperature compared to the $B = 0$ case, i.e. $G(B = \infty) - e^2/h \propto T^4$ and $S(B = \infty) \propto T^5$. Again second order perturbation theory was used to lowest order in temperature.

To describe the conductance versus temperature beyond the perturbative regime, $(W_i k_F^2/\varepsilon_F)^2 (T/T_F)^2 \ll 2e^2/h$, we derived a useful current formula for the point-like interaction model $V(x, x') = V_0 \delta(x) \delta(x')$. The point-like interaction is the simplest way to mimic the non-momentum conserving interactions (i.e. the $L \rightarrow 0$ limit). This non-perturbative current formula only depend on the local spectral function $A(0, \omega)$ (i.e. at $x = x' = 0$) and therefore the local self-energy (by the Dyson equation). To model the self-energy, the second order diagrams are made self-consistent (i.e. replasing non-interacting Green's function by interacting ones). We argued that this is like using the full distribution function in the collision integral of a Boltzmann equation and therefore a simple way to describe the relaxation of the right and left movers due to the interaction in the QPC beyond perturbation theory³³. Numerically, we found that the conductance versus temperature beyond the T^2 dependence flattens out to $\sim e^2/h$ by using the self-consistent 2nd order approach.

All the quantities found in this chapter are in qualitative agreement with the experimental observations on the 0.7 anomaly in quantum point contacts (see section 1.9). To recapitulate, we found: Conductance $G = I_e/V$ reduction for increasing temperature or bias from zero, thermopower enhancement for increasing temperature, suppression of the effect on the e^2/h plateau ($B = \infty$), noise reduction, and finally the conductance flattens out to $\sim e^2/h$ at higher temperature (but still below T_F). Furthermore, the interactions will be strongest in the beginning of the plateau due to the lack of screening for low density of the electrons.

³³However, one should note that due to the short interacting region a Boltzmann equation approach does not make sense here.

To make a quantitative agreement further studies are needed. A simple estimation of the interaction showed that it seems to be big enough to give the anomaly. However, to verify (or falsify) the explanation a better calculation of the interaction is a very important step forward. This should determine the magnitude of the non-momentum conserving interactions including e.g. a realistic geometry and screening. Another interesting direction is to try to find the non-perturbative saturation value of the conductance by analytical considerations or by other means. Yet another interesting direction is to include a single-particle potential barrier and study the interplay with the non-momentum conserving interactions to mimic the gate-voltage dependence better.

Appendix A:

A general current formula including interactions

In this appendix, we present a general current formula including interactions. It describes the situation of a general mesoscopic system connected to leads using scattering states and furthermore. The interaction is described in terms of the full (i.e. not the irreducible) self-energy and can be electron-electron interactions or interaction with phonons or impurities. In the end, we consider this formula in our perturbative setup for a fully open QPC.

This section is not included in the thesis, since it is work in progress, where the loose ends still need to be considered [146].

A.1 The Hamiltonian

We study a mesoscopic system connected to reservoirs with different chemical potentials and/or temperatures. We can e.g. use the scattering states as our basis set and the unperturbed Hamiltonian is given by

$$H_0 = \sum_{n\eta} \int dE \, \nu(E) c_{nE\eta}^\dagger c_{nE\eta} \equiv \sum_1 E_1 c_1^\dagger c_1, \quad (\text{A.1})$$

where the operator $c_{nE\eta}^\dagger$ creates an electron in the scattering state in direction η , incoming from channel n , and with energy E . Here ν is the density of states. We use the notation $1 = nE\eta$ and $1' = n'E'\eta'$ (spin is included in the n quantum number). (We can also see the states as k states, as in the previous calculations. However, both are included in the present derivation.) We include electron-electron interaction in the form

$$H_{\text{int}} = \frac{1}{2} \sum_{11'22'} V_{1'2',12} c_{1'}^\dagger c_{2'}^\dagger c_2 c_1, \quad (\text{A.2})$$

where

$$V_{1'2',12} = \int d\mathbf{r}_a \int d\mathbf{r}_b \, \psi_{1'}^*(\mathbf{r}_a) \psi_{2'}^*(\mathbf{r}_b) V(\mathbf{r}_a, \mathbf{r}_b) \psi_1(\mathbf{r}_a) \psi_2(\mathbf{r}_b). \quad (\text{A.3})$$

Here $\psi_i(\mathbf{r})$ is the wavefunction *including the spin part*. Further, we note that $[V_{1'2',12}]^* = V_{12,1'2'}$ and $V_{1'2',12} = V_{2'1',21}$, since $V(\mathbf{r}_a, \mathbf{r}_b) = V(\mathbf{r}_b, \mathbf{r}_a)$.

A.2 The current

We use the non-equilibrium Green's function formalism regarding the interaction terms as the perturbation. The current is given by ($e > 0$)

$$\begin{aligned} I_e &= -e \sum_{nn'\eta\eta'} \int dE dE' \nu^2 \langle n' E' \eta' | \hat{I}_x | n E \eta \rangle \langle c_{n' E' \eta'}^\dagger c_{n E \eta} \rangle \\ &= -e \sum_{11'} \langle 1' | \hat{I}_x | 1 \rangle \langle c_1^\dagger c_1 \rangle, \end{aligned} \quad (\text{A.4})$$

where \hat{I}_x is the current operator. This translates into a lesser Green's function as

$$I_e = ei \sum_{11'} \langle 1' | \hat{I}_x | 1 \rangle \mathcal{G}^<(11', tt) = -e \text{Im} \sum_{11'} \langle 1' | \hat{I}_x | 1 \rangle \mathcal{G}^<(11', tt). \quad (\text{A.5})$$

The calculation thus starts with the time-ordered electron Green's function (given by $\mathcal{G}(11', \tau\tau') = -i \langle T_c(c_1(\tau) c_1^\dagger(\tau')) \rangle$), where the time ordering is along the contour \mathcal{C} seen in figure 6.3. The time-ordered Green's function is written as (neglecting time and space integrations)

$$\mathcal{G} = \mathcal{G}_0 + \mathcal{G}_0 \Sigma \mathcal{G}_0 = \mathcal{G}_0 + \delta\mathcal{G}, \quad (\text{A.6})$$

where Σ is the *full* self-energy including all diagrams and not just the irreducible ones as in the Dyson equations $\mathcal{G} = \mathcal{G}_0 + \mathcal{G}_0 \Sigma^{\text{irr}} \mathcal{G}$ (see section 6.3.3). The second term thus gives the correction to the non-interacting current. For the lesser part we have in detail (in the diagonal basis for H_0)

$$\delta\mathcal{G}(11', \tau\tau') = \int_{\mathcal{C}} d\tau_1 d\tau_2 \mathcal{G}_0(1, \tau\tau_1) \Sigma(11', \tau_1\tau_2) \mathcal{G}_0(1', \tau_2\tau'). \quad (\text{A.7})$$

Using the Langreth rules eq.(6.37) and Fourier transforming, this becomes

$$\begin{aligned} \delta\mathcal{G}^<(11', \omega) &= \mathcal{G}_0^r(1, \omega) \Sigma^r(11', \omega) \mathcal{G}_0^<(1', \omega) + \mathcal{G}_0^r(1, \omega) \Sigma^<(11', \omega) \mathcal{G}_0^a(1', \omega) \\ &\quad + \mathcal{G}_0^<(1, \omega) \Sigma^a(11', \omega) \mathcal{G}_0^a(1', \omega). \end{aligned} \quad (\text{A.8})$$

The correction to the current is then

$$\delta I_e = -e \text{Im} \sum_{11'} \int \frac{d\omega}{2\pi} \langle 1' | \hat{I}_x | 1 \rangle \delta\mathcal{G}^<(11', \omega). \quad (\text{A.9})$$

Before proceeding, some useful relations for G_0

$$G_0^r(1, \omega) = \frac{1}{\omega - E_1 + i\eta}, \quad (\text{A.10a})$$

$$G_0^a(1, \omega) = \frac{1}{\omega - E_1 - i\eta}, \quad (\text{A.10b})$$

$$G_0^<(1, \omega) = 2\pi i \delta(\omega - E_1) n_1, \quad (\text{A.10c})$$

where n_1 is the occupation of the quantum number 1. Note that n_1 depends on the direction of i.e. on η , when the two reservoirs have different chemical potentials and/or temperatures. Some general relations for a lesser function are

$$[A^<(11', t, t')]^* = -A^<(1'1, t', t) \Rightarrow [A^<(11', \omega)]^* = -A^<(1'1, \omega), \quad (\text{A.11})$$

and for retarded functions

$$[A^r(11', t, t')]^* = A^a(1'1, t', t) \Rightarrow [A^r(11', \omega)]^* = A^a(1'1, \omega). \quad (\text{A.12})$$

These are used extensively in the following.

A.3 A general formula for the current

The current is now rewritten into an elastic and an inelastic part. Using the expression (A.10) the current is rewritten:

$$\begin{aligned} \delta I_e = -e \text{Im} \sum_{11'} \int \frac{d\omega}{2\pi} \langle 1' | \hat{I}_x | 1 \rangle \frac{1}{E_1 - E_{1'} - i\eta} \\ \times [-\Sigma^r(11', \omega) \mathcal{G}_0^<(1', \omega) + \mathcal{G}_0^<(1, \omega) \Sigma^a(11', \omega) + (\mathcal{G}_0^r(1, \omega) - \mathcal{G}_0^a(1', \omega)) \Sigma^<(11', \omega)]. \end{aligned} \quad (\text{A.13})$$

There are now two contributions corresponding the real and imaginary parts of $[E_1 - E_{1'} - i\eta]^{-1}$. The real part does not conserve current, since $\langle 1' | \hat{I}_x | 1 \rangle$ depends on x when $E_1 \neq E_{1'}$ and hence it should vanish for a conserving approximation of Σ . This has to be checked for every approximation used. The non-zero part is

$$\begin{aligned} \delta I_e = -e\pi \text{Re} \sum_{11'} \int \frac{d\omega}{2\pi} \langle 1' | \hat{I}_x | 1 \rangle \delta(E_1 - E_{1'}) \\ \times [-\Sigma^r(11', \omega) \mathcal{G}_0^<(1', \omega) + \mathcal{G}_0^<(1, \omega) \Sigma^a(11', \omega) + (\mathcal{G}_0^r(1, \omega) - \mathcal{G}_0^a(1', \omega)) \Sigma^<(11', \omega)] \\ = 2e\pi^2 \text{Im} \sum_{11'} \int \frac{d\omega}{2\pi} \langle 1' | \hat{I}_x | 1 \rangle \delta(E_1 - E_{1'}) \delta(\omega - E_1) \\ \times [-\Sigma^r(11', \omega) n_{1'} + n_1 \Sigma^a(11', \omega) - \Sigma^<(11', \omega)] \\ = 2e\pi^2 \text{Im} \sum_{11'} \int \frac{d\omega}{2\pi} \langle 1' | \hat{I}_x | 1 \rangle \delta(E_1 - E_{1'}) \delta(\omega - E_1) [-2\Sigma^r(11', \omega) n_{1'} - \Sigma^<(11', \omega)]. \end{aligned} \quad (\text{A.14})$$

Using $\Sigma^r(tt') = \theta(t - t') (\Sigma^>(tt') - \Sigma^<(tt'))$, we rewrite

$$\Sigma^r(\omega) = i \int \frac{d\omega'}{2\pi} \frac{\Sigma^>(\omega') - \Sigma^<(\omega')}{\omega - \omega' + i\eta} = \frac{1}{2} [\Sigma^>(\omega) - \Sigma^<(\omega)] + \frac{i}{2} \mathcal{H}_\omega(\Sigma^> - \Sigma^<), \quad (\text{A.15})$$

where \mathcal{H} is the Hilbert transform defined as

$$\mathcal{H}_x(f) = P \int \frac{dy}{\pi} \frac{f(y)}{x - y}. \quad (\text{A.16})$$

We then find

$$\delta I_e = e\pi \text{Im} \sum_{11'} \langle 1' | \hat{I}_x | 1 \rangle \delta(E_1 - E_{1'}) \quad (\text{A.17})$$

$$\times \left[-\Sigma^<(11', E_1)(1 - n_{1'}) - \Sigma^>(11', E_1)n_{1'} + \frac{i}{2} \mathcal{H}_{E_1}[\Sigma^>(11') - \Sigma^<(11')](n_1 - n_{1'}) \right].$$

The last part can be interpreted as an elastic term (i.e. correction to the first order Hartree-Fock term), whereas the first part is inelastic, which we concentrate on here:

$$\delta I_{\text{inelas}} = -e\pi \text{Im} \sum_{11'} \langle 1' | \hat{I}_x | 1 \rangle \delta(E_1 - E_{1'}) [\Sigma^<(11', E_1)(1 - n_{1'}) + \Sigma^>(11', E_1)n_{1'}]. \quad (\text{A.18})$$

Note that this expression has a form of a scattering in and out of some states, like a impurity collision integral, where the self-energy takes the role of a distribution-like function.

A.4 Electron-electron interactions for a general basis and interaction

In this section, we find the inelastic current eq.(A.18) to second order in the interaction for a general electron-electron interaction $V_{1'2',12}$ and for a general basis of quantum states.

The full second order self-energy is the same as the irreducible second order self-energy, even though this is not generally the case. Note that we do not include diagrams that contribute to the self-consistent Hartree-Fock potential. The bubble diagram self-energy seen on figure A.1 is

$$\Sigma_B(11', \tau\tau') = i^2 \sum_2 \mathcal{G}_0(2, \tau\tau') B(11'2, \tau\tau'), \quad (\text{A.19})$$

where B is the bubble (or loop) in figure A.1(left):

$$B(11'2, \tau\tau') = - \sum_{34} V_{24,1'3} V_{13,24} \mathcal{G}_0(3, \tau'\tau) \mathcal{G}_0(4, \tau\tau'). \quad (\text{A.20})$$

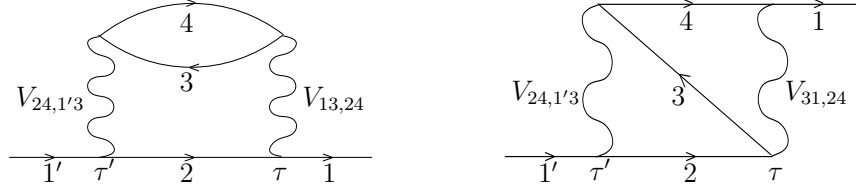


Figure A.1: The bubble diagram (left) and the zigzag diagram (right) for the self energy. Note that the external legs (i.e. $\mathcal{G}_0(1), \mathcal{G}_0(1')$) also are included.

Thus using the Langreth rules of a product of functions and Fourier transforming the lesser component becomes

$$\begin{aligned}
 \Sigma_B^<(11', \omega) &= - \sum_2 \int \frac{d\omega'}{2\pi} \mathcal{G}_0^<(2, \omega - \omega') B^<(11'2, \omega'), \\
 &= -i \sum_2 n_2 B^<(11'2, \omega - E_2), \\
 &= i \sum_2 n_2 \int \frac{d\omega'}{2\pi} \sum_{34} V_{24,1'3} V_{13,24} \mathcal{G}_0^>(3, \omega') \mathcal{G}_0^<(4, \omega - E_2 + \omega'), \\
 &= 2\pi i \sum_2 n_2 \sum_{34} V_{24,1'3} V_{13,24} (1 - n_3) n_4 \delta(\omega - E_2 + E_3 - E_4),
 \end{aligned} \tag{A.21a}$$

and the greater component is found to be

$$\Sigma_B^>(11', \omega) = -2\pi i \sum_{234} (1 - n_2)(1 - n_4) n_3 V_{24,1'3} V_{13,24} \delta(\omega - E_2 + E_3 - E_4). \tag{A.21b}$$

Similarly, the zigzag diagram figure A.1(right) yields

$$\Sigma_Z(11', \tau\tau') = - \sum_2 \mathcal{G}_0(2, \tau\tau') Z(11'2, \tau\tau'), \tag{A.22}$$

where Z is

$$Z(11'2, \tau\tau') = \sum_{34} V_{24,1'3} V_{31,24} \mathcal{G}_0(3, \tau'\tau) \mathcal{G}_0(4, \tau\tau'), \tag{A.23}$$

and $\Sigma_Z^>$ can be generated as in eq.(A.21) by interchanging the arguments of the second V (and multiplying by -1). When inserting these results into (A.18), we find (note that 1 and 1' are interchanged)

$$\begin{aligned}
 \delta I_{\text{inelas}}^{(2)} &= -2e\pi^2 \text{Re} \sum_{11'} \sum_{234} \langle 1 | \hat{I}_x | 1' \rangle \delta(E_1 - E_{1'}) V_{24,13} \{V_{1'3,24} - V_{31',24}\} \\
 &\quad \times [(1 - n_1) n_2 (1 - n_3) n_4 - n_1 (1 - n_2) n_3 (1 - n_4)] \delta(E_1 - E_2 + E_3 - E_4).
 \end{aligned} \tag{A.24}$$

Again the familiar form of a collision integral is observed as in the Boltzmann case.

A.4.1 The free-electron plane wave basis

Next we simplify the above formula to the case of k states as we used for the fully open QPC, but still keeping the interaction general.

Using plane wave quantum numbers correspond to

$$\sum_1 (\cdots) = \sum_{k_1 \sigma_1} (\cdots). \quad (\text{A.25})$$

The current matrix element is

$$\langle 1' | \hat{I}_x | 1 \rangle = \frac{1}{\mathcal{L}} \frac{\hbar}{2m} (k_{1'} + k_1) e^{i(k_1 - k_{1'})x} \delta_{\sigma_1 \sigma_{1'}} \quad (\text{A.26})$$

Note that we have included the factor of $1/\mathcal{L}$ in the matrix element to get the current and not the current density. For a quadratic band, we get

$$\delta(E_1 - E_{1'}) = \frac{2m}{\hbar^2} \left[\frac{\delta(k_1 - k_{1'})}{|2k_1|} + \underbrace{\frac{\delta(k_1 + k_{1'})}{|2k_1|}}_{\text{does not contribute}} \right], \quad (\text{A.27})$$

where the last delta function leads to zero current matrix element and therefore it does not contribute. The current change from eq.(A.24) is therefore:

$$\begin{aligned} \delta I_{\text{inelas}}^{(2)} = & -e\pi \text{Re} \sum_{k_2 k_4 k_1 k_3} \frac{k_1}{|k_1|} [(1 - n_1)n_2(1 - n_3)n_4 - n_1(1 - n_2)n_3(1 - n_4)] \\ & \times \delta(E_1 - E_2 + E_3 - E_4) \sum_{\sigma_1 \sigma_2 \sigma_3 \sigma_4} V_{24,13} \{V_{13,24} - V_{31,24}\}, \end{aligned} \quad (\text{A.28})$$

where $n_i = f_{\text{R/L}}^0(\varepsilon_{k_i})$ is the left (right) Fermi function of the lead for $k_i > 0$ ($k_i < 0$). By the variable change $(1324) \rightarrow (121'2')$ a more familiar form appears

$$\begin{aligned} \delta I_{\text{inelas}}^{(2)} = & -e\pi \text{Re} \sum_{k_1 k_2 k_{1'} k_{2'}} \frac{k_1}{|k_1|} [(1 - n_1)(1 - n_2)n_{1'}n_{2'} - (1 - n_{1'})(1 - n_{2'})n_1n_2] \\ & \times \delta(E_1 + E_2 - E_{1'} - E_{2'}) \sum_{\sigma_1 \sigma_2 \sigma_{1'} \sigma_{2'}} V_{1'2',12} \{V_{12,1'2'} - V_{21,1'2'}\}. \end{aligned} \quad (\text{A.29})$$

Note that the zigzag diagram corresponds to an exchange term in the interaction. This relation is useful in our situation, since it allows for a perturbative calculation for a general interaction.

Note that in the simple case of a contact interaction $V(x, x') = V_0 \delta(x) \delta(x')$, so $V_{1'2',12} = \frac{V_0}{\mathcal{L}^2} \delta_{\sigma_1 \sigma_{1'}} \delta_{\sigma_2 \sigma_{2'}}$, then we obtain the result in eq.(6.84) as expected.

Paper I

Anders Mathias Lunde and Karsten Flensberg:

On the Mott formula for thermopower of non-interactions electrons in quantum point contacts

Journal of Physics: Condensed Matter **17**, 3879 (2005).

Errata:

1. The overall sign of eq.(3) should be changed.
2. The signs in front of the second and third terms in Eq.(4) are wrong, it should read:

$$f_i^0(\varepsilon) \simeq f^0(\varepsilon) - \partial_\varepsilon f^0(\varepsilon)(\mu_i - \mu) - (\varepsilon - \mu) \partial_\varepsilon f^0(\varepsilon) \frac{T_i - T}{T}. \quad (4)$$

3. Just above eq.(4) the definition of ΔT should be $\Delta T = T_R - T_L$.
4. In eq.(9) a factor of $2e^2/h$ is missing.

None of these misprints change the conclusions nor other equations.

On the Mott formula for the thermopower of non-interacting electrons in quantum point contacts

Anders Mathias Lunde and Karsten Flensberg

Niels Bohr Institute, University of Copenhagen, DK-2100 Copenhagen, Denmark

E-mail: lunan@fys.ku.dk

Received 12 April 2005

Published 10 June 2005

Online at stacks.iop.org/JPhysCM/17/3879

Abstract

We calculate the linear response thermopower S of a quantum point contact using the Landauer formula and therefore assume non-interacting electrons. The purpose of the paper is to compare analytically and numerically the linear thermopower S of non-interacting electrons to the low-temperature approximation, $S^{(1)} = (\pi^2/3e)k_B^2 T \partial_\mu [\ln G(\mu, T = 0)]$, and the so-called Mott expression, $S^M = (\pi^2/3e)k_B^2 T \partial_\mu [\ln G(\mu, T)]$, where $G(\mu, T)$ is the (temperature-dependent) conductance. This comparison is important, since the Mott formula is often used to detect deviations from single-particle behaviour in the thermopower of a point contact.

1. Introduction

A narrow constriction in for example a two-dimensional electron gas makes a small channel between two electron reservoirs. This constriction is called a quantum point contact [1]. The width of the channel can be controlled by a gate voltage, and by applying a small bias the phenomenon of quantized conductance as a function of the width (i.e. gate voltage) is observed at low temperatures [2]. This quantization is due to the wave nature of the electronic transport through the short ballistic point contact. Experimentally [3–7], it is also possible to heat up one of the sides of the point contact, thereby producing a temperature difference ΔT across the contact, which in turn gives an electric current (and a heat current) through the point contact. By applying a bias V in the opposite direction to the temperature difference ΔT , the two contributions to the electric current I can be made to cancel, which defines the thermopower S as

$$S = - \lim_{\Delta T \rightarrow 0} \left. \frac{V}{\Delta T} \right|_{I=0}. \quad (1)$$

For a quantum point contact, the thermopower as a function of gate voltage has a peak every time the conductance plateau changes from one subband of the transverse quantization to the next [5, 8].

In order to compare experiment and theory for the thermopower of a point contact, the so-called Mott formula,

$$S^M \propto \partial_{V_g} [\ln G(V_g, T)], \quad (2)$$

is often a valuable tool, because by differentiating the experimentally found conductance $G(V_g, T)$ with respect to the gate voltage V_g one can see if there is more information in the thermopower than in the conductance. This additional information could for example be many-body effects [7], since S^M is an approximation to the single-particle thermopower. Note that this approximation is independent of the specific form of the transmission $\mathcal{T}(\varepsilon)$ through the point contact. It is the purpose of this paper to determine the validity of the Mott approximation S^M , and thereby decide if it is really deviations from single-particle behaviour the experiments [6, 7, 9] reveal or rather artefacts of this approximation.

2. Thermopower from the Landauer formula

For the sake of completeness, we begin by deriving the single-particle thermopower formula in linear response to the applied bias V and temperature difference ΔT . The current through a ballistic point contact is found from the Landauer formula [10, p 111, equation (7.30)]:

$$I = \frac{2e}{h} \int_0^\infty d\varepsilon \mathcal{T}(\varepsilon) [f_L^0(\varepsilon) - f_R^0(\varepsilon)], \quad (3)$$

where $\mathcal{T}(\varepsilon)$ is the transmission and $f_i^0(\varepsilon)$ is the Fermi function for the right/left ($i = R, L$) lead. The Landauer formula assumes non-interacting electrons and therefore so will the derived thermopower formula. When a small bias $V = (\mu_L - \mu_R)/(-e)$ and temperature difference $\Delta T = T_L - T_R$ are applied, we can expand the distribution functions around μ , T as ($|\Delta T|/T \ll 1$ and $|eV| \ll \mu$):

$$f_i^0(\varepsilon) \simeq f^0(\varepsilon) - \partial_\varepsilon f^0(\varepsilon)(\mu - \mu_i) - (\varepsilon - \mu) \partial_\varepsilon f^0(\varepsilon) \frac{T - T_i}{T}, \quad (4)$$

where $f^0(\varepsilon)$ is the Fermi function with the equilibrium chemical potential μ and temperature T and $i = L, R$. To obtain the thermopower equation (1) we insert the distribution functions in equation (3), set it equal to zero and obtain

$$S(\mu, T) = \frac{1}{eT} \frac{\int_0^\infty d\varepsilon \mathcal{T}(\varepsilon)(\varepsilon - \mu)[- \partial_\varepsilon f^0(\varepsilon)]}{\int_0^\infty d\varepsilon \mathcal{T}(\varepsilon)[- \partial_\varepsilon f^0(\varepsilon)]}, \quad (5)$$

which is our exact single-particle formula.

3. Approximations to the thermopower and their validity

3.1. The low-temperature (first-order) approximation

For $T = 0$ we have $-\partial_\varepsilon f^0(\varepsilon) = \delta(\varepsilon - \mu)$, so the numerator in equation (5) is zero, i.e. $S(\mu, T = 0) = 0$. For temperatures $k_B T$ much lower than the scale of variation of $\mathcal{T}(\varepsilon)$ and $k_B T \ll \mu$, we can expand $\mathcal{T}(\varepsilon)$ around μ to first order (i.e. a Sommerfeld expansion) to obtain

$$S^{(1)}(\mu, T) = \frac{\pi^2}{3} \frac{k_B}{e} k_B T \frac{1}{\mathcal{T}(\mu)} \frac{\partial \mathcal{T}(\mu)}{\partial \varepsilon} = \frac{\pi^2}{3} \frac{k_B}{e} k_B T \frac{1}{G(\mu, T = 0)} \frac{\partial G(\mu, T = 0)}{\partial \mu}, \quad (6)$$

where $G(\mu, T = 0)$ is the conductance for zero temperature, i.e. $G(\mu, T = 0) = \frac{2e^2}{h} \mathcal{T}(\mu)$.

3.2. The Mott approximation and analytical considerations of its validity

The Mott approximation¹ [6, 7] is

$$S^M(\mu, T) = \frac{\pi^2 k_B}{3e} k_B T \frac{1}{G(\mu, T)} \frac{\partial G(\mu, T)}{\partial \mu}, \quad (7)$$

where $G(\mu, T)$ is the temperature-dependent conductance

$$G(\mu, T) = \frac{2e^2}{h} \int_0^\infty d\varepsilon T(\varepsilon) [-\partial_\varepsilon f^0(\varepsilon)]. \quad (8)$$

The form of S^M stated in equation (2) assumes that the chemical potential and gate voltage are linear dependent. The Mott approximation to the single-particle thermopower equation (5) and its range of validity are not so obvious compared to the approximation of the first-order Sommerfeld expansion equation (6).

One way of comparing S from equation (5) and S^M is to differentiate equation (8) to obtain (assuming that $T(\varepsilon)$ is independent of μ):

$$S^M(\mu, T) = \frac{\pi^2 k_B}{3e} \frac{1}{G(\mu, T)} \int_0^\infty d\varepsilon T(\varepsilon) \tanh\left(\frac{\varepsilon - \mu}{2k_B T}\right) [-\partial_\varepsilon f^0(\varepsilon)], \quad (9)$$

i.e. by using the Mott formula we approximate $(\varepsilon - \mu)/k_B T$ in the integral by $(\pi^2/3) \tanh[(\varepsilon - \mu)/(2k_B T)]$.

To compare S and S^M in another way, we observe that for low temperatures $k_B T \ll \mu$ the Mott approximation S^M simplifies to the $S^{(1)}$ equation (6), because $G(\mu, T) \rightarrow \frac{2e^2}{h} T(\mu)$ for $T \rightarrow 0$, i.e. $S(\mu, T) = S^{(1)}(\mu, T) = S^M(\mu, T)$ for $k_B T/\mu \rightarrow 0$. Therefore, we compare S and S^M by expanding both quantities in orders of $k_B T$ and comparing order by order. Using

$$T(\varepsilon) = \sum_{n=0}^{\infty} \frac{1}{n!} \frac{\partial^n T(\mu)}{\partial \varepsilon^n} (\varepsilon - \mu)^n, \quad (10)$$

we can exactly rewrite equation (8):

$$\begin{aligned} G &= \frac{2e^2}{h} \sum_{n=0}^{\infty} \frac{1}{n!} \frac{\partial^n T(\mu)}{\partial \varepsilon^n} \int_0^\infty d\varepsilon (\varepsilon - \mu)^n [-\partial_\varepsilon f^0(\varepsilon)] \\ &= \frac{2e^2}{h} \sum_{n=0}^{\infty} \frac{1}{n!} \frac{\partial^n T(\mu)}{\partial \varepsilon^n} (k_B T)^n \mathfrak{B}_n\left(\frac{\mu}{k_B T}\right), \end{aligned} \quad (11)$$

where $y = (\varepsilon - \mu)/k_B T$

$$\mathfrak{B}_n\left(\frac{\mu}{k_B T}\right) \equiv \int_{-\frac{\mu}{k_B T}}^{\infty} dy \frac{y^n}{4 \cosh^2(y/2)} \rightarrow I_n \equiv \int_{-\infty}^{\infty} dy \frac{y^n}{4 \cosh^2(y/2)} \quad \text{for } k_B T \ll \mu, \quad (12)$$

where we note that $I_{2n+1} = 0$ for all integer n . Numerically, it turns out that $\mathfrak{B}_n(\mu/k_B T)/\mathfrak{B}_n(0) \simeq 0$ for $\mu \gtrsim (10 + n)k_B T$ as seen in figure 1. The integral I_n can be calculated, and the first values are

$$I_0 = 1, \quad I_2 = \frac{\pi^2}{3}, \quad I_4 = \frac{7\pi^4}{15}, \quad I_6 = \frac{31\pi^6}{21}, \quad I_8 = \frac{127\pi^8}{15}, \quad \dots \quad (13)$$

Using the approximation equation (12) we get

$$G(\mu, T) \simeq \frac{2e^2}{h} \sum_{n=0}^{\infty} \frac{1}{(2n)!} \frac{\partial^{2n} T(\mu)}{\partial \varepsilon^{2n}} I_{2n} (k_B T)^{2n}. \quad (14)$$

¹ In the early works by Mott and co-workers [11, 12] it was actually the first-order approximation equation (6) which was referred to as the Mott formula.

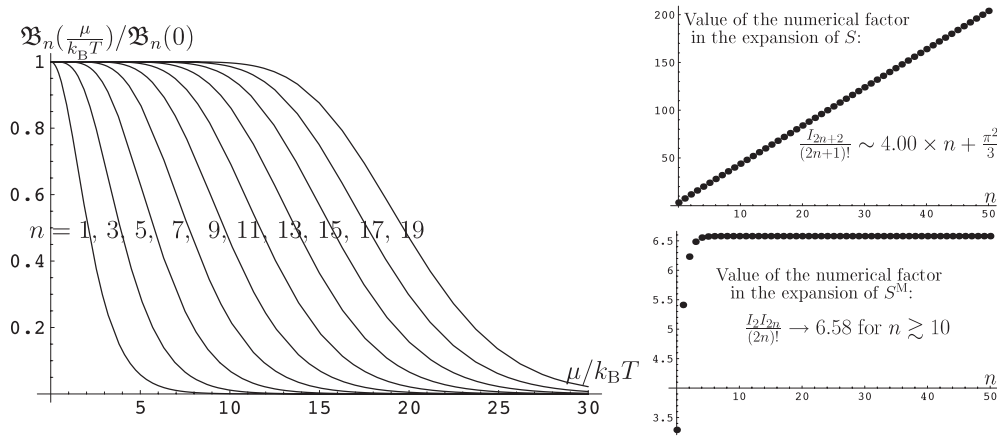


Figure 1. Left: the approximation in equation (12) is pictured for odd integer values of n from 1 (left) to 19 (right) in $\mathfrak{B}_n(\mu/k_B T)$. We note that $\mathfrak{B}_n(\mu/k_B T)/\mathfrak{B}_n(0) \simeq 0$ for $\mu \gtrsim (10+n)k_B T$. Right: the numerical values of the factors in the series expansions of the Mott approximation equation (15) (lower) and the exact linear single-particle series expansion equation (16) (upper).

This leads to a Mott approximation to the thermopower for low temperatures as

$$S^M(\mu, T) \simeq \frac{k_B}{e} \frac{1}{G(\mu, T)} \frac{2e^2}{h} \left[\sum_{n=0}^{\infty} \frac{I_2 I_{2n}}{(2n)!} \frac{\partial^{2n+1} \mathcal{T}(\mu)}{\partial \varepsilon^{2n+1}} (k_B T)^{2n+1} \right]. \quad (15)$$

Writing the exact single-particle thermopower S equation (5) by using equation (10) and the approximation of low temperatures equation (12), we get

$$S(\mu, T) \simeq \frac{k_B}{e} \frac{1}{G(\mu, T)} \frac{2e^2}{h} \left[\sum_{n=0}^{\infty} \frac{I_2 I_{2n+2}}{(2n+1)!} \frac{\partial^{2n+1} \mathcal{T}(\mu)}{\partial \varepsilon^{2n+1}} (k_B T)^{2n+1} \right]. \quad (16)$$

We see that both formulae only have odd terms in $k_B T$, and the first-order term is the same (which is $S^{(1)}$). However, none of the higher-order terms are the same, and in figure 1(right) the different numerical factors of the two series expansions are seen to behave very differently as the power of $k_B T$ grows:

$$\frac{I_2 I_{2n+2}}{(2n+1)!} \sim 4.00 \times n + \frac{\pi^2}{3} \quad \text{and} \quad \frac{I_2 I_{2n}}{(2n)!} \rightarrow 6.58 \quad \text{for } n \gtrsim 10. \quad (17)$$

So the Mott approximation is better the smaller the temperature compared to μ , but it is not a bad approximation for moderate temperatures (i.e. $k_B T$ comparable to other energy scales), as we shall see numerically. Note that if the approximation equation (12) is not valid, then we have all powers of $k_B T$.

4. Comparison of the approximations to the exact single-particle thermopower from numerical integration

We need a specific model for the transmission to do a numerical comparison of S from equation (5) to S^M and $S^{(1)}$. Using a harmonic potential in the point contact, i.e. a saddle point potential, a transmission in the form of a Fermi function can be derived [13]:

$$\mathcal{T}(\varepsilon) = \sum_{n=1}^{n_{\max}} \frac{1}{\exp(\frac{n\varepsilon_0 - \varepsilon}{\varepsilon_s}) + 1}, \quad (18)$$

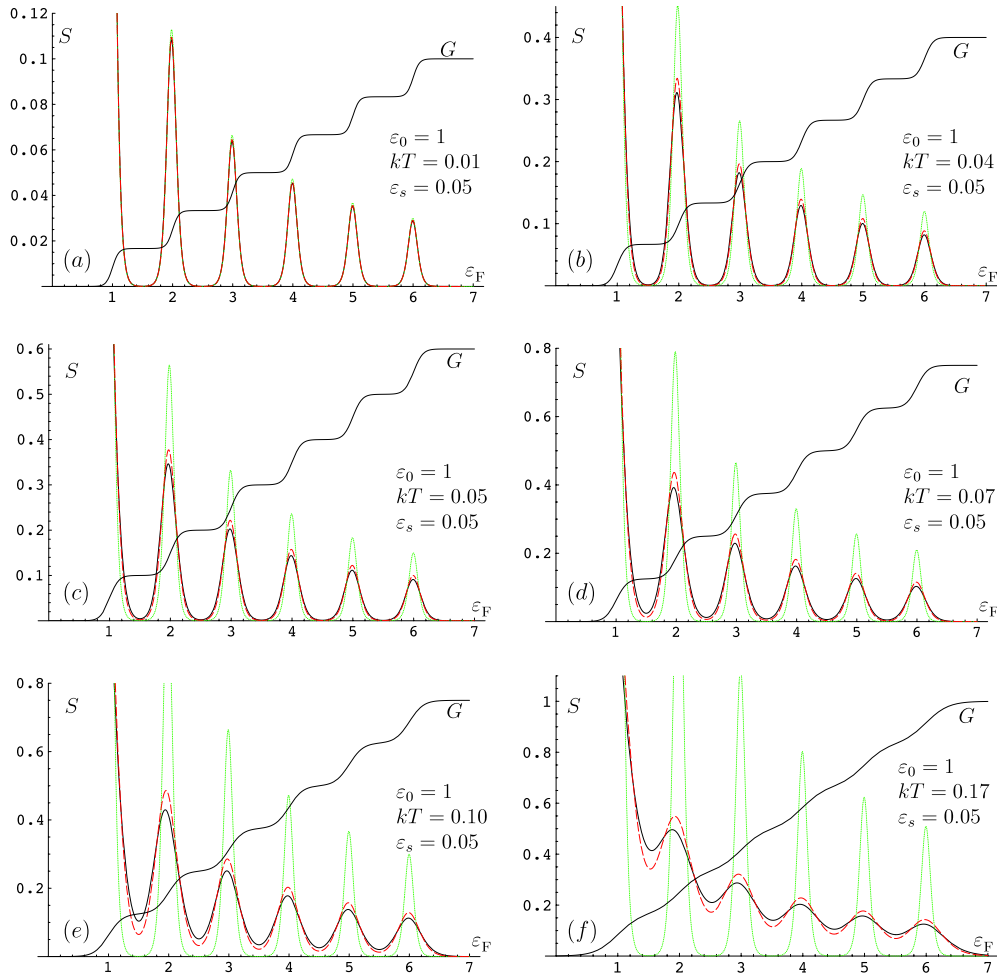


Figure 2. Thermopower S from numerical integration of equation (5) (black solid line), the Mott formula S^M equation (7) (red dashed line) and the first-order approximation $S^{(1)}$ equation (6) (green dotted line). From (a) to (f) the temperature is changed from the low-temperature regime $k_B T < \varepsilon_s$ to $k_B T > \varepsilon_s$ in small steps. The smearing of the transmission ε_s is kept constant, and note that $\varepsilon_s, k_B T \ll \varepsilon_0$ and $\varepsilon_s, k_B T \ll \varepsilon_F$ in all the graphs. The thermopowers are all in units of k_B/e , but note the different magnitudes of the thermopower from (a) to (f). The conductance G is shown (in arbitrary units) for comparison.

(This figure is in colour only in the electronic version)

where ε_s is the smearing of the transmission between the steps and ε_0 is the length of the steps (often called the subband spacing). In terms of the harmonic potential $V(x, y) = \text{const} - m\omega_x^2 x^2/2 + m\omega_y^2 y^2/2$, where x is along the channel, we have $\varepsilon_0 = \hbar\omega_y$ and $\varepsilon_s = \hbar\omega_x/(2\pi)$. Other functional forms of T have also been tested, but provided they have the same graphical structure (such as for example a tanh dependence) the same conclusions are obtained.

Three regimes of temperatures relevant to experiments are investigated numerically:

$$\begin{aligned}
 k_B T < \varepsilon_s \text{ (figure 2(a)),} \quad & k_B T \sim \varepsilon_s \text{ (figures 2(b)–(d))} \\
 \text{and} \quad & k_B T > \varepsilon_s \text{ (figures 2(e), (f)).}
 \end{aligned}
 \tag{19}$$

The thermopower S for the transmission model equation (18) is found from numerical integration of equation (5) and compared to the Mott approximation S^M equation (7) and the first-order approximation $S^{(1)}$ equation (6). In all three regimes, we have a staircase conductance, so $k_B T \ll \varepsilon_0$, and $G(\mu, T)$ is also shown in the figures (in arbitrary units) for comparison. Furthermore, $\mu = \varepsilon_F$ is of order ε_0 , so the approximation $k_B T \ll \varepsilon_F$ used for example in equation (12) is indeed very good. Note that all energies in the figures are given in units of the step length ε_0 .

The information obtained from the numerical calculations is the following. Figures 2(a), (b) show that for $k_B T$ being the lowest energy scale both approximations work very well, as expected from the analytical considerations. When the temperature becomes comparable to the smearing of the steps, $k_B T \sim \varepsilon_s$, the Culter–Mott formula works well and is better than the first-order approximation, as seen in figures 2(b)–(d). For $k_B T$ bigger than ε_s , the Mott approximation still works quite well, whereas $S^{(1)}$ is no longer a good approximation. The reason that the Mott approximation works well is found in the similar terms in the analytic temperature expansions equations (15) and (16). Note that as $k_B T$ increases both $S^{(1)}$ and S^M show a tendency to overestimate S at the peaks and underestimate it at the valleys.

In summary, we have found that the Mott approximation to the single-particle thermopower is a fairly good approximation provided the temperature is smaller than the Fermi level, but $k_B T$ can be both compatible and larger than the smearing of the transmission ε_s . However, to rule out any doubt one could use an experimental determination of $\mathcal{T}(\varepsilon)$ from the (very low-temperature) conductance to find the single-particle thermopower from equation (5), which could perhaps give an interesting comparison to the experimental result. Thereby one would obtain an even more convincing statement of deviations from single-particle behaviour in the thermopower.

Acknowledgment

We would like to thank James T Nicholls for sharing his experimental results with us and for discussions of the thermopower in point contacts in general.

References

- [1] Houten H V and Beenakker C 1996 *Phys. Today* (July) 22 for an minor review
- [2] van Wees B J *et al* 1988 *Phys. Rev. Lett.* **60** 848
- [3] Molenkamp L W *et al* 1990 *Phys. Rev. Lett.* **65** 1052
- [4] Molenkamp L W *et al* 1992 *Phys. Rev. Lett.* **68** 3765
- [5] van Houten H, Molenkamp L W, Beenakker C W J and Foxon C T 1992 *Semicond. Sci. Technol.* **7** B215
- [6] Appleyard N J *et al* 1998 *Phys. Rev. Lett.* **81** 3491
- [7] Appleyard N J *et al* 2000 *Phys. Rev. B* **62** 16275(R)
- [8] Streda P 1989 *J. Phys.: Condens. Matter* **1** 1025
- [9] Proskuryakov Y Y *et al* 2004 unpublished
- [10] Bruus H and Flensberg K 2004 Many-body quantum theory in condensed matter physics *Oxford Graduate Texts* 1st edn (New York: Oxford University Press)
- [11] Mott N F and Jones H 1936 *The Theory of the Properties of Metals and Alloys* 1st edn (Oxford: Clarendon)
- [12] Cutler M and Mott N F 1969 *Phys. Rev.* **181** 1336
- [13] Büttiker M 1990 *Phys. Rev. B* **41** 7906(R)

Paper II

Anders Mathias Lunde, Karsten Flensberg
and Leonid I. Glazman:

Interaction-induced resonance in conductance and thermopower of quantum wires

Physical Review Letters **97**, 256802 (2006).

Note:

For clearness, a normalization length and the length of the wire should have been introduced separately as in the thesis, see section 3.2.3, p. 39. However, the normalization length cancels out, so the distinction does not change the results.

Interaction-Induced Resonance in Conductance and Thermopower of Quantum Wires

Anders Mathias Lunde,^{1,2} Karsten Flensberg,¹ and Leonid I. Glazman²

¹Nano-Science Center, Niels Bohr Institute, University of Copenhagen, DK-2100 Copenhagen, Denmark

²William I. Fine Theoretical Physics Institute, University of Minnesota, Minneapolis, Minnesota 55455, USA

(Received 9 September 2006; published 20 December 2006)

We study the effect of electron-electron interaction on the transport properties of short clean quantum wires adiabatically connected to reservoirs. Interactions lead to resonances in a multichannel wire at particular values of the Fermi energy. We investigate in detail the resonance in a two-channel wire. The (negative) conductance correction peaks at the resonance, and decays exponentially as the Fermi energy is tuned away, the resonance width being given by the temperature. Likewise, the thermopower shows a characteristic structure, which is surprisingly well approximated by the so-called Mott formula. Finally, fourfold splitting of the resonance in a magnetic field provides a unique signature of the effect.

DOI: 10.1103/PhysRevLett.97.256802

PACS numbers: 73.21.Hb, 73.23.-b, 73.50.Lw

It is well established by now that ballistic motion of electrons in quantum wires results in the conductance quantization [1,2]. With the increase of wire width, the conductance increases by one quantum, $2e^2/h$, each time a new channel becomes available for the electron propagation. The experimental observation of the low-temperature conductance quantization was explained successfully within the model of noninteracting electrons [3]. In this model, corrections to the quantized conductance values come from the electron diffraction at the edges of the wire and from thermal broadening. At the conductance plateaus the latter corrections are exponentially small at low temperatures.

There is little reason to believe that the electron-electron interactions are weak in the studied quantum wires. Nevertheless, apart maybe from the so-called “0.7 anomaly”, they apparently do not show up in the experimental observations of quantized steps in the dependence of conductance on the wire width. The lack of the effect of interaction on the low-temperature conductance at the first plateau can be easily understood within the Luttinger liquid picture [4] and from the fact that the density-density interaction does not redistribute electrons between the left-moving and right-moving species.

Within the model of noninteracting electrons, the thermopower is related to the derivative of the electron transmission coefficient with respect to energy in the vicinity of the Fermi level [giving rise to the so-called Mott’s formula, see Eq. (3) below]. Therefore such a model predicts zero thermopower at the conductance plateaus in good agreement with experiments [5–7]. Again, interactions, if accounted for within the Luttinger liquid approximation, do not alter this result due to the particle-hole symmetry built into the approximation.

In this Letter, we find interaction-induced features in the electron transport of a multichannel wire. The features have the form of resonances in the dependence of conductance and thermopower on the Fermi energy (or, equivalently, on the gate voltage). The origin of the features is in the possibility of interaction-induced electron scattering

between the channels at some specific relations of the Fermi wave vectors of electrons in different channels. These relations are determined by energy and momentum conservation. The interchannel scattering events do not necessarily preserve the number of right and left movers. For example, in Fig. 1 a right and a left mover become two left movers. Since the number of right (left) movers is not conserved in this scattering event, it changes the particle current. We evaluate in detail the corrections to the conductance G and the thermopower S for a two-channel wire due to such processes.

We show that near the resonance point displayed in Fig. 1, the interaction-induced correction to the quantized value of conductance, $4e^2/h$, has the form

$$\delta G = \frac{4e^2}{h} \frac{L}{l_{ee}} \frac{k_B T}{\varepsilon_F} F_0 \left(\frac{\varepsilon_F - \varepsilon_R}{k_B T} \right), \quad (1)$$

where $\varepsilon_R = (9/8)\varepsilon_0$, with ε_0 being the difference of the quantized energies of the transverse motion corresponding to the two channels, 1 and 2, see Fig. 1; L is the wire length, and l_{ee} is the electron mean free path corresponding to the described type of scattering. We assume weak scattering, so the wire is sufficiently short, $L \ll (\varepsilon_F/k_B T)l_{ee}$, see Eq. (12) below. The dimensionless function $F_0(x)$ [given in Fig. 2 and Eq. (11)] is of the order of unity when $|x| \lesssim 1$ and falls off exponentially at large $|x|$. The wire width and thus the difference $\varepsilon_F - \varepsilon_R$ can be controlled electrostatically [1,2] by a gate voltage. The shape of the conductance dip can be easily understood from the process in Fig. 1. For an excess of right movers created by the bias voltage, it

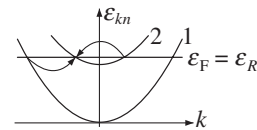


FIG. 1. An example of interchannel scattering event discussed in this Letter. This scattering event becomes possible at the Fermi level only if the ratio of the Fermi momenta of the two channels equals 3:1.

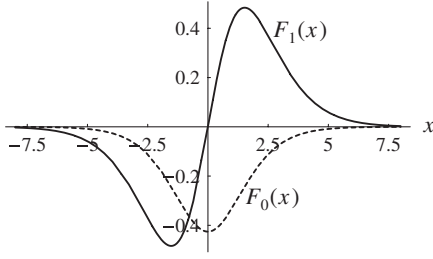


FIG. 2. The dimensionless scaling functions $F_0(x)$ and $F_1(x)$ entering the conductance correction Eq. (1) and the interaction-induced thermopower Eq. (2), respectively.

allows for a relaxation of the right movers into the left-moving species.

When the conductance is quantized at the value $4e^2/h$, the thermopower vanishes in *absence* of interactions. Accounting for the interactions, we find the leading contribution to the thermopower coefficient S for two open channels

$$S = \frac{k_B}{e} \frac{L}{l_{ee}} \frac{k_B T}{\varepsilon_F} F_1\left(\frac{\varepsilon_F - \varepsilon_R}{k_B T}\right). \quad (2)$$

The thermopower S is proportional to T at the maximum. Here S is conventionally defined by the relation $\Delta V = S\Delta T$, with ΔT and ΔV being, respectively, the temperature difference at the ends of the wire and the voltage caused by it. Again, the function $F_1(x)$ falls off exponentially at $|x| \gg 1$, see Fig. 2, and its analytical form is given by Eq. (11). Since S is the leading contribution, it is a direct measure of the interchannel interaction. Furthermore, since S and δG are functions of $(\varepsilon_F - \varepsilon_R)/k_B T$, measurements performed at different temperatures are predicted to collapse to the two curves of Fig. 2, when properly scaled. The shape of the curve $F_1(x)$ and, in particular, the sign change can be understood in terms of allowed interchannel relaxation processes, as explained and illustrated in Fig. 3.

A remarkably good estimate, $F_1(x) \approx (\pi^2/3)dF_0/dx$, can be obtained from the Mott's formula [8],

$$S^M = \frac{\pi^2}{3} \frac{k_B}{e} k_B T \frac{1}{G} \frac{dG}{d\varepsilon_F}, \quad (3)$$

which is expected to be a good approximation at low temperatures for noninteraction electrons [9]. There is no *a priori* reason for Mott's formula to work here, as we consider effects of inelastic scattering. We therefore stress that interaction effects can be seen in an experiment even without a manifesting violation of the Mott formula. (We note though, that violation of the Mott formula has been detected in experiments [7].)

The magnetic field introduces Zeeman splitting of the electron states. This, in turn, splits the single resonance for both conductance and thermopower into four resonances, see Fig. 4. Two of the resonances correspond to the transitions involving electrons with the *same* spins. With the increase of the magnetic field B , splitting in this doublet, in

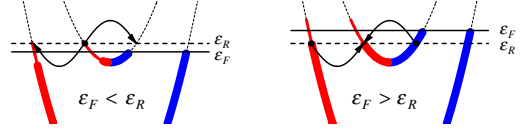


FIG. 3 (color online). Illustration of the dominant scattering events on either side of the resonance, $\varepsilon_F = \varepsilon_R$, for a finite-temperature difference across the wire. Here the right movers are cold (blue) and left movers are warmer (red); for simplicity we consider $\mu_L = \mu_R$ and $T = 0$ for right movers. Because of momentum and energy conservation the scattering has to take place close to ε_R (the dotted line). In the left panel, only scattering of electrons from warm to cold is possible and, consequently, an excess of right movers is created. In contrast, in the right panel this process is blocked by a filled Fermi sea and instead a scattering, where a right mover is transformed to a left mover prevails. This explains the sign change of thermopower seen in Fig. 2.

terms of ε_F , equals $g\mu_B B$ and coincides with the Zeeman splitting of the quantized steps in the conductance (here g and μ_B are the electron g factor in a quantum wire and Bohr magneton, respectively). The amplitude of the resonances involving electrons with the same spin is smaller than the one given by Eqs. (1) and (2) by a parameter $\propto (k_B T/\varepsilon_F)^2$. This suppression is a manifestation of the Pauli principle: at $T = 0$ the scattering process we consider would involve two electrons in the same orbital and spin state, see Fig. 1. The full form of the conductance correction and the thermopower in this doublet is given below in Eq. (16). The two remaining resonances form another doublet with splitting $g\mu_B B/2$ at small fields, see Eq. (14) and Fig. 4 for details. These resonances correspond to the transitions involving electrons with *opposite* spins and are therefore not suppressed by the Pauli principle; Eqs. (1) and (2) can be used for an estimate of the amplitude of these two resonances. However, as seen on Fig. 4, the position of the lower of these resonances approach the bottom of the spin-split band, $\varepsilon_0 + g\mu_B B/2$, which tends to mask the interaction-induced structure.

We thus find that the interaction-induced features in transport properties scale with the temperature as T or T^3 . They are associated with electron scattering at energies close to the Fermi level. This should be compared to the

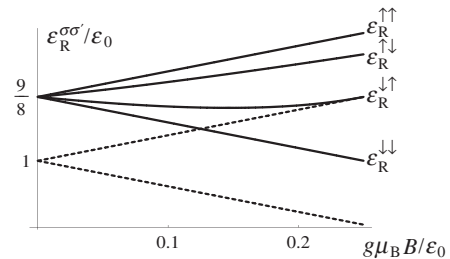


FIG. 4. Splitting of the resonance features in conductance and thermopower into four features as a function of magnetic field B . Dashed lines represent the evolution of the positions of single-particle peaks in the thermopower.

situation without interactions where finite-temperature corrections to the quantized conductance and to the zero value of S are of the order of $\exp(-\varepsilon_0/8k_B T)$, which stems from the exponentially small probability of having holes at the bottom of band 2. Thus, at sufficiently low temperatures, the features we consider are dominant.

Next, we outline the derivation of the electron-electron interaction effects on the current. We start from the Boltzmann equation,

$$v_{kn} \partial_x f_{kn}(x) = I_{knx}[f], \quad (4)$$

where $f_{kn}(x)$ is the distribution function, n the channel index, $v_{kn} = \frac{1}{\hbar} \partial_k \varepsilon_{kn}$ the velocity, and $I_{knx}[f]$ is the electron-electron collision integral. The reflectionless contacts of the quantum wire [3] and the shift in chemical potential and temperatures [10] are introduced by the boundary conditions

$$f_{kn}(x=0) = f_{L,kn}^0 \quad \text{for } k > 0, \quad (5a)$$

$$f_{kn}(x=L) = f_{R,kn}^0 \quad \text{for } k < 0, \quad (5b)$$

where $f_{L/R,kn}^0$ is the Fermi distribution for the left and right lead, respectively, including their temperatures $T_{L/R}$ and chemical potentials $\mu_{L/R}$. In Eq. (5) we have assumed that the collision term is turned on abruptly at $x=0$ and $x=L$, which, of course, is not the case. However, as long as the length of the wire is much larger than its width the results are not sensitive to the details of the openings. In the absence of interactions ($I_{knx}[f]=0$), the solution to the Boltzmann equation is simply given by

$$f_{kn}^{(0)} = f_{L,kn}^0 \theta(k) + f_{R,kn}^0 \theta(-k). \quad (6)$$

The interaction between electrons yields the collision integral

$$I_{k_1 n_1 x}[f] = - \sum_{\sigma_1' \sigma_2'} \sum_{n_1' n_2'} \sum_{k_1' k_2'} W_{12;1'2'} [f_1 f_2 (1-f_{1'}) (1-f_{2'}) - f_{1'} f_{2'} (1-f_1) (1-f_2)], \quad (7)$$

where $f_i = f_{k_i n_i}(x)$, and primes denote electron states after the collision. The scattering rate $W_{12;1'2'}$ is found using the Fermi golden rule. To find the distribution, we expand it powers of $W_{12;1'2'}$ as $f = f^{(0)} + f^{(1)} + \dots$. To the leading order, we can therefore insert $f_{kn}^{(0)}$ from Eq. (6) into the collision integral in the right-hand side of Eq. (4) to get

$$f_{kn}^{(1)}(x) = \left[\frac{x}{v_{kn}} \theta(k) + \frac{x-L}{v_{kn}} \theta(-k) \right] I_{kn}[f^{(0)}]. \quad (8)$$

The electric current now follows as (with $e > 0$)

$$I = I^{(0)} + I^{(1)}, \quad I^{(0)} = \frac{(-e)}{L} \sum_{\sigma n k} v_{kn} f_{kn}^{(0)}, \quad (9)$$

$$I^{(1)} = e \sum_{\sigma n k < 0} I_{kn}[f^{(0)}],$$

where $I^{(0)}$ corresponds to the Landauer formula for fully

open channels, and the term $I^{(1)}$ is the correction to the current due to interactions. To calculate $I^{(1)}$, we linearize $I_{kn}[f^{(0)}]$ in $eV = \mu_L - \mu_R$ and $\Delta T = T_R - T_L$ and divide the summation over quasiwave vectors into positive and negative values using $W_{12;1'2'} = W_{21;1'2'} = W_{1'2';12}$, etc. [11]. We obtain

$$I^{(1)} = 2(-e) \sum_{\sigma_1' \sigma_2'} \sum_{n_1' n_2'} \sum_{k_1' < 0, k_2' > 0} W_{12;1'2'} f_1^0 f_2^0 (1-f_{1'}^0) (1-f_{2'}^0) \times \left[\frac{\Delta T}{k_B T^2} (\varepsilon_1 - \mu) - \frac{eV}{k_B T} \right], \quad (10)$$

where $f_i^0 = 1/[\exp((\varepsilon_{k_i n_i} - \mu)/k_B T) + 1]$ is the Fermi function. For two channels, we find that the only combination of channel indices, which gives a contribution nonexponential in temperature, is $n_2 = 1$ and $n_1 = n_1' = n_2' = 2$. Moreover, this combination is nonexponential only if the Fermi energy is within a range of $k_B T$ from ε_R . An important point of the result (10) is that the number of left- and right-moving electrons has to change in order for the current to change. In essence, this is due to the cancellation of the velocity in the distribution function, Eq. (8), and in the current definition, Eq. (9). In fact, the cancellation can be shown to be valid to all orders in the interaction [11]. A similar situation occurs for the Coulomb drag response [12,13] of mesoscopic structures.

At low temperatures, $T \ll (\varepsilon_F - \varepsilon_0)/k_B$, we can now find the thermopower and conductance for both zero and nonzero magnetic field. From Eq. (10), we obtain the linear response current as $I = (G_T^{(0)} + G_T^{(1)}) \Delta T - (G^{(0)} + G^{(1)}) V$, where G is the conductance and G_T is the thermoelectric coefficient. Furthermore, since $G_T^{(0)} \propto e^{-(\varepsilon_F - \varepsilon_0)/k_B T}$ at the plateaus [5] and $G_T^{(1)} \propto T$ or T^3 one obtains at low temperatures the thermopower $S \approx G_T^{(1)}/G^{(0)}$. Moreover, the contribution to lowest order in temperature is found by linearizing the quadratic dispersion and using a constant interaction in Fourier space in Eq. (10). For ε_F near ε_R , we finally obtain, after some algebra, the zero-magnetic-field conductance correction, $\delta G = G^{(1)}$, and thermopower given in Eqs. (1) and (2) (plotted in Fig. 2). The dimensionless scaling functions F_0 and F_1 are determined by

$$F_n(x) = \int_{-\infty}^{\infty} dz z^n h(z, x), \quad (11a)$$

$$h(z, x) = \frac{-(2x + z)}{4 \sinh(2x + z) \cosh(\frac{z}{2}) \cosh(2x + \frac{3z}{2})}. \quad (11b)$$

Further, in Eqs. (1) and (2) we have defined the effective interchannel electron-electron scattering length as

$$l_{ee} = \frac{2}{27} \frac{2\pi}{k_{F1}} \left(\frac{\hbar v_{F1}}{|V_{2k_{F2}}^{2122}|} \right)^2, \quad (12)$$

where $V_{2k_{F2}}^{2122}$ is the electron-electron interaction at twice the Fermi vector for the second channel (i.e., upper subband) $2k_{F2}$. Both the curvature of the electron dispersion relation

and the momentum dependence of the interaction give rise to small corrections, e.g., $S(\varepsilon_F = \varepsilon_R) \propto T^2$. These corrections to higher order in temperature shift the point where the thermopower coefficient changes sign, but the overall behavior is still the same.

Magnetic field splits the resonance at $\varepsilon_F = \varepsilon_R$ into four points corresponding to scattering between electrons with identical or different spins. For scattering between electrons with identical spins, momentum and energy conservation lead to resonances occurring at $(\sigma = \pm 1 = \uparrow\downarrow)$

$$\varepsilon_R^{\sigma\sigma} = \frac{9}{8}\varepsilon_0 + \sigma\frac{1}{2}g\mu_B B. \quad (13)$$

However, the features which originate from scattering

between different spins split up in a different way ($\bar{\sigma} = -\sigma$),

$$\varepsilon_R^{\sigma\bar{\sigma}} = \varepsilon_0 \frac{9 + 20\sigma g\mu_B B/\varepsilon_0 + 8(g\mu_B B/\varepsilon_0)^2}{8(1 + 2\sigma g\mu_B B/\varepsilon_0)}. \quad (14)$$

For $g\mu_B B > \varepsilon_0/4$ only three resonances remain, since the scattering at $\varepsilon_F = \varepsilon_R^{\uparrow\uparrow}$ can no longer conserve both momentum and energy (similarly when $g\mu_B B < -\varepsilon_0/4$ the $\varepsilon_F = \varepsilon_R^{\downarrow\downarrow}$ resonance is absent).

In the regime $k_B T \ll g\mu_B B \ll \varepsilon_F - \varepsilon_0$, the thermopower and conductance change around each of the points $\varepsilon_F = \varepsilon_R^{\sigma\sigma'}$ can be found separately. The matrix element of the interaction potential

$$\langle k_1' 2\sigma_1' k_2' 2\sigma_2' | V | k_1 2\sigma_1 k_2 1\sigma_2 \rangle = \frac{\delta_{k_1+k_2, k_1'+k_2'}}{L} [V_{k_1'-k_1}^{2122} \delta_{\sigma_1, \sigma_1'} \delta_{\sigma_2, \sigma_2'} - V_{k_2'-k_1}^{2122} \delta_{\sigma_1, \sigma_2'} \delta_{\sigma_2, \sigma_1'}], \quad (15)$$

consist of a direct (first) and exchange (second) term leading to the remarkable difference between the resonance amplitude at $\varepsilon_R^{\sigma\bar{\sigma}}$ and $\varepsilon_R^{\sigma\sigma}$. The direct and exchange contributions to the scattering amplitude cancel each other for a pointlike interaction and equal spins (Pauli principle). Finite contributions to the transport characteristics appear due to the momentum dependence of the interaction matrix elements (15) and are of higher power in temperature:

$$S_{\sigma\sigma} = \frac{k_B}{e} \frac{6L}{l'_{ee}} \left(\frac{k_B T}{\varepsilon_F} \right)^3 \tilde{F}_1 \left(\frac{\varepsilon_F - \varepsilon_R^{\sigma\sigma}}{k_B T} \right), \quad (16a)$$

$$\delta G_{\sigma\sigma} = \frac{4e^2}{h} \frac{6L}{l'_{ee}} \left(\frac{k_B T}{\varepsilon_F} \right)^3 \tilde{F}_0 \left(\frac{\varepsilon_F - \varepsilon_R^{\sigma\sigma}}{k_B T} \right), \quad (16b)$$

where

$$l'_{ee} = \frac{2}{27} \frac{2\pi}{k_{F1}} \left(\frac{\hbar v_{F1}^\sigma}{k_{F1}^\sigma |\partial_q V_{2k_{F2}}^{2122}|} \right)^2. \quad (17)$$

The new dimensionless functions \tilde{F}_0 and \tilde{F}_1 are defined as

$$\tilde{F}_n(x) = \frac{1}{16} \int_{-\infty}^{\infty} dz z^n h(z, x) \left[\frac{4\pi^2}{3} + \frac{1}{3}(4x + 2z)^2 \right], \quad (18)$$

being well approximated by F_0 and F_1 in Fig. 2. The predicted evolution of the resonance structure with the increase of magnetic field should be a good candidate for experimental verification of the interaction effects.

In summary, we found interaction-induced resonance points in the Fermi energy in the conductance and thermopower S of a short clean multichannel quantum wire adiabatically connected to leads. The resonances in thermopower offer a way to observe the effect of inter-channel electron-electron interaction and to measure its strength. We found S to be dominated entirely by interactions for $|\varepsilon_F - \varepsilon_R|/k_B T \lesssim 5$ at low temperatures and to have the scaling form presented in Eq. (2). Furthermore,

the thermopower coefficient and the conductance develop distinct features in a finite magnetic field.

The work at the University of Minnesota is supported by NSF Grants No. DMR 02-37296 and No. DMR 04-39026. We thank H. Buhmann, M. Garst, A.-P. Jauho, M. Khodas, L. W. Molenkamp, M. Pustilnik, and H. Smith for discussions. The hospitality of MIPKs-Dresden (L. I. G.) and of the William I. Fine Theoretical Physics Institute, University of Minnesota (A.M.L.) is gratefully acknowledged.

-
- [1] B. J. van Wees *et al.*, Phys. Rev. Lett. **60**, 848 (1988).
 - [2] D. A. Wharam *et al.*, J. Phys. C **21**, L209 (1988).
 - [3] L. I. Glazman, G. B. Lesovik, D. E. Khmelnitskii, and R. I. Shekhter, JETP Lett. **48**, 238 (1988).
 - [4] D. I. Maslov and M. Stone, Phys. Rev. B **52**, R5539 (1995).
 - [5] H. van Houten, L. W. Molenkamp, C. W. J. Beenakker, and C. T. Foxon, Semicond. Sci. Technol. **7**, B215 (1992).
 - [6] L. W. Molenkamp *et al.*, Phys. Rev. Lett. **65**, 1052 (1990); L. W. Molenkamp *et al.*, Phys. Rev. Lett. **68**, 3765 (1992); N. J. Appleyard *et al.*, Phys. Rev. Lett. **81**, 3491 (1998).
 - [7] N. J. Appleyard *et al.*, Phys. Rev. B **62**, R16275 (2000).
 - [8] N. F. Mott and H. Jones, *The Theory of the Properties of Metals and Alloys* (Clarendon, Oxford, 1936).
 - [9] A. M. Lunde and K. Flensberg, J. Phys. Condens. Matter **17**, 3879 (2005).
 - [10] The term $\dot{k}\partial_k f$ is not present in the Boltzmann equation, since the bias and temperature difference are included in the boundary condition.
 - [11] A. M. Lunde, K. Flensberg, and L. I. Glazman (to be published).
 - [12] V. L. Gurevich, V. B. Pevzner, and E. W. Fenton, J. Phys. Condens. Matter **10**, 2551 (1998).
 - [13] N. A. Mortensen, K. Flensberg, and A.-P. Jauho, Phys. Rev. Lett. **86**, 1841 (2001).

Paper III

Anders Mathias Lunde, Karsten Flensberg
and Leonid I. Glazman:

Three-particle collisions in quantum wires: Corrections to thermopower and conductance

Physical Review B **75**, 245418 (2007).

Notes:

1. To be precise one should have introduced a normalization length and a length of the wire separately as in the thesis (section 3.2.3, p. 39). However, the normalization length cancels out, so the qualitative and quantitative results are not changed.
2. The statement discussed in Appendix A is actually more general than presented here: It does not require a symmetric scattering rate $W_{123;1'2'3'} = W_{1'2'3';123}$. However, it still requires that $W_{123;1'2'3'}$ is symmetric under interchange among the final and initial states, respectively, e.g. $W_{1'2'3';213} = W_{1'2'3';123}$, as stated in the article. For the general case see section 3.3, p. 41.

Three-particle collisions in quantum wires: Corrections to thermopower and conductance

Anders Mathias Lunde,^{1,2} Karsten Flensberg,¹ and Leonid I. Glazman²¹*Nano-Science Center, Niels Bohr Institute, University of Copenhagen, DK-2100 Copenhagen, Denmark*²*William I. Fine Theoretical Physics Institute, University of Minnesota, Minneapolis, Minnesota 55455, USA*

(Received 1 March 2007; published 15 June 2007)

We consider the effect of electron-electron interaction on the electron transport through a finite length single-mode quantum wire with reflectionless contacts. The two-particle scattering events cannot alter the electric current and therefore we study the effect of three-particle collisions. Within the Boltzmann equation framework, we calculate corrections to the thermopower and conductance to the leading order in the interaction and in the length of wire L . We check explicitly that the three-particle collision rate is identically zero in the case of several integrable interaction potentials. In the general (nonintegrable) case, we find a positive contribution to the thermopower to leading order in L . The processes giving rise to the correction involve electron states deep in the Fermi sea. Therefore, the correction follows an activation law with the characteristic energy of the order of the Fermi energy for the electrons in the wire.

DOI: [10.1103/PhysRevB.75.245418](https://doi.org/10.1103/PhysRevB.75.245418)

PACS number(s): 73.21.Hb, 72.10.-d, 73.63.Nm

I. INTRODUCTION

Short clean one-dimensional (1D) mesoscopic wires, often referred to as quantum point contacts, show conductance quantization^{1,2} as a function of the channel width. The quantization is well described by the theory of adiabatic propagation of free electrons.³ For noninteracting particles, conductance quantization should occur in longer channels too, as long as there is no backscattering off inhomogeneities within the channel.

A lot is known about the role of electron-electron interaction of 1D channels. Electron-electron repulsion in a wire enhances dramatically the reflection coefficient, making it energy dependent.⁴ However, interaction between electrons does not alter the quantization (in units of $2e^2/h$) of an ideal channel conductance in the limit of zero temperature.^{5,6} What is still an open question is whether there are other manifestations of interactions due to inelastic processes, which influence the transport properties.

In the absence of interactions, left- and right-moving particles in a wire are at equilibrium with the reservoirs they originate from. If a bias is applied between the reservoirs, then these equilibria differ from each other, giving rise to a particular form of the nonequilibrium distribution inside the channel. On the other hand, in a long ideal channel and in the presence of interactions, one may expect equilibration to occur between the left and right movers into a single distribution characterized by an equilibrium with respect to a reference frame moving with some drift velocity. Interestingly, in a model with momentum-independent electron velocity for left and right movers (as it is the case in the Tomonaga-Luttinger model), there is no difference between the two distributions. Effects originating from the particle-hole asymmetry, however, may discriminate between the two. Thermopower and Coulomb drag⁷⁻⁹ are examples of such effects.

At present, little is known about equilibration in a 1D electron system. In higher dimensions, the electron-electron interaction provides the most effective relaxation mechanism at low temperatures and therefore we include this relaxation

mechanism as the first approach. However, in 1D pair collisions cannot change the distribution function for quadratic dispersion, since the momentum and energy conservation¹⁰ laws result in either zero-momentum exchange or an interchange of the two momenta.¹¹ In either case, the distribution function remains the same. Thus, the leading equilibration mechanism is due to three-particle collisions, which we study in this paper.¹²

We investigate here the effects of three-particle collisions in reasonably short wires (see Fig. 1), where electron-electron scattering can be considered perturbatively. As measurable quantities, we evaluate the temperature dependence of the thermopower and conductance. Note that for more than one mode, pair collisions become important for certain fillings.¹³

The paper is organized as follows. First we review the noninteracting limit of thermopower and give a qualitative explanation of the effects due to three-particle collisions. Then, we describe how to include the electron interactions using the Boltzmann equation. Next, we calculate the main ingredient for our perturbation theory, namely, the three-particle matrix element and scattering rate using a T -matrix expansion. We note several interesting properties of this scattering rate. Finally, we derive the conductance and thermopower corrections and discuss the deviation from the so-called Mott formula. Furthermore, some technical details are

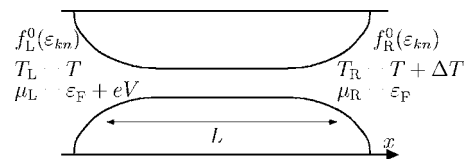


FIG. 1. A schematic picture of two metallic gates depleting the underlying two-dimensional electron gas and thereby forming a short 1D quantum wire of length L . This fabrication method has the advantage of producing reflectionless contacts to the leads (Ref. 3), so that the boundary conditions of the distribution function are given by the Fermi function of the reservoirs. We define the thermopower as $S = V / \Delta T|_{I=0}$, i.e., the voltage V required to counteract a current due to the temperature difference ΔT .

put in two appendices, and in Appendix A we show that the number of left and right movers have to change in a scattering event for the current to change.

A. Thermopower in the noninteracting limit

For a wire without interactions, the distribution function $f^{(0)}$ is determined solely by the electron reservoirs,

$$f_k^{(0)} = \begin{cases} f_L^0(\varepsilon_k - \mu_L, T_L) \equiv f_L^0(\varepsilon_k) & \text{for } k > 0, \\ f_R^0(\varepsilon_k - \mu_R, T_R) \equiv f_R^0(\varepsilon_k) & \text{for } k < 0, \end{cases} \quad (1)$$

where ε_k is the dispersion relation for momentum k and spin σ (suppressed in the notation), and $f^0(\varepsilon - \mu, T) = (1 + \exp[(\varepsilon - \mu)/k_B T])^{-1}$ is the Fermi function with $\mu_{L/R}$ and $T_{L/R}$ denoting the chemical potential and temperature of the left/right contact, respectively (see Fig. 1). The electric current for low temperature $T \ll T_F$ and in linear response to the applied bias V and temperature difference $\Delta T \ll T$ then follows as ($e > 0$) (Ref. 14)

$$I^{(0)} = \frac{(-e)}{L} \sum_{\sigma k > 0} v_k [f_L^0(\varepsilon_k) - f_R^0(\varepsilon_k)], \quad (2)$$

$$\simeq -\frac{2e^2}{h} V (1 - e^{-T_F/T}) + \frac{2e}{h} k_B \Delta T \frac{T_F}{T} e^{-T_F/T}. \quad (3)$$

From this, the well-known leading-order results for conductance,

$$G^{(0)} = \frac{2e^2}{h} (1 - e^{-T_F/T}), \quad (4)$$

and for thermopower,

$$S^{(0)} = \frac{k_B T_F}{e T} e^{-T_F/T}, \quad (5)$$

for a fully open channel are obtained. Here $T_F \equiv \varepsilon_F/k_B$ is the Fermi temperature.

B. Main results and a simple picture of the effect of the three-particle scattering

One of the main results of this paper is that the three-particle collisions give a *positive* contribution to the thermopower, i.e., the current due to a temperature difference is *increased* by the three-particle scattering. This can be explained in simple terms. Firstly, to change the current the number of left- and right-moving electrons need to change, since it is the number of electrons going through a mesoscopic structure that determines the current and not their velocity (see Appendix A). Secondly, we find the dominant scattering process at low temperature to only involve a single electron changing direction. This occurs near the bottom of the band, as pictured on Fig. 2(a). For the initial electronic distribution, the left-moving electrons have a higher temperature than the right-moving ones, which favors scattering into the warmer distribution, as seen on Fig. 2(b). This thus creates more left-moving electrons and thereby increases the

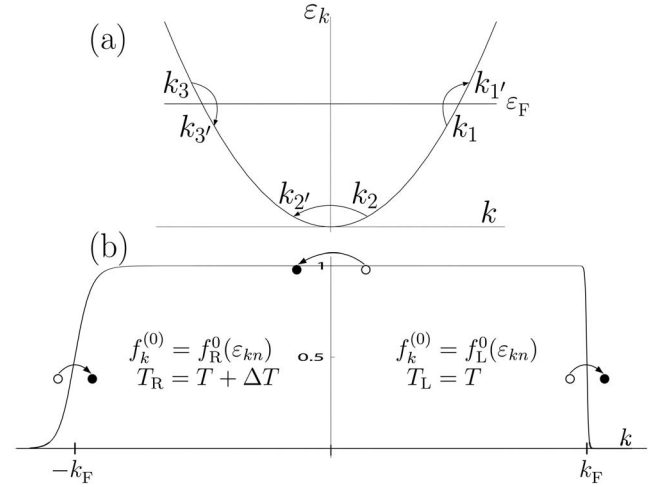


FIG. 2. (a) The dominant three-particle scattering process at low temperature in a single energy band. (b) The three-particle scattering process perturbing the initial distributions shown with warm left-moving electrons ($k < 0$) and cold right-moving electrons ($k > 0$). Due to the temperature difference of the initial distributions, the scattering process creating left movers dominates compared to the opposite scattering and therefore it gives a positive correction to the thermopower.

particle current toward the colder reservoir, i.e., increasing the thermopower.

Another important point is that the thermopower and conductance corrections are exponential in temperature, i.e., proportional to $\exp(-T_F/T)$. This is a direct consequence of the dominant three-particle scattering process requiring an empty state near the bottom of the band. We find the form of the thermopower correction at low temperatures due to the three-particle scattering to be given by

$$S^{\text{int}} \propto L |V|^4 \left(\frac{T}{T_F} \right)^6 \exp(-T_F/T) > 0, \quad (6)$$

where V is the electron-electron interaction strength and T_F the Fermi temperature. This is found perturbatively in the short-wire limit. The long-wire limit remains an open question, and we expect that the length dependence of thermopower saturates once L exceeds some relaxation length (which increases for decreasing temperature).

In contrast, the conductance correction is negative. To understand this, note that the chemical potential of the initial distribution is higher for the right-moving electrons than the left-moving ones. This favors scattering into the left-moving branch [still with the process shown in Fig. 2(a)] for nonzero temperature and thereby decreasing the current. The form of the conductance correction is similar to the thermopower correction,

$$G^{\text{int}} \propto -L |V|^4 \left(\frac{T}{T_F} \right)^7 \exp(-T_F/T) < 0. \quad (7)$$

II. CURRENT CALCULATION IN THE BOLTZMANN EQUATION FORMALISM

A. Effect of interactions on the current

To model the current through a short 1D quantum wire including perturbatively the three particle interactions, we use the Boltzmann equation

$$v_k \partial_x f_k(x) = \mathcal{I}_{kx}[f], \quad (8)$$

where $f_k(x)$ is the distribution function at a space point x between zero and L (see Fig. 1), $v_k = \frac{1}{\hbar} \partial_k \epsilon_k$ is the velocity, and $\mathcal{I}_{kx}[f]$ is the three-body electronic collision integral, i.e., no impurity or interface roughness effects are included here. We include the voltage and temperature difference in the boundary conditions of the reflectionless contacts,³ i.e.,

$$f_k(x=0) = f_L^0(\epsilon_k) \quad \text{for } k > 0, \quad (9a)$$

$$f_k(x=L) = f_R^0(\epsilon_k) \quad \text{for } k < 0, \quad (9b)$$

and therefore omit the term $k \partial_k f_k(x)$ in the Boltzmann equation allowed in the linear-response regime.¹⁵ A similar method has been used to investigate electron-phonon interactions in short quantum wires,¹⁶ quantum Hall effect in quantum wires,¹⁷ and ballistic Coulomb drag.¹⁸

The three-particle collision integral is assumed to be local in space and is given by

$$\begin{aligned} \mathcal{I}_{k_1 x}[f] = & - \sum_{\sigma_2 \sigma_3} \sum_{k_2 k_3} W_{123;1'2'3'} [f_1 f_2 f_3 (1-f_1')(1-f_2') \\ & \times (1-f_3') - f_1' f_2' f_3' (1-f_1)(1-f_2)(1-f_3)], \end{aligned} \quad (10)$$

where the quantum numbers are primed (unprimed) after (before) the scattering event, $f_i \equiv f_{k_i}(x)$, and the scattering rate $W_{123;1'2'3'}$ is found in the next section. Without interactions ($W_{123;1'2'3'}=0$), the solution of the Boltzmann equation is simply given by $f^{(0)}$ in Eq. (1). When interactions are included, it becomes a very difficult task to solve the Boltzmann equation to all orders in the interaction. However, for a short wire the interactions only have a short time to change the distribution function away from the initial distribution $f^{(0)}$ and therefore we expand the distribution function in orders of $W_{123;1'2'3'}$ as

$$f = f^{(0)} + f^{(1)} + \dots \quad (11)$$

To find $f^{(1)}$ to the first order in W , we insert the expansion of f in the Boltzmann equation and realize that only $f^{(0)}$ is necessary in the collision integral. Since $\mathcal{I}_{kx}[f^{(0)}] = \mathcal{I}_k[f^{(0)}]$ is independent of x , we find that

$$f_k^{(1)}(x) = \frac{x}{v_k} \mathcal{I}_k[f^{(0)}] \quad \text{for } k > 0, \quad (12a)$$

$$f_k^{(1)}(x) = \frac{x-L}{v_k} \mathcal{I}_k[f^{(0)}] \quad \text{for } k < 0, \quad (12b)$$

using the boundary conditions [Eq. (9)]. Therefore, the current to the first order in W is

$$I = I^{(0)} + e \sum_{\sigma k < 0} \mathcal{I}_k[f^{(0)}] \equiv I^{(0)} + I^{\text{int}}, \quad (13)$$

where $I^{(0)}$ is the noninteracting (Landauer) part of the current from Eq. (2) and I^{int} is the part due to interactions.

B. The linear-response limit

The form of the interacting part of the current is now known and the next step is therefore to evaluate it to linear response to V and ΔT to obtain the thermopower and conductance corrections. To this end, we define $\psi_k^{(0)}$ via

$$f_k^{(0)} \equiv f^0(\epsilon_k) + f^0(\epsilon_k)[1 - f^0(\epsilon_k)]\psi_k^{(0)}, \quad (14)$$

where $f^0(\epsilon_k)$ is the Fermi function with temperature T and Fermi level ϵ_F . It turns out that $\psi_k^{(0)}$ is proportional to either V or ΔT . This is seen by using the identity

$$-k_B T \partial_\epsilon f^0(\epsilon_k) = f^0(\epsilon_k)[1 - f^0(\epsilon_k)], \quad (15)$$

so we can identify $\psi_k^{(0)}$ by expanding the noninteracting distribution function $f_k^{(0)}$ [see Eq. (1) and Fig. 1],

$$f_L^0(\epsilon_k) \approx f^0(\epsilon_k) + [-\partial_\epsilon f^0(\epsilon_k)]eV, \quad (16a)$$

$$f_R^0(\epsilon_k) \approx f^0(\epsilon_k) + [-\partial_\epsilon f^0(\epsilon_k)](\epsilon - \epsilon_F) \frac{\Delta T}{T}, \quad (16b)$$

i.e.,

$$\psi_k^{(0)} = \begin{cases} \frac{eV}{k_B T} & \text{for } k > 0 \\ \frac{\epsilon_k - \epsilon_F}{k_B T} \frac{\Delta T}{T} & \text{for } k < 0. \end{cases} \quad (17)$$

Therefore, to get I^{int} in linear response to V and ΔT , we linearized the collision integral $\mathcal{I}_k[f^{(0)}]$ [Eq. (10)] with respect to $\psi_k^{(0)}$ and insert it into I^{int} [Eq. (13)] to obtain

$$\begin{aligned} I^{\text{int}} = & (-e) \sum_{\sigma_1 \sigma_2 \sigma_3} \sum_{k_1 < 0, k_2 k_3} \Delta_{123;1'2'3'} \\ & \times [\psi_1^{(0)} + \psi_2^{(0)} + \psi_3^{(0)} - \psi_1'^{(0)} - \psi_2'^{(0)} - \psi_3'^{(0)}], \end{aligned} \quad (18)$$

where we defined

$$\Delta_{123;1'2'3'} = W_{123;1'2'3'} f_1^0 f_2^0 f_3^0 (1-f_1')(1-f_2')(1-f_3'), \quad (19)$$

using the shorthand notation $\psi_i^{(0)} \equiv \psi_{k_i}^{(0)}$ and $f_i^0 \equiv f^0(\epsilon_{k_i})$. To linearize the collision integral and thereby the correction to the current due to interactions I^{int} , we have used the relation

$$\begin{aligned} f_1^0 f_2^0 f_3^0 (1-f_1')(1-f_2')(1-f_3') \\ = f_1^0 f_2^0 f_3^0 (1-f_1^0)(1-f_2^0)(1-f_3^0), \end{aligned} \quad (20)$$

valid at $\epsilon_1 + \epsilon_2 + \epsilon_3 = \epsilon_1' + \epsilon_2' + \epsilon_3'$.

Since $\psi_i^{(0)}$ is different for positive and negative k_i , we need to divide the summation in I^{int} [Eq. (18)] into positive

and negative k sums, which gives $2^5=32$ terms. For this purpose, we introduce the notation

$$\sum_{\substack{k_1 < 0, k_2 > 0, k_3 < 0 \\ k_1' > 0, k_2' > 0, k_3' < 0}} (\cdot) \equiv \sum_{\substack{-- \\ ++}} (\cdot), \quad \sum_{\substack{\sigma_1 \sigma_2 \sigma_3 \\ \sigma_1' \sigma_2' \sigma_3'}} (\cdot) \equiv \sum_{\text{spin}} (\cdot), \quad (21)$$

and similarly for other combinations of the summation intervals. The 32 terms can be simplified to only three terms using energy conservation and symmetry properties of

$\Delta_{123;1'2'3'}$ in Eq. (19) under interchange of indices. There are pairwise exchanges of indices $\Delta_{123;1'2'3'} = \Delta_{213;1'2'3'} = \Delta_{123;1'3'2'}$, etc., and interchanges between primed and unprimed indices, $\Delta_{123;1'2'3'} = \Delta_{1'2'3';123}$, using Eq. (20) and the fact that $W_{123;1'2'3'}$ contains a matrix element squared. This leads to six terms. Furthermore, $\Delta_{123;1'2'3'}$ is invariant under $k_i \rightarrow -k_i$ for all $i=1,2,3,1',2',3'$ simultaneously due to time-reversal symmetry, also seen explicitly from the form of $W_{123;1'2'3'}$ (derived below). An example of how the simplifications occurs can be seen in Eq. (A6). Thus, we obtain the result

$$\begin{aligned} I^{\text{int}} = & 2(-e) \sum_{\text{spin}} \sum_{\substack{+++ \\ ---}} \Delta_{123;1'2'3'} \left[\frac{\Delta T}{k_B T^2} (\varepsilon_1 - \varepsilon_F) - \frac{eV}{k_B T} \right] \\ & + 4(-e) \sum_{\text{spin}} \sum_{\substack{--+ \\ +++}} \Delta_{123;1'2'3'} \left\{ \frac{\Delta T}{k_B T^2} [(\varepsilon_1 - \varepsilon_F) + (\varepsilon_2 - \varepsilon_F)] - \frac{2eV}{k_B T} \right\} \\ & + 3(-e) \sum_{\text{spin}} \sum_{\substack{++- \\ +--}} \Delta_{123;1'2'3'} \left\{ \frac{\Delta T}{k_B T^2} [-(\varepsilon_3 - \varepsilon_F) + (\varepsilon_2' - \varepsilon_F) + (\varepsilon_3' - \varepsilon_F)] - \frac{eV}{k_B T} \right\}, \end{aligned} \quad (22)$$

where the definition of $\psi_i^{(0)}$ in Eq. (17) was inserted. An important point is that the number of positive and/or negative wave-vector intervals is not the same before and after the scattering. Therefore, we note that only scattering events that change the number of left- and right-moving electrons contribute to the interaction correction to the current. The origin of this is the cancellation of the velocity in the definition of the current and in the distribution functions [Eq. (12)].

This cancellation thus leads to an expression for the interaction correction to the current in Eq. (22) where all the in-going and out-going momenta enter on equal footing. In Appendix A, we show that this is valid to all orders in perturbation theory. Due to this property and momentum conservation, there are no processes that alter the current possible near the Fermi level. Consequently, states far away from the Fermi level have to be involved in the scattering, which, as we will see, leads to a suppression of I^{int} by a factor $\exp(-T_F/T)$. The distribution function, on the other hand, can be changed by scattering processes near the Fermi level.

To identify the important processes, we find in the next section the scattering rate $W_{123;1'2'3'}$.

III. THREE-PARTICLE SCATTERING RATE

The three-particle scattering rate $W_{123;1'2'3'}$ is calculated using the generalized Fermi golden rule inserting the T matrix, $T \equiv V + VG_0T$, iterated to second order in the interaction V to get the three-particle interaction amplitude, i.e.,

$$W_{123;1'2'3'} = \frac{2\pi}{\hbar} |\langle 1'2'3' | VG_0V | 123 \rangle_c|^2 \delta(E_i - E_f), \quad (23)$$

where $E_i = \varepsilon_1 + \varepsilon_2 + \varepsilon_3$ is the initial energy, $E_f = \varepsilon_{1'} + \varepsilon_{2'} + \varepsilon_{3'}$ the final energy, G_0 is the resolvent operator (or free Green's function), j is shorthand for k_j , and the subscript “c” means connected in the sense that the scattering process cannot be effectively a two-particle process, where one of the incoming particles does not participate in the scattering. Explicitly G_0 and V are given by

$$G_0 = \frac{1}{E_i - H_0 + i\eta}, \quad (\eta \rightarrow 0^+), \quad (24)$$

$$V = \frac{1}{2L} \sum_{k_1 k_2 q} \sum_{\sigma_1 \sigma_2} V_q c_{k_1+q\sigma_1}^\dagger c_{k_2-q\sigma_2}^\dagger c_{k_2\sigma_2} c_{k_1\sigma_1}. \quad (25)$$

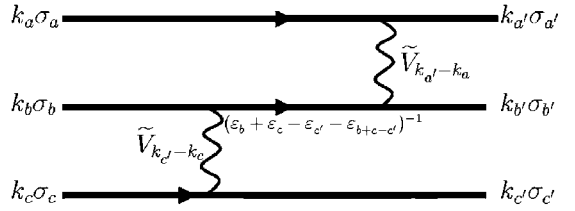
Here, H_0 is the unperturbed Hamiltonian (i.e., kinetic energy with some dispersion), V_q the Fourier-transformed interaction potential, and $c_{k\sigma}$ ($c_{k\sigma}^\dagger$) is the annihilation (creation) operator. To calculate the matrix element $\langle 1'2'3' | VG_0V | 123 \rangle_c$, we write the initial and final states as

$$|123\rangle = c_{k_1\sigma_1}^\dagger c_{k_2\sigma_2}^\dagger c_{k_3\sigma_3}^\dagger |0\rangle, \quad (26)$$

$$|1'2'3'\rangle = c_{k_{1'}\sigma_{1'}}^\dagger c_{k_{2'}\sigma_{2'}}^\dagger c_{k_{3'}\sigma_{3'}}^\dagger |0\rangle, \quad (27)$$

where $|0\rangle$ is the empty state. Using the anticommutator algebra $\{c_i, c_j^\dagger\} = \delta_{i,j}$, we obtain

(a)

$$\frac{1}{4L^2} \frac{\tilde{V}_{a'-a} \tilde{V}_{c'-c}}{\varepsilon_b + \varepsilon_c - \varepsilon_{c'} - \varepsilon_{b+c-c'} + i\eta} \delta_{a'+b+c, a'+b'+c'} \delta_{\sigma_{a'}, \sigma_a} \delta_{\sigma_{b'}, \sigma_b} \delta_{\sigma_{c'}, \sigma_c} \equiv$$


(b)

$$\langle 1'2'3' | VG_0 V | 123 \rangle_c = \frac{1}{3} \left(\begin{array}{c} \text{---} \\ \text{---} \\ \text{---} \end{array} + \begin{array}{c} \text{---} \diagup \diagdown \text{---} \\ \text{---} \end{array} + \begin{array}{c} \text{---} \diagdown \diagup \text{---} \\ \text{---} \end{array} - \begin{array}{c} \text{---} \diagup \diagup \text{---} \\ \text{---} \end{array} - \begin{array}{c} \text{---} \diagdown \diagdown \text{---} \\ \text{---} \end{array} - \begin{array}{c} \text{---} \diagup \diagdown \diagup \text{---} \\ \text{---} \end{array} \right) \times \left(\begin{array}{c} \text{---} \\ \text{---} \\ \text{---} \end{array} \right)$$

$$\times \left(\begin{array}{c} \text{---} \\ \text{---} \\ \text{---} \end{array} + \begin{array}{c} \text{---} \diagup \diagdown \text{---} \\ \text{---} \end{array} + \begin{array}{c} \text{---} \diagdown \diagup \text{---} \\ \text{---} \end{array} - \begin{array}{c} \text{---} \diagup \diagup \text{---} \\ \text{---} \end{array} - \begin{array}{c} \text{---} \diagdown \diagdown \text{---} \\ \text{---} \end{array} - \begin{array}{c} \text{---} \diagup \diagdown \diagup \text{---} \\ \text{---} \end{array} \right) \begin{array}{c} 1' \\ 2' \\ 3' \end{array}$$

FIG. 3. A visualization of the connected three-particle scattering matrix element [Eq. (30)], where three particles interchange their momenta and energy. This matrix element enters the scattering rate via the generalized Fermi golden rule [Eq. (23)]. (a) The basic three-particle interaction consisting of two interaction lines and a free propagation [see Eq. (30)]. (b) Picture of the exchange processes times the basic interaction needed to form the matrix element [Eq. (30)].

$$G_0 V | 123 \rangle = \frac{1}{2L} \sum_q V_q \sum_{(abc) \in P(123)} \frac{\text{sgn}(abc)}{\varepsilon_{ba}(q)} \times c_{k_a+q, \sigma_a}^\dagger c_{k_b-q, \sigma_b}^\dagger c_{k_c, \sigma_c}^\dagger | 0 \rangle, \quad (28)$$

where we introduced

$$\varepsilon_{ba}(q) = \varepsilon_b + \varepsilon_a - \varepsilon_{b-q} - \varepsilon_{a+q} + i\eta = \frac{\hbar^2}{m} q(k_b - k_a - q) + i\eta \quad (29)$$

(the last equality is only valid for a quadratic dispersion), and where the set of permutations is given by $P(123) = [(123)^+, (231)^+, (312)^+, (132)^-, (321)^-, (213)^-]$. Here, the signs of the permutation, $\text{sgn}(abc)$, are shown as superscripts.

In order to exclude the effectively two-particle processes when multiplying Eq. (28) by $\langle 1'2'3' | V$ from the left, k_c ($c=1,2,3$) needs to be different from $k_{j'}$ ($j=1,2,3$). The result is

$$\begin{aligned} \langle 1'2'3' | VG_0 V | 123 \rangle_c &= \frac{1}{(2L)^2} \sum_{(abc) \in P(123)} \sum_{(a'b'c') \in P(1'2'3')} \text{sgn}(abc) \text{sgn}(a'b'c') \\ &\times \frac{\tilde{V}_{a'-a} \tilde{V}_{c'-c} \delta_{a'+b+c, a'+b'+c'}}{\varepsilon_b + \varepsilon_c - \varepsilon_{c'} - \varepsilon_{b+c-c'} + i\eta} \delta_{\sigma_{a'}, \sigma_a} \delta_{\sigma_{b'}, \sigma_b} \delta_{\sigma_{c'}, \sigma_c}, \quad (30) \end{aligned}$$

where $\tilde{V}_q = V_q + V_{-q}$ is the symmetrized interaction. The matrix element consists of 36 terms and the scattering rate thus has $36^2 = 1296$ terms. To obtain this result, we did not use energy conservation. For a quadratic dispersion, the denominator is only zero if we have an effective pair collision or if the momentum transfer is zero, as seen from the expression $\varepsilon_{ba}(q) = \frac{\hbar^2}{m} q(k_b - k_a - q) + i\eta$. A picture of the matrix element is found in Fig. 3(b), where the exchange processes (including the sign) are visualized as different ways to connect two interaction lines and an intermediate propagation (G_0) seen on Fig. 3(a). The inclusion of the Fermi statistics makes a substantial difference for the properties of the scattering rate as compared to the case described in Ref. 19, which is obtained by setting all $\text{sgn}(\dots) = +1$.

We can rewrite the matrix element [Eq. (30)] in a more transparent way in terms of quantum-mechanical exchange symmetry. First, we introduce the following combination of three-particle scattering amplitudes:

$$\begin{aligned} V(11', 22', 33') &= \frac{\delta_{\sigma_{1'}, \sigma_1} \delta_{\sigma_{2'}, \sigma_2} \delta_{\sigma_{3'}, \sigma_3}}{4L^2} \left(\frac{\tilde{V}_{1'-1} \tilde{V}_{3'-3}}{\varepsilon_3 + \varepsilon_2 - \varepsilon_{3'} - \varepsilon_{2+3-3'}} + \frac{\tilde{V}_{2'-2} \tilde{V}_{1'-1}}{\varepsilon_1 + \varepsilon_3 - \varepsilon_{1'} - \varepsilon_{3+1-1'}} + \frac{\tilde{V}_{3'-3} \tilde{V}_{2'-2}}{\varepsilon_2 + \varepsilon_1 - \varepsilon_{2'} - \varepsilon_{1+2-2'}} \right. \\ &\quad \left. + \frac{\tilde{V}_{1'-1} \tilde{V}_{2'-2}}{\varepsilon_2 + \varepsilon_3 - \varepsilon_{2'} - \varepsilon_{3+2-2'}} + \frac{\tilde{V}_{3'-3} \tilde{V}_{1'-1}}{\varepsilon_1 + \varepsilon_2 - \varepsilon_{1'} - \varepsilon_{2+1-1'}} + \frac{\tilde{V}_{2'-2} \tilde{V}_{3'-3}}{\varepsilon_3 + \varepsilon_1 - \varepsilon_{3'} - \varepsilon_{1+3-3'}} \right), \quad (31) \end{aligned}$$

and after some rewriting, we then obtain

$$\begin{aligned} \langle 1'2'3'|VG_0V|123\rangle_c &= \delta_{k_1+k_2+k_3, k_1'+k_2'+k_3'} [V(11', 22', 33') \\ &\quad + V(12', 23', 31') + V(13', 21', 32') \\ &\quad - V(11', 23', 32') - V(13', 22', 31') \\ &\quad - V(12', 21', 33')]. \end{aligned} \quad (32)$$

We interpret this result in a way similar to a two-particle matrix element,

$$\begin{aligned} \langle 1'2'|V|12\rangle &= \frac{\delta_{k_1+k_2, k_1'+k_2'}}{L} (V_{k_1, -k_1} \delta_{\sigma_1, \sigma_1'} \delta_{\sigma_2, \sigma_2'} \\ &\quad - V_{k_2, -k_1} \delta_{\sigma_1, \sigma_2'} \delta_{\sigma_2, \sigma_1'}), \end{aligned} \quad (33)$$

which contains a direct (first term) and an exchange term (where $1' \leftrightarrow 2'$).

In the three-particle case, $V(11', 22', 33')$ is the direct term and one can make five exchange processes (instead of one) by exchanging the three final states $1'$, $2'$, and $3'$. This gives Eq. (32). The sign in front of each $V(\cdots)$ is determined by the number of exchanges made, e.g., in $V(11', 23', 32')$ a single exchange, $2' \leftrightarrow 3'$, gives a minus $(-1)^1$ whereas for $V(12', 23', 31')$ two exchanges ($1' \leftrightarrow 3'$ followed by $3' \leftrightarrow 2'$) give a positive sign $(-1)^2$. Furthermore, the arguments in $V(11', 22', 33')$ are ordered in three pairs such that the differences between the elements in each pair are the only arguments of the interaction potential [see Eq. (31)]. This is useful when constructing approximations having a specific scattering process in mind.

How the matrix element was rewritten into the form of Eq. (32) can also be described in terms of the drawings of

Fig. 3. The direct term $V(11', 22', 33')$ is the sum of the six terms having mirror-symmetric exchanges before and after the scattering. The other terms in Eq. (32) then can be obtained by suitable changes of out-going lines.

A. Zero three-particle scattering rate for integrable models

The expressions we obtain for the three-particle scattering rates [Eq. (23)] are quite cumbersome. Nevertheless, the obtained results allow for some consistency checks. Remarkably, for some two-body potentials, scattering of the particles of an N -body system is exactly equivalent to a sequence of two-body collisions. Such “special” potentials were studied in the context of integrable quantum many-body problems.¹¹ We recall now that for a quadratic band, a pair collision does not change the momenta of the incoming particles or simply permutes the two momenta. Therefore, three-particle scattering for the integrable potentials may result *only* in permutations within the group of three momenta of the colliding particles; all other three-particle scattering amplitudes must be zero for such potentials. In the context of this work, it means that even three-particle (or higher-order) collisions would not bring electron equilibration for such types of electron-electron interaction.

In this section, we check that the three-particle scattering amplitudes are indeed zero for two special potentials.

1. Pointlike interaction

In the case of contact interaction, $\tilde{V}_q = \text{const} \equiv \tilde{V}_0$, and for any kind of electron dispersion relation (i.e., not necessarily quadratic), we find by using the energy conservation law that

$$\begin{aligned} \sum_{\text{spin}} |\langle 1'2'3'|VG_0V|123\rangle_c|^2 &= \frac{2\tilde{V}_0^4}{(2L)^4} \delta_{k_1+k_2+k_3, k_1'+k_2'+k_3'} (|A_{121'} - A_{122'} - A_{131'} + A_{132'}|^2 + |A_{121'} - A_{123'} - A_{131'} + A_{133'}|^2 \\ &\quad + |A_{122'} - A_{123'} - A_{132'} + A_{133'}|^2 + |A_{121'} - A_{122'} - A_{231'} + A_{232'}|^2 + |A_{131'} - A_{132'} - A_{231'} + A_{232'}|^2 \\ &\quad + |A_{121'} - A_{123'} - A_{231'} + A_{233'}|^2 + |A_{131'} - A_{133'} - A_{231'} + A_{233'}|^2 + |A_{122'} - A_{123'} - A_{232'} + A_{233'}|^2 \\ &\quad + |A_{132'} - A_{133'} - A_{232'} + A_{233'}|^2), \end{aligned} \quad (34)$$

where $A_{abc} = (\varepsilon_a + \varepsilon_b - \varepsilon_c - \varepsilon_{a+b-c} + i\eta)^{-1}$. This is a major simplification from $36^2 = 1296$ to $9 \times 4^2 = 144$ terms by performing the spin summation. If, furthermore, the dispersion is quadratic, $\varepsilon_k \propto k^2$, then we find the (at first sight) surprising cancellation

$$\sum_{\text{spin}} |\langle 1'2'3'|VG_0V|123\rangle_c|^2 \delta(\varepsilon_1 + \varepsilon_2 + \varepsilon_3 - \varepsilon_{1'} - \varepsilon_{2'} - \varepsilon_{3'}) = 0. \quad (35)$$

This can be seen directly from Eq. (34) or by noting that

$$V(1a', 2b', 3c') \delta(\varepsilon_1 + \varepsilon_2 + \varepsilon_3 - \varepsilon_{a'} - \varepsilon_{b'} - \varepsilon_{c'}) = 0, \quad (36)$$

for a quadratic dispersion and constant interaction for $(a'b'c') \in P(1'2'3')$, i.e., each term of Eq. (32) is zero. $V(11', 22', 33')$ cancels in such a way that the three first terms of Eq. (31) cancel each other [the even permutations of (123) combined with the same primed permutation] and the three last terms cancel each other [the odd permutations of

(123) combined with the same primed permutation].

In fact, the cancellation described above is in agreement with the general factorization results for the S matrix of one-dimensional N -body problem with δ -function interaction in real space.²⁰ In this context, it is crucial that the particles have a quadratic dispersion relation; if we use, e.g., $\varepsilon_k \propto k^4$, then the cancellation does not occur. Notice also that the cancellation we demonstrate is not a trivial zero. Indeed, the underlying two-particle amplitudes [Eq. (33)] are finite for a q -independent potential if one includes spins. (For spinless fermions and contact interaction, the matrix element would be zero because the direct and the exchange terms cancel in accordance with the Pauli principle.)

2. $\tilde{V}_q = V_0(1 - q^2/q_0^2)$ interaction

We also observed that the energy conserving part of the matrix element $\langle 1'2'3' | VG_0V | 123 \rangle_c$ in the case of *spinless* fermions, quadratic dispersion, and the Fourier transformed interaction potential of the form

$$\tilde{V}_q = V_0 \left(1 - \frac{q^2}{q_0^2} \right) \quad (37)$$

becomes equal to zero. This is also possible to expect because of the relation of the potential [Eq. (37)] to the integrable 1D bosonic Lieb-Liniger model.²¹ Indeed, the bosonic model with contact interaction potential $\propto g_B \delta(x_1 - x_2)$ may be exactly mapped²² onto the spinless fermionic model with interaction $V_F(x_1 - x_2) \propto -(1/g_B) \delta'(x_1 - x_2)$. The integrability of the bosonic model guarantees the integrability of the corresponding fermionic one. Adding a contact interaction to V_F does no harm, as we are considering spinless fermions. Finally, Fourier transformation takes us to Eq. (37).

We observed that including the spin degree of freedom spoils the remarkable cancellation for a three-particle amplitude.

In the following sections, we assume a general case interaction potential for which the three-particle scattering amplitudes lead to a nontrivial redistribution of the momenta between the particles.

IV. THERMOPOWER AND CONDUCTANCE CORRECTIONS DUE TO THREE-PARTICLE INTERACTION

In this section, we go through the main ideas and approximations in evaluating the current correction due to interactions I^{int} [Eq. (22)] to lowest order in the temperature, $T \ll T_F$. We give a more detailed calculation in Appendix B.

As noted previously, all three terms in I^{int} [Eq. (22)] are exponentially suppressed, since momentum conservation

$$k_1 + k_2 + k_3 = k_{1'} + k_{2'} + k_{3'}$$

forbids scattering processes near the Fermi level for the given combinations of positive and negative k intervals. To be more specific, it is the phase-space restrictions of the Fermi functions that give the exponential suppression, i.e.,

$$f_{1'}^0 f_2^0 f_3^0 (1 - f_{1'}^0)(1 - f_2^0)(1 - f_3^0) \propto e^{-T_F/T}. \quad (38)$$

We begin by identifying the most important three-particle scattering process. The three terms in I^{int} [Eq. (22)] are the following: (i) two right movers backscattering a left mover while remaining right movers, (ii) one right mover keeping its direction while backscattering two left movers, and (iii) a left and a right mover keeping their directions while backscattering the third particle. From now on, we will concentrate on the case of Coulomb interaction \tilde{V}_q , which is the largest for small q ; therefore we want to identify processes where the initial and final states are close in momentum space.²³ Further, the process(es) should not require more than one electron in states suppressed exponentially by the Fermi functions. One can see that due to the constraints stemming from momentum and energy conservation, in fact, only process (iii) allows both initial and final states to be close to each other in momentum space and at the same time having only a single exponentially suppressed factor. The corresponding scattering process is of the type shown in Fig. 2(a). Therefore, to the first order in $\exp(-T_F/T)$, we include only the third one in Eq. (22). This leads to

$$I^{\text{int}} \simeq 3(-e) \sum_{\text{spin } ++-} \sum_{+-+} \Delta_{123;1'2'3'} \times \left[\frac{\Delta T}{k_B T^2} (-\varepsilon_3 + \varepsilon_{2'} + \varepsilon_{3'} - \varepsilon_F) - \frac{eV}{k_B T} \right]. \quad (39)$$

Here, $\Delta_{123;1'2'3'}$ expresses the available phase space in form of the Fermi functions and the three-particle scattering rate [see Eq. (19)].

One essential approximation is that for the scattering process depicted in Fig. 2(a), we may replace the full Fermi distribution functions by the exponential tails or the low-temperature limit expressions, i.e.,

$$f_1^0 \simeq \theta(k_F - k_1) \theta(k_1), \quad 1 - f_{1'}^0 \simeq \theta(k_{1'} - k_F), \quad (40a)$$

$$f_2^0 \simeq \theta(k_F - k_2) \theta(k_2), \quad 1 - f_{2'}^0 \simeq e^{(\varepsilon_{2'} - \varepsilon_F)/k_B T}, \quad (40b)$$

$$f_3^0 \simeq e^{-(\varepsilon_3 - \varepsilon_F)/k_B T}, \quad 1 - f_{3'}^0 \simeq e^{(\varepsilon_{3'} - \varepsilon_F)/k_B T}. \quad (40c)$$

Note that k_1 , $k_{1'}$, and k_2 are all positive. We see that the product of the Fermi functions is indeed exponentially suppressed, i.e., $\propto \exp(-T_F/T)$.

The second essential approximation is that for the scattering process seen in Fig. 2(a), the initial and final states differ by a small momentum. Therefore, the matrix element in the transition rate $W_{123;1'2'3'}$ is dominated by the direct term $V(11', 22', 33')$ in Eq. (32), since the five exchange terms are suppressed by the Coulomb interaction $|\tilde{V}_{|q| \sim k_F}| \ll |\tilde{V}_{|q| \ll k_F}|$, i.e.,

$$\langle 1'2'3' | VG_0V | 123 \rangle_c \simeq \delta_{k_1+k_2+k_3, k_{1'}+k_{2'}+k_{3'}} V(11', 22', 33'). \quad (41)$$

The direct term [Eq. (41)] would be zero for $\tilde{V}_q = \text{const.}$ In the case of quadratic dispersion relation and general \tilde{V}_q , it vanishes in the limit $(k_{i'} - k_i) \rightarrow 0$ and $(k_{j'} - k_j) \rightarrow 0$ for $i, j \in \{1, 2, 3\}$ due to the Pauli principle. For a quadratic dispersion and for a general symmetrized interaction $\tilde{V}_q = V_q + V_{-q}$, the direct term $\mathbb{V}(11', 22', 33')$ simplifies to the following expression:

$$\begin{aligned} & \mathbb{V}(11', 22', 33') \\ &= \frac{\delta_{\sigma_1', \sigma_1} \delta_{\sigma_2', \sigma_2} \delta_{\sigma_3', \sigma_3}}{4L^2 \hbar^2 / m} (q_1 + q_3) \\ & \times \frac{[-(q_1 + q_3) \tilde{V}_{q_1} \tilde{V}_{q_3} + \tilde{V}_{q_1+q_3} (q_3 \tilde{V}_{q_1} + q_1 \tilde{V}_{q_3})]}{(k_1 - k_3 + q_1) q_1 q_3 (k_1 - k_3 - q_3)}, \quad (42) \end{aligned}$$

where we used energy conservation and introduced $q_1 = k_1' - k_1$ and $q_3 = k_3' - k_3$.

Next, we give a qualitative explanation for the power law in T for the interacting current correction [Eq. (39)] using the quadratic dispersion. First, we consider the phase-space constraint. To do the sum over all k in Eq. (39), we use the momentum and energy conservation and introduce new variables $q_1 = k_1' - k_1$ and $q_3 = k_3' - k_3$, i.e., change the summation variables,

$$k_1, k_2, k_3, k_1', k_2', k_3' \rightarrow k_1, k_3, q_1, q_3. \quad (43)$$

The energy conservation for a quadratic dispersion gives a factor of $1/|q_1 + q_3|$ [see, e.g., Eq. (B6)]. For the process at hand, k_1 and k_3 are close to the Fermi level and each of their sums contributes with a factor of q_1 and q_3 , respectively. The Fermi functions give the exponential suppression and a contribution to the phase space in form of an exponential tail, i.e.,

$$f_1^0 f_2^0 f_3^0 (1 - f_1^0) (1 - f_2^0) (1 - f_3^0) \propto e^{-T_F/T} e^{(\varepsilon_2' - \varepsilon_3 + \varepsilon_3')/k_B T} \quad (44)$$

[see Eqs. (40a)–(40c)]. To get the low-temperature result for I^{int} [Eq. (39)], we use the method of steepest decent to calculate the integral. To this end, we note that the exponent $\varepsilon_2' - \varepsilon_3 + \varepsilon_3'$ is a function of q_1 and q_3 and in the limit $T/T_F \rightarrow 0$ the most important part is around the origin $q_1 = q_3 = 0$. Here, $\varepsilon_2' - \varepsilon_3 + \varepsilon_3'$ vanishes as $-\frac{1}{2} \hbar v_F (q_1 + q_2)$ (see Appendix B for details). Therefore, collecting the phase-space factors, the current correction due to three-particle interactions [Eq. (39)] becomes

$$\begin{aligned} I^{\text{int}} & \propto \varepsilon^{-T_F/T} \int dq_1 \int dq_3 \frac{q_1 q_3}{|q_1 + q_3|} e^{-(T_F/T)(q_1 + q_3)/k_F} \\ & \times |\mathbb{V}(11', 22', 33')|^2 \left[\frac{\Delta T}{T} \frac{T_F}{T} \left(-\frac{q_1 + q_3}{k_F} - 1 \right) - \frac{eV}{k_B T} \right], \quad (45) \end{aligned}$$

in the limit $T \ll T_F$. Furthermore, it turns out that the constraints $k_2 > 0$ and $k_2' < 0$ in the sum [Eq. (39)] only leaves phase space close to $q_1 = q_3$ for $T/T_F \rightarrow 0$, so we can set $q_3 = q_1$ in the integrand and do the integral over q_3 , which is

$\propto q_1^2$ due to the phase-space limits. To lowest order in temperature, this yields

$$\begin{aligned} I^{\text{int}} & \propto \varepsilon^{-T_F/T} \int_0^\infty dq q^3 e^{-(T_F/T)2q/k_F} |\mathbb{V}(11', 22', 33')|^2 \\ & \times \left(\frac{\Delta T}{T} \frac{T_F}{T} + \frac{eV}{k_B T} \right). \quad (46) \end{aligned}$$

From this, we conclude that phase space alone (i.e., assuming $|\mathbb{V}(11', 22', 33')|^2$ to be a constant) gives a temperature dependence of the form

$$I^{\text{int}} \propto \varepsilon^{-T_F/T} T^4 \left(\frac{\Delta T}{T} \frac{T_F}{T} + \frac{eV}{k_B T} \right) \quad (\text{phase space only}). \quad (47)$$

However, as we have seen the three-particle interaction rate has a delicate momentum dependence that needs to be taken into account. Therefore, to calculate the direct interaction term $\mathbb{V}(11', 22', 33')$, we expand the symmetrized potential \tilde{V}_q for small q as

$$\tilde{V}_q = V_0 \left[1 - \left(\frac{q}{q_0} \right)^2 + \mathcal{O}(q^4) \right], \quad (48)$$

where the parameter $q_0 \ll k_F$ describes the screening due to the metallic gates near the quantum wire and V_0 is (twice) the $q=0$ Fourier transform of the Coulomb potential cut off by the screening. Setting $q_3 = q_1 \equiv q$ into the three-particle scattering rate [Eq. (42)], we obtain

$$\mathbb{V}(11', 22', 33') \propto V_0^2 \left(\frac{k_F}{q_0} \right)^2 q^2 \quad (49)$$

to lowest order in q . Inserting this into Eq. (46), the final result for the current correction, including both phase-space factors and the momentum dependent scattering rate, becomes

$$I^{\text{int}} \propto e^{-T_F/T} T^8 V_0^4 \left(\frac{k_F}{q_0} \right)^4 \left(\frac{\Delta T}{T} \frac{T_F}{T} + \frac{eV}{k_B T} \right). \quad (50)$$

(Here we noticed that the nonconstant three-particle scattering rate gave rise to four extra powers in temperature.) The detailed calculation given in Appendix B yields a prefactor, and the end result is

$$\begin{aligned} I^{\text{int}} &= \frac{8505}{2048 \pi^4} e^{-T_F/T} \frac{e}{\hbar} \frac{(V_0 k_F)^4}{\varepsilon_F^3} (L k_F) \left(\frac{k_F}{q_0} \right)^4 \left(\frac{T}{T_F} \right)^7 \left(\frac{\Delta T}{T} + \frac{eV}{\varepsilon_F} \right) \\ &+ \mathcal{O} \left[\left(\frac{T}{T_F} \right)^8 \right]. \quad (51) \end{aligned}$$

Combining this result with the zero order in the interaction terms see [Eqs. (4) and (5)], we find for the thermopower and conductance in the low-temperature limit,

$$S = \frac{k_B T_F}{e T} e^{-T_F/T} \left(1 + \frac{L}{\ell_{ee}} \right), \quad (52)$$

$$G = \frac{2e^2}{h} - \frac{2e^2}{h} e^{-T_F/T} \left(1 + \frac{L}{\ell_{eee}} \right). \quad (53)$$

Here, we introduced the effective length ℓ_{eee} by the relation²⁴

$$\ell_{eee}^{-1} = \frac{8505}{2048\pi^3} \frac{(V_0 k_F)^4}{\varepsilon_F^4} \left(\frac{k_F}{q_0} \right)^4 \left(\frac{T}{T_F} \right)^7 k_F, \quad (54)$$

which may be viewed as a mean free path with respect to backscattering for a hole near the bottom of the band.

To recapitulate, the temperature dependence $T \propto T^7$ in Eq. (54) can be understood in the following way: the three-particle scattering of a single particle leaves five free momenta, and since two are taken by energy and momentum conservation this gives T^3 . In addition, the interaction, V_q , is proportional to q^2 , and when squared it gives rise to four more powers, which results in the T^7 dependence.

In the limit of a pointlike interaction, $q_0 \rightarrow \infty$, the corrections are zero in agreement with the result of Sec. III A.

It is known from the Luttinger liquid theory that in the limit of linear spectrum, which corresponds to $T_F \rightarrow \infty$, the conductance remains finite even if the wire is infinitely long ($L \rightarrow \infty$). Therefore, it is tempting to speculate that the two terms in the square brackets of Eq. (53) are the first terms of an expansion in $\lambda = L/\ell_{eee}$ of some function $F_G(\lambda)$ which saturates at a constant value in the limit $\lambda \rightarrow \infty$. One may also have a similar speculation generalizing Eq. (52) for the thermopower, $[\dots] \rightarrow F_S(L/\ell_{eee})$.

As a final remark, we note that the so-called Mott formula²⁵ relating the thermopower to the low-temperature conductance,

$$S = \frac{\pi^2 k_B}{3e} k_B T \frac{1}{G} \frac{dG}{d\varepsilon_F}, \quad (55)$$

is clearly violated by Eqs. (53) and (52). This violation could be expected because the conventional derivation of the Mott formula (for the noninteracting case) assumes that the main contribution to the conductance *and* thermopower comes from the states around the Fermi level in an energy interval of the order of temperature.²⁶ However, in the considered case the main contribution to S comes from the “deep” states, even in the zeroth order with respect to the interaction potential. Correspondingly, there is no surprise that Eqs. (52) and (53) being substituted, respectively, in the left- and right-hand sides of Eq. (55) produce a parametrically large mismatch $\sim T_F/T$.

V. SUMMARY AND DISCUSSION

We have calculated the leading interaction correction to the transport properties of a clean mesoscopic wire adiabatically connected to the leads, using perturbation theory in the length of the wire.

For a single-mode wire, the leading interaction corrections turns out to be given by three-particle scattering processes. This is because two-particle processes cannot change the current due to momentum and energy conservation. To calculate the effect of the three-body processes, we have utilized the Boltzmann equation formalism, with three-particle

scattering events defining the collision integral. We have identified the leading-order scattering processes and found that they involve at least one state near the bottom of the band, i.e., far from the Fermi level. The involvement of such “deep” states results in an exponentially small, $\propto e^{-T_F/T}$, interaction-induced correction to thermopower and conductance at low temperatures.

The account for interaction in this paper is performed for relatively short wires, where perturbation theory in the interaction or equivalently in the wire length is valid. For longer wires, one needs to find the distribution function by treating the collision integral in the Boltzmann equation nonperturbatively. It is not clear whether the relaxation of the distribution function would instead yield nonexponential corrections to the transport coefficients for longer wires. However, since the scattering processes that contribute to the current must involve a particle that changes direction (which is proven in Appendix A), one might speculate that the exponential suppression is valid for all lengths, as long as electron-electron scattering is the only active relaxation mechanism.

The question of what the relaxed distribution function looks like for a mesoscopic wire is an interesting and unsolved problem. Here, we have only given a partial answer for the leading contributions for a short wire, i.e., to lowest order in the interaction. Further studies should involve a self-consistent determination of the distribution function.

Since thermopower is sensitive to the electron distribution function, it might be a good experimental tool for answering the fundamental questions regarding the effect of electron-electron collisions. Indeed, refined measurements of thermopower of short 1D quantum wires have been performed, yielding reasonably good agreement with the free-electron theory.^{27–29} It remains an open question whether the accuracy of thermopower measurements is high enough to see the interaction effects in longer wires.

ACKNOWLEDGMENTS

We acknowledge illuminating discussions with M. Garst, A. Kamenev, M. Khodas, T. L. Larsen, and M. Pustilnik. A.M.L. appreciates and enjoyed the hospitality of the William I. Fine Theoretical Physics Institute, University of Minnesota. This work is supported by NSF Grant Nos. DMR 02-37296 and DMR 04-39026.

APPENDIX A: SCATTERING PROCESSES CONTRIBUTING TO THE CURRENT

In this appendix, we show that the particle current changes due to electronic scattering *if and only* if the scattering changes the number of left- and right-moving electrons. In the main text [see Eq. (22)], this was shown to first order in the transition rate, but here we show it to *all orders in the interaction*.

We show it explicitly in the Boltzmann equation framework; however, we suspect it to be a general feature of mesoscopic systems. Intuitively, the statement means that it is the *number* of particles that passes through the mesoscopic system that matters and not their velocity. In contrast to this

is, e.g., a long 1D wire or a bulk metal, where a velocity change of the particles is enough to change the current.

To show the above statement explicitly, we formally rewrite the Boltzmann equation [Eq. (8)] including the boundary conditions [Eq. (9)] as

$$f_k(x) = f_L^0(\epsilon_k) + \int_0^x dx' \frac{\mathcal{I}_{kx'}[f]}{v_k} \quad \text{for } k > 0, \quad (\text{A1})$$

$$f_k(x) = f_R^0(\epsilon_k) + \int_L^x dx' \frac{\mathcal{I}_{kx'}[f]}{v_k} \quad \text{for } k < 0. \quad (\text{A2})$$

Note that this is not a closed solution of the Boltzmann equation, since the distribution function is still contained inside the collision integral. However, this rewriting enables us to find the current without finding the distribution function first, i.e., by inserting Eqs. (A1) and (A2) into the current definition

$$I = \frac{(-e)}{L} \sum_{\sigma k} v_k f_k(x) \quad (\text{A3})$$

and obtain (after a few manipulations)

$$I = \frac{(-e)}{L} \sum_{\sigma k > 0} v_k [f_L^0(\epsilon_k) - f_R^0(\epsilon_k)] - \frac{(-e)}{L} \int_0^L dx \sum_{\sigma k < 0} \mathcal{I}_{kx}[f] + \frac{(-e)}{L} \int_0^x dx' \sum_{\sigma k} \overbrace{\mathcal{I}_{kx'}[f]}^{=0} \equiv I^{(0)} + I^{(\text{int})}, \quad (\text{A4})$$

where the x -dependent part can be seen to be zero by changing variables. We note the cancellation of the velocity in the distribution function [Eqs. (A1) and (A2)] and the current definition [Eq. (A3)], which is the origin of the statement we are showing (as in the first order calculation). A similar cancellation occurs in the Landauer formula, thus relating the transmission to the conductance. By using the explicit form of the collision integral Eq. [(10)], the current from the interactions is

$$I^{(\text{int})} = \frac{(-e)}{L} \int_0^L dx \sum_{\substack{\sigma_1 \sigma_2 \sigma_3 \\ \sigma_1' \sigma_2' \sigma_3'}} \sum_{\substack{k_1 < 0, k_2, k_3 \\ k_1' k_2' k_3'}} W_{123;1'2'3'} [f_1 f_2 f_3 (1 - f_{1'}) \times (1 - f_{2'}) (1 - f_{3'}) - f_{1'} f_{2'} f_{3'} (1 - f_1) (1 - f_2) (1 - f_3)]. \quad (\text{A5})$$

We can divide the summation over k quantum number into positive and negative intervals as in the main text (see Sec. II B). The essential point is now that all terms that have the same number of positive (and negative) intervals for the primed and unprimed wave numbers k are zero. In other words, if the number of left- and right-moving electrons does not change, then the contribution is zero by symmetry of the transition rate. We show this cancellation in practice by an example [using the notation of Eq. (21)],

$$\begin{aligned} & \sum_{\text{spin } \begin{smallmatrix} + & + & - \\ - & + & - \end{smallmatrix}} \sum W_{123;1'2'3'} [f_1 f_2 f_3 (1 - f_{1'}) (1 - f_{2'}) (1 - f_{3'}) - f_{1'} f_{2'} f_{3'} (1 - f_1) (1 - f_2) (1 - f_3)] \\ &= \sum_{\text{spin } \begin{smallmatrix} + & + & - \\ - & + & - \end{smallmatrix}} \sum W_{123;1'2'3'} [f_1 f_2 f_3 (1 - f_{1'}) (1 - f_{2'}) (1 - f_{3'}) - f_{1'} f_{2'} f_{3'} (1 - f_1) (1 - f_2) (1 - f_3)] \\ &= \sum_{\text{spin } \begin{smallmatrix} + & + & - \\ - & + & - \end{smallmatrix}} \sum W_{123;1'2'3'} f_1 f_2 f_3 (1 - f_{1'}) (1 - f_{2'}) (1 - f_{3'}) - \sum_{\text{spin } \begin{smallmatrix} + & + & - \\ - & + & - \end{smallmatrix}} \underbrace{\sum W_{123;1'2'3'} f_{1'} f_{2'} f_{3'} (1 - f_1) (1 - f_2) (1 - f_3)}_{\text{interchange } (123) \leftrightarrow (1'2'3')} = 0, \end{aligned} \quad (\text{A6})$$

interchanging 1' and 2' at the first equality using $W_{123;1'2'3'} = W_{123;2'1'3'}$ and interchanging $(123) \leftrightarrow (1'2'3')$ in the second term as indicated. Thereby, we have shown to all orders that to change the current by electronic interactions, the number of left and right movers have to change.

The statement is *not limited* to only three-particle

scattering and can be shown equivalently for pair interaction including several bands, electron-phonon coupling, or any other interaction with the same kind of symmetry under particle interchange. Furthermore, the statement is still true if the collision is nonlocal in space, since that only introduce some spatial integrals in the collision integral that can be

handled similarly. Note, however, that the distribution function can be changed by processes that do not change the number of left and right movers.

APPENDIX B: DETAILED CALCULATION OF THE THERMOPOWER AND CONDUCTANCE CORRECTION DUE TO THE THREE-PARTICLE SCATTERING

The purpose of this appendix is to calculate I^{int} in Eq. (39),

$$I^{\text{int}} \simeq 3(-e) \sum_{\text{spin } ++-} \sum_{+-} \Delta_{123;1'2'3'} \times \left[\frac{\Delta T}{k_B T^2} (-\varepsilon_3 + \varepsilon_{2'} + \varepsilon_{3'} - \varepsilon_F) - \frac{eV}{k_B T} \right], \quad (\text{B1})$$

in the low-temperature limit, $T \ll T_F$, step by step to find the prefactor given in Eq. (51). As already mentioned, we perform the calculation with the scattering process seen in Fig. 2(a) in mind. Therefore, we use the Fermi functions as given in Eq. (40) and the matrix element entering in the scattering rate from Eqs. (41) and (42), i.e. using a quadratic dispersion.

We perform the summation over all the k in Eq. (B1) in the following way. First of all, we note that due to the momentum and energy conservation in the interaction process described, the scattering of k_3 to $k_{3'}$ has to be from above to below the Fermi level, i.e.,

$$k_3 < -k_F < k_{3'} \Rightarrow \theta(-k_F - k_3) \theta(k_F + k_{3'}). \quad (\text{B2})$$

This is due to the signs of k_2 and $k_{2'}$ and can be understood as a sign of the difference between the curvature of the dispersion near the bottom of the band and near the Fermi level. Next, we introduce the momentum transfer around the Fermi level $q_i \equiv k_{i'} - k_i$ for $i=1,3$ and using the momentum conservation to do the $k_{2'}$ summation, we obtain

$$\sum_{++-} (\dots) \rightarrow \sum_{k_1 > 0, k_2 > 0, k_3 < 0} \sum_{q_1, q_3} (\dots), \quad (\text{B3})$$

remembering the constraint $k_{1'} = k_1 + q_1 > 0$, $k_{2'} = k_2 + q_1 + q_3 < 0$, and $k_{3'} = k_3 + q_3 < 0$. The Fermi factors $f_1^0(1-f_{1'}^0)$ and $f_3^0(1-f_{3'}^0)$ restrict the momentum transfer q_1 and q_3 to be much smaller than k_F and the k_1 and k_3 to be near the Fermi level for the process in mind. Therefore, we can use the Fermi functions $f_1^0(1-f_{1'}^0)$ to do the summation over k_1 . Assuming slow variation of the scattering rate over a range of $q_1 \ll k_F$ at the Fermi level, the k_1 summation becomes

$$\sum_{k_1 > 0} \theta(k_F - k_1) \theta(k_1 + q_1 - k_F) = \frac{L}{2\pi} q_1 \theta(q_1). \quad (\text{B4})$$

Similarly, the k_3 summation is done using the phase-space constraint in Eq. (B2),

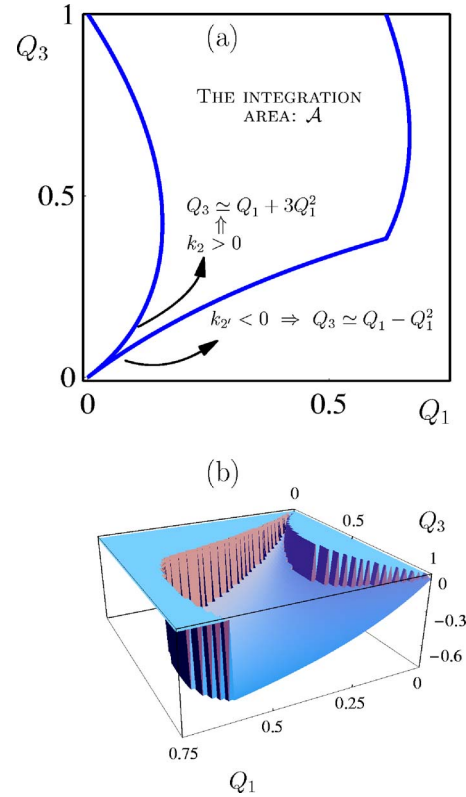


FIG. 4. (Color online) (a) The integration region \mathcal{A} for the integral [Eq. (B13)] to calculate the current due to interactions. The two boundaries for the integration area *close to the origin* stemming from the signs of k_2 and $k_{2'}$ are indicated. (b) The $\Xi(Q_1, Q_3) = \xi(k_F Q_1, k_F Q_3) / \varepsilon_F$ function, a dimensionless version of $\xi(q_1, q_3)$ [Eq. (B9)], important in the calculation using the method of steepest decent.

$$\sum_{k_3 < 0} \theta(-k_F - k_3) \theta(k_F + k_{3'}) = \frac{L}{2\pi} q_3 \theta(q_3). \quad (\text{B5})$$

We see that since k_1 and k_3 are restricted to the Fermi level, we can insert $k_1 \simeq k_F$ and $k_3 \simeq -k_F$ in the rest of the integrand. To do the $k_2 > 0$ summation, we use the energy conservation contained in the scattering rate. It is rewritten as (inserting $k_1 = k_F$ and $k_3 = -k_F$)

$$\delta(\varepsilon_1 + \varepsilon_2 + \varepsilon_3 - \varepsilon_1 - \varepsilon_2 - \varepsilon_3) \simeq \frac{m}{\hbar^2} \frac{1}{|q_1 + q_3|} \times \delta\left(k_2 - k_F \frac{q_1 - q_3}{q_1 + q_3} - \frac{1}{2}(q_1 + q_3) - \frac{1}{2} \frac{q_1^2 + q_3^2}{q_1 + q_3}\right). \quad (\text{B6})$$

We have now done the summation over k_1 , k_2 , and k_3 and are left with the summation over q_1 and q_3 of the scattering rate, some Fermi functions, and the phase factors described above. To this end, we introduce $u(q_1, q_3)$ by inserting $k_1 = k_F$ and $k_3 = -k_F$ in Eq. (42),

$$V(11', 22', 33') = \frac{\delta_{\sigma_1, \sigma_1'} \delta_{\sigma_2, \sigma_2'} \delta_{\sigma_3, \sigma_3'}}{4L^2 \hbar^2 / m} u(q_1, q_3) \quad (\text{B7})$$

for a general symmetrized interaction $\tilde{V}_q = V_q + V_{-q}$.

Furthermore, we collect the exponential tales of the Fermi functions [Eqs. (40b) and (40c)],

$$(1 - f_2^0)f_3^0(1 - f_3^0) = e^{(\varepsilon_2' - \varepsilon_3 + \varepsilon_3' - \varepsilon_F)/k_B T}, \quad (\text{B8})$$

defining

$$\begin{aligned} \xi(q_1, q_3) \equiv & \varepsilon_2' - \varepsilon_3 + \varepsilon_3' = \varepsilon_F \left(\frac{q_1 - q_3}{q_3 + q_1} \right)^2 - \frac{1}{2} \hbar v_F (q_1 + q_3) \\ & + \frac{1}{2} \hbar v_F \frac{(q_1 - q_3)(q_1^2 + q_3^2)}{(q_3 + q_1)^2} \\ & + \frac{\hbar^2}{2m} \frac{q_3^2(2q_1^2 + 2q_1q_3 + q_3^2)}{(q_1 + q_3)^2}, \end{aligned} \quad (\text{B9})$$

inserting $k_2' = k_2 - q_1 - q_3$, k_2 from the energy conservation Eq. (B6) and $k_1 = k_F$ and $k_3 = -k_F$. Therefore, we finally get the interacting contribution to the current in Eq. (B1) as

$$\begin{aligned} I^{\text{int}} = & \frac{3(-e)Lm^3}{32\pi^4\hbar^7} \int_0^\infty dq_1 \int_0^\infty dq_3 \frac{q_1 q_3}{q_1 + q_3} |u(q_1, q_3)|^2 \\ & \times \theta(k_F - k_2) \theta(k_2) \theta(-k_2 + q_1 + q_3) \\ & \times \theta(k_F - q_3) e^{(\xi(q_1, q_3) - \varepsilon_F)/k_B T} \\ & \times \left\{ \frac{\Delta T}{k_B T^2} [\xi(q_1, q_3) - \varepsilon_F] - \frac{eV}{k_B T} \right\}. \end{aligned} \quad (\text{B10})$$

Here, only the step functions that restricts the integral are included. Next, we introduce the dimensionless integration variables $Q_i = q_i/k_F$ for $i=1, 3$ and the dimensionless functions

$$U(Q_1, Q_3) = k_F^2 u(k_F Q_1, k_F Q_3), \quad (\text{B11})$$

$$\Xi(Q_1, Q_3) = \frac{\xi(k_F Q_1, k_F Q_3)}{\varepsilon_F} \quad (\text{B12})$$

in the integral

$$\begin{aligned} I^{\text{int}} = & \frac{3(-e)Lm^3}{32\pi^4\hbar^7 k_F} e^{-T_F/T} \int_{\mathcal{A}} dQ_1 dQ_3 \frac{Q_1 Q_3}{Q_1 + Q_3} |U(Q_1, Q_3)|^2 \\ & \times e^{\Xi(Q_1, Q_3)T_F/T} \left\{ \frac{T_F \Delta T}{T^2} [\Xi(Q_1, Q_3) - 1] - \frac{eV}{k_B T} \right\}, \end{aligned} \quad (\text{B13})$$

where \mathcal{A} is the integration area shown in Fig. 4(a). Note that this expression is valid for a general interaction \tilde{V}_q and that it

is not possible to extract a power law in temperature times some integral by defining new integration variables.

To proceed, we consider the low-temperature limit $T/T_F \ll 1$ by using the method of steepest decent. Due to the exponential function $e^{\Xi(Q_1, Q_3)T_F/T}$, the maximum of $\Xi(Q_1, Q_3)$ will dominate the integral for $T/T_F \rightarrow 0$, since $\Xi(Q_1, Q_3) \leq 0$. The maxima are $\Xi(0, 0) = 0$ and $\Xi(0, 1) = 0$, and $\Xi(Q_1, Q_3)$ is shown in Fig. 4(b). For a decreasing interaction, the area of $Q_1 \ll 1$ and $Q_3 \ll 1$ dominates even though the integrand is zero for $Q_1 = Q_3 \rightarrow 0$. Therefore, we expand around the maximum $(Q_1, Q_3) = (0, 0)$ to get the lowest-order result in T/T_F . In view of the integration region [Fig. 4(a)], we use $Q_3 = Q_1 \equiv Q$ in the integral [Eq. (B13)] and thereby do the Q_3 integral using the approximate limits seen in Fig. 4(a), i.e.,

$$\int_{Q_1 - Q_1^2}^{Q_1 + 3Q_1^2} 1 dQ_3 = 4Q_1^2. \quad (\text{B14})$$

To model the symmetrized potential \tilde{V}_q for small q , we include the deviation from a constant, as described in Eq. (48). This gives

$$\frac{Q_1 Q_3}{Q_1 + Q_3} |U(Q_1, Q_3)|^2 \Big|_{Q_3 = Q_1 = Q} \rightarrow V_0^4 \left(\frac{k_F}{q_0} \right)^4 \frac{9}{2} Q^5 \quad (\text{B15})$$

to lowest order in Q . In the exponential, we keep Ξ to lowest order in Q , i.e.,

$$e^{\Xi(Q_1, Q_3)T_F/T} \rightarrow e^{-2QT_F/T}. \quad (\text{B16})$$

So using the lowest order in Q in the integrand (leading to lowest order in T), the interacting contribution to the current is

$$\begin{aligned} I^{\text{int}} = & \frac{3(-e)Lm^3}{32\pi^4\hbar^7 k_F} e^{-T_F/T} \int_0^\infty dQ V_0^4 \left(\frac{k_F}{q_0} \right)^4 \frac{9}{2} Q^5 4Q^2 e^{-2QT_F/T} \\ & \times \left[\frac{T_F \Delta T}{T^2} (0 - 1) - \frac{eV}{k_B T} \right] \end{aligned} \quad (\text{B17})$$

$$\simeq \frac{8505}{2048\pi^4} e^{-T_F/T} \frac{e}{\hbar} \frac{(V_0 k_F)^4}{\varepsilon_F^3} (Lk_F) \left(\frac{k_F}{q_0} \right)^4 \left(\frac{T}{T_F} \right)^7 \left(\frac{\Delta T}{T} + \frac{eV}{\varepsilon_F} \right) \quad (\text{B18})$$

to lowest order in temperature. This is the result stated in the text in Eq. (51).

¹B. J. van Wees, H. van Houten, C. W. J. Beenakker, J. G. Williamson, L. P. Kouwenhoven, D. van der Marel, and C. T. Foxon, Phys. Rev. Lett. **60**, 848 (1988).

²D. A. Wharam, T. J. Thornton, R. Newbury, M. Pepper, H. Ahmed, J. E. F. Frost, D. G. Hasko, D. C. Peacock, D. A. Ritchie, and G. A. C. Jones, J. Phys. C **21**, L209 (1988).

³L. I. Glazman, G. B. Lesovik, D. E. Khmelnitskii, and R. I. Shek-

hter, JETP Lett. **48**, 238 (1988).

⁴A. M. Chang, Rev. Mod. Phys. **75**, 1449 (2003).

⁵M. P. A. Fisher and L. I. Glazman, in *Mesoscopic Electron Transport*, NATO Advanced Studies Institute, Series E: Applied Science, edited by G. S. L. Kowenhoven and L. Sohn (Kluwer Academic, Dordrecht, 1997).

⁶D. L. Maslov, arXiv:cond-mat/0506035 (unpublished).

- ⁷N. A. Mortensen, K. Flensberg, and A.-P. Jauho, Phys. Rev. Lett. **86**, 1841 (2001).
- ⁸M. Pustilnik, E. G. Mishchenko, L. I. Glazman, and A. V. Andreev, Phys. Rev. Lett. **91**, 126805 (2003).
- ⁹B. Y.-K. Hu and K. Flensberg, in *Hot Carriers in Semiconductors (HCIS-9)*, edited by K. Hess, J. P. Leburton, and U. Ravaioli (Plenum, New York, 1996), p. 421.
- ¹⁰This statement is still true for all 1D bands with positive curvature (e.g., like $\varepsilon_k \propto k^4$ or $\varepsilon_k \propto k^2 + ak^4$ for $a > 0$). A special case is linear dispersion where two-particle collisions *can* change the distribution. However, even for this case the two-particle collisions *cannot* change the number of left and right movers and hence not the current, as shown in Appendix A.
- ¹¹Bill Sutherland, *Beautiful Models* (World Scientific, Singapore, 2004), Secs. 1.3–1.5.
- ¹²A related recent work studied a different aspect of three-particle processes, namely, their influence on the spectral function of 1D fermions, M. Khodas, M. Pustilnik, A. Kamenev, and L. I. Glazman, arXiv:cond-mat/0702505 (unpublished).
- ¹³A. M. Lunde, K. Flensberg, and L. I. Glazman, Phys. Rev. Lett. **97**, 256802 (2006).
- ¹⁴H. van Houten, L. W. Molenkamp, C. W. J. Beenakker, and C. T. Foxon, Semicond. Sci. Technol. **7**, B215 (1992).
- ¹⁵Y. V. Sharvin, Zh. Eksp. Teor. Fiz. **48**, 984 (1965) [Sov. Phys. JETP **21**, 655 (1965)].
- ¹⁶V. L. Gurevich, V. B. Pevzner, and K. Hess, Phys. Rev. B **51**, 5219 (1995).
- ¹⁷H. Akera and T. Ando, Phys. Rev. B **41**, 11967 (1990).
- ¹⁸V. L. Gurevich, V. B. Pevzner, and E. W. Fenton, J. Phys.: Condens. Matter **10**, 2551 (1998).
- ¹⁹Y. M. Sirenko, V. Mitin, and P. Vasilopoulos, Phys. Rev. B **50**, 4631 (1994).
- ²⁰C. N. Yang, Phys. Rev. **168**, 1920 (1968).
- ²¹E. H. Lieb and W. Liniger, Phys. Rev. **130**, 1605 (1963).
- ²²See, e.g., M. A. Cazalilla, Phys. Rev. A **67**, 053606 (2003). The interaction potential between fermions is written there in a slightly different form, which, however, can be reduced [M. Khodas, A. Kamenev, and L. I. Glazman (unpublished)] to the one we present in the text.
- ²³We assume that electrons in the channel produce some image charges in a distant gate. As the result, the Coulomb interaction is cut off at some distance $\sim 2\pi/q_0$ large compared to the Fermi wavelength.
- ²⁴Note here that the sign of the conductance correction is negative even though there is a positive sign in Eq. (51). This is due to the way the bias is defined the left contact having the higher chemical potential.
- ²⁵N. F. Mott and H. Jones, *The Theory of the Properties of Metals and Alloys*, 1st ed. (Clarendon, Oxford, 1936).
- ²⁶Surprisingly, Mott formula still yields a reasonably good approximation for thermopower even if the temperature is comparable to the energy scale over which the transmission amplitude changes value, see A. M. Lunde and K. Flensberg, J. Phys.: Condens. Matter **17**, 3879 (2005).
- ²⁷L. W. Molenkamp, H. van Houten, C. W. J. Beenakker, R. Eppenga, and C. T. Foxon, Phys. Rev. Lett. **65**, 1052 (1990).
- ²⁸L. W. Molenkamp, Th. Gravier, H. van Houten, O. J. A. Buijk, M. A. A. Mabesoone, and C. T. Foxon, Phys. Rev. Lett. **68**, 3765 (1992).
- ²⁹N. J. Appleyard, J. T. Nicholls, M. Y. Simmons, W. R. Tribe, and M. Pepper, Phys. Rev. Lett. **81**, 3491 (1998).

Paper IV

Anders Mathias Lunde, Alessandro De Martino,
Reinhold Egger and Karsten Flensberg:

Electron-electron interaction effects in quantum point contacts

Submitted. (cond-mat/07071989).

Notes:

1. The definition of T^* in the thesis and in the paper differs by a numerical prefactor, however, the idea is the same.
2. In reference [24], we should have stated that $\varepsilon_0 = \varepsilon_F - \text{Re}[\Sigma^r(00, \omega)]$.

Electron-electron interaction effects in quantum point contacts

Anders Mathias Lunde,¹ Alessandro De Martino,² Reinhold Egger,² and Karsten Flensberg¹

¹ *Nano-Science Center, Niels Bohr Institute, University of Copenhagen, DK-2100 Copenhagen, Denmark*

² *Institut für Theoretische Physik, Heinrich-Heine-Universität, D-40225 Düsseldorf, Germany*

(Dated: July 13, 2007)

We consider interaction effects in quantum point contacts on the first quantization plateau, taking into account all non momentum-conserving processes. We compute low-temperature linear and non-linear conductance, shot noise, and thermopower by perturbation theory, and show that they are consistent with experimental observations on the so-called "0.7 anomaly". The full temperature-dependent conductance is obtained from self-consistent second-order perturbation theory and approaches $\approx e^2/h$ at higher temperatures, but still smaller than the Fermi temperature.

PACS numbers: 72.10.-d, 73.23.-b, 72.10.Fk

Conductance quantization in a quantum point contact (QPC), first observed in 1988 [1], constitutes a classic textbook effect of mesoscopic physics. On top of the integer conductance plateaus $G = nG_0$ (where $G_0 = 2e^2/h$) observed as a function of gate voltage V_g , many experiments have pointed to the existence of a so-called "0.7 anomaly" in the conductance and other transport quantities [2, 3, 4, 5, 6]. Most prominently, the 0.7 anomaly implies a shoulder-like feature in the conductance $G(V_g)$ around $G \approx 0.7 G_0$ seen at elevated temperature T (or finite voltage V) near the first quantized plateau [2, 3, 4], accompanied by a shot noise reduction [6]. Given the conceptual simplicity of a QPC and the fact that the 0.7 anomaly has been observed in a variety of material systems by different groups over more than a decade, it is quite amazing that still no generally accepted microscopic theory exists, apart from an overall consensus that one is dealing with some spin-related many-body effect. Such a theory should be able to explain all the experimental data in a unified and physically consistent manner.

While phenomenological models [7], assuming the existence of a density-dependent spin gap, can provide rather good fits to experimental data, the presumed static spin polarization due to interactions within the *local* QPC region is not expected in the presence of unpolarized *bulk* reservoirs. Recently it was also pointed out that spin symmetry-broken mean-field theory is unable to recover the correct T dependence of the conductance [8]. Other proposals assume the existence of a quasi-bound state in the QPC region, leading to a Kondo-type scenario as encountered in transport through interacting quantum dots [9, 10]. Such a quasi-bound state was indeed found in spin density functional theory (SDFT) calculations [9], but other SDFT works did not reach such conclusions [11]. Further proposals involve phonon effects [12]. Several publications have suggested that taking into account only electron-electron (e-e) interactions may result in a reduced conductance at elevated temperatures, without the need for additional assumptions of spin polarization or a localized state [13, 14, 15, 16, 17]. However, a physically consistent picture explaining the temperature, voltage, and magnetic field dependence of the conductance,

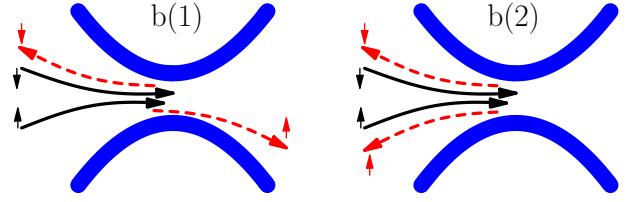


FIG. 1: (Color online) Illustration of the two-electron non momentum-conserving scattering processes that give rise to a correction to the transport properties at the beginning of the first plateau. The full (black) lines represent incoming electrons, while the dashed (red) lines are the outgoing electrons. The thick (blue) lines define the edge of the QPC. Only scattering between different spins is present to leading order in T/T_F due to the Pauli principle.

as well as thermopower and noise experiments, is still lacking. In this paper, we show that a careful consideration of *non momentum-conserving* e-e interaction processes in QPCs may allow for a consistent theory of the 0.7 anomaly.

The lack of momentum conservation in e-e scattering processes is due to an emerging lack of translational invariance relevant for the low density regime $k_F L \sim 1$, where k_F is the local Fermi momentum and L a typical interaction length-scale of the QPC (see below). Therefore this effect is dominant at the onset of the plateau and gradually disappears for larger electron density in the QPC. We will focus on the first conductance plateau, where the QPC has only one open channel (1D mode) [18, 19]. Now e-e interactions give the contribution

$$H_I = \frac{1}{2} \sum_{\sigma\sigma'} \int dx dx' W(x, x') \Psi_{\sigma}^{\dagger}(x) \Psi_{\sigma'}^{\dagger}(x') \Psi_{\sigma'}(x') \Psi_{\sigma}(x) \quad (1)$$

to the Hamiltonian, where $\Psi_{\sigma}(x)$ is the 1D electron field operator for spin $\sigma = \uparrow, \downarrow$. The pair potential $W(x, x')$ takes into account screening processes due to closed channels and nearby gates, as well as semiclassical slowing down [17], and therefore depends not only on the relative coordinate $x - x'$ but also on the center of mass $X = (x + x')/2$. In fact, the range of the interaction

$W(X)$ is determined by the above length-scale L . The e-e interaction now enters the 1D description in two different ways. There are (i) one-particle effects described through a self-consistent potential, given by the real part of the self energy (in the simplest case, this is the Hartree-Fock potential). At $T = 0$, the imaginary part of the self energy for our Fermi liquid starting point is zero [20], and the plateau then occurs where the open channel suffers no backscattering. This part is thus already contained in the potential forming the QPC. In addition, at finite T , we have (ii) inelastic e-e scattering processes, which are the focus of our work and give rise to a reduced conductance by changing the number of left- and right-movers, and hence the current. This is illustrated in Fig. 1, where two important types of non momentum-conserving scattering events are illustrated. Process b(2) describes the simultaneous backscattering of two electrons with opposite spins and has been discussed on a perturbative level in Ref. [14]. The process b(1), where a single electron is backscattered, has not been studied before. On top of these two, there are e-e forward scattering and backscattering processes (momentum-conserving in a long 1D wire). While high- T transport properties are affected by all interactions, we show now that the leading low- T behavior is *fully* determined by the two processes in Fig. 1.

Let us calculate the non-linear conductance, the thermopower, and the shot noise to leading order in the interaction. Perturbation theory gives the *interaction correction to the current* (here, $\hbar = 1$ and $e > 0$)

$$\frac{I(V, T)}{G_0 V} = 1 - (A_{b(1)} + A_{b(2)}) (\pi T / T_F)^2 - (A_{b(1)}/4 + A_{b(2)}) (eV / \varepsilon_F)^2 + \mathcal{O}(W^3), \quad (2)$$

with coefficients $A_{b(1,2)} = W_{b(1,2)}^2 k_F^4 / (48\pi^2 \varepsilon_F^2)$ corresponding to the b(1) and b(2) processes, where $\varepsilon_F = k_B T_F$ is the Fermi energy and $W_{b(1,2)} = \int dx dx' W(x, x') e^{ik_F(x+x')} e^{ik_F(x \mp x')}$. Already at this point, we observe a correspondence to experimental observations, namely the reduced conductance I/V with increasing T and/or V . Furthermore, to leading order in T/T_F , where all scattering happens at the Fermi level, only opposite spins interact due to the Pauli principle: for equal spins, the exchange term tends to cancel the direct term. As a consequence, we can also understand the behavior at *large magnetic fields*, where the $T = 0$ plateau occurs at e^2/h . In that case, to order $(T/T_F)^2$ no interaction renormalization of the conductance arises [21]. This is consistent with experiments, where no suppression is observed at the half-plateaus.

Another experimental observable probing the enhanced phase space for e-e scattering at higher T is the *thermopower* $\mathcal{S}(T)$ [22], for which perturbation theory predicts

$$\mathcal{S}(T) = \frac{k_B}{e} \frac{2\pi^4}{5} (A_{b(1)} + A_{b(2)}) (T/T_F)^3. \quad (3)$$

Since the non-interacting thermopower is exponentially small [$\propto \exp(-T_F/T)$] at the conductance plateau, the interaction correction completely determines the low-temperature thermopower [23]. The enhanced thermopower (as compared to the non-interacting one) is in qualitative agreement with experiments at the anomalous plateau [5].

Next we calculate consequences for another observable, namely non-equilibrium noise. The zero-frequency *shot noise* follows from the (symmetrized) two-point correlation function of the current operator. Perturbation theory yields for the backscattering noise power

$$S_B(V, T) = 2e \left[2I_{bs(2)}(V, T) \coth(eV/k_B T) + I_{bs(1)}(V, T) \coth(eV/2k_B T) \right], \quad (4)$$

where $I_{bs(1,2)}$ are the current corrections due to $W_{b(1,2)}$ quoted in Eq. (2) (defined positive for $V > 0$). This is nothing but the famous Schottky shot noise relation, encoding the charge of the backscattered particles. Equation (4) predicts an additional factor of two for the b(2) contribution, because two electrons are backscattered in that event [14]. Direct calculation then yields the full noise power of the transmitted current as $S_T = S_B + 4G_0 k_B T - 8k_B T \partial_V I_{bs}$, where $I_{bs} = I_{bs(1)} + I_{bs(2)}$. Recent noise measurements on the first quantized plateau were compared to the corresponding single-particle picture [6], and a reduced noise power was observed on the conductance anomaly. For that comparison, one subtracts the thermal noise and defines the excess noise as $S_I = S_T - 4G(V, T)k_B T$. For a non-interacting system, $S_I^{SP} = 2G_0 R \{eV \coth(eV/2k_B T) - 2k_B T\}$ to lowest order in the reflection coefficient $R = I_{bs}/G_0 V$, see Ref. [6]. Thus the difference between the true excess noise and its single-particle value is

$$\frac{S_I - S_I^{SP}}{2G_0 eV (T/T_F)^2} = -2A_{b(1)} \frac{eV}{k_B T} + A_{b(2)} h(eV/k_B T), \quad (5)$$

where $h(x) = -8x + (\pi^2 + x^2) \tanh(x/2)$. This expression shows that for $eV < 6.507 k_B T$, regardless of $A_{b(1,2)}$, the measured noise is always smaller than predicted by a single-particle analysis. This situation corresponds to the experimental work of Ref. [6], where $eV \lesssim 5k_B T$.

It is clear from all these perturbative results that for low energies, $V, T \rightarrow 0$, all interaction effects disappear. The perturbation theory results presented above, however, obviously break down at higher temperatures or voltages. From Eq. (2), we find the temperature scale for this crossover to a strong-interaction regime,

$$k_B T^* \approx \frac{\varepsilon_F}{\sqrt{A_b}} \propto \frac{\varepsilon_F^2}{W_b k_F^2}, \quad (6)$$

where $A_b = A_{b(1)} + A_{b(2)}$ and $W^2 = W_{b(1)}^2 + W_{b(2)}^2$. Contrary to the usual situation encountered in mesoscopic physics, the nontrivial question to be answered thus concerns the *high-temperature* limit (but still $T \ll T_F$). To

make progress in the relevant temperature regime

$$T^* \lesssim T \ll T_F, \quad (7)$$

let us consider a simplified model pair potential entering Eq. (1), see Ref. [17],

$$W(x, x') = V_0 \delta(x) \delta(x'), \quad (8)$$

which implies $W_{b(1)} = W_{b(2)}$. We express the interaction strength in the dimensionless parameter $\lambda = mV_0/2\pi^{3/2}$. Estimates for λ in GaAs heterostructures gives $\lambda \approx 1$, see Refs. [8, 17], which then yields $k_B T^*/T_F \approx 0.1$ allowing for a study of the temperature range (7).

In order to treat the local interaction (8), we start from the Dyson equation for the full Keldysh single-particle Green's function (GF) $\mathbf{G}(x, x'; \omega)$,

$$\mathbf{G}(x, x'; \omega) = \mathbf{G}_0(x, x'; \omega) + \mathbf{G}_0(x, 0; \omega) \mathbf{\Sigma}(\omega) \mathbf{G}(0, x'; \omega), \quad (9)$$

which is a 2×2 matrix in Keldysh space. The self energy due to Eq. (8) acts only at $x = x' = 0$. Note that $\mathbf{G}_\uparrow = \mathbf{G}_\downarrow$, i.e., we can suppress the spin index. For simplicity, we now assume a parabolic dispersion, $\varepsilon_k = k^2/2m$, for the open channel. The charge current operator is $I = \frac{ie}{2m} \sum_\sigma [\Psi_\sigma^\dagger(x) \partial_x \Psi_\sigma(x) - (\partial_x \Psi_\sigma^\dagger(x)) \Psi_\sigma(x)]$, and we evaluate $\langle I \rangle$ at $x = 0$, where it can be expressed in terms of the local GF $\mathbf{G}(\omega) \equiv \mathbf{G}(0, 0; \omega)$ and the self energy $\mathbf{\Sigma}(\omega)$. In fact, some algebra shows that only the local spectral function $A(\omega) = -2 \text{Im} G^r(\omega)$ enters the current formula for the contact interaction (8),

$$I = \frac{2e}{h} \int_0^\infty d\omega [f_R^0(\omega) - f_L^0(\omega)] \frac{A(\omega)}{A_0(\omega)}, \quad (10)$$

where $f_{R/L}^0$ are Fermi functions in the right/left lead, and $A_0(\omega) = 2\pi d(\omega)$ is the non-interacting spectral function. Here, $d(\omega)$ is the density of states $2\pi d(\omega) = (2m/\omega)^{1/2} \theta(\omega)$. Remarkably, the nonequilibrium current through the interacting QPC is thereby fully expressed in terms of the local retarded GF only. So far, the given relations are exact, but to make progress, one needs to approximate the self energy. We take the full *second-order self energy*,

$$\begin{aligned} \Sigma^r(\omega) = & V_0^2 \int_0^\infty dt e^{i\omega t} [G^<(-t)G^>(t)G^>(t) \\ & - G^>(-t)G^<(t)G^<(t)], \end{aligned} \quad (11)$$

and make it self-consistent by using the interacting (lesser/greater) GFs. The corresponding diagrams are shown in the inset to Fig. 2. The approximation (11) is the simplest way to describe equilibration between left- and right-moving electrons in an interacting QPC. In what follows, we confine ourselves to the linear conductance regime, where the spectral function in Eq. (10) can be calculated in equilibrium by solving Eq. (11), and where we can replace $f_R^0 - f_L^0 \rightarrow eV[-\partial_\omega f(\omega)]$, where $f(\omega)$ is the Fermi function. In linear response, the

lesser/greater GFs can be written in terms of the local spectral function $A(\omega)$,

$$G^{</>}(t) = \pm i \int_0^\infty \frac{d\omega}{2\pi} e^{-i\omega t} A(\omega) f(\pm\omega). \quad (12)$$

This suggests a natural iterative way to self-consistently solve for the conductance: Starting with the initial guess $A(\omega) = A_0(\omega)$, one computes $\Sigma^r(\omega)$ from Eq. (11), which in turn defines a new retarded GF and a new guess for $A(\omega)$. This procedure is iterated until convergence has been reached. For the parameters below, this numerical scheme is convergent and can be implemented in an efficient manner.

The numerical results, for $\lambda = 0.8$ shown in Fig. 2, accurately reproduce the above perturbative results at low T , but also allow to cover the interesting high-temperature limit. Our data for different λ fall to high accuracy on the simple function

$$\frac{G(T)}{G_0} = b + \frac{1-b}{1+(T/T_\lambda^b)^2}, \quad (13)$$

where b sets the high-temperature saturation value. While this functional dependence is somewhat similar to the phenomenological Kondo-type function used in Ref. [4], our numerical data fit better to Eq. (13). It is also possible to obtain equally good fits to the activated T dependence reported in Ref. [3], see also Ref. [7],

$$\frac{G(T)}{G_0} = 1 - (1-a)e^{-T_\lambda^a/T}, \quad (14)$$

where a again denotes the high- T limit. The values for T_λ^b and T_λ^a extracted from best fits to our numerical data are summarized in the inset in Fig. 2. Remarkably, both temperature scales are of the same order. Moreover, they are lowered by increasing the interaction strength λ . For high T , the conductance appears to approach the saturation value $G \approx e^2/h$. Similar saturation value has also been reported for *long* wires [13], with the same $T = 0$ conductance G_0 . The new feature for QPCs comes from the non-momentum conserving interactions, resulting in a distinct low-to-intermediate temperature dependence $G(T)$. The perturbative T^2 correction is not present in the long wire results [13], but is seen experimentally [4].

As a final remark on the numerical solution of the self-consistent approach, we mention that thermopower (data not shown) exhibits a crossover from the $\mathcal{S} \propto T^3$ law at low T , see Eq. (3), to a linear-in- T behavior at elevated temperatures.

It is also instructive to discuss our model in terms of an Anderson model. For the model pair potential (8), by spatial discretization our Hamiltonian maps to a 1D tight-binding chain with hopping matrix elements t and on-site interaction U acting at one site ($x = 0$) only [24]. We thus arrive at an Anderson-type impurity model, similar to the one used in Ref. [9] to describe interactions in a QPC in the Kondo regime. However, we consider a rather

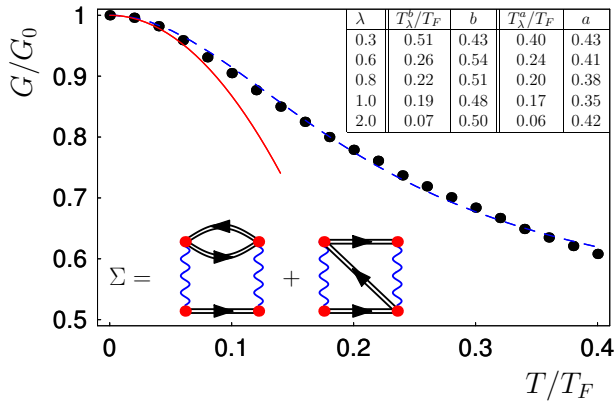


FIG. 2: (Color online) Temperature dependence of the linear conductance G for $\lambda = 0.8$. Dots denote self-consistent numerical results, the solid curve gives the perturbative estimate (2), and the dotted curve is a fit to Eq. (13). Inset: Fit parameters entering best fits of Eqs. (13) and (14) to numerical data for $T/T_F < 0.4$. Note that a and b are somewhat different. The lower inset shows the two second order self-consistent energy diagrams in Eq. (11).

different parameter regime, where U is of the same order as the hybridization Γ and can be parametrically larger than the bandwidth $D \sim |t|$. Employing Eq. (6), with $\varepsilon_F \approx D$, the interesting temperature range (7) translates to $D^2/U \ll k_B T \ll D$, where our claim is that G approaches $\approx e^2/h$. While the Kondo model requires the formation of a local moment, this is not the case for the

present approach. Instead, our high-temperature limit may be described as an *incoherent Fermi liquid*, with *full relaxation* between left- and right-movers. In fact, one can establish that a simple Boltzmann-type approach has a high-temperature solution where the out-going distribution function is a mixture of the incoming left- and right-mover's distributions. Such an Ansatz leads to the conductance formula (13) with $b = 1/2$, which is the reason for using that as a fitting formula. Unfortunately, a Boltzmann approach is conceptually difficult to justify due to an inherent normalization problem[17], i.e. one cannot define a proper local distribution function in k -space for this model.

In conclusion, we have considered interaction effects in short QPCs and shown that taking into account non momentum-conserving processes, we can qualitatively account for the experimentally observed behavior of the linear and non-linear conductance, thermopower (including their magnetic field dependencies) and shot noise at the so-called 0.7 anomaly. The gate voltage dependence can also be explained within the present scheme, because the backscattering is suppressed for larger values of $k_F L$. In the high-temperature (but still $T \ll T_F$) non-perturbative regime, our second-order self-consistent approach predicts that the conductance approaches $\approx e^2/h$. It is an open and interesting problem to verify this result by other non-perturbative methods.

We thank P. Brouwer, W. Häusler, and J. Paaske for discussions. This work was supported by the SFB TR 12 of the DFG and by the ESF network INSTANS.

-
- [1] D.A. Wharam *et al.*, J. Phys. C **21**, L209 (1988); B.J. van Wees *et al.*, Phys. Rev. Lett. **60**, 848 (1988).
 - [2] K.J. Thomas, J.T. Nicholls, M.Y. Simmons, M. Pepper, D.R. Mace, and D.A. Ritchie, Phys. Rev. Lett. **77**, 135 (1996).
 - [3] A. Kristensen *et al.*, Phys. Rev. B **62**, 10950 (2000).
 - [4] S.M. Cronenwett *et al.*, Phys. Rev. Lett. **88**, 226805 (2002).
 - [5] N.J. Appleyard, J.T. Nicholls, M. Pepper, W.R. Tribe, M.Y. Simmons, and D.A. Ritchie, Phys. Rev. B **62**, R16275 (2000).
 - [6] P. Roche *et al.*, Phys. Rev. Lett. **93**, 116602 (2004); L. DiCarlo *et al.*, Phys. Rev. Lett. **97**, 036810 (2006).
 - [7] H. Bruus, V.V. Cheianov, and K. Flensberg, Physica E **10**, 97 (2001); D.J. Reilly, Phys. Rev. B **72**, 033309 (2005).
 - [8] A. Lassel, P. Schlagheck, and K. Richter, Phys. Rev. B **75**, 045346 (2007).
 - [9] Y. Meir, K. Hirose, and N.S. Wingreen, Phys. Rev. Lett. **89**, 196802 (2002); T. Rejec and Y. Meir, Nature **442**, 900 (2006); S. Ihnatsenka and I.V. Zozoulenko, cond-mat/0701657.
 - [10] P.S. Cornaglia and C.A. Balseiro, Europhys. Lett. **67**, 634 (2004); P.S. Cornaglia, C.A. Balseiro, and M. Avignon, Phys. Rev. B **71**, 024432 (2005).
 - [11] C.K. Wang and K.-F. Berggren, Phys. Rev. B **54**, 14257(R) (1996); A.A. Starikov, I.I. Yakimenko, and K.-F. Berggren, Phys. Rev. B **67**, 235319 (2003).
 - [12] G. Seelig and K.A. Matveev, Phys. Rev. Lett. **90**, 176804 (2003).
 - [13] K.A. Matveev, Phys. Rev. Lett. **92**, 106801 (2004); M. Kindermann and P.W. Brouwer, Phys. Rev. B **74**, 125309 (2006).
 - [14] D. Meidan and Y. Oreg, Phys. Rev. B **72**, 121312 (2005).
 - [15] D. Schmeltzer, A. Saxena, A.R. Bishop, and D.L. Smith, Phys. Rev. B **71**, 045429 (2005).
 - [16] O.F. Syljuåsen, Phys. Rev. Lett. **98**, 166401 (2007).
 - [17] C. Sloggett, A.I. Milstein, and O.P. Sushkov, cond-mat/0606649.
 - [18] L.I. Glazman and R.I. Shekhter, Zh. Eksp. Teor. Fiz. **94**, 292 (1988) [Sov. Phys. JETP **67**, 163 (1988)].
 - [19] Assuming a fully transmitting one-particle potential is not in conflict with the condition $k_F L \sim 1$, since the length L is essentially given by the region with only one subband, see also Ref. [17].
 - [20] J.M. Luttinger, Phys. Rev. **121**, 942 (1961).
 - [21] For a local interaction, the direct and exchange terms cancel to any order in T/T_F . However, for a non-local interaction the cancellation tendency implies that scattering between equal spins is to higher order in (T/T_F) with a reduced prefactor due to the cancellation.
 - [22] H. van Houten, L.W. Molenkamp, C.W.J. Beenakker,

- and C.T. Foxon, *Semicond. Sci. Technol.* **7**, B215 (1992).
- [23] A.M. Lunde, K. Flensberg, and L.I. Glazman, *Phys. Rev. Lett.* **97**, 256802 (2006).
- [24] Again, in order to have perfect transmission at $T = 0$, the one-particle on-site energy must be canceled out, so that $\epsilon_0 = -\text{Re}[\Sigma^r(0)]$ at zero temperature.

Bibliography

- [1] N. Ashcroft and N. Mermin, *Solid State Physics*. Harcourt College Publishers, college ed., 1976.
- [2] Y. Aharonov and D. Bohm, “Significance of electromagnetic potentials in the quantum theory,” *Phys. Rev.*, vol. 115, p. 485, 1959.
- [3] C. W. J. Beenakker and H. van Houten, “Quantum transport in semiconductor nanostructures,” *Solid State Physics*, vol. 44, p. 1, 1991. (cond-mat/0412664).
- [4] B. Altshuler, “Fluctuations in the extrinsic conductivity of disordered conductors,” *JETP Lett.*, vol. 41, p. 648, 1985.
- [5] P. A. Lee and A. D. Stone, “Universal conductance fluctuations in metals,” *Phys. Rev. Lett.*, vol. 55, p. 1622, 1985.
- [6] B. Altshuler and P. Lee, “Disordered electronic systems,” *Phys. Today*, vol. 41, p. 36, 1988.
- [7] A. I. Yanson, G. R. Bollinger, H. E. van den Brom, N. Agraït, and J. M. van Ruitenbeek, “Formation and manipulation of a metallic wire of single gold atoms,” *Nature*, vol. 395, p. 783, 1998.
- [8] A. Yacoby, H. L. Stormer, N. S. Wingreen, L. N. Pfeiffer, K. W. Baldwin, and K. W. West, “Nonuniversal conductance quantization in quantum wires,” *Phys. Rev. Lett.*, vol. 77, p. 4612, 1996.
- [9] B. J. van Wees, H. van Houten, C. W. J. Beenakker, J. G. Williamson, L. P. Kouwenhoven, D. van der Marel, and C. T. Foxon, “Quantized conductance of point contacts in a two-dimensional electron gas,” *Phys. Rev. Lett.*, vol. 60, p. 848, 1988.
- [10] D. A. Wharam, T. J. Thornton, R. Newbury, M. Pepper, H. Ahmed, J. E. F. Frost, D. G. Hasko, D. A. R. D. C. Peacock, and G. A. C. Jones, “One-dimensional transport and the quantisation of the ballistic resistance,” *J. Phys. C*, vol. 21, p. L209, 1988.

- [11] L. I. Glazman, G. B. Lesovik, D. E. Khmelnitskii, and R. I. Shekhter, "Reflectionless quantum transport and fundamental ballistic-resistance steps in microscopic constrictions," *JETP Lett.*, vol. 48, p. 238, 1988.
- [12] L. Kouwenhoven and L. Glazman, "Revival of the kondo effect," *Physics World*, vol. January, p. 33, 2001.
- [13] I. L. Aleiner, P. W. Brouwer, and L. I. Glazman, "Quantum effects in coulomb blockade," *Phys. Rep.*, vol. 358, p. 309, 2002.
- [14] H. Bruus and K. Flensberg, *Many-Body Quantum Theory in Condensed Matter Physics*. Oxford Graduate Texts, New York: Oxford University press, 1st ed., 2004.
- [15] Y. Imry, *Introduction to Mesoscopic Physics*. USA: Oxford University Press, 2nd ed., 2002.
- [16] L. I. Glazman, "Resource letter: Mesp-1: Mesoscopic physics," *American Journal of Physics*, vol. 70, p. 376, 2002.
- [17] A. Kristensen, H. Bruus, A. E. Hansen, J. B. Jensen, P. E. Lindelof, C. J. Marckmann, J. N. rd, C. B. S. rensen, F. Beuscher, A. Forchel, and M. Michel, "Bias and temperature dependence of the 0.7 conductance anomaly in quantum point contacts," *Phys. Rev. B*, vol. 62, p. 10950, 2000.
- [18] H. van Houten and C. W. J. Beenakker, "Quantum point contacts," *Phys. Today*, vol. july, p. 22, 1996. (condmat/0512609).
- [19] B. J. van Wees, L. P. Kouwenhoven, H. van Houten, C. W. J. Beenakker, J. E. Mooij, C. T. Foxon, and J. J. Harris, "Quantized conductance of magnetoelectric subbands in ballistic point contacts," *Phys. Rev. B*, vol. 38, p. 3625, 1988.
- [20] A. Szafer and A. D. Stone, "Theory of quantum conduction through a constriction," *Phys. Rev. Lett.*, vol. 62, p. 300, 1989.
- [21] S. Tarucha, T. Honda, and T. Saku, "Reduction of quantized conductance at low temperatures observed in 2 to 10 μm -long quantum wires," *Solid State Commun.*, vol. 94, p. 413, 1995.
- [22] B. E. Kane, G. R. Facer, A. S. Dzurak, N. E. Lumpkin, R. G. Clark, L. N. Pfeiffer, and K. W. West, "Quantized conductance in quantum wires with gate-controlled width and electron density," *Appl. Phys. Lett.*, vol. 72, p. 3506, 1998.

- [23] C.-T. Liang, M. Y. Simmons, C. G. Smith, D. A. Ritchie, and M. Pepper, "Fabrication and transport properties of clean long one-dimensional quantum wires formed in modulation-doped GaAs/AlGaAs heterostructures," *Appl. Phys. Lett.*, vol. 75, p. 2975, 1999.
- [24] T. Morimoto, M. Henmi, R. Naito, K. Tsubaki, N. Aoki, J. P. Bird, and Y. Ochiai, "Resonantly enhanced nonlinear conductance in long quantum point contacts near pinch-off," *Phys. Rev. Lett.*, vol. 97, p. 096801, 2006.
- [25] U. Sivan and Y. Imry, "Multichannel landauer formula for thermoelectric transport with application to thermopower near the mobility edge," *Phys. Rev. B*, vol. 33, p. 551, 1986.
- [26] H. van Houten, L. W. Molenkamp, C. W. J. Beenakker, and C. T. Foxon, "Thermo-electric properties of quantum point contacts," *Semicond. Sci. Technol.*, vol. 7, p. B215, 1992.
- [27] D. E. Angelescu, M. C. Cross, and M. L. Roukes, "Heat transport in mesoscopic systems," *Superlattices and Microstructures*, vol. 23, p. 673, 1998.
- [28] L. W. Molenkamp, T. Gravier, H. van Houten, O. J. A. Buijk, M. A. A. Mabesoone, and C. T. Foxon, "Peltier coefficient and thermal conductance of a quantum point contact," *Phys. Rev. Lett.*, vol. 68, p. 3765, 1992.
- [29] O. Chiatti, J. T. Nicholls, Y. Y. Proskuryakov, N. Lumpkin, I. Farrer, and D. A. Ritchie, "Quantum thermal conductance of electrons in a one-dimensional wire," *Phys. Rev. Lett.*, vol. 97, p. 056601, 2006.
- [30] L. W. Molenkamp, H. van Houten, C. W. J. Beenakker, R. Eppenga, and C. T. Foxon, "Quantum oscillations in the transverse voltage of a channel in the nonlinear transport regime," *Phys. Rev. Lett.*, vol. 65, p. 1052, 1990.
- [31] N. J. Appleyard, J. T. Nicholls, M. Y. Simmons, W. R. Tribe, and M. Pepper, "Thermometer for the 2d electron gas using 1d thermopower," *Phys. Rev. Lett.*, vol. 81, p. 3491, 1998.
- [32] R. Landauer, "Spatial variation of currents and fields due to localized scatterers in metallic conduction," *IBM J. Res. Dev.*, vol. 1, p. 223, 1957.
- [33] M. Büttiker, "Four-terminal phase-coherent conductance," *Phys. Rev. Lett.*, vol. 57, p. 1761, 1986.
- [34] Y. Imry, in *Directions in condensed matter physics*. Singapore: World Scientific, 1986.
- [35] Y. Imry and R. Landauer, "Conductance viewed as transmission," *Rev. Mod. Phys.*, vol. 71, p. S306, 1999.

- [36] P. Streda, “Quantised thermopower of a channel in the ballistic regime,” *J. Phys.: Condens. Matter*, vol. 1, p. 1025, 1989.
- [37] R. de Picciotto, H. L. Stormer, L. N. Pfeiffer, K. W. Baldwin, and K. W. West, “Four-terminal resistance of a ballistic quantum wire,” *Nature*, vol. 411, p. 51, 2001.
- [38] A. M. Chang, “Fundamental physics - resistance of a perfect wire,” *Nature*, vol. 411, p. 39, 2001. [Note that this paper explains the paper by Picciotto *et al.* in *Nature* **411**, p. 51 (2001)].
- [39] A. D. Stone and A. Szafer, “What is measured when you measure a resistance? – the landauer formula revisited,” *IBM J. Res. Dev.*, vol. 32, p. 384, 1988.
- [40] T. Dittrich, P. Hänggi, G.-L. Ingold, B. Kramer, G. Schön, and W. Zwerger, *Quantum Transport and Dissipation*. Wiley-VCH Verlag GmbH, 1998.
- [41] M. Büttiker, “Quantized transmission of a saddle-point constriction,” *Phys. Rev. B*, vol. 41, p. 7906(R), 1990.
- [42] W. H. Miller, “Semiclassical treatment of multiple turning-point problems – phase shifts and eigenvalues,” *J. Chem. Phys.*, vol. 48, p. 1651, 1968.
- [43] J. N. L. Connor, “On the analytical description of resonance tunnelling reactions,” *Mol. Phys.*, vol. 15, p. 37, 1968.
- [44] L. I. Glazman and I. A. Larkin, “Lateral position control of an electron channel in a split-gate device,” *Semicond. Sci. Technol.*, vol. 6, p. 32, 1991.
- [45] D. B. Chklovskii, B. I. Shklovskii, and L. I. Glazman, “Electrostatics of edge channels,” *Phys. Rev. B*, vol. 46, p. 4026, 1992.
- [46] Y. Y. Proskuryakov, J. T. Nicholls, D. I. Hadji-Ristic, A. Kristensen, and C. B. Sørensen, “Energy-loss rate of a two-dimensional electron gas measured using a mesoscopic thermometer,” *Phys. Rev. B*, vol. 75, p. 045308, 2007.
- [47] R. Taboryski, A. Kristensen, C. B. Sørensen, and P. E. Lindelof, “Conductance-quantization broadening mechanisms in quantum point contacts,” *Phys. Rev. B*, vol. 51, p. 2282, 1995.
- [48] F. D. M. Haldane, “Luttinger liquid theory of one-dimensional quantum fluids. I. Properties of the luttinger model and their extension to the general 1d interacting spinless fermi gas,” *J. Phys. C: Solid State Phys.*, vol. 14, p. 2585, 1981.

- [49] J. M. Luttinger, “An exactly soluble model of a many-fermion system,” *J. Math. Phys.*, vol. 4, p. 1154, 1963.
- [50] S. Tomonaga, “Remarks on blochs method of sound waves applied to many-fermion problems,” *Prog. Theor. Phys.*, vol. 5, p. 544, 1950.
- [51] M. Khodas, M. Pustilnik, A. Kamenev, and L. I. Glazman, “One-dimensional Fermi-Luttinger liquid,” 2007. cond-mat/0702505.
- [52] M. P. A. Fisher and L. I. Glazman, “Transport in a one-dimensional luttinger liquid,” in *Mesoscopic Electron Transport* (G. S. L. Kowenhoven and L. Sohn, eds.), (Dordrecht), NATO ASI Series E, Kluwer Ac. Publ., 1997.
- [53] T. Giamarchi, *Quantum Physics in One Dimension*. Clarendon Press, 2003.
- [54] K. A. Matveev and L. I. Glazman, “Conductance and coulomb blockade in a multi-mode quantum wire,” *Physica B: Condens. Matter*, vol. 189, p. 266, 1993.
- [55] D. L. Maslov and M. Stone, “Landauer conductance of luttinger liquids with leads,” *Phys. Rev. B*, vol. 52, p. R5539, 1995.
- [56] C. L. Kane and M. P. A. Fisher, “Transport in a one-channel luttinger liquid,” *Phys. Rev. Lett.*, vol. 68, p. 1220, 1992.
- [57] C. L. Kane and M. P. A. Fisher, “Transmission through barriers and resonant tunneling in an interacting one-dimensional electron gas,” *Phys. Rev. B*, vol. 46, p. 15233, 1992.
- [58] K. J. Thomas, J. T. Nicholls, M. Y. Simmons, M. Pepper, D. R. Mace, and D. A. Ritchie, “Possible spin polarization in a one-dimensional electron gas,” *Phys. Rev. Lett.*, vol. 77, p. 135, 1996.
- [59] S. M. Cronenwett, H. J. Lynch, D. Goldhaber-Gordon, L. P. Kouwenhoven, C. M. Marcus, K. Hirose, N. S. Wingreen, and V. Umansky, “Low-temperature fate of the 0.7 structure in a point contact: A kondo-like correlated state in an open system,” *Phys. Rev. Lett.*, vol. 88, p. 226805, 2002.
- [60] B. J. van Wees, L. P. Kouwenhoven, E. M. M. Willems, C. J. P. M. Harmans, J. E. Mooij, H. van Houten, C. W. J. Beenakker, J. G. Williamson, and C. T. Foxon, “Quantum ballistic and adiabatic electron transport studied with quantum point contacts,” *Phys. Rev. B*, vol. 43, p. 12431, 1991.
- [61] K. J. Thomas, J. T. Nicholls, M. Pepper, W. R. Tribe, M. Y. Simmons, and D. A. Ritchie, “Spin properties of low-density one-dimensional wires,” *Phys. Rev. B*, vol. 61, p. R13365, 2000.

- [62] A. Kristensen, P. E. Lindelof, J. B. Jensen, M. Zaffalon, J. Hollingbery, S. W. Pedersen, H. B. J. Nygård and, C. B. S. S. M. Reimann, M. Michel, and A. Forchel, “Temperature dependence of the $0.7\ 2e^2/h$ quasi-plateau in strongly confined quantum point contacts,” *Physica B*, vol. 249, p. 180, 1998.
- [63] K. J. Thomas, J. T. Nicholls, N. J. Appleyard, M. Y. Simmons, M. Pepper, D. R. Mace, W. R. Tribe, and D. A. Ritchie, “Interaction effects in a one-dimensional constriction,” *Phys. Rev. B*, vol. 58, p. 4846, 1998.
- [64] E. Koop, A. Lerescu, J. Liu, B. van Wees, D. Reuter, A. Wieck, and C. van der Wal, “Persistence of the 0.7 anomaly of quantum point contacts in high magnetic fields,” *cond-mat/07060792*, 2007.
- [65] L. P. Kouwenhoven, B. J. van Wees, C. J. P. M. Harmans, J. G. Williamson, H. van Houten, C. W. J. Beenakker, C. T. Foxon, and J. J. Harris, “Nonlinear conductance of quantum point contacts,” *Phys. Rev. B*, vol. 39, p. 8040, 1989.
- [66] N. K. Patel, L. Martin-Moreno, M. Pepper, R. Newbury, J. E. F. Frost, D. A. Ritchie, G. A. C. Jones, J. T. M. B. Janssen, J. Singleton, and J. A. A. J. Perenboom, “Ballistic transport in one dimension: additional quantisation produced by an electric field,” *J. Phys.: Condens. Matter*, vol. 2, p. 7247, 1990.
- [67] K. S. Pyshkin, C. J. B. Ford, R. H. Harrell, M. Pepper, E. H. Linfield, and D. A. Ritchie, “Spin splitting of one-dimensional subbands in high quality quantum wires at zero magnetic field,” *Phys. Rev. B*, vol. 62, p. 15842, 2000.
- [68] N. J. Appleyard, J. T. Nicholls, M. Pepper, W. R. Tribe, M. Y. Simmons, and D. A. Ritchie, “Direction-resolved transport and possible many-body effects in one-dimensional thermopower,” *Phys. Rev. B*, vol. 62, p. 16275(R), 2000.
- [69] Y. M. Blanter and M. Büttiker, “Shot noise in mesoscopic conductors,” *Physics Reports*, vol. 336, p. 1, 2000.
- [70] M. Büttiker, “Scattering theory of thermal and excess noise in open conductors,” *Phys. Rev. Lett.*, vol. 65, p. 2901, 1990.
- [71] P. Roche, J. Ségala, D. C. Glatthli, J. T. Nicholls, M. Pepper, A. C. Graham, K. J. Thomas, M. Y. Simmons, and D. A. Ritchie, “Fano Factor Reduction on the 0.7 Conductance Structure of a Ballistic One-Dimensional Wire,” *Physical Review Letters*, vol. 93, p. 116602, 2004.

- [72] M. Reznikov, M. Heiblum, H. Shtrikman, and D. Mahalu, “Temporal correlation of electrons: Suppression of shot noise in a ballistic quantum point contact,” *Phys. Rev. Lett.*, vol. 75, p. 3340, 1995.
- [73] A. Kumar, L. Saminadayar, D. C. Glattli, Y. Jin, and B. Etienne, “Experimental test of the quantum shot noise reduction theory,” *Phys. Rev. Lett.*, vol. 76, p. 2778, 1996.
- [74] L. Dicarlo, Y. Zhang, D. T. McClure, D. J. Reilly, C. M. Marcus, L. N. Pfeiffer, and K. W. West, “Shot-Noise Signatures of 0.7 Structure and Spin in a Quantum Point Contact,” *Physical Review Letters*, vol. 97, p. 036810, 2006.
- [75] W. D. Oliver, *The generation and detection of electron entanglement*. PhD thesis, Stanford University, 2003.
- [76] L. DiCarlo, Y. Zhang, D. T. McClure, D. J. Reilly, C. M. Marcus, L. N. Pfeiffer, K. W. West, M. P. Hanson, and A. C. Gossard, “Current noise in quantum point contacts,” *Proceedings of the 6th Rencontres du Vietnam, Hanoi*, 2006. (condmat/07043892).
- [77] A. Kristensen, J. B. Jensen, M. Zaffalon, C. B. Sørensen, S. M. Reimann, P. E. Lindelof, M. Michel, and A. Forchel, “Conductance quantization above 30k in GaAlAs shallow-etched quantum point contacts smoothly joined to the background 2deg,” *Journal of Applied Physics*, vol. 83, p. 607, 1998.
- [78] D. J. Reilly, G. R. Facer, A. S. Dzurak, B. E. Kane, R. G. Clark, P. J. Stiles, R. G. Clark, A. R. Hamilton, J. L. O’Brien, N. E. Lumpkin, L. N. Pfeiffer, and K. W. West, “Many-body spin-related phenomena in ultra low-disorder quantum wires,” *Phys. Rev. B*, vol. 63, p. 121311, 2001.
- [79] R. Danneau, W. R. Clarke, O. Klochan, A. P. Micolich, A. R. Hamilton, M. Y. Simmons, M. Pepper, and D. A. Ritchie, “Conductance quantization and the $0.7 \times 2e^2/h$ conductance anomaly in one-dimensional hole systems,” *Appl. Phys. Lett.*, vol. 88, p. 012107, 2006.
- [80] R. de Picciotto, L. N. Pfeiffer, K. W. Baldwin, and K. W. West, “Non-linear response of a clean one-dimensional wire,” *Phys. Rev. Lett.*, vol. 92, p. 036805, 2004.
- [81] M. J. Biercuk, N. Mason, J. Martin, A. Yacoby, and C. M. Marcus, “Anomalous conductance quantization in carbon nanotubes,” *Phys. Rev. Lett.*, vol. 94, p. 026801, 2005.
- [82] K. A. Matveev, “Conductance of a Quantum Wire in the Wigner-Crystal Regime,” *Phys. Rev. Lett.*, vol. 92, p. 106801, 2004.

- [83] K. A. Matveev, “Conductance of a quantum wire at low electron density,” *Phys. Rev. B*, vol. 70, p. 245319, 2004.
- [84] B. Spivak and F. Zhou, “Ferromagnetic correlations in quasi-one-dimensional conducting channels,” *Phys. Rev. B*, vol. 61, p. 16730, 2000.
- [85] J. S. Meyer, K. A. Matveev, and A. I. Larkin, “Transition from a One-Dimensional to a Quasi-One-Dimensional State in Interacting Quantum Wires,” *Physical Review Letters*, vol. 98, p. 126404, 2007.
- [86] A. D. Klironomos, R. R. Ramazashvili, and K. A. Matveev, “Exchange coupling in a one-dimensional Wigner crystal,” *Phys. Rev. B*, vol. 72, p. 195343, 2005.
- [87] A. D. Klironomos, J. S. Meyer, and K. A. Matveev, “Spontaneous spin polarization in quantum wires,” *Europhysics Letters*, vol. 74, p. 679, 2006.
- [88] O. F. Syljuåsen, “Length-Dependent Conductance of a Spin-Incoherent Hubbard Chain: MonteCarlo Calculations,” *Physical Review Letters*, vol. 98, p. 166401, 2007.
- [89] G. A. Fiete, “The spin-incoherent luttinger liquid,” 2007. To appear in *Reviews of Modern Physics* (condmat/0611597).
- [90] M. Kindermann, P. W. Brouwer, and A. J. Millis, “Interference as a Probe of Spin Incoherence in Strongly Interacting Quantum Wires,” *Phys. Rev. Lett.*, vol. 97, p. 036809, 2006.
- [91] M. Kindermann and P. W. Brouwer, “Conductance reduction without shot noise in quantum wires,” *Phys. Rev. B*, vol. 74, p. 125309, 2006.
- [92] Y. Meir, K. Hirose, and N. S. Wingreen, “Kondo model for the 0.7 anomaly in transport through a quantum point contact,” *Phys. Rev. Lett.*, vol. 89, p. 196802, 2002.
- [93] L. Glazman and M. Pustilnik, “Coulomb blockade and kondo effect in quantum dots,” *New Directions in Mesoscopic Physics (Towards Nanoscience)*, eds. R. Fazio, V.F. Gantmakher, and Y. Imry (Kluwer, Dordrecht, 2003), pp. 93-115, 2003 (cond-mat/0302159).
- [94] D. Goldhaber-Gordon, J. Göres, M. A. Kastner, H. Shtrikman, D. Mahalu, and U. Meirav, “From the kondo regime to the mixed-valence regime in a single-electron transistor,” *Phys. Rev. Lett.*, vol. 81, p. 5225, 1998.
- [95] A. Golub, T. Aono, and Y. Meir, “Suppression of Shot Noise in Quantum Point Contacts in the “0.7 Regime”,” *Phys. Rev. Lett.*, vol. 97, p. 186801, 2006.

- [96] T. Rejec and Y. Meir, “Magnetic impurity formation in quantum point contacts,” *Nature*, vol. 442, p. 900, 2006.
- [97] C.-K. Wang and K.-F. Berggren, “Spin splitting of subbands in quasi-one-dimensional electron quantum channels,” *Phys. Rev. B*, vol. 54, p. R14257, 1996.
- [98] A. A. Starikov, I. I. Yakimenko, and K.-F. Berggren, “Scenario for the 0.7-conductance anomaly in quantum point contacts,” *Phys. Rev. B*, vol. 67, p. 235319, 2003.
- [99] O. P. Sushkov, “Restricted and unrestricted hartree-fock calculations of conductance for a quantum point contact,” *Phys. Rev. B*, vol. 67, p. 195318, 2003.
- [100] H. Bruus, V. V. Cheianov, and K. Flensberg, “From mesoscopic magnetism to the anomalous 0.7 conductance plateau,” 2000. (cond-mat/0002338).
- [101] H. Bruus, V. V. Cheianov, and K. Flensberg, “The anomalous 0.5 and 0.7 conductance plateaus in quantum point contacts,” *Physica E*, vol. 10, p. 97, 2001. (cond-mat/0106504).
- [102] D. J. Reilly, “Phenomenological model for the 0.7 conductance feature in quantum wires,” *Phys. Rev. B*, vol. 72, p. 033309, 2005.
- [103] G. Seelig and K. A. Matveev, “Electron-phonon scattering in quantum point contacts,” *Phys. Rev. Lett.*, vol. 90, p. 176804, 2003.
- [104] G. Seelig, K. A. Matveev, and A. V. Andreev, “Phonon-Induced Resistivity of Electron Liquids in Quantum Wires,” *Phys. Rev. Lett.*, vol. 94, p. 066802, 2005.
- [105] H. Bruus and K. Flensberg, “Localized plasmons in point contacts,” *Semicond. Sci. Technol.*, vol. 13, p. A30, 1998.
- [106] D. Meidan and Y. Oreg, “Multiple-particle scattering in quantum point contacts,” *Phys. Rev. B*, vol. 72, p. 121312, 2005.
- [107] C. Sloggett, A. I. Milstein, and O. P. Sushkov, “Correlated electron current and temperature dependence of the conductance of a quantum point contact,” unpublished (cond-mat/0606649), 2006.
- [108] D. Schmeltzer, A. Saxena, A. R. Bishop, and D. L. Smith, “Electron transmission through a short interacting wire: 0.7 conductance anomaly,” *Phys. Rev. B*, vol. 71, p. 045429, 2005.

- [109] M. Cutler and N. F. Mott, "Observation of anderson localization in an electron gas," *Phys. Rev.*, vol. 181, p. 1336, 1969.
- [110] N. F. Mott and H. Jones, *The Theory of the Properties of Metals and Alloys*. Oxford: Clarendon, 1st ed., 1936.
- [111] Y. Y. Proskuryakov, J. T. James, D. I. Hadji-Ristic, A. Kristensen, and C. B. S. rensen, "Linear thermopower of a constriction: Evidence of a bound electron," (*unpublish*), 2004.
- [112] M. Jonson and G. D. Mahan, "Mott's formula for the thermopower and the Wiedemann-Franz law," *Phys. Rev. B*, vol. 21, p. 4223, 1980.
- [113] M. Jonson and G. D. Mahan, "Electron-phonon contribution to the thermopower of metals," *Phys. Rev. B*, vol. 42, p. 9350, 1990.
- [114] G. Catelani and I. Aleiner, "Interaction corrections to the thermal transport coefficients in disordered metals: Quantum kinetic equation approach," *Journal of Experimental and Theoretical Physics*, vol. 100, p. 331, 2005. (cond-mat/0405333).
- [115] H. Smith and H. H. Jensen, *Transport Phenomena*. Clarendon Press, Oxford, 1989.
- [116] B. Shchamkhalova and V. Sablikov, "Potential landscape of a biased quantum wire," *Physica E: Low-dimensional Systems and Nanostructures*, vol. 27, p. 51, 2005.
- [117] H. Akeru and T. Ando, "Theory of the hall effect in quantum wires: Effects of scattering," *Phys. Rev. B*, vol. 41, p. 11967, 1990.
- [118] V. L. Gurevich, V. B. Pevzner, and E. W. Fenton, "Coulomb drag in the ballistic electron transport regime," *J. Phys.: Condens. Matter*, vol. 10, p. 2551, 1998.
- [119] H. Bruus, K. Flensberg, and H. Smith, "Magnetoeconductivity of quantum wires with elastic and inelastic scattering," *Phys. Rev. B*, vol. 48, p. 11144, 1993.
- [120] V. L. Gurevich, V. B. Pevzner, and K. Hess, "Phonon-assisted ballistic resistance," *Phys. Rev. B*, vol. 51, p. 5219, 1995.
- [121] J. Sone, "Electron transport in quantum wires and its device applications," *Semicond. Sci. Technol.*, vol. 7, p. B210, 1992.
- [122] M. I. Muradov, "Phonon drag in ballistic quantum wires in the nonlinear regime," *Phys. Rev. B*, vol. 66, p. 115417, 2002.

- [123] C. Bena and L. Balents, “Spin transport in a quantum wire,” *Phys. Rev. B*, vol. 65, p. 115108, 2002.
- [124] M. Nedjalkov, E. A. Dragica Vasileska, and V. Palankovski, “Ultrafast wigner transport in quantum wires,” *Journal of Computational Electronics*, vol. 6, p. 1572, 2007.
- [125] S. K. Lyo and D. Huang, “Effect of electron-electron scattering on the conductance of a quantum wire studied with the boltzman transport equation,” *Phys. Rev. B*, vol. 73, p. 205336, 2006.
- [126] E. Lifshitz, L. Pitaevskii, and A. Kosevich, *Physical Kinetics*, vol. 10 of *Landau and Lifshitz: Course of Theoretical Physics*. Butterworth-Heinemann Ltd, 1.st ed., 1981.
- [127] R. Liboff, *Introductory Quantum Mechanics*. USA: Addison Wesley, 4th ed., 2002.
- [128] Y. M. Sirenko, V. Mitin, and P. Vasilopoulos, “Triple-electron collisions in a quantum wire,” *Phys. Rev. B*, vol. 50, p. 4631, 1994.
- [129] L. V. Keldysh *Zh. Eksp. Teor. Fiz.*, vol. 47, p. 1515, 1964.
- [130] G. D. Mahan, *Many Particle Physics*. Springer, 3nd ed., January 2000.
- [131] H. Haug and A.-P. Jauho, *Quantum Kinetics in Transport and Optics of Semiconductors*. Springer, 1st ed., 1996.
- [132] T. Frederiksen, “Inelastic electron transport in nanosystems,” master thesis, Technical university of Denmark, 2004. (Chapter 2 contains an excellent introduction to Non-equilibrium Green’s function ordered on a Keldysh contour. An electronic version can be found at www.mic.dtu.dk under the theoretical nanotechnology group.).
- [133] J. Rammer and H. Smith, “Quantum field-theoretical methods in transport theory of metals,” *Rev. Mod. Phys.*, vol. 58, p. 323, 1986.
- [134] J. Rammer master thesis, University of Copenhagen, The Niels Bohr Institute, 1981. (in Danish).
- [135] A. Kamenev, “Many-body theory of non-equilibrium systems,” 2004. Lectures notes for the 2004 Les Houches Summer School on Nanoscopic Quantum Transport (cond-mat/0412296).
- [136] D. C. Langreth, *Linear and Nonlinear Electron Transport in Solids*. New York and London: Plenum Press, 1976.

- [137] Y. Meir and N. S. Wingreen, “Landauer formula for the current through an interacting electron region,” *Phys. Rev. Lett.*, vol. 68, p. 2512, 1992.
- [138] A. Lassl, P. Schlagheck, and K. Richter, “Effects of short-range interactions on transport through quantum point contacts: A numerical approach,” *Phys. Rev. B*, vol. 75, p. 045346, 2007.
- [139] K. F. Berggren and I. I. Yakimenko, “Effects of exchange and electron correlation on conductance and nanomagnetism in ballistic semiconductor quantum point contacts,” *Phys. Rev. B*, vol. 66, p. 085323, 2002.
- [140] K. Flensberg and B. Y.-K. Hu, “Plasmon enhancement of coulomb drag in double-quantum-well systems,” *Phys. Rev. B*, vol. 52, p. 14796, 1995.
- [141] A. M. Lunde, “Coulomb drag in multiwall carbon nanotubes,” Master’s thesis, Niels Bohr Institute and MIC–Department of Micro and Nanotechnology, see www.nbi.ku.dk/flensberg under students, 2004.
- [142] L. Kadanoff and G. Baym, *Quantum Statistical Mechanics*. Westview Press, 1962.
- [143] G. Baym, “Conservation laws and the quantum theory of transport: the early days,” *Progress in Non-equilibrium Green’s Functions*, p. 17, 2000. World Scientific, Singapore (see also the homepage of Leo Kadanoff for an electronic version).
- [144] K. S. Thygesen and A. Rubio, “Non-equilibrium gw approach to quantum transport in nano-scale contacts,” *J. Chem. Phys.*, vol. 126, p. 091101, 2007.
- [145] J. M. Luttinger, “Analytic properties of single-particle propagators for many-fermion systems,” *Phys. Rev.*, vol. 121, p. 942, 1961.
- [146] A. M. Lunde and K. Flensberg *et al.*, (unpublished).